STRUCTURAL STUDIES OF AN ASPARTIC PROTEASE INHIBITOR FROM AN EXTREMOPHILIC *BACILLUS* SP.: INTERACTIONS OF ASPARTIC PROTEASES WITH THE INHIBITOR

THESIS SUBMITTED
TO
THE UNIVERSITY OF PUNE
FOR
THE DEGREE OF DOCTOR OF PHILOSOPHY
IN
BIOTECHNOLOGY

BY
CHANDRAVANU DASH

DIVISION OF BIOCHEMICAL SCIENCES
NATIONAL CHEMICAL LABORATORY
PUNE-411 008
INDIA

SEPTEMBER 2001

Acknowledgement

I am indeed fortunate to work under the able guidance of Dr (Mrs) Mala Rao, whose consistent interest, continuous encouragement, inspiration, and the genuine insight into the problems have helped me to gain the deepest thoughts in research. I express my deep sense of gratitude for her open mindedness and patience during the course of this work.

I take this opportunity to thank Dr. Murali Sastry, Material Chemistry Division, National Chemical Laboratory, for introducing and guiding me into the fascinating field of "Nanotechnology" and to give me a chance to work in the area of Nanobiotechnology.

I am grateful to Dr (Mrs) Vasanti Deshpande for invaluable discussions, timely advice, and support throughout my work.

I am thankful to Dr. Absar Ahmed for all the Microbiological work and fruitful discussions.

I thank my ex-labmates Drs. Sangeeta, Neeta, Urmila, Sneha, Kavita for their help and co-operation.

I am thankful to Dr. Mohini, and Dr Sushma for their timely help and inspirations.

Thanks are also due to my labmates Anish, Nilesh, Prashant, Kavita, Swati, Aparna, Sharmili, and Pankaj for the cordial and friendly atmosphere in the lab.

A special thanks goes to Vinod for his timely help and the lighter moments shared.

I am indeed thankful to my senior and friend, Devyani for her inspiration, encouragement, help and valuable discussions during the course of the work.

I fall short of words to express my feelings towards my all time friends, Sudeep, Rajesh, and Jui. They have made an outstanding impact on my outlook towards life and science. They have been there all the time with me in my ups and downs.

Special thanks are to my friends Anand, Ashwini, Maneesha, Lata, and Ramchander with whom I have shared many memorable moments and for their help, co-operation, and inspiration throughout this work.

I owe my deepest gratitude to my parents, brother, sister, niece, and sister-in-law, without whose enduring support and encouragement, it would not have been possible to embark upon this journey in life.

I am thankful to our office staffs Usha, Indira, Satyali, Karunakaran, and Mari for their timely help rendered during the course of this work.

I also express my thanks to our efficient instrumentation staffs, Mr. Kamthe, Mr. Karanjkar, Mr. Trehan for the help and maintenance of the instruments.

I am thankful to our lab attendant Mr. R. Lambharte for his untiring help in routine chores.

I am thankful to Dr. P. K. Ranjekar, Head, Division of Biochemical Sciences for allowing me to use the facilities of the Department.

I am thankful to Dr. Paul Ratnasamy, Director, National Chemical Laboratory, for granting me permission to submit this work in the form of thesis.

The fellowship awarded by the Council of Scientific and Industrial Research is duly acknowledged.

Chandravanu Dash

Dedicated to My Family……..

TABLE OF CONTENTS

DECLARATION

This is to certify that the work incorporated in the thesis entitled **"STRUCTURAL STUDIES OF AN ASPARTIC PROTEASE INHIBITOR FROM AN EXTREMOPHILIC *BACILLUS* SP.: INTERACTIONS OF ASPARTIC PROTEASES WITH THE INHIBITOR"** submitted by **Mr. Chandravanu Dash** was carried out under my supervision at the Division of Biochemical Sciences, National Chemical Laboratory, Pune, India. Materials obtained from other sources have been duly acknowledged.

Dr. (Mrs) Mala Rao
Research Guide

ABBREVIATIONS

AIDS	Acquired immunodeficiency virus	**TFP**	Transframe peptide
ANS	8-Anilinonapthalene-1-sulfonic acid	**TFR**	Transframe region
AP	Aspartic protease	**UV**	Ultra violet
AP-ATBI	First reversible aspartic protease-inhibitor complex	**WRK**	Woodward's reagent K
		XPS	X-ray photoelectron spectroscopy
AP-ATBI*	Second slow dissociating aspartic protease-inhibitor complex		
ATBI	Alkalo-thermophilic *Bacillus* inhibitor		
ATP	Adenosine 5'-triphosphate		
CD	Circular dichroism		
DNSA	3,5-dinitrosalicylic acid		
EDTA	Ethylene diamine tetraacetic acid		
EDAX	Energy dispersive analysis of X-rays		
ES-MS	Electrospray mass spectrometer		
F-prot	Fungal protease from *Aspergillus saitoi*		
FTIR	Fourier Transform Infrared Spectroscopy		
Gdm/HCl	Guanidine hydrochloride		
HIV	Human immunodeficiency virus		
HIV-1 PR	Human immunodeficiency virus type 1 protease		
IC_{50},	50% inhibitory concentration		
IPTG	Isopropyl β-D- thiogalactoside		
LB	Luria bertani		
MIC	Minimum inhibitory concentration		
NCIM	National center for industrial microorganisms		
ODA	Octadecyl amine		
PCA	Perchloric acid		
PD	Potato dextrose		
PSI	Protease specific insert		
QCM	Quartz crystal microgravimetry		

rp-HPLC	Reverse phase high performance liquid chromatography
SEM	Scanning electron microscope
TEM	Transmission electron microscope

ABSTRACT

Proteases are responsible either, directly or indirectly for all bodily functions including cell growth, nutrition, differentiation, and protein turn over. The aspartic proteases constitute one of the primary classes of proteolytic enzymes utilizing two aspartic acid residues in the active site for the catalytic activity with the direct participation of a water molecule. The study of the kinetic properties of this class of enzymes frequently has been motivated by their involvement in physiological and pathological processes of human, thus their effective regulators, i.e., aspartic protease inhibitors, are tremendously essential for physiological regulations. The enzymatic properties of pepsin, plasma renin, lysosomal cathepsin D, as well as several other mammalian and fungal aspartic proteases of commercial importance have evoked considerable interest for investigating the role of inhibitors kinetically. Recent developments in the involvement of aspartic proteases in the life cycle of human immunodeficiency virus and in the degradation of hemoglobin by malarial parasite have generated enormous attention to investigate the interaction between potent inhibitors and the target enzymes. Determination of the kinetic parameters of the inhibition of aspartic proteases will provide insight into the mechanism of the interaction between the enzyme-inhibitor complex. Thus to understand the mechanism of inhibition of aspartic proteases and to shed light on their interactions with the inhibitors, the present work has been undertaken with following main objectives.

1. Purification and characterization of an aspartic protease inhibitor, ATBI from an extremophilic *Bacillus* sp.
2. Interaction of ATBI with HIV-1 protease: implications in the mechanism of inactivation.
3. Structural and mechanistic insight into the inhibition of aspartic proteases by ATBI.
4. Bifunctional role of ATBI: implications in fungal growth inhibition.
5. Unfolding and chaperone mediated refolding of the aspartic proteases.
6. Interactions of the aspartic proteases with lipids and gold nanoparticles.

A summary of the important findings is described in the following seven chapters.

Chapter 1. General Introduction

This chapter is an overview of the classes of aspartic proteases, their occurrence, and mechanism of catalysis. It covers the role of aspartic protease inhibitors in various physiological regulations, and their distribution, design, mechanism of action, and the review of literature.

Chapter 2. Purification and Characterization of an Aspartic Protease Inhibitor, ATBI from an Extremophilic *Bacillus* sp.

The indispensable nature of the aspartic proteases in numerous physiological functions has evoked tremendous response towards isolating new inhibitors from various resources. After extensive screening, we have isolated an extremophilic *Bacillus* sp., which produces an aspartic protease inhibitor (ATBI). Maximum

production of ATBI was observed after 48 h after the commencement of the fermentation. The production of ATBI was optimized in terms of the carbon, nitrogen sources, and amino acids. Presence of glucose, soyameal and beef extract, and arginine in the fermentation medium induced the production of ATBI substantially. ATBI was purified from the extracellular culture filtrate by the treatment of activated charcoal and ultra filtration. The resulting filtrate was concentrated by lyophilization and the concentrated inhibitor sample was further purified by reverse phase-HPLC. The fractions collected were tested for their aspartic protease inhibitory activity by using pepsin as the representative enzyme. The active fractions were further purified by rp-HPLC. Homogeneity of the active fractions was indicated by the single peak as analyzed on rp-HPLC. The purified ATBI showed a single band on an analytical iso-electric focusing gel with a pI of 10.0. The amino acid composition data revealed the abundance of Asp residues. The amino acid sequence of the purified inhibitor determined by a protein sequencer was Ala-Gly-Lys-Lys-Asp-Asp-Asp-Asp-Pro-Pro-Glu. The predominance of the charged amino acid residues in the inhibitor sequence indicated its hydrophilic nature and the net charge per molecule calculations from the amino acid composition was negative indicating that ATBI is an anionic peptide. The molecular mass (M_r) of ATBI as determined from ES-MS was 1147 Da. The stability of the inhibitor was checked with respect to temperature and pH. ATBI was resistant to heat treatment up to 90°C for 1 h and was stable over a pH range of 2-10. ATBI specifically inhibited aspartic proteases such as pepsin, HIV-1 protease and the protease from *Aspergilllus saitoi*, however, it failed to inhibit other classes of proteases such as chymotrypsin, trypsin, papain, and subtilisin.

Chapter 3. Interaction of ATBI with HIV-1 Protease, Implications in the Mechanism of Inactivation

HIV produces a small dimeric aspartyl proteases, which specifically cleaves the polyprotein precursors. This proteolytic activity is absolutely required for the production of mature, infectious virions and is therefore an attractive target for therapeutic. The active site cleft of the HIV-1 protease (PR) is bound by two identical conformationally mobile loops known as flaps, which are important for substrate binding and catalysis. ATBI, being an aspartic protease inhibitor has been tested for its potency towards the recombinant HIV-1 PR. Investigation of the kinetics of the enzyme-inhibitor interactions revealed that ATBI is a non-competitive inhibitor with the IC_{50} and K_i values 18.0 nM and 17.8 nM respectively. The non-dissociative nature of HIV-1 PR-ATBI complex with multiple dilutions prompted us to apply a model of tight binding inhibition for the determination of the kinetic parameters of HIV-1 PR inhibition. Sequence homology exhibited no similarity with the reported peptidic inhibitors of HIV-1 PR. The binding of the inhibitor with the enzyme and the subsequent induction of the localized conformational changes in the flap-region of the HIV-1 PR were monitored by exploiting the intrinsic fluorescence of the surface exposed Trp-42 residues, which are present at the proximity of the flaps. We have demonstrated by fluorescence and circular dichroism studies that ATBI binds in the active site of the HIV-1 PR. The localized conformational changes induced in the HIV-1 PR due to the interaction with ATBI were investigated by fluorescence spectroscopic studies. The titration of the enzyme with increasing concentrations of

ATBI resulted in a concentration dependent quenching of the tryptophan fluorescence. A comparative analysis in the fluorescence spectra of the HIV-1 PR upon binding of the substrate or the known active site directed inhibitors was found to be similar to that of ATBI, suggesting that ATBI binds in the active site of the enzyme. To evaluate the effects of the inhibitor on the secondary structure of the enzyme, we have analyzed the CD spectra of HIV-1 PR-ATBI complex. Interestingly, the HIV-1 PR-ATBI complex and HIV-1 PR-substrate complex exhibited a similar pattern of negative ellipticity in the far-UV region, suggesting that the inhibitor causes similar structural changes in the enzyme as that of the substrate. Based on our results, we propose that the inactivation is due to the reorganization of the flaps impairing its flexibility leading towards inaccessibility of the substrate to the active site of the enzyme.

Chapter 4. Structural and Mechanistic Insight into the Inhibition of Aspartic Proteases by ATBI

ATBI exhibited two-step inhibition mechanism against the aspartic proteases, pepsin and F-prot. The evaluation of kinetic parameters displayed competitive inhibition for pepsin and F-prot by ATBI. The progress-curves for the degree of inhibition are time-dependent and consistent with a two-step, slow-tight binding inhibition mechanism:

$$E + I \underset{k_4}{\overset{k_3}{\rightleftharpoons}} EI \underset{k_6}{\overset{k_5}{\rightleftharpoons}} EI^*$$

The K_i values associated with the formation of the first reversible complex (EI) of ATBI with pepsin and F-prot, were 17±0.5 x 10^{-9} M and 3.2±0.6 x 10^{-6} M, whereas the overall inhibition constant K_i* values were 55±0.5 x 10^{-12} M and 5.2±0.6 x 10^{-8} M, respectively. The rate constant k_5, determining the slow inhibition revealed a faster isomerization rate of the initial reversible enzyme-inhibitor complex, EI, for F-prot (2.3±0.4 x 10^{-3} sec^{-1}) than pepsin (7.7±0.3 x 10^{-4} sec^{-1}). However, ATBI dissociated from the tight enzyme-inhibitor complex (EI*) of F-prot faster (3.8±0.5 x 10^{-5} sec^{-1}) than pepsin (2.5±0.4 x 10^{-6} sec^{-1}). Comparative analysis of the kinetic parameters with pepstatin, the known inhibitor of pepsin, revealed a higher value of k_5/k_6 for ATBI. The binding of the inhibitor with the aspartic proteases and the subsequent conformational changes induced, were monitored by exploiting the intrinsic tryptophanyl fluorescence. The rate constants derived from the fluorescence data were in agreement with those obtained from the kinetic analysis, therefore the induced conformational changes were correlated to the isomerization of EI to EI*. Chemical modification of the Asp or Glu by WRK and Lys residues by TNBS abolished the anti-proteolytic activity and revealed the involvement of two carboxyl and one amine group of ATBI in the enzymatic inactivation.

Chapter 5. Bifunctional Role of ATBI, Implications in Fungal Growth Inhibition

ATBI exhibited anti-fungal activity against a broad spectrum of phytopathogenic fungi including *Alternaria*, *Aspergillus*, *Curvularia*, *Colletotricum*, *Fusarium*, *Phomopsis*, and the saprophytic fungus *Trichoderma.* During the purification of ATBI, the anti-fungal activity of the inhibitor was co-purified with the aspartic protease

inhibitory activity. The concentration of ATBI required for the 50 % growth inhibition (IC_{50}) ranged from 0.30 to 5.9 μg/ml, whereas the minimum inhibitory concentration varied from 0.60 to 3.5 μg/ml. The amino acid sequence of ATBI, did not exhibit primary structural homology to any known anti-fungal peptides. The negative charge and the absence of periodic secondary structure in ATBI suggested an alternative mechanism of action for fungal growth inhibition. ATBI was found to inhibit xylanase and aspartic protease (F-prot) competitively with the K_i values 1.75 and 3.25 μM respectively, suggesting higher binding affinity of ATBI to xylanase than aspartic protease. Growth of representative fungi on selective media for the production of xylanase and aspartic protease and their growth inhibition by ATBI on synthetic media containing specified carbon source for the production of the enzymes, revealed the role of these enzymes in fungal growth. Rescue of the growth inhibition by the reaction products of xylanase and aspartic protease indicated the involvement of these enzymes in the cellular growth. The chemical modification of Asp/Glu or Lys residues of ATBI abolished its anti-fungal activity, indicating the crucial role of these amino acids for the functional aspects of ATBI. The kinetic analysis of the TNBS and WRK modified ATBI abolished its anti-xylanolytic and anti-proteolytic activity and subsequently its anti-fungal activity. Our results envisage a paradigm shift in the concept of fungal growth inhibition for the role of antixylanolytic activity. The structural and functional characteristics of ATBI indicated that, this is the first report of a novel class of anti-fungal peptide, exhibiting bifunctional inhibitory activity.

Chapter 6. Unolding and Chaperone Mediated Refolding of the Aspartic Proteases

Elucidating the mechanistic details underlying the efficient refolding of proteins by chaperones appears to be an important consideration for defining how protein fold *in vivo*. We have studied the unfolding and refolding pathways of the HIV-1 protease and F-prot.

Section I. Equilibrium Unfolding of HIV-1 Protease: Evidence for an Alterative Conformation, which Resembles a Molten Globule. Elucidating the mechanistic details underlying the efficient refolding of proteins now appears to be an important consideration for defining how proteins fold to their native structure. Denaturation studies using the structure-perturbing agent guanidinium hydrochloride (GdmHCl) indicated that the HIV-1 PR folds through a partially folded molten-globule state. The molten globule state of the enzyme was characterized by its perturbed tertiary structure, intact secondary structure, and the exposure of the hydrophobic surfaces, as analyzed by the fluorescence and circular dichroism studies. The present work demonstrates the active participation of α-crystallin in the refolding of the HIV-1 PR. Fluorescence and light scattering experiments revealed that α-crystallin interacts with the molten-globule state of HIV-1 PR and prevents its aggregation. However, the enzyme failed to regain its functional integrity as revealed by the small recovery of enzymatic activity (8%) with the assistance of α-crystallin. Interestingly, in the presence of ATP and α-crystallin, reactivation of HIV-1 PR increased by five fold. Further, thermal denaturation of the enzyme at 50°C resulted in the rapid aggregation and loss of enzymatic activity. Although, α-crystallin prevented aggregation of thermally unfolded HIV-1 PR, there was no indication of reconstitution of the active enzyme. Addition of ATP along with α-crystallin,

assisted further in preventing aggregation of thermally denatured HIV-1 PR. Consistent with these findings *in vitro*, *in vivo* experiments demonstrated that cell viability at 50°C, increased five fold in *Escherichia coli* expressing α-A and α-B crystalline, suggesting that α-crystallin protects cells against physiological stress *in vivo* by maintaining cytosolic proteins in their native and functional conformations. The experimental evidences presented here serve to conclude that HIV-1 PR refolds through a molten globule state and α-crystallin acts like a molecular chaperone *in vitro* and *in vivo*, in an ATP dependent manner.

Section II. Interaction of the molten globule state of F-prot with a -crystallin. Denaturation studies of F-prot using the structure-perturbing agent (GdmHCl) were carried out. The protein completely unfolded in the presence of 4-6 M GdmHCl as revealed by the loss of tertiary structure, secondary structure, and enzymatic activity. However, at 3 M GdmHCl, although the tertiary structure of F-prot was perturbed, the secondary structure of the protein was substantial. Binding of the hydrophobic fluorophore, ANS, to this state of the protein resulted in the increase in the maximum increase in the fluorescence of ANS, suggesting the presence of a molten globule state like structure. Complete unfolding of F-prot as achieved at 6 M GdmHCl failed to refold in the renaturation condition and underwent a rapid aggregation leading towards the inactivation of the enzyme. Thermal aggregation of the protein as reflected by the light scattering experiments revealed that F-prot aggregates very fast at 60°C. α-crystallin, are group of structural proteins which share both sequence and structural homology with small heat shock proteins, whose chaperone like activity has been described in suppressing protein unfolding and aggregation in response to thermal or chemical stress. Refolding of F-prot in the presence of α-crystallin prevented aggregation, however it failed to reconstitute the enzyme to its active form as revealed by the activity data. To investigate the role of ATP on the chaperone activity of α-crystallin, renaturation of the denatured F-prot at 2 M GdmHCl, was initiated in the presence of α-crystallin and ATP. The chaperone activity was found to be enhanced by 5 fold in the presence of ATP as revealed by the 80% recovery of the enzymatic activity. Based on our above results we propose the enhanced chaperone activity of α-crystallin in the presence of ATP for the refolding of chemically denatured F-prot.

Chapter 7. Interactions of the Aspartic Proteases with Lipid Membranes and Colloidal Gold

The commercial exploitation of enzymes requires the development of efficient immobilization protocols that help convenient handling, ease of separation from the product, possibility for reuse, pH and temporal stability of the biocatalysts. The entrapment of the aspartic protease in lipid bilayers and colloidal gold particles have been undertaken and the aspects relating to the structural and functional integrity of the encapsulated enzyme have been discussed.

Section I. Interaction of Pepsin with Octadecyl Amine, Lipid Bilayers. The entrapment of proteins in different inert matrices with the aim of protection, retention of the native structure and accessibility of the encapsulated proteins to cofactors, and substrates has evoked considerable interest currently. The interaction

of the aspartic protease, pepsin, with thermally evaporated lipid, octadecyl amine, has been demonstrated. The approach is based on diffusion of the enzyme from aqueous solution, driven primarily by attractive electrostatic interaction between charged groups on the enzyme surface and ionized lipid molecules in the film. The kinetics of pepsin diffusion into the amine films was followed using quartz crystal microgravimetry (QCM) measurements. The encapsulated pepsin showed catalytic activity comparable to that of the enzyme molecules in solution indicating facile access of biological analytes/reactants in solution to the entrapped enzyme. The time required for the biocomposite formation was less in comparison to some of the techniques currently in vogue, which demonstrated the commercial application of the protocol used. We propose that secondary interactions such as hydrophobic and hydrogen bonding could also be responsible for the diffusion process. The conformational integrity of the entrapped pepsin was investigated by the Fourier Transformed Infrared spectroscopy, UV-vis spectroscopy and by activity measurements. The presence of well distinct amide bands in the FTIR spectrum and the activity measurements of the encapsulated enzyme ruled out any significant distortion to the native structure of the enzyme.

Section II. Interaction of Pepsin with Colloidal Gold Nanoparticles. Pepsin-colloidal gold conjugates were prepared by a protein-friendly process and the structural and functional integrity of the bioconjugates have been investigated. The pepsin-gold conjugates were obtained by mixing colloidal gold and pepsin solutions at pH 3 and, thereafter, centrifugation, washing, and redispersion of the pepsin-gold conjugate material in water. Films of the bioconjugate obtained by solvent evaporation on suitable substrates were further analyzed by scanning electron microscopy (SEM), energy dispersive analysis of X-rays (EDAX), transmission electron spectroscopy (TEM), Fourier transform infrared spectroscopy (FTIR) and X-ray photoelectron spectroscopy (XPS). While TEM and SEM measurements showed aggregates of the enzyme/colloidal gold conjugates, the intactness of secondary and tertiary structures of the enzyme, as determined by FTIR, and fluorescence spectroscopies. The functional integrity of the bioconjugate was analyzed by the catalytic activity measurements, clearly indicates that the enzyme is stable in its natural state and is possibly stabilized by the colloidal gold particles. The enzyme in the pepsin-Au bioconjugate retained substantial biocatalytic activity and was more stable than the free enzyme in solution. In the case of pepsin-gold nanoparticle bioconjugates, we believe that cysteine residues present on the enzyme surface forms covalent linkage with the nanoparticles. It is also possible that amine residues in the enzyme will also bind to the metal surface.

PUBLICATIONS

1. **Dash, C.**, and Rao, M. (2001). Interactions of a novel inhibitor from an extremophilc *Bacillus* sp with HIV-1 protease: implications in mechanism of inactivation. ***J. Biol. Chem.*** 276, 2487-2493.

2. **Dash, C.**, Ahmad, A., Nath, D., and Rao, M. (2001). A novel bifunctional inhibitor of xylanase and aspartic protease: implications in fungal growth inhibition. ***Antimicrob. Agents Chemother.*** 45,2008-2017.

3. **Dash, C.**, Phadtare, S., Deshpande, V., and Rao, M. (2001). Structural and mechanistic insight into the inhibition of aspartic proteases by a slow-tight binding inhibitor from an extremophilic *Bacillus* sp.: correlation of the kinetic parameters with the inhibitor induced conformational changes. ***Biochemistry*** (In press).

4. **Dash, C.,** Pallazi, V., George, S. P., and Rao, M. Inhibition of xylanase by an aspartic protease inhibitor, the kinetic parameters that determine the affinity and selectivity of the bifunctional nature of the inhibitor. (Communicated).

5. **Dash, C.,** and Rao, M. Correlation between the *in vivo and in vitro* chaperone mediated unfolding and refolding of HIV-1 protease. (Communicated).

6. **Dash, C.,** and Rao, M. Unfolding and assisted refolding of the fungal aspartic protease: evidence for a molten globule like intermediate. (Communicated).

7. **Dash, C.,** and Rao, M. Factors determining the production of an aspartic protease inhibitor from an extremophilic *Bacillus* sp. (Manuscript under preparation).

8. **"Indian Scientists Target HIV"**, an invited article published in the "**News India"**, a supplementary of **Nature,** for the subscribers of Nature in India, October 1999.

9. Gole, A., **Dash, C.**, Rao, M., and Sastry, M. (2000). Encapsulation and biocatalytic activity of the enzyme pepsin in fatty lipid films by selective electrostatic interactions. ***JCS Chem. Com.*** 2000, 297-298.

10. Gole, A., **Dash, C.**, Mandale, A. B., Rao, M., and Sastry, M. (2000). Fabrication, characterization and enzymatic activity of encapsulated fungal protease-fatty lipid biocomposite films. ***Anal. Chem.*** 72,4301-4309.

11. Gole, A., **Dash, C.**, Ramakrishnan, V., Sainkar, S. R., Mandale, A. B., Rao, M., and Sastry, M. (2001). Pepsin: gold colloid conjugates - preparation, characterization and enzymatic activity. ***Langmuir*** 17, 1674-1679.

12. Gole, A., **Dash, C.**, Soman, C., Sainkar, S. R., Sainkar, S. R., Rao, M., and Sastry, M. (2001). On the preparation, characterization and enzymatic activity of fungal protease: gold colloid bioconjugates. ***Bioconjugate Chem.*** (in press).

13. Gole, A., **Dash, C.**, Pallazi, V., Rao, M., and Sastry, M. Patterning of F-prot in lead assisted lipid films. (Manuscript under preparation).

14. Sastry, M., Gole, A., **Dash, C.,** Vyas, S., Lachke, A., Rao, M., and Ganesh, K. N. Entrapment of proteins and DNA in thermally evaporated lipid films. Review article in ***Trends in Biotechnol.*** (Communicated).

PATENTS/POSTERS/ABSTRACTS/WORKSHOPS

1. **Dash, C.**, Phadtare, S. U., Ahmed, A., Deshpande, V. V., and Rao, M. B. (1998) *Indian patent no*. **3560-DEL-98**.

2. **Dash, C.**, Phadtare, S. U., Ahmed, A., Deshpande, V. V., and Rao, M. B. (1998) *US patent filed*.

3. **Dash, C.,** and Rao, M. Poster presented at the International Symposium on **"Frontiers in Structural Biology"**, at the **National Center for Biological Sciences, Bangalore**, India, from October 25-27, 1999.

4. Gole, A., **Dash, C.**, Ramakrishnan, V., Sainkar, S. R., Mandale, A. B., Rao, M., and Sastry, M. Paper presented in the National Conference on "**Recent Advances in Material Sciences"** at **Nehru Memorial College**, **Tiruchirappalli**, India, from September 29-30, 2000.

5. **Dash, C.**, and Rao, M., Paper presented in the International Conference on "**Women: Biotechnology, Environment, and Non-conventional Energy**" at **Indian Institute of Chemical Technology, Hyderbad**, India, from October 17-21, 2000.

6. Gole, A., **Dash, C.**, Rao, M., and Sastry, M. Paper presented in the National Symposium on "**Instrumentation**", at **Indian Institute of Science, Bangalore**, India, from November 8-11, 2000.

7. **Dash, C.**, Ahmad, A., and Rao, M. Abstract published in the 41st Annual Conference of Association of Microbiologists of India "**Microbiotech 2000**" at **Birla Institute of Scientific Research, Jaipur**, India, from November 25-27, 2000.

8. Gole, A., **Dash, C.**, Ramakrishnan, V., Sainkar, S. R., Mandale, A. B., Rao, M., and Sastry, M. Poster presented in the 3rd National Symposium in "**Chemistry**" at **Center of Advanced Studies in Chemistry, Punjab University, Chandigarh**, India, from February 2-4, 2001.

9. **Dash, C.**, and Rao, M. Paper to be presented in "Thermophiles 2001", International Symposium to be held at the Department of Microbiology at Delhi University, South Campus, New Delhi, India, from December 3-7, 2001.

10. Attended the "**Orientation Course in Bioinformatics**" at **Bioinformatics Centre**, **DIC**, Pune University, Pune, India., from

11. Attended the International Workshop on "**Protein Structural Bioinformatics, and Genomics**" at the **National Center for Biological Sciences, Bangalore**, India, on October 28, 1999.

Chapter 1

General Introduction

Introduction

Proteases, once considered primarily as "enzymes of digestion" are one of the largest and most diverse families of enzymes known and are involved in every aspect of organismal function. They play a critical role in many physiological and pathological processes such as protein catabolism, blood coagulation, cell growth and migration, tissue arrangement, morphogenesis in development, inflammation, tumor growth and metastasis, activation of zymogens, release of hormones and pharmacologically active peptides from precursor proteins, and transport of secretory proteins across membranes. Proteases catalyze the addition of water across amide (and ester) bonds to effect cleavage using a reaction involving nucleophilic attack on the carbonyl carbon of the scissile bond. The exact mechanisms of cleavage and the active site substituents vary widely among different protease subtypes. This provides the basis for the classification of proteases into the serine proteases, cysteine proteases, metallo proteases, and aspartic proteases (Barett et al., 1998). There are a few miscellaneous proteases, which do not precisely fit into the standard classification, e.g., ATP-dependent proteases, which require ATP for activity (Menon and Goldberg, 1987).

The serine proteases

This class comprises two distinct families, the chymotrypsin family, which includes the mammalian enzymes such as chymotrypsin, trypsin, elastase or kallikrein and the subtilisin family including the bacterial enzymes such as subtilisin. Although, the three-dimensional structure is different in the two families, they possess similar active site geometry and catalytic mechanism. The serine proteases exhibit different substrate specificities, which are related to amino acid substitutions in the various enzyme subsites interacting with the substrate residues. Some enzymes have an extended interaction site with the substrate whereas others have a specificity restricted to the P1 substrate residue. The catalytic triad of the serine protease, essential in the catalytic process is His, Asp, and Ser. The first step in the catalysis is the formation of an acyl enzyme intermediate between the substrate and the essential Ser. Formation of this covalent intermediate proceeds through a negatively charged tetrahedral transition state intermediate and followed by the cleavage of the peptide bond. During the second step or deacylation, the acyl-enzyme intermediate is hydrolyzed by a water molecule to release the peptide and to restore the Ser-hydroxyl of the enzyme. The deacylation, which also involves the formation of a tetrahedral transition state intermediate, proceeds through the reverse reaction pathway of acylation. A water molecule is the attacking nucleophile instead of the Ser residue. The His residue provides a general base and accepts the OH-group of the reactive Ser.

The cysteine proteases

This family includes the plant proteases such as papain, actinidin or bromelain, several mammalian lysosomal cathepsins, the cytosolic calpains (calcium-activated) as well as several parasitic proteases (e.g., Trypanosoma, Schistosoma). Papain is the archetype and the best-studied member of the family. A novel type of fold for cysteine proteases has been revealed from the recent elucidation of the X-ray structure of the Interleukin-

1-beta Converting Enzyme (ICE). Like the serine proteases, catalysis proceeds through the formation of a covalent intermediate and involves a cysteine and a histidine residue. The essential Cys and His play the same role as Ser and His respectively. The nucleophile is a thiolate ion rather than a hydroxyl group. The thiolate ion is stabilized through the formation of an ion pair with neighboring imidazolium group of His. The attacking nucleophile is the thiolate-imidazolium ion pair in both steps and hence a water molecule is not required.

The metallo proteases

The metallo proteases are one of the older classes of proteases and are found in bacteria, fungi as well as in higher organisms. They differ widely in their sequences and their structures but the great majority of enzymes contain a zinc atom, which is catalytically active. In some cases, zinc may be replaced by cobalt or nickel without loss of the activity. Bacterial thermolysin has been well characterized and its crystallographic structure indicates that two histidines and one glutamic acid bind to zinc. Many enzymes contain the sequence HEXXH, which provides two histidine ligands for the zinc whereas the third ligand is either a glutamic acid (thermolysin, neprilysin, alanyl aminopeptidase) or a histidine (astacin). Other families exhibit a distinct mode of binding of the Zn atom. The catalytic mechanism leads to the formation of a non-covalent tetrahedral intermediate after the attack of a zinc-bound water molecule on the carbonyl group of the scissile bond. This intermediate is further decomposed by transfer of the glutamic acid proton to the leaving group.

The aspartic proteases

Aspartic proteases are a group of proteolytic enzymes of the pepsin family that share the same catalytic apparatus and usually function in acidic conditions. This latter aspect limits the function of aspartic proteases to some specific locations in different organisms; thus, the occurrence of aspartic proteases is less abundant than other groups of proteases, such as serine proteases. However, aspartic proteases have been isolated and studied from a wide range of organisms, varying from vertebrates to plants, fungi, parasites, retroviruses, and very recently bacteria (James et al., 1998; Hill and Phylip, 1997). Of the five currently documented from the human body, three (pepsin, gastricsin, and renin) are secretory and have well-defined physiological roles. The fourth protease, cathepsin D, is found ubiquitously in the lysosomes of most cells (Saftig et al. 1995), while the fifth, cathepsin E, is neither secretoy nor lysosomal but it is located within the endoplasmic reticulum/trans-Golgi network/endosomal compartments of cells (Kageyama, 1995). The cathepsin E molecule is readily distinguished from the other aspartic proteases not only by this cytomorphological compartmentation but also by its unique molecular architecture (Rao-Naik et al., 1995) and its limited tissue distribution. Aspartic proteases have been extensively studied for their structure and function relationships and have been the topics of several reviews or monographs (Tang, 1977; Tang, 1979; Kay, 1985; Dunn, 1992; Dunn et al., 1995).

Aspartic proteases are directly dependent on aspartic acid residues for their catalytic activity and represent the simplest sub-subclass of peptidases in that only three families are known. Among the three families, two families are known to be related are those of pepsin (A1) and retropepsin (A2). The enzymes from pararetroviruses such as the cauliflower mosaic virus that form family A3 shows signs of relationship to

retropepsins. Crystallographic studies have shown that the enzymes of the pepsin family are bilobed molecules with the active-site cleft located between the lobes, and each lobe contributes one aspartate residue of the catalytically active diad of aspartates. These two aspartyl

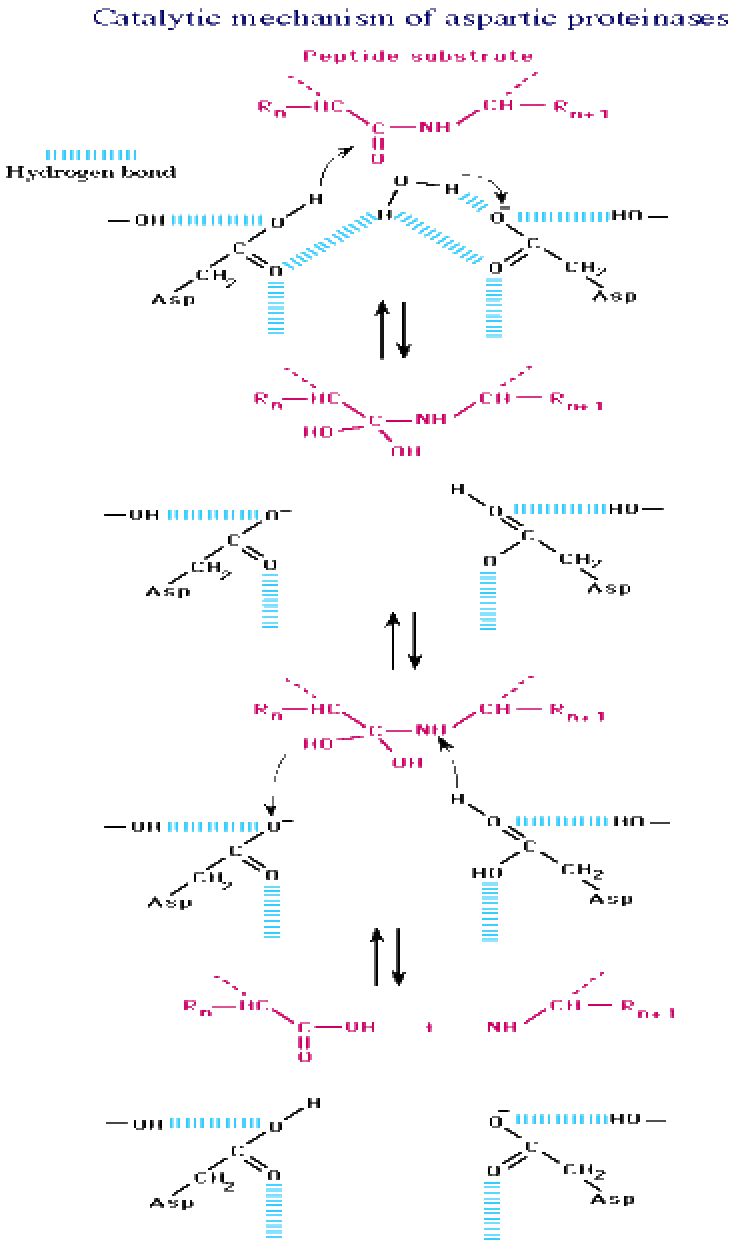

Figure 1. Catalytic mechanism of aspartic proteases.

residues are in close geometric proximity in the active molecule and one aspartate is ionized whereas the second one is unionized at the optimum pH range of 2-3 (Sielicki et al., 1991; Blundell et al., 1991). The lobes are homologous to one another, having arisen by gene duplication. Retropepsins, are monomeric, i.e. carry only one catalytic aspartate and thus dimerization is required to form an active enzyme (Blundell et al., 1991; Miller et al., 1989). In contrast, to serine and cysteine proteases, catalysis by aspartic proteases does not involve a covalent intermediate though a tetrahedral intermediate exists. The nucleophilic attack is achieved by two simultaneous proton transfers, one from a water molecule to the diad of the two-carboxyl groups and a second one from the diad to the carbonyl oxygen of the substrate with the concurrent CO-NH bond cleavage (Figure 1). This general acid-base catalysis, which may be called a "push-pull" mechanism, leads to the formation of a non-covalent neutral tetrahedral intermediate (Miller et al., 1989; Holm et al., 1984).

In family A1 of pepsin (clan AA), the catalytic Asp residues occur within the motif Asp-Xaa-Gly, in which Xaa can be Ser or Thr. The presence of this motif in a protein has often been taken as evidence that it is an aspartic peptidase, which is rather unsound. The Asp residue in the catalytic triad of the serine peptidases of the subtilisin family (S8) occurs in such a motif and the motif is also present in many proteins that are not peptidases. Members of clan AA are all more or less strongly inhibited by pepstatin by a mechanism that is known to be similar at least for families A1 and A2 (Fitzgerald et al., 1989; Cooper et al., 1989). Leader peptidase II (family U11) and thermopsin (family U16) also are sensitive to this inhibitor. Covalently reacting inhibitors of pepsin, namely diazoacetylnorleucine methyl ester (DANLME), 1,2-epox-3-(*p*-nitrophenoxy) propane (EPNE), and *p*-bromophenacyl bromide, have also been used as diagnostic reagents for aspartic endopeptidases. An acidic pH optimum is certainly not the sole criterion of a relationship to pepsin. Unrelated peptidases that are maximally active at acidic pH include lysosomal cysteine endopeptidases (family C1), serine carboxypeptidases (S10), thermopsin (U16), and the enzymes of the scytalidopepsin (U18) and pseudomonapepsin (U25) families.

Pepsin Family

All members of the pepsin family have been found in eukaryotes. The family includes animal enzymes from the digestive tract, such as pepsin and chymosin, lysosomal enzymes such as cathepsin D, and enzymes involved in posttranslational processing such as renin and yeast aspartic protease 3. There are also examples from protozoa (e.g., *Eimeria, Plasmodium)*, fungi, and plants. Members of the family are listed in Table-I. Family A1 contains many enzymes that enter the secretory pathway, and it is probable that all the proteins are synthesized with signal peptides and propeptides. Unusually, barrierpepsin from yeast has a long C-terminal extension, which can be excised without affecting enzymatic activity (Mackay et al., 1988).

Retropepsin Family

Retropepsin is required for processing of all three viral polyproteins, although cellular enzymes perform initial stages of *env* polyprotein cleavage. Processing occurs at a very late stage in virion assembly, usually after budding of virus particles from the cell membrane; inactive virions containing only *gag* polyprotein can be formed. Processing seems to be essential for RNA dimerization within the virion, and hence for infectivity. There is

therefore intense interest in the development of retropepsins as antiretroviral agents (Hellen and Wimmer, 1992). A subset of the retropepsins from oncoviruses and avian retroviruses are larger proteins with N-terminal domain homologous to dUTPases.

Cauliflower Mosaic Virus Peptidase Family

Cauliflower mosaic virus belongs to a group of plant viruses known as pararetroviruses. Although the viral genome is double-stranded DNA, it contains an open reading frame (ORF V) which is analogous to the *pol* gene of retroviruses. ORF V encodes a polyprotein, which includes a reverse transcriptase, which is homologous to that of retroviruses and, based on an Asp-Thr-Gly triplet near the N terminus, was suggested to be included as an aspartic protease as well (Fuetterer and Hohn, 1987). The existence of an endopeptidase was confirmed by mutational studies, which implicated the involvement of Asp-45 in catalysis. There was also weak inhibition by pepstatin. The peptidase is larger than retropepsin, however, since it contains only one Asp-Thr-Gly sequence, it is assumed to be active only as a dimer (Torruella et al., 1989). Other pararetroviruses contain sequences homologous to the cauliflower mosaic virus peptidases.

Putative Aspartic Peptidases

Families of peptidases (U22, U33, U34, U23, U24, U25, U11, and U4) are strictly categorized as of unknown catalytic type but exhibit certain indications of aspartic type.

Putative Transposition Endopeptidases: *Families of Drosophila Transposon 297 Endopeptidase (U22), copia Endopeptidase (U23), and Maize Transposon bs1 Endopeptidase (U24)*.

The putative endopeptidases of family U22 are encoded by open reading frames that correspond to the *pol* gene of retroviruses (Inouye et al., 1986), whereas that of the *copia* transposon (U23) is encoded by the open reading frame corresponding to the Rous sarcoma virus *gag* gene (Yoshika et al., 1990). The *gypsy* transposon from *Drosophila* is homologous to *Drosophila* transposons in family U22, and has been suggested to contain a peptidase (Garfinkel et al., 1991). For family U23, deletion of part of the 5' end of yeast *TyB* (including the Asp-Ser-Gly tripeptide) prevents processing (Adams et al., 1987), and similar results were obtained by another group subsequently (Garfinkel et al., 1991). For the product of *copia* transposon in *Drosophila*, autocatalytic processing has been shown to be necessary for the release of the protein VPL from the polyprotein precursor, and mutation of the putative catalytic Asp prevents processing (Yoshika et al., 1990). The autocatalytic processing of the *copia* transposon of *Drosophila*, thought to be mediated by the transposon endopeptidase, was not significantly inhibited by pepstatin. Family U24 comprises only the putative endopeptidase of maize transposon *bs1* (Johns et al., 1989).

Thermopsin family (U16)

Among the few peptidases that are known from archaebacteria, there is a subtilisin (family S8) and a multicatalytic endopeptidase complex (S25). However, thermopsin from the thermophilic *Sulfolobus acidocaldarius* shows no relationship to any other protein. The enzyme has a pH optimum of 2, maximally active at 70°C, and is covalently attached to the cell membrane. Thermopsin is apparently synthesized as a precursor

with a 41-residue prepropeptide. Sensitivity to inhibition by pepstatin suggests a possible distant relationship to the pepsin clan, however, the typical Asp-Xaa-Gly motif is not present, and there is no evidence of an internal duplication.

Scytalidopepsin B Family (U18)

Pepstatin-insensitive peptidases active at low pH values are known from a variety of fungi (*Aspergillus, Scytalidum*) and bacteria (*Xanthomonas, Pseudomonas, Bacillus*). The bacterial enzymes are inhibited by the carboxyl-specific carbodiimides and also by peptide aldehyde tyrostatin (Oda et al., 1989). Unlike enzymes from the pepsin family, these endopeptidases are thermostable. Scytalidopepsin B from *Scytalidium* and aspergillopepsin II (*Aspergillus* protease A) have been sequenced and are found to be homologous. Aspergillopepsin II is a secreted enzyme, synthesized as a precursor. Activation involves not only removal of the 59-residue prepropeptide, but also excision of an internal 11-residue peptide to produce a two-chain molecule. The gene for the protease does not include introns (Inoue et al., 1991).

Leader Peptidase II Family (U11)

Bacterial cell walls contain large quantities of murein lipoprotein. This is a small protein that has N-terminal cysteine substituted on sulfur with the $CH_2(OOCR_1)CH(OOCR_2)CH_2$- group, and the C-terminal lysine is bound to the membrane peptidoglycan (murein) through the ε-amino group. Secretion of the lipoprotein from the cytoplasm is mediated by a leader peptide, which is cleaved by a specialized peptidase of the inner membrane known as leader peptidase II. Leader peptidase II is strongly inhibited by the antibiotic globomycin, but it is also inhibited by pepstatin, which suggests that the enzyme may be an aspartic endopeptidase.

Pseudomonapepsin Family (U25)

Pseudomonapepsin, an acid endopeptidase from *Pseudomonas* species, is not inhibited by the standard inhibitors for the pepsin family, pepstatin, DANLME, or EPNP, but is inhibited by tyrostatin (*N*-isovaleryl-tyrosyl-leucyl-tyrosinal). Pseudomonapepsin is a secreted enzyme, synthesized as a precursor with a signal peptide and a large propeptide, which is autocatalytically activated by cleavage at a Leu-Ala bond (Oda et al., 1994).

Sporulation Sigma Factor Processing Peptidase Family (U4)

Bacilli produce spores under the direction of a protein known as σ (sigma)^E, which switches on the genes necessary for sporulation. The σ factor is produced as a precursor, and the peptidase believed to be responsible for processing it is the product of the *spoIIGA* gene. Because of the presence of an Asp-Ser-Gly motif in the processing peptidase, the enzyme has been assumed to be an aspartic protease. The peptidase is located in the inner membrane and possesses five membrane-spanning domains and large cytoplasmic domain that contain the putative catalytic Asp (Stragier et al., 1988).

Plant Aspartic Proteases

Aspartic proteases produced by plants are mostly confined to seeds and are involved in the processing of storage proteins during ripening and in their degradation during germination (Takahasi, 1995; James, 1998; Shutov and Vaintraub, 1987; Tormakangas et al., 1994; Mutlu et al., 1998; Hiraiwa et al., 1997; Runeberg-Roos

et al., 1994). Aspartic proteases in plant seeds have been purified from barley (Tormakangas et al., 1994), wheat (Belozersky et al., 1989; Bleukx et al., 1998), rice (Asakura et al., 1997, Doi et al., 1980), castor bean (Hiraiwa et al., 1997), and buckwheat (Belozersky et al., 1984) and their enzymatic properties have been investigated. Many plant aspartic proteases are synthesized as the preproform. cDNA cloning of plant aspartic protease's has demonstrated the presence of an insert of approximately 100 amino acids at the C-terminal region that is not found in animal or microbial aspartic proteases. This plant aspartic protease-specific insert (PSI) may thus characterize aspartic proteases of plant origin (Runeberg-Roos et al., 1994; Asakura et al., 1995; Cordeiro et al., 1994; Brodelius et al., 1994; Faro et al., 1999; Schaller and Ryan, 1996; D'Hondt et al., 1997; D'Arcy-Lameta et al., 1996; Verissimo et al., 1996). The phytophysical role of the PSI has been inferred from several findings. Secondary structural analysis of the phytepsin PSI showed it to resemble saposin, which exists in the lysosome, indicating that this PSI may act as a vacuole-targeting signal (Guruprasad et al., 1994). Investigations of the crystal structures of phytepsin (Kervinen et al., 1999) and cardosin A (Frazao et al., 1999) also showed that the PSI should be located in the surface of the molecule, as each of these proAPs binds to the plasma membrane at the PSI site prior to being transported into the vacuole, where the PSI is eventually removed by processing (Kervinen et al., 1999). Cyprosin, an aspartic protease of cardoon, *Pichia pastoris*, is a disulfide-linked dimer lacking PSI, has been expressed extracellularly (White et al., 1999). It has been reported that the PSI-deletion mutant of cyprosin is not processed by itself, which concluded that without the PSI, plant aspartic proteases fail to autolyze from the pro-form to the mature form. Although the function of PSI (Ramalho-Santos et al., 1998) is not completely understood, but it does share considerable sequence identity with sapposins, the group of mammalian sphingolipid activator proteins (Guruprasad et al., 1994; O'Brien et al., 1988). Saposins have been postulated to bind selectively to certain lipids and thus direct the precursor form of the aspartic protease into the appropriate cytomorphological compartment in the plant cell (Guruprasad et al., 1994). Nothing is known of the enzyme(s) responsible in planta, but the excision of each insert is imprecise, resulting in the generation of a complex mixture of heterogenous, mature aspartic protease within the tissues of each of the plants that has been studied, e. g., from seeds of barley (Sarkinnen et al., 1992), pumpkin (Hiraiwa et al., 1997), and *Arabidopsis thaliana* (Mutlu et al., 1998), from rice (Asakura et al., 1997), and from flowers of the cardoon, *Cynara cardunculus* (Ramalho-Santos et al., 1998; Heimgartner et al., 1990; Verissimo et al., 1996). Commonly, the enzymes thus generated are heterodimers with molecular weights in the region of 40, 000-45, 000. These complexity of natural isoforms is compounded even further by the expression of several genes in the plant tissues, each encoding closely related enzymes so that physicochemical and enzymatic characterization of naturally occurring aspartic proteases isolated directly from plants has been made rather difficult.

Families of Peptidases of Unknown Catalytic Mechanism

There are a number of incompletely characterized peptidases that cannot be assigned to any catalytic type yet and show no homology to peptidases of known type. These are listed in Table II.

TABLE I

MEMBERS OF FAMILIES OF ASPARTIC PROTEASES[a]

Family	EC	Database Code	Structure
Family A1: Pepsin			
Aspartic endopeptidase P111	-	PIR JT0398	
Aspartic protease (barley)	-	(X56136)	
Aspartic protease (cattle)	-	(L06151)	
Aspartic protease (*Eimeria*)	-	(Z24676)	
Aspartic protease 3 (yeast)	-	YAP3_YEAST	
Aspergillopepsin I	3.4.23.18	PEPA_ASPAW, (D13894)	
Barrierpepsin (*Saccharomyces*)	-	BAR1_YEAST	
Candidapepsin	3.4.23.24	CAR1_CANAL, CARP_CANTR, CARL_CANPA, (L22358), (X62289)	
Cathepsin D	3.4. 23.5	CATD_*, (M88822), (M95187), (S49650)	*b*
Cathepsin E	3.4. 23.34	CATE_*, (L08418)	
Chymosin	3.4.23.4	CHYM_*	
b			
Endothiapepsin	3.4.23.22	CARP_CRYPA	*b*
Gastricsin	3.4.23.3	PEPC_*	
Mucorpepsin	3.4.23.23	CARP_RHIMI, CARP_RHIPU CAR2_CANAL, CAR2_CANAL, CARR_CANPA	*b*
Penicillopepsin	3.4.23.20	PENP_PENJA	*b*
Pepsin A	3.4.23.1	PEPA_*, PEP1_MACFU, PEP2_MACFU, PEP4_MACFU	
b			
Pepsin F	3.4.23.1	PEPF_RABIT	
Pepsin II	3.4.23.1	PEP1_RABIT, PEP2_RABIT, PEP4_RABIT	
Pepsin III	3.4.23.1	PEP3_RABIT	
Embryonic pepsin (chicken)	-	PEPE_CHICK	
Polyporopepsin	3.4.23.29	CARP_POLTU	
Renin, renal	3.4.23.15	RENI_*	*b*

Renin, submandibular	3.4.23.15	RENS_MOUSE	

TABLE I (*continued*)

Family	EC	Database Code	Structure
Family A1: Pepsin (*continued*)			
Rizopuspepsin	3.4.23.21	CARP_RHICH, CARP_RHINI	*b*
Rizopuspepsin	3.4.23.21	CRP2_RHINI, (D13939)	
Rizopuspepsin	3.4.23.21	CRP3_RHINI	
Rizopuspepsin	3.4.23.21	(X56992)	
Saccharopepsin	3.4.23.25	CARP_SACFI, CARP_YEAST, SAX1_SCHPO, SAX2_SCHPO	
Family A2: Retropepsin			
Retropepsin	3.4.23.16	GAG_AVIMA, GAG_RSVP, POL_BAEVM, POL_BIV06, POL_EIAV, PLO_FIVPE, POL_FLV, POL_GALV, POL_HIV1A, POL_HIV2D, POL_MLVAV, POL_OMVVS, POL_SIVMK, POL_VILV, VPRT_BLV, VPRT_JSRV, VPRT_MPMV, VPRT_MMTVB, VPRT_HTL1A, VPRT_SMRVH, VPRT_SRV1, VPRT_HUMAN	*b*
Family A3: Cauliflower mosaic virus peptidase			
Pararetropepsin endopeptidase	-	POL_CAMVD, POL_CERV, POL_FMVD, POL_SOCMV	
Family U22: *Drosophila* transposon 297 endopeptidase			
Endopeptidase (*Drosophila* transposon 297)	-	POL2_DROME	
Endopeptidase (*Drosophila* transposon 17.6)	-	POL3_DROME	
Endopeptidase (*Drosophila* transposon 412)	-	POL4_DROME	
Retrovirus-related endopeptidase (*Schizosaccharomyces*)	-	(L10324)	

TABLE I (*continued*)

Family	EC	Database Code	Structure
Family U23: *Drosophila* transposon copia endopeptidase			
Endopeptidase (*Drosophila* transposon *copia*)	-	COPI_DROME	
Endopeptidase (tobacco transposon Tnt1)	-	POLX_TOBAC	
Endopeptidase (yeast transposon Ty1-17)	-	YCB9_YEAST	
Family U24: Maize transposon *bs1* endopeptidase			
Endopeptidase (maize transposon *bs1*)	-	POLB_MAIZED	
Family U16: Thermopsin			
Thermopsin	3.4.99.43	THPS_SULAC	
Family U18: Scytalidopepsin			
Scytalidopepsin B	3.4.23.32	PRTB_SCYLI	
Aspergillopepsin	3.4.23.19	PRTA_ASPNG	
Family U25: Pseudomonapepsin			
Pseudomonapepsin	3.4.23.37	(D37970)	
Family U11: Leader peptidase II			
Leader peptidase II	3.4.99.35	LPSA_*	
Family U4: Sporulation sigma^{E} factor Processing peptidase			
Sporulation sigma factor^{E} processing Peptidase (*Bacillus subtilis*)	-	SP2G_*	

[a] EC is the enzyme nomenclature number (Nomenclature Committee of the International Union of Biochemistry and Molecular Biology, "Enzyme Nomenclature 1992," Academic Press, Orlando, Florida, 1992, and supplement); - indicate that no EC number has been assigned. Literature references to the individual proteins are generally to be found in the database entries for which the codes are given.

[b] Structure is included in the Brookhaven database.

TABLE II

MEMBERS OF FAMILIES OF ASPARTIC PROTEASES[a]

Family	EC	Database Code	Structure
Family U7: Endopeptidase IV			
Endopeptidase IV (*Escherichia coli*)	-	SPA_ECOLI, LICA_HAEIN	
Minor capsid protein presursor C (bacteriophage λ)	-	VCAC_LAMBD	
soh B gene product (*E. coli*)	-	(M73320)	
Family U2: Aminopeptidase iap			
Alkaline phosphatase isozyme conversion protein (*E. coli*)	-	IAP_ECOLI	
Family U5: Tail-specific protease			
Tail-specific protease (*E. coli*)	-	(M75634)	
OrfX (*Agmenellum*)	-	(X63049)	
Family U5: Murein endopeptidase			
Penicillin-insensitive murein endopeptidase (*E. coli*)	-	MEPA_ECOLI	
Family U8: Bacterophage murein endopeptidase			
Murein endopeptidase (bacterophage)	-	ENPP_*	
Family U9: Prohead endopeptidase			
Prohead endopeptidase (bacteriophage T4)	-	PCCP_BPT4	
Family U3: Spore endopeptidase			
Spore endopeptidase (*Bacillus*)	-	(M55262), (9124)	
Family U20: γ-D-Glutamyl-L-diamino acid opeptidase II			
γ-D-Glutamyl-L-diamino acid opeptidase II (*Bacillus spaericus*)	-	(X64809)	
Family U26: *Enterococcus* D-Ala-D-Ala carboxypeptidase			
D-Ala-D-Ala carboxypeptidase (*Enterococcus*)	-	(M90647)	
Family U29: Encephalomyelitis virus proteinase 2A			
Proteiase 2A (Theiler's muriene encephalomyletis virus)	-	POLG_TMEVD	
Proteiase 2A (Encephalomyocarditis virus)	-	POLG_EMCV	
Family U27: *Lactococcus* ATP-dependent proteinase			
ATP-dependent proteinase (*Lactococcus*)	-	(X67821)	
Family U28: Aspartyl dipeptidase			
Aspartyl dipeptidase (*Salmonella*)	-	*b*	

[a] See Table I for explanation.

[b] Conlin, C. A., Hakensson, K., Lijas, A., and Miller C. G. (1994) *J. Bacteriol.* **176**, 166.

It is the great diversity and potential for selectivity of proteases that provides the basis for the variety of their actions and different aspects of physiological activity. Proteases are ubiquitous enzymes involved in both specific peptide bond cleavages, for example in processing precursor proteins, and non-specific cleavage. Their activity, if uncontrolled, would be destructive to the cell or organism and must therefore be precisely regulated. The most difficult and arguably most important aspect of protease action is the control of protease activity to limit cleavage to intended substrates without general destruction of functional proteins within and outside otherwise normal tissue. Thus, inhibitors of such proteases are emerging with promising therapeutic uses (Craik et al., 1995; Shaw, 1990; Seife, 1997), in the treatment of diseases such as cancers (Backett et al., 1996; Johnson et al., 1998; Yan et al., 1998), parasitic, fungal, and viral infections (e.g. schistosomiasis, malaria, *C. albicans*, HIV, hepatitis, herpes) (Becker et al., 1995; Brindley et al., 1997; Silva et al., 1996; Li et al., 1994; Abad-Zapatero et al., 1996; Abad-Zapatero et al., 1998; Wlodawer et al., 1993; Darke and Huff, 1994; West and Fairlei, 1995; Kim et al., 1996; Love et al., 1996; Gibson and Hall, 1997; Shieh, 1996), and inflammatory, immunological, respiratory, cardiovascular, and neurodegenerative disorders (Bernstein et al., 1994; Hugli, 1996; Fath et al., 1998; Tanak et al., 1995; Stubbs and Bode, 1993; Vassar et al., 1999).

The elucidation of catalytic mechanism operative in other types of proteases has been facilitated by the ready availability of naturally occurring inhibitors of these enzymes. Indeed inhibitors of serine, cysteine, and metalloproteases are distributed ubiquitously throughout the biological world. In sharp contrast, however, naturally occurring inhibitors of aspartic proteases are relatively uncommon and are found in only certain specialized locations.

Protease Inhibitors

Proteases are responsible either directly or indirectly for all bodily functions including cell growth, differentiation, and death (apoptosis), cell nutrition, intra- and extra-cellular protein turnover (house-keeping and repair), cell migration and invasion, and fertilization and implantation. These functions extend from the cellular level to the organ and organism level to produce cascade systems such as homeostasis and inflammation, and complex processes at all levels of physiology and pathophysiology. Any system that encompasses normal and abnormal bodily functions must have effective regulatory counterparts, i.e. protease inhibitors. Hence, the research interest in protease inhibitors has evoked tremendous attention in many disciplines. Multicellular organisms possess endogenous protein protease inhibitors to control proteolytic activity. Most of these inhibitory proteins are directed against serine proteases, although some are known to target cysteine, aspartyl or metalloproteases (Bode and Huber, 1991). Protease inhibitors have been traditionally developed by natural product screening for lead compounds with subsequent optimization or by empirical substrate-based methods (West and Fairlie, 1995). The optimization involves replacement of the cleavable amide bonds by a noncleavable isostere and optimizing inhibitor potency through trial and error structural modifications that progressively reduce the peptide nature of the molecule. This substrate based drug design has been substantially improved in recent years with the availability of three-dimensional structure information for proteases, permitting receptor-based

design. The structural information about the active site of the receptor (or protease) and selection of designed molecules with the aid of computers has helped to design receptor-based inhibitors. Combinatorial chemistry also presents opportunities both to discover new molecular entities for assaying and to optimize lead structures for development of protease inhibitors.

Inhibitors of Aspartic Protease

As an enzyme family, aspartic proteases are a relatively small group. Nevertheless, they have received enormous interest because of their significant roles in human diseases. The best-known examples are the involvement of renin in hypertension, cathepsin D in metastasis of breast cancer, and the protease of human immunodeficiency virus (HIV) in acquired immune deficiency syndrome (AIDS). Therefore, the new understanding of the structure and function relationships of these enzymes has a direct impact on the design of inhibitor drugs. Moreover, as structure and function are closely related among the aspartic proteases, model enzymes have been particularly informative.

Aspartic proteases are uniquely susceptible to inhibition by pepstatin and by the active site-directed affinity labels, diazoacetyl norleucine methyl ester and EPNP [epoxy-(*p*-nitrophenoxy)propane]. Each of the latter reacts specifically with the side chain carboxyl of a distinct aspartic acid residue to inactivate the enzyme. Together, these residues contribute to the catalytic mechanism and provide the basis for nomenclature for this class of enzyme. Aspartic protease-inhibitor crystal structures are currently available on the PDB database for viral proteases (HIV-1. HIV-2, SIV, FIV), Cathepsin D, renin, renin/chymosin, penicillopepsin, secreted aspartic protease, pepsin, mucoropepsin, retropepsin, saccharopepsin, rhizopuspepsin, and plasmapepsin II.

Aspartic proteases generally bind 6-10 amino acid regions of their polypeptide substrates, which are typically processed, with the aid of two catalytic aspartic acid residues in the active site (James and Sielecki, 1997). Thus, there is usually considerable scope for building inhibitor specificity for a particular aspartic protease by taking advantage of the collective interactions between a putative inhibitor, on both sides of its scissile amide bond, and a substantial portion of the substrate-binding groove of the enzyme. Some aspartic protease also have one or more flaps that close down on top of the inhibitor further adding to inhibitor protease interactions and increasing the basis for selectivity. The general acid-base mechanism that is considered most likely for polypetide hydrolysis catalyzed by aspartic proteases is depicted in the figure 1. The scissile amide bond undergoes nucleophilic attack by a water molecule, which is itself partially activated by deprotonated catalytic aspartic acid residue. The protonated aspartic acid donates a proton to the amide bond nitrogen, generating a zwitterionic intermediate, which collapses to the cleaved products. The water molecule that binds between the enzyme and inhibitor is thought to position a peptide substrate, stretching the peptide bond out of planarity toward a tetrahedral transition state that is stabilized by a second water molecule (Chatfield and Brooks, 1995).

Aspartic protease inhibitors can be grouped under two categories, i) Proteinaceous nhibitors, and ii) Low-molecular weight inhibitors.

i) *Proteinaecous Inhibitors*. In a sharp contrast to the ubiquitous presence of multiple forms of proteinaceous inhibitors of other classes of proteases from different sources of plants, animals and microorganisms, there is a paucity of proteinaceous inhibitors of aspartic proteases. With the exception of macroglobulins, which inhibit proteases of all classes, individual protein inhibitors inhibit only proteases belonging to a single mechanistic class. Protein inhibitors of aspartic proteases are relatively uncommon and are found in only a few specialized locations (Bennet et al., 2000). Few of the examples include renin-binding protein in mammalian kidney (Kay et al., 1983), a 17-kDa inhibitor of pepsin and cathepsin E from the parasite *Ascaris lumbicoides* (Kageyama, 1998), proteins from plants such as potato, tomato, and squash (Kreft et al., 1997; Christiller et al., 1998), and a pluoripotent inhibitor from sea anemone of cysteine protease as well as cathepsin D (Lenarcic and Turk, 1999). There is a report of an 8-kDa polypeptide inhibitor from yeast of the vacuolar aspartic protease (protease A or saccharopepsin) (Saheki et al., 1972).

ii) *Low-Molecular Weight Inhibitors*. In contrast to the proteinaceous nature of the protease inhibitors from plants and animals, the inhibitors produced by microorganisms are of smaller molecular nature. Presence of protease inhibitors in microorganisms came into existence from the studies on antibiotics as they act as inhibitors of enzymes which are involved in growth and multiplication. Extracellular proteolytic enzymes hydrolyze organic nitrogen compounds in the medium and are thought to be harmful to cells. The production of inhibitors of the proteolytic enzymes by microorganisms has probably evolved as a mechanism to provide cell protection. Specific inhibitors of microbial origin have been used as useful tools in biochemical analysis of biological functions and diseases. Polysaccharide sulfates have been reported to be pepsin inhibitors, however, their antipepsin activity is weak, and the effect of such polyanionic compounds is not specific. Pepstatin, a low molecular weight aspartic protease inhibitor, isolated from various species of *Streptomyces*, is a specific inhibitor of pepsin (Morishima et al., 1970; Umezawa et al., 1970). *Streptomyces testacus* was reported to produce various pepstatins that differed from one another in the fatty acid moiety (C_2-C_{10}) (Ayogi et al., 1973). A pepstatin containing an isovaleryl group has been most widely used for biological and biochemical studies. Moreover, as minor components, pepstanone (Miyano et al., 1972), containing (S)-3-amino-5-methylhexane-2-one instead of the C-terminal (3S, 4S)-4-amino-3-hydroxy-6-methylheptanoic acid (AHMHA), and hydroxypepstatin (Umezawa et al., 1973), containing L-serine instead of L-alanine, have also been isolated. Pepstatin containing an acetyl group and propanoyl or isobutyryl groups were isolated from *Streptomyces naniwaensis* (Murao and Satoi, 1970) and *Streptomyces* No. 2907 (Kakinuma and Kanamaru, 1976). Pepstatins, pepstanones, and hydroxypepstatins have almost identical activity against pepsin and cathepsin D. However, Pepstatin is more effective against renin than are pepstanone or hydroxypepstatin (Ayogi et al., 1971; Ayogi et al., 1972) and its potency against renin increases with the increasing numbers of carbon atoms in the fatty acid moiety (Ayogi et al., 1973). Esters of pepstatin, pepstatinal and pepstatinol, possess anti-pepsin activity similar to pepstatins. Several pepstatin analogs have also been synthesized to date. AHMHA and its N-acyl derivative exhibit no potency towards pepsin, however, N-acetyl-valyl-AHMHA is active, and the addition of another valine between the acetyl and valyl groups does not increase their

activity. Addition of L-alanine to the C-terminal group increases the activity about 100 times. This suggests that the acetyl-valyl-AHMHA-L-alanine is the smallest molecular structure that exhibits inhibition against pepsin and cathepsin D similar to pepstatin (Ayogi et al., 1972). Acetyl-L-valyl-L-valyl-[(3S, 4R)-4-amino-3-hydroxy-6-methyl] heptanoic acid prepared by chemical synthesis shows absence of activity (Kinoshita et al., 1973). This suggests that the 4S-configuration of AHMHA is essential for activity. The bacterial enzyme that hydrolyzes the isovaleryl bond in pepstatin has been identified, and from the residual peptide, benzoyl-L-valyl-AHMHA-L-alanyl-AHMHA and L-lactyl-L-valyl-AHMHA-L-alanyl-AHMHA have been synthesized. These analogs are more water-soluble than pepstatin and have almost identical activity against pepsin and cathepsin D, as that of pepstatin. However, these water-soluble analogs have much weaker activity against renin as compared to pepstatin (Matsushita et al., 1975; Tone et al., 1975). The addition of aspartic acid or arginine to the C-terminus of pepstatin increases its water solubility. Such water-soluble analogs have same activity against renin as does pepstatin and also have a hypotensive action. Pepstatin also inhibits carageenin-induced edema and suppresses the generation of Shay rat ulcer. Therapeutic effects on stomach ulcers in man have also been observed. Pepstatin has been reported to be effective against experimental muscle dystrophy and enhances the effect of leupeptin (Chelmicka-Schorr et al., 1978; McGowan et al., 1976). Pepstatin also inhibits leukokinin formation and ascites accumulation in ascites carcinoma of mice (Greenbaum et al., 1975). Pepstatin inhibits the growth of *Plasmodium beghei* (Levy and Chow, 1974; Levy and Chow, 1975), and also inhibits focus formation in murine sarcoma virus (Yuasa et al., 1975.)

HIV-1 Protease Inhibitors

The protease of the human immunodeficiency virus (HIV-1 PR) has proved to be an attractive drug target due to its essential role in the replicative cycle of HIV. Several low molecular weight inhibitors of HIV-1 PR are now used in humans, including saquinavir, ritonavir, indinavir, nelfinavir, and amprenavir. These are the first successful examples of receptors/structure-based designer drugs and were developed using structures of compounds bound in the active site of HIV-1 PR and with the knowledge of inhibitors of other aspartic proteases (e.g. renin) (Kempf and Sham, 1996). All HIV-1 PR inhibitors developed so far target the active site substrate-binding groove of the homodimeric enzyme, a long cylindrical cavity that binds 6-7 amino acids via ionic, van der Waals, or hydrogen bonding interactions (Kempf and Sham, 1996). Two catalytic aspartates in the center of this cavity promote amide bond hydrolysis. Saquinavir became the first protease inhibitor designed from a three-dimensional structure of a protease (structure-based design) to be approved for human use in 1996 (Patick and Potts, 1998; Pakyz and Israel, 1997), despite its low oral bioavailability due to poor absorption and extensive first-pass degradation by cytochrome P450 (Wacher et al., 1998). It is active in cell culture against both HIV-1 and HIV-2 viruses and in combinations with ritonavir, an inhibitor of cytochrome P450 (Kempf et al., 1997), lead to greatly increased plasma concentrations. Ritonavir is itself a potent inhibitor of HIV-1 PR with high oral bioavailability (Lea and Faulds, 1996). Indinavir or Crixivan is another potent inhibitor of HIV-1 and HIV-2 protease, which halts the spread of HIV infection in MT4 lymphoids cells and is orally bioavailable. In humans,

Indinavir is rapidly absorbed in fasting state, there is significant binding to plasma proteins, and the main degradation pathway is via cytochrome P450 (Lacy and Abriola, 1996). The mesylate salt of nelfinavir, approved for human use in 1997, is a lipophilic protease inhibitor with good oral bioavailability in rats and monkeys (Shetty et al., 1996). Ampenavir, is a water-soluble, orally bioavailable inhibitor with long half life, allows less frequent administration of drug thereby having the potential for less side effects with respect to other marketed HIV protease inhibitors described above (Kim et al., 1995; Adkins and Faulds, 1998).

Viral resistance to "monotherapy" with any of these drugs is a significant problem (Erickson, 1995). Serial passages of HIV-1 *in vitro* in the presence of increasing concentrations of a protease inhibitor cause rapid emergence of drug-resistant viral strains of HIV-1 (Patick and Potts, 1998). Thus, new HIV protease inhibitors with different resistance profiles are still being actively pursued. A number of second-generation inhibitors have been developed. ABT -378 was designed to inhibit mutant proteases produced in response to ritonavir. It is 10 fold more potent against ritonavir-resistant strains and displays lower binding to serum proteins. Although, it's oral bioavailability is very poor, when administered with ritonavir the bioavailability was enhanced (Sham et al., 1998). CGP-73547 inhibits indinavir resistant and saquinavir resistant strains of HIV-1, is orally bioavailable (Bold et al., 1998). One of the most promising preclinical candidates for HIV protease inhibition is palinavir. This compound is a very potent, orally active inhibitor of HIV-1 and HIV-2 proteases with high antiviral activity (Lamerre et al., 1997).

Renin Inhibitors

The aspartic protease, renin, is involved in the rate-limiting step of the renin-angiotensin (RAS) system, by hydrolyzing the α_2-globulin angiotensinogen to release the 10-residue peptide angiotensin I. Because of its specificity, renin inhibitors are antihypertensive agents similar in action to ACE inhibitors, and AII antagonists, but are free of some side effects associated with ACE inhibitor administration. For example Zankiren (A-72517), a potent inhibitor of human plasma renin, is the peptidic inhibitor with significant oral absorption (Kleinert et al., 1992). Renin inhibitors have mainly been developed by modifying substrate fragments from the angiotensinogen cleavage site (Rosenberg, 1995), but their clinical progress has been hampered by their peptidic character, which confers low stability and poor oral bioavailability in humans. Another hurdle in the development of renin inhibitors has been the high cost of production, compared with current antihypertensives such as ACE inhibitors and AII receptor antagonists. Renin inhibitors generally need to interact with five subsites (S4-S1') of the enzyme to bind tightly and selectively compared with only three for ACE inhibitors. Consequently, renin inhibitors tend to have higher molecular weight, have more stereo centers, and are thus more expensive to manufacture.

Several renin inhibitors with low molecular weight, less peptidic character, and improved oral bioavailabilty have emerged recently. CP-108 671 was designed from the cleavage site of angiotensinogen and the structure of the general aspartic protease inhibitor pepstatin (Hoover et al., 1995). It uses a cyclohexylnorstatine transition-state analogue, a(*R*)-benzylsuccinate, at P3 for chymotrypsin stability and is a potent inhibitor of human plasma renin. It is highly selective over most aspartic proteases but does weakly inhibit cathepsin D. BILA 2157 BS is another potent renin inhibitor with some selectivity towards cathepsin D and oral

activity (Simoneau et al., 1999). A combination of the X-ray crystal structure of CGP38560 bound renin (Buhlmayer et al., 1988), and previous information (Goschke et al., 1997) that the S3 subsite can be accessed by extending the P1 residue has helped in developing several other nonpeptidic inhibitors with good activity and specificity. These nonpeptidic, low molecular weight compounds represent excellent progress towards the necessary features (oral bioavailability and economic production) for renin-binding drugs but may require improved selectivity.

Plasmepsins Inhibitors

Plasmepsins I and II, found in the malarial parasite *Plasmodium falciparum*, are aspartic proteases that are believed to be essential for the degradation of its major food source, human hemoglobin (Hill et al., 1994; Dame et al., 1994). Inhibition of these enzymes, which have 73% and 35% sequence homology with human cathepsin D, is therefore considered to be a viable therapeutic strategy for the treatment of malaria. Both plasmepepsin I and II are believed to initially cleave the Phe33-Leu34 peptide bond of the α-chain of hemoglobin, followed by cleavage of the polypeptides into smaller fragments which are subsequently processed by the cysteine protease falcipain (Francis et al., 1997). SC-5003, the first peptidomimetic inhibitor reported to selectively inhibit plasmepsin I and II, was active *in vitro* against the live parasite preventing hemoglobin degradation (Francis et al., 1994). X-ray crystallographic structure of plasmepepsin II complexed to pepstatin A have been used to develop peptidic inhibitors which starves the live parasite *in vitro* as well as inhibits human cathepsin D (Silva et al., 1996). Combinatorial synthesis is currently being used to generate inhibitor libraries for these enzymes. All compounds developed to date are potent inhibitors of human cathepsin D, so better selectivity needs to be attained in orally active inhibitors of these enzymes. Interestingly, a combination of cysteine and aspartic protease inhibitors was recently found to be more effective than either compound alone in inhibiting *Plasmodium*-mediated hemoglobin degradation in both culture and a murine malaria model (Semenov et al., 1998). This synergy suggests that combination therapy may be a viable strategy for antimalarial treatment regimes of the future.

Cathepsin D Inhibitors

Human cathepsin D is an intracellular aspartic protease mainly found in lysosomes. It has a number of "house-keeping" functions including degradation of cellular and phagocytosed proteins for reprocessing. The enzymes may be involved in a variety of disease states, including cancer and Alzheimer's disease. Clinical studies have shown that cathepsin D is overexpressed in breast cancer cells, and this seems to be associated with an increased risk of metastasis due to enhanced cell growth (Rochefort and Liaudet-Coopman, 1999). Cathepsin D or a similar aspartic protease is also thought to be involved in formation of β-amyloid peptide in Alzheimer's disease (Papssotiropoulos et al., 1999; Wolfe et al., 1999). The availability of selective and potent inhibitors will help to further define the role of cathepsin D in disease and possibly lead to therapeutic agents.

Relatively few inhibitors of cathepsin D have been reported, partly because of its uncertain role as a viable target for therapeutic intervention. Human cathepsin D was co-crystallized with pepstatin A, and its

structure (Baldwin et al., 1993) has promoted some inhibitor studies. One study suggests that the entropy and solvation effects are key determinants of high affinity for pepstatin-cathepsin D binding (Majer et al., 1997). Although a general inhibitor of aspartic proteases, pepstatin A remains the most potent inhibitor known. There have been reports of cyclic inhibitors designed from the X-ray structures using the fact that the enzyme-bound conformation of the P2 and P3' residues of pepstatin are in close proximity to each other (Silva et al., 1996). This allows cyclization of the inhibitor thereby increasing the proteolytic stability of the three-amide bonds in the cycle. Combinatorial approaches have been carried out for the development of inhibitors to prove the methodology for the optimized specificity against other aspartic proteases.

Secreted Aspartic Protease Inhibitors

The *Candida* yeast strains *C. albicans, C. tropicalis,* and *C. parapsilosis* exist in small quantities in a healthy intestinal tract but become a health problem when the immune system is compromised. Such opportunistic infections arise in AIDS patients where *C. albicans* is a serious pathogen of the mucous membranes (Gruber et al., 1999). It is also the major cause of vaginitis (De Bernardis et al., 1999) and has been implicated in liver toxicity and in development of multiple chemical allergies. *C. tropicalis* is the predominant cause of fungal infections in neutropenic cancer patients. These organisms have the ability to secrete into the host (Naglik et al., 1999) several aspartic proteases (SAP, secreted aspartic protease) of broad specificity. These proteases are thought to be linked to the virulent effects of *Candida* strains in humans as protease-deficient mutants reduce the virulence (Hube et al., 1997; Sanglard et al., 1997). The HIV-1 PR inhibitor indinavir is a weak but specific inhibitor of SAP and greatly reduces the viability and growth of *C. albicans* (Gruber et al., 1999). These enzymes are therefore becoming attractive targets for therapeutic attack. Nine SAPs have been identified in the genome of *C. albicans* to date (SAP1-9) (Monod et al., 1998). From mutation experiments, SAP2 seems to be the dominant isoenzyme for the normal progression of systemic infection, while SAP1 and 3, are also important for overall virulence of *C. albicans* (Naglik et al., 1999). SAP4-6 appears to play a role in the process of induction of SAP2 (Sanglard, D. et al., 1997). X-ray crystal structures have been determined for SAP2 complexed to pepstatin (Cutfield et al., 1995), a close homologue SAP2X bound to the same inhibitor (Abad-Zapetero et al., 1998), and a SAP enzyme of *C. tropicalis* (Symerski et al., 1997).

Very little inhibitor design has been reported for SAP2. A-70450 was originally designed to inhibit renin and later found to be nonselective inhibitor of the SAP of *C. albicans*. This inhibitor incorporates the (*S*)-hydroxylethylene isostere with the hydroxyl group positioned in the crystal structure between two catalytic aspartate residues. Interestingly, the terminal methylpiperazine ring of A-70450 is found in a boat conformation, which occupies the S3 subsite of the enzyme together with the benzyl group of the ketopiperazine ring. The large S3 subsite is not found in other aspartic proteases, and this difference could be exploited to develop selective inhibitors for SAP2 (Abad-Zapetero et al., 1996).

Inhibitor Design and Future Prospects

Most aspartic protease inhibitors that have been developed to date bind to their target enzyme through noncovalent interactions (i.e. hydrogen bonds, ionic or van der Waal's contacts). These compounds are therefore reversible inhibitors of proteases, and effective inhibition relies on the enzyme having greater affinity for the inhibitor than its natural substrate. High affinity for any particular aspartic protease has been achieved by trying to maximize the number of noncovalent interactions that the inhibitor makes with the enzyme. One approach that has proved very successful in this regard is the incorporation of a transition-state isostere into designed inhibitors. A transition-state isostere is defined as a functional group that can mimic the tetrahedral transition-state of amide bond hydrolysis but cannot itself be hydrolyzed by the enzyme. It has been hypothesized that stable structures, which can resemble the transition state of an enzyme reaction, will be bound more tightly than the substrate for the enzyme-catalyzed reaction. Studies on the general aspartic protease inhibitor pepstatin (which incorporates the statine transition-state isostere) suggest that this increased affinity, which can be as great as 10^4-fold, is not only due to mimicry of the transition state of amide bond hydrolysis but also due to the displacement of the catalytic water molecule hydrogen bonded to the catalytic aspartates.

The susceptibility of the individual aspartic proteases to inhibition by these compounds varies considerably. The Ascaris proteins for example are effective inhibitors of human (Abu-Erreish and Peanasky, 1974), pig, and chicken pepsins, pig gastricin, and (rabbit) cathepsin E with a weaker influence on human gastricin and little or no effect of the other aspartic proteases tested. This selectivity of inhibition is also observed with the pepsin inhibitor peptide obtained upon activation of pepsinogen. It has been known that one of the peptides released on activation of (pig) pepsinogen binds to pepsin above pH 4.5 to stabilize the enzyme at higher pH values and to inhibit it. This inhibitor has been identified as the peptide released in the first step in the sequential activation of pig (and cow) pepsinogen(s) and is derived from the first 16/17 residues in the zymogens (Harboe et al., 1984; Dunn et al., 1983). This differential susceptibility to inhibition by naturally occurring compounds persists into what is perhaps the best-known category, the pepstatins. Members of this protease family, *e.g.* renin, pepsin, cathepsin D, and human immunodeficiency virus-protease are generally typecast on basis of their susceptibility to inhibition by acetylated pentapeptides, isovaleryl- and acetyl-pepstatin. However, the two most recently identified human aspartic proteases, *b*-site Alzheimer's precursor protein cleavage enzyme and *b*-site Alzheimer's precursor protein cleavage enzyme 2 (Dunn et al., 1983; Vassar et al., 1999), are not inhibited by this classical type of inhibitor of this family of enzymes. On the basis of these observations with naturally-occurring inhibitors, it would seem to be possible to design synthetic counterparts that should be specific for individual enzymes. The rationale behind such inhibitors has been to synthesize a peptide of an appropriate length and containing the amino acid residues known to be present in the naturally occurring substrate for the enzyme but with the introduction of statine in place of the two residues contributing to the scissile bond of the substrate. Such an approach has led to the synthesis of highly potent inhibitors of human renin (Boger et al., 1983) and calf chymosin (Powell et al., 1984).

An analogous yet different strategy where a chemical modification of the scissile peptide bond is used to introduce a non-hydrolyzable analogue of the tetrahedral transition-state formed during hydrolysis was also reported (Szelke et al., 1982). Instead of using the naturally-occurring statine residues as the centerpiece around which the inhibitor is constructed, the complete amino acid sequence of the substrate is retained in the inhibitor except that the scissile peptide bond between P_1- P_1' of the substrate is replaced by the non-hydrolyzable analogue of the transition state. Using this approach, a tight-binding inhibitor of human renin has been developed which is a synthetic analogue based on the sequence of residues known to occur on either side of the scissile peptide bond of the angiotensinogen but with a reduced -CH_2-NH- isostere in place of the -CONH- of the substrate.

It is also possible, of course, to device such inhibitors not on the sequence of residues found in naturally-occurring protein substrates but based on synthetic peptides that are known to be good substrates for certain enzymes. It would thus appear that while naturally occurring inhibitors of aspartic proteases may have little physiological significance in regulating their target enzymes *in vivo*, nevertheless such compounds and their synthetic counterparts have probed of inestimable value in facilitating distinction among the different types of aspartic proteases. Such inhibitors can be utilized for diagnostic purposes to establish the nature of a "newly-isolated" protease. As an illustration of this, consider inhibition of human pepsin and gastricin by isovaleryl and lactyl-pepstatin. While considerable progress has been made with the structure, activity, and importance (biological and commercial) of the aspartic proteases (Acid protease 1997), much remains to be learned about the distinctions of the various architecture and how these are reflected in the functions of the various enzymes. Inhibitors (naturally occurring and synthetic) have permitted detailed biochemical and crystallographic investigations to be made but an understanding of the selectivity of such inhibitors may be of just as much importance for the design and synthesis of specific inhibitors for use therapeutically in controlling individual aspartic proteases.

Present Investigation

The present work details various aspects of aspartic proteases and their inhibition. The findings of the investigations have been presented in the following seven chapters:

1. General introduction.
2. Purification and characterization of an aspartic protease inhibitor, ATBI, from an extremophilic *Bacillus* sp.
3. Interaction of ATBI with HIV-1 protease, implications in the mechanism of inactivation.
4. Structural and mechanistic insight into the inhibition of aspartic proteases by ATBI.
5. Bifunctional role of ATBI, implications in fungal growth inhibition.
6. Unfolding and chaperone mediated refolding of the aspartic proteases.
7. Interaction of aspartic protease with lipid and gold nanoparticles.

References

Abad-Zapetero, C., Goldman, R., Muchmore, S. W., Hutchins, C., Oie, T., Stewart, K., Cutfield, S. M., Cutfield, J. F., Foundling, S. I., and Ray, T. L. (1998) *Adv. Exp. Med. Biol.* **436**, 297-313.

Abad-Zapetero, C., Goldman, R., Muchmore, S. W., Hutchins, C., Stewart, K., Navaza, J., Payne, C. D., and Ray, T. L. (1996) *Protein Sci*. **5**, 640-652.

Abu-Erreish, G. M., and Peanasky, R. J. (1974) *J. Biol. Chem.* **249**, 1566-1578.

Adams, S. E., Mellor, J., Gull, K., Sim, R. B., Tuite, M. F., Kindsman, S. M., and Kingsman, A. J. (1987) *Cell* **49**, 111-119.

Adkins, J. C., and Faulds, D. (1998) *Drugs* **55**, 837-842.

Asakura, T., Watanabe, H., Abe, K., and Arai, S. (1995) *Eur. J. Biochem.* **232**, 77-83.

Asakura, T., Watanabe, H., Abe, K., and Arai, S. (1997) *J. Agril. Food Chem.* **45**, 1070-1075.

Ayogi, T., Kunimoto, S., Morishima, H., Takeuchi, T., and Umezawa, H. (1971) *J. Antibiot.* **24**, 687-694.

Ayogi, T., Morishima, H., Nishizawa, R., Kunimoto, S., Takeuchi, T., and Umezawa, H. (1972) *J. Antibiot.* **25**, 689-694.

Ayogi, T., Yagisawa, Y., Kumagai, M., Hamada, M., Morishima, H., Takeuchi, T., and Umezawa, H. (1973) *J. Antibiot.* **26**, 539-541.

Babine, R. E., and Bender, S. L. (1997) *Chem. Rev.* **97**, 1359-1472.

Backett, R. P., Davidson, A. H., Drummond, A. H., and Whittaker, M. (1996) *Drug Discov. Today* **1**, 16-26.

Baldwin, E. T., Baht, T. N., Gulnik, S., Hosur, M. V., Sowder, R. C. D., Cachau, R. E., Collins, J., Silvam A. M., and Erickson, J. W. (1993) *Proc. Natl. Acad. Sci. U.S.A.* **90**, 6796-6800.

Barett, A. J., Rawlings, N. D., and Woessner, J. F. (1998) *"Handbook of Proteolytic Enzymes"* Academic Press Inc., London.

Becker, M. M., Harrop, S. A., Dalton, J. P., Kalina, B. H., McMansu, D. P., and Brindley, P. J. (1995) *J. Biol. Chem.* **270**, 24496-501.

Belozersky, M. A., Dunaevsky, Y. E., Rudenskaya, G. N., and Stepanov, V. M. (1984) *Biokhimiya* **49**, 479-485.

Belozersky, M. A., Sarbakanova, S. T., and Dunaevsky, Y. E. (1989) *Planta* **177**, 321-326.

Bennet, B. D., Babu-Khan, S., Leoloff, R., Louis, J.-C., Curran, E., Citron, M., and Vassar, R. (2000) *J. Biol. Chem.*, **275**, 20647-20651.

Bernstein, P. R., Edwards, P. D., and Williams, J. C. (1994) *Prog. Med. Chem.* **31**, 59-120.

Bleukx, W., Brijs, K., Torrenkens, S., Van Leuven, F., and Arsene Delcour, J. A. (1998) *Biochim. Biophys. Acta* **1387**, 317-324.

Blundell, T. L., Cooper, J. B., Sali, A., and Zhu, Z. (1991) in *"Structure and Function of the Aspartic Proteases"* (B. N. Dunn, Eds.), pp 443, Plenum, New York.

Bode W., and Huber R. (1991) *Curr. Opin. Struct. Biol.* **1**, 45-52.

Boger, G. S., Lohr, N. S., Ulm, E. H., Poe, M., Blaine, E. H., Fanelli, G. M., Lin, T.-Y., Payne, L.-S., Schorn, T. W., Lamont, B. I., Vassil, T. C., Stabilito, I. I., Veber, D. F., Rich, D. H., and Bopari, A. S. (1983) *Nature* **303**, 83-86.

Bold, G., Faessler, A., Capraro, H.-G., Cozens, R., Klimkait, T., Lazdins, J., Mestan, J., Poncioni, B., Roesel, J., Stover, D., Tintelnot-Blomley, M., Acemoglu, F., Beck, W., Boss, E., Eschbach, M., Huerlimann, T., Masso, E., Roussel, S., Ucci-Stoll, K., Wyss, D., and Lang, M. (1998) *J. Med. Chem.* **41**, 3387-3401.

Brindley, P. J., Kalinna, B. H., Dalton, J. P., Day, S. R., Wong, J. W., Smythe, M. L., and McManus, D. P. (1997) *Mol. Biochem. Parasitol.* **89**, 1-9.

Brodelius, P. E., Cordeiro, M., Mercke, P., Domingos, A., Clements, A., and Paris, M. S. (1994) *Adv. Exp. Med. Biol.* **436**, 435-439.

Buhlmayer, P., Caselli, A., Furher, W., Goshke, R., Rasett, V., Reuger, H., Stanton, J. L., Criscione, L., and Wood, J. M. (1988) *J. Med. Chem.* **31**, 1839-1846.

Chatfield, D. C., and Brooks, B. R. (1995) *J. Am. Chem. Soc.* **117**, 5561-5572.

Christeller, J. T., Rafley, P. C., Ramsey, R. J., Sullivan, P. A., and Laing, W. A. (1998) *Eur. J. Biochem.* **254,** 160-167**.**

Cooper, J. B., Foundling, S. I., Blundell, T. L., Boger, J., Jupp, R. A., and Kay, J. (1989) *Biochemistry* **28**, 8596-8603.

Cordeiro, M. C., Xue, Z.-T., Pietrzak, M., Pais, M. S., and Brodelius, P. E. (1994) *Plant Mol. Biol.* **24**, 733-741.

Craik, M. S., and Debouck, C. (1995) In *"Perspectives in Drug Discovery and Design"* (McKerrow, J. H., and James, M. N. G., Eds.), ESCOM, Leiden, Vol 2, pp1-125.

Cutfield, S. M., Dodson, E. J., Anderson, B. F., Moody, P. C., Marshall, C. J., Sullivan, P. A., and Cutfield, J. F. (1995) *Structure* **3**, 1261-1271.

D'Arcy-Lameta, A., Zuily-Fodil, Y., Pham Thi, A. T., and Ferrari-Iliou, R. (1996) *Vigna unguiculata* aspartic proteinase mRNA. Complete cds, accession no. U61396.

D'Hondt, K., Stack, S., Gutterridge, S., Vandekerckhove, J., Krebbers, E., and Gal, S. (1997) *Plant Mol. Biol.* **33**, 187-192.

Dame, J., Berry, C., Dunn, B. M., and Kay, J. (1994) *Mol. Biochem. Parasitol.* **64**, 177-190.

Darke, P. L., and Huff, J. L. (1994) *Adv. Pharmacol. (San Diego)* **5**, 399-454.

De Bernardis, F., Arancia, S., Morelli, L., Hube, B., Sanglard, D., Schafer, W., and Cassone, A. (1999) *J. Infect. Dis.* **179**, 201-208.

Doi, E., Shibata, D., Mataba, T., and Yonezawa, D. (1980) *Agric. Biol. Chem.* **44**, 741-747.

Dunn, B. M. (1992) In *"Advances in Detailed Reaction Mechanisms"* (Coxon, J. Eds.), Vol. 2, JA1 Press, Greenwich, Connecticut, pp 213-241.

Dunn, B. M., Scarborough, P. E., Lowther, W. T., and Rao-Naik, C. (1995) In *"Aspartic Proteinases"* (Takahashi, K. Eds.), Plenum Press, pp 1-9.

Dunn, B., Lewwitt, M., and Pham. C. (1983) *Biochem. J.* **209**, 355-362.

Erickson, J. W. (1995) *Nature Struct. Biol.* **2**, 523-529.

Faro, C., Ramalho-Santos, M., Vieira, M., Mendes, A., Simoes, I., Andade, R., Verissimo, P., Lin, X., Tang, J., and Pires, E. (1999) *J. Biol. Chem.* **274**, 28724-28729.

Fath, M. A., Wu, X., Hileman, R. E., Linhardt, R. J., Kashem, M. A., Nelson, R. M., Wright, C. D., and Abraham, W. M. (1998) *J. Biol. Chem.* **273**, 13563-13569.

Fitzgerald, P. M. D., McKeever, B. M., VanMiddlesworth, J. F., Springer, J. P., Heimbach, J. C., Leu, C. T., Herber, W. K., Dixon, R. A. F., and Darke, P. L. (1990) *J. Biol. Chem.* **265**, 142009-142019.

Francis, S. E., Gluzman, I. Y., Oksman, A., Knickerboker, A., Lueller, R., Bryant, M. L., Sherman, D. R., Russell, D. G., and Goldberg, D. E. (1994) *EMBO J.* **13**, 306-317.

Francis, S. E., Sullivan, D. J. Jr., and Goldberg, D. E. (1997) *Annu. Rev. Microbiol.* **51**, 97-123.

Frazao, C., Bento, I., Costa, J., Soares, C. M., Verissimo, P., Faro, C., Pires, E., Cooper, J., and Carrondo, M. A. (1999) *J. Biol. Chem.* **274**, 27694-27701.

Fuetterer, J., and Hohn, T. (1987) *Trends Biochem. Sci.* **12**, 92-95.

Garfinkel, D. J., Hedge, A. M., Youngren, S. D., and Copeland, T. D. (1991) *J. Virol.* **65**, 4573-4581.

Gibson, W., and Hall, M. R. (1997) *Drug Des. Discov.* **15**, 39-47.

Goeschke, R., Cohen, N. C., Wood, J. M., and Mailaum, J. (1997) *Bioorg. Med. Chem. Lett.* **7**, 2735-2740.

Greenbaum, L. M., Grebow, P., Johnston, M., Prekash, A., and Semente, G. (1975) *Cancer Res.* **35**, 706-710.

Gruber, A., Speth, C., Lukasser-vogl, E. Zangerle, R. Borg-von Zopelin, M., and Dierich, M. P. (1999) *Immunopharmacology* **41**, 227-234.

Guruprasad, K., Tormakangas, K., Kervinen, J., and Blundell, T. L. (1994) *FEBS Lett.* **352**, 131-136.

Harboe, M., Andersen, P. M., Foltman, B., Kay, J., and Kassell, B. (1984) *J. Biol. Chem.* **249**, 4487-4494.

Heimgartner, U., Piertrzak, M., Geertsen, R., Brodelius, P. E., da Silva Figueirdo, A. C., and Pais, M. S. S. (1990) *Phytochemistry* **29**, 1405-1410.

Hellen, C. U. T. and Wimmer, E. (1992) *Experntia* **48**, 201-205.

Hill, J., and Phylip, L. H. (1997) *FEBS Lett.* **409**, 357-360.

Hill, J., Tyas, L., Phylip, L. H., Kay, J., Dunn, B. M., and Berry, C. (1994) *FEBS Letts.* **352**, 155-158.

Hiraiwa, N., Kondo, M., Nishimura, M., and Hara-Nishimura, I. (1997) *Eur. J. Biochem.* **246**, 133-141.

Holm, I., Ollo, R., Panthier, J. J., and Rougeon, F. (1984) *EMBO J.* **3**, 557-562.

Hoover, D. J., Lefker, B. A., Rosati R, L., Westerm R. T., Kleinman, E. F., Bindram J, S., Holt, W. F., Murphy, W. R., Mangiapane, M. L. Hockel, G. M., et al. (1995) *Adv. Exp. Med. Biol.* **362**, 167-180.

Hube, B., Sanglard, D., Odds, F. C., Hess, D., Monod, M., Schafer, W., Brown, A. J. P., and Gow, N. A. R. (1997) *Infect. Immun.* **65**, 3529-3538.

Hugli, T. E. (1996) *Trends Biotechnol.* **14**, 409-412.

Inoue, H., Kimura, T., Makabe, O., and Takahashi, K. (1991) *J. Biol. Chem.* **266**, 19484-19489.

Inouye, S., Yuki, S., and Saigo, K. (1986) *Eur. J. Biochem.* **154**, 417-425.

James, M. N. G. (1998) *Aspartic Proteinases*. Plenum Press. New York and London.

James, M. N. G. (1998) In *"Structure and Function of Aspartic Protease: Retroviral and Cellular Enzymes"* Plenum Press, New York, pp 1-481.

James, M. N. G., and Sielecki, A. R. (1987) In *"Biological macromolecules and assemblies: Active sites of enzymes"* (Jurnak, F. A., McPherson, A., Eds.), John Wiley & Sons, New York, Vol. 3, p-413.

Johns, M. A., Babcock, M. S., Fuerstenberg, S. M., Fuerstenberg, S. I., Freeling, M., and Simpson, R. B. (1989) *Plant Mol. Biol.***12**, 633-642.

Johnson, L. L., Dyer, R., and Hupe, D. J. (1998) *Curr. Opin. Chem. Biol.* **2**, 466-71.

Kageyama, T. (1995) *Meth. Enzymol.* **248**, 120-136.

Kageyama, T. (1998) *Eur. J. Biochem.* **253**, 804-809.

Kakinuma, A., and Kanamaru, T. (1976) *J. Takeda Res. Lab.* **35**, 123-127.

Kay, J. (1985) In *"Aspartic Proteases and Their Inhibitors"* (Kostka, V. ed.) Walter de Gruyter, Berlin pp 1-17.

Kay, J., Valler, M. J., and Dunn, B. N. (1983) In *"Protease Inhibitors Medical and Biological Aspects"* (Katunuma, N., Umezawa, H., and Holzer, H., Eds.), pp 201-210, Japan Scientific Societies Press, Tokyo.

Kempf, D. J., and Sham, H. L. (1996) *Curr. Pharm. Des.* **2**, 225-246.

Kempf, D. J., Marsh, K. C., Kumar, G., Rodrigues, A. D., Denissen, J. F., McDonald, E., Kukulka, M. J., Hsu, A., Granneman, G. R., Baroldi, P. A., Sun, E., Pizzuti, D., Plattner, J. J., Norbeck, D. W., and Leonard, J. M. (1997) *Antimicrob. Agents Chemother.* **41**, 654-660.

Kervinen, J., Tobin, G. J., Costa, J., Waugh, D. S., Wlodawer, A., and Zdanov, A. (1999) *EMBO J.* **18**, 3947-3955.

Kim, E. E., Baker, C. T., Dwyer, M. D., Murcko, M. A., Rao, B. G., Tung, R. D., and Navia, M. A. (1995) *J. Am. Chem. Soc.* **117**, 1181-1182.

Kim, J. L., Morgenstern, K. A., Lin, C., Fox, T., Dwyer, M. D., Landro, J. A., Chambers, S. P., Markland, W., Lepre, C. A., O'Malley, E. T., Harbeson, S. L., Rice, C. M., Mureko, M. A., Caron, P. R., and Thomson, J. A. (1996) *Cell* **87**, 343-355.

Kinoshita, M., Aburaki, S., Hagiwara, A., and Imai, J. (1973) *J. Antibiot.* **26**, 249-251.

Kleinert, H. D., Stein, H. H., Boyd, S., Fung, A. K., Baker, W. R., Verburg, K. M., Polakowski, J. S., Kovar, P., Barlow, J., Cohen, J. et al. (1992) *Hypertension* **20**, 768-775.

Kreft, S., Ravnikar, M., Mesko, P., Pungercar, J., Umek, A., Kregar, I., and Strukelj, B. (1997) *Phytochemistry*, **44**, 1001-1006.

Lacy, M. K., and Abriola, K. P. (1996) *Conn. Med.* **60**, 723-737.

Lamarre, D., Croteau, G., Wardrop, E., Bourgon, L., Thibeault, D., Clouette, C., Vaillancourt, M., Cohen, E. Pargellis, C., Yoakim, C., and Anderson, P. C. (1997) *Antimicrob. Agents Chemother.* **41**, 965-971.

Lea, A. P., and Faulds, D. (1996) *Drugs* **52**, 541-546.

Lenarcic, B., and Turk, V. (1999) *J. Biol. Chem.***274**, 563-566.

Levy, M. R., and Chow, S. C. (1974) *Biochim. Biophys. Acta.* **334**, 423-430.

Levy, M. R., and Chow, S. C. (1975) *Experintia* **31**, 52-54.

Li, Z., Chen, X., Davidson, E., Zwang, O., Mendis, C., Ring, C. S., Roush, W. R., Fegley, G., Li, R., Rosenthal, P. J., et al. (1994) *Chem. Biol.* 1, 31-7.

Love, R. A., Parge, H. E., Wickersham, J. A., Hostomsky, Z., Habuks, M., Moomaw, E. W., Adachi, T., and Hostomska, Z. (1996) *Cell* **87**, 331-342.

Mackay, V. L., Welch, S. K., Insley, M. Y., Manney, T. R., Holly, J., Saari, G. C., and Parker, M. L. (1988) *Proc. Natl. Acad. Sci. U. S. A.* **85**, 55-58.

Majer, P., Collings, J. R., Gulnik, S. V., and Erikson, J. W. (1997) *Protein Sci.* **6**, 1458-1466.

Matsushita, Y., Tone, H., Hori, S., Yagi, Y., Tamamatsu, A., Morishima, H., Ayogi, T., Takeuchi, T., and Umezawa, H. (1975) *J. Antibiot.* **28**, 1016-1018.

McGowan, E. B., Shafiq, S. A., and Stracher, A. (1976) *Exp. Neurol.* **50**, 649-657.

Menon, A. S., and Goldberg, A. L. (1987) *J. Biol. Chem.* **262**, 14929-14934.

Miller, M., Jaskolski, M., Rao, J. K. M., Leis, J., and Wlodawer, A. (1989) *Nature (London)* **337**, 576-578.

Miyano, T., Tomiyasu, M., Iizuka, H., Tomisaka, S., Takita, T., Ayogi, T., and Umezawa, H. (1972) *J. Antibiot.* **25**, 489-491.

Monod, M., Hube, B., Hess, D., and Sanglard, D. (1998) *Microbiology* **144**, 2731-2377.

Morishima, H., Takita, T. Ayogi, T., Takeuchi, T., and Umezawa, H. (1970) *J. Antibiot.* **23**, 263-265.

Murao, S., and Satoi, S. (1970) *Agric. Boil. Chem.* **34**, 1265-1267.

Mutlu, A., Pfeil, J. E., and Gal, S. (1998) *Phytochemistry* **47**, 1453-1459.

Naglik, J. R., Newport, G., White, T. C., Fernandes-Naglik, L. L., Greenspan, J. S., Greenspan, D., Challacomber, S. J., and Agabian, N. (1999) *Infect. Immun.* **67**, 2482-2490.

O'Brien, J. S., Kertz, K. A., Dewji, N., Wenger, D. A., Esch, F., and Fluharty, A. L. (1988) *Science* **241**, 1098-1101.

Oda, K., Fukuda, Y., Murao, S., Uchida, K., and Kainosho, M. (1989) *Agric. Biol. Chem.* **53**, 405-415.

Oda, K., Takahashi, T., Tokuda, Y., Shibano, Y., and Takahashi, S. (1994) *J. Biol. Chem.* **269**, 26518-26524.

Pakyz, A., and Israel, D. (1997) *J. Am. Pharm. Assoc. (Washington)* **NS37**, 543-551.

Papssotiropoulos, A., Bagli, M., Feder, O., Jessen, F., Maier, W., Rao, M. L., Ludwig, M., Schwab, S. G., and Heun, R. (1999) *Neurosci. Lett.* **262**, 171-174.

Patick, A. K., and Potts K. E. (1998) *Clin. Microbiol. Rev.* **11**, 614-627.

Powell, M. J., Holdsworth, R. J., Baker, T. S., Titmas, R. C., Bose, C. C., Phipps, A., Eaton, M., Rolph, C. E., Valler, M. J., Kay, J. (1984) in *"Aspartic Proteases and their Inhibitors"* pp 479-483.

Ramalho-Santos, M., Verissimo, P., Cortes, L., Samyn, B., van Beeumen, J., Pires, E., and Faro, C. (1998) *Eur. J. Biochem.* **255**, 133-138.

Rao-Naik, C., Guruprasad, K., Batley, B., Rapundalo, S., Hill, J., Blundell, T., Kay, J., and Dunn, B. N. (1995) *Proteins Struct. Funct. Genet.* **22**, 168-181.

Reid, W. A., Vongsorasak, L., Svasti, J., Valler, M. J., and Kay, J. (1984) *Cell Tissue Res.* **236**, 597-600.

Rich D. H. (1985) *J. Med. Chem.* **28**, 263-273.

Rochefort, H., and Liaudet-Coopman, E. (1999) *APMIS* **107**, 86-95.

Rosenberg, S. H. (1995) In *"Progress in Medicinal Chemistry"* (Ellis G. P., Loscombe, D. K., Eds.), Elsevier Science, New York, Vol.32, pp 37-115.

Runeberg-Roos, P., Kervinen, J., Kovaleva, V., Rakhel, N. V., and Gal, S. (1994) *Plant Physiol.* **105**, 321-329.

Runeberg-Roos, P., Tormakangas, K., and Ostman, A. (1991) *Eur. J. Biochem.* **202**, 1021-1027.

Saftig, P., Hetman, M., Schmahl, W., Weber, W., Heine, L., Mossman, H., Kostere, A., Hess, B., Evers, M., von Figura, K., and Peters, C. (1995) *EMBO J.* **14**, 3599-3608.

Saheki, T., Matsuda, Y., and Holzer, H. (1972) *Eur. J. Biochem.* **47**, 325-327.

Sanglard, D., Hube, B., Monod, M., Odds, F. C., and Gow, N. A. A. (1997) *Infect. Immun.* **65**, 3539-3546.

Sarkinnen, P., Kalkkinen, N., Tigmann, C., Siuro, J., Kervinen, J., and Mikola, L. (1992) *Planta* **186**, 317-323.

Schaller, A., and Ryan, C. A. (1996) *Plant. Mol. Biol.* **31**, 1073-1077.

Seife, C. (1997) *Science* **277**, 1602-11603.

Semenov, A., Olson, J. E., and Rosenthal, P. J. (1998) *Antimicrob. Agents Chemother.* **42**, 2254-2258.

Sham, H. L., Kempf, D. L., Molla, A., Marsh, K. C., Kumar, G. N., Chen, C.-M., Kati, W., Stewart, K., Lal, R., Hsu, A., et al., (1998) *Antimicrob. Agents Chemother.* **42**, 3218-3224.

Shaw, W. (1990) *Adv. Enzymol. Relat. Areas Mol. Biol.* **63**, 271-347.

Shetty, B. V., Kosa, M. B., Khalil, D. A., and Webber, S. (1996) *Antimicrob. Agents Chemother.* **40**, 110-114.

Shieh, S. H., Kurumbail, R. G., Stevens, A. M., Stegeman, R. A., Sturman, E. J., Pak, J. Y., Witwer, A., J., Palmier, M. O., Weigand, R. C., Holwerda, B. C., and Stallings, W. C. (1996) *Nature* **383**, 279-282.

Shutov, A. D., and Vaintraub, I. A. (1987) *Biochemistry* **26**, 1557-1566.

Sielecki, R., Fujinanga, M., Read, R. J., and James, M. N. G. (1991) *J. Mol. Biol.* **219**, 671-692.

Silva, A. M., Lee, A. Y., Gulnik, S. V., Maier, P., Collins, J., Bhat, T. N., Collins, P. J., Cachau, R. E., Luker, K. E., Gluzman, I. Y., Francis, S. E., Oksman, A., Goldberg, D. E., and Erickson, J. (1996) *Proc. Natl. Acad. Sci. U.S.A* **93**, 10034-10039.

Simoneau, B., Lavallee, P., Anderson, P. C., Bailey, M., Bantle, G., Berthiaume, S., Chabot, C., Fazal, G., Halmos, T., Ogilvie, W. W., Poupart, M. A., Thavonekham, B., Xin, Z., Thibeault, D., Bolger, G., Panzenbeck, M., Winquist, R., and Jung, G. L. (1999) *Bioorg. Med. Chem.* **7**, 489-508.

Stragier, P., Bonamy, C., and Karmazyn-Campelli, C. (1988) *Cell* **52**, 697-704.

Stubbs, M. T., and Bode, W. (1993) *Thromb. Res.* **69**, 1-53.

Symersky, J. Monod, M., and Foundling, S. I. (1997) *Biochemistry* **36**, 12700-12710.

Szelke, M., Leckie, B., Hallet, A., Jones, D. M., Sueiras, J.. Atrash, B., and Lever, A. F. (1982) *Nature* **299**, 555-557.

Takahasi, K. (1995) In *"Function, Biology, and Biomedical Implications"* Plenum Press. New York and London.

Tanak, R. D., Clark, J. M., Warne, R. L., Abraham, W. M., and Moore, W. R. (1995) *Int. Arch. Allergy Immunol.* **107**, 408-409.

Tang, J. (1977) In *"Acid Proteases, Structure, Function, and Biology*" New York: Plenum Press.

Tang, J. (1979) *Mol. Cell Biochem.* **26**, 93-109.

Tone, H., Matsushita, Y., Yagi, Y., and Tamamatsu, A. (1975) *J. Antibiot.* **28**, 1012-1045.

Tormakangas, K., Kervinen, J., Ostman, A., and Teeri, T. (1994) *Plant* **195**, 116-125.

Torruella, M., Gordon, K., and Hohn, T. (1989) *EMBO J.* **8**, 2819-2825.

Umezawa, H., Ayogi, T., Morishima, H., Matsuzaki, M., Hamada, M., and Takeuchi, T. (1970) *J. Antibiot.* **23**, 259-262.

Umezawa, H., Miyano, T., Murakami, T., Takita, T., Ayogi, T., Takeuchi, T., Naganawa, H., and Morishima, H. (1973) *J. Antibiot.* **27**, 615-617.

Vassar, R., Bennet, B. D., Babu-Khan, S., Kahn, S., Mendiaz, E. A., Denis, P., Teplow, B. D., Ross, S., Amarante, P., Leoloff, R., Luo, Y., Fisher, S., Fuller, J., Edenson, S., Lile, J., Jaronsinski, M. A., Biere, A. L., Curran, E., Burgess, T., Louis, J.-C., Collins, F., Treanor, J., Roger, G., and Citron, M., (1999) *Science* **286**, 735-741.

Verissimo, P., Faro, C., Moir, A. J. G., Lin, Y., Tang, J., and Pires, E. (1996) *Eur. J. Biochem.* **235**, 762-768.

Wacher, V. J., Silverman, J. A., Zhang, Y., and Benet, L. Z. (1998) *J. Pharm. Sci.* **87**, 1322-30.

West, M. L., and Fairlei, D. P. (1995) *Trends Pharmacol. Sci* .**16**, 67-75.

White, P. C., Cordeiro, M. C., Arnold, D., Brodelius, P. E., and Kay, J. (1999) *J. Biol. Chem.* **274**, 16685-16693.

Wilimowska-Pelc, A., Polanowski, A., Kolaczkowska, M. K., Wieczorek, M., and Wilusz, T. (1983) *Acta Biochim. Pol.* **30**, 23-31.

Wlodawer, A., and Erickson, J. W. (1993) *Annu. Rev. Biochem.* **62**, 543-585.

Wolfe, M. S., Xia, W., Moore, C. L., Leatherwood, D. D., Ostaszewski, B., Rahmati, T., Donker, I. O., and Selkoe, D. J. (1999) *Biochemistry* **38**, 4720-4727.

Yan, S., Sameni, M., and Sloane, B. F. *Biol. Chem.* 1998, 379, 113-23.

Yoshika, K., Honma, H., Zushi, M., Kondo, S., Togashi, S., Miyake, T., and Shiba, T. (1990) *EMBO J.* **9**, 535-541.

Yuasa, Y., Shimojo, H., Ayogi, T., and Umezawa, H. (1975) *J. Natl. Cancer Inst.* **54**, 1255-1256.

Chapter 2

Purification and Characterization of an Aspartic Protease Inhibitor, ATBI, from an Extremophilic *Bacillus* sp.

Summary

The indispensable nature of the aspartic proteases in numerous physiological functions has evoked tremendous response towards isolating new inhibitors from various resources. After extensive screening, we have isolated an extremophilic *Bacillus* sp., which produces an aspartic protease inhibitor (ATBI). Maximum production of ATBI was observed after 48 h after the commencement of the fermentation. The production of ATBI was optimized in terms of the carbon, nitrogen sources, and amino acids. Presence of glucose, soyameal and beef extract, and arginine in the fermentation medium induced the production of ATBI substantially. ATBI was purified from the extracellular culture filtrate by the treatment of activated charcoal and ultra filtration. The resulting filtrate was concentrated by lyophilization and the concentrated inhibitor sample was further purified by reverse phase-HPLC. The fractions collected were tested for their aspartic protease inhibitory activity by using pepsin as the representative enzyme. The active fractions were further purified by rp-HPLC. Homogeneity of the active fractions was indicated by the single peak as analyzed on rp-HPLC. The purified ATBI showed a single band on an analytical iso-electric focusing gel with a pI of 10.0. The amino acid composition data revealed the abundance of Asp residues. The amino acid sequence of the purified inhibitor determined by a protein sequencer was Ala-Gly-Lys-Lys-Asp-Asp-Asp-Asp-Pro-Pro-Glu. The predominance of the charged amino acid residues in the inhibitor sequence indicated its hydrophilic nature and the net charge per molecule calculations from the amino acid composition was negative indicating that ATBI is an anionic peptide. The molecular mass (M_r) of ATBI as determined from ES-MS was 1147 Da. The stability of the inhibitor was checked with respect to temperature and pH. ATBI was resistant to heat treatment up to 90°C for 1 h and was stable over a pH range of 2-10. ATBI specifically inhibited aspartic proteases such as pepsin, HIV-1 protease and the protease from *Aspergilllus saitoi*, however, it failed to inhibit other classes of proteases such as chymotrypsin, trypsin, papain, and subtilisin.

Introduction

Aspartic proteases participate in a variety of physiological processes, and the onset of pathological conditions such as hypertension, gastric ulcers, and neoplastic diseases (Phylip et al., 2001). The elucidation of catalytic mechanism operative in other types of proteolytic enzymes has been facilitated by the ready availability of naturally occurring inhibitors of these enzymes. Indeed inhibitors of serine, cysteine, and metalloproteinases are distributed ubiquitously throughout the biological world. In sharp contrast, however, naturally occurring inhibitors of aspartic proteases are relatively uncommon and are found in only certain specialized locations, e. g., proteins from *Ascaris lumbricoides*, the inhibitor peptide released on activation of pepsinogen(s), acetylated pentapeptides (pepstatins) from various species of Actinomycetes, renin-binding proteins, and the inhibitor of proteinase A from yeast.

The development of potent enzyme inhibitors has led to a detailed understanding of enzyme mechanisms and has provided effective therapeutic agents for the treatment of diseases. Inhibitors serve as probes for kinetic and chemical processes during catalysis. For example, they help in elucidating the mode of ligand binding, where the ligand may be an inhibitor, substrate, or substrate analogue. Alternative applications for inhibitors are the detection of short-lived enzyme-bound reaction intermediates, or the identification of amino acid residues at the active site that are necessary for the catalytic activity of the enzyme. Inhibitors are also used for *in vivo* studies to localize and quantify enzymes in organs or to mimic certain genetic diseases that involve the absence of an enzyme in given biosynthetic pathway. An increased understanding of the enzymes specificity for the substrate and inhibitor binding enables a more rational design of potent inhibitors, selective for a particular enzyme. Although in the past decade, the rational drug discovery has taken the movement away from the development of enzyme inhibitors by screening of natural products, the biodiversity prevalent in soil, water, insects, and tropical plants still possess tremendous potential for the isolation of novel and effective enzyme inhibitors.

The involvement of aspartic proteases in various human diseases has made these enzymes an important target for the drug discovery. Therefore, the new understanding of the structure and function relationships of these enzymes has a direct impact on the design of inhibitor drugs. Moreover, as structure and function are closely related among the aspartic proteases, model enzymes have been particularly informative. There have been a plethoras of reports of synthetic aspartic protease inhibitors, however, there is a paucity of reports of such inhibitors from microorganisms. Furthermore, to our knowledge, there are no reports of peptidic inhibitors of aspartic proteases from extremophiles. We have exploited the vast diversity of the soil sample and isolated an extremophilic *Bacillus* sp., which produces an aspartic protease inhibitor, ATBI. The present chapter deals with the purification and biochemical characterization of the inhibitor.

Materials and Methods

Materials

Activated charcoal, beef extract, yeast extract, malt extract, peptone, and other media components were purchased from Himedia, India. Glucose, sodium chloride, magnesium sulfate, dipotassium hydrogen phosphate were from Qualigens, Glaxo India. UM-10, UM-2 membranes were from Amicon Inc. USA. Acetonitrile was from E-Merck, Germany. Trifluoroacetate (TFA) was from Sigma Chem. Co. USA. Ampholines were from Pharmacia, Sweden. All other chemicals were of analytical grade.

Bacterial Strain and Growth Conditions

The extremophilic *Bacillus* sp. was isolated from the hot spring from the Vajreswari District, Maharashtra, India (Dey et al., 1991). The *Bacillus* sp. was routinely maintained on alkaline wheatbran (10%) and yeast extract (0.5%) slants, or on malt extract (0.3%), glucose (1%), yeast extract (0.3%), and peptone (0.5%) (MGYP) agar slants. The pH of the slants was adjusted to pH 10 by the addition of sterile 10% sodium carbonate separately. The bacterial culture was grown at 50°C for16 h and slants were preserved at 4°C. For long-term storage, 25% glycerol suspension of the 16 h grown culture was kept frozen at -70°C.

Production of the Aspartic Protease Inhibitor (ATBI)

The media composition for the production of ATBI was as given below:

Glucose - 1%

Beef extract - 0.75%

Sodium chloride - 0.3%

Magnesium sulfate - 0.1%

Dipotassium hydrogen phosphate - 0.1%

Soyameal - 2%

The pH of the autoclaved medium was adjusted to 10 by addition of sterile 10% sodium carbonate separately. Production of the inhibitor was carried out by inoculating a loop full of freshly grown culture on wheatbran slant into the inoculum flask containing the liquid media with the above composition at 50°C. The inoculum was developed in for 24 h in the inoculum flasks at 50°C. 10 ml of the inoculum was transferred into 500 ml Erlenmeyer flasks containing 100 ml of the above medium and was incubated under shaking conditions (250 rpm) at 50°C for 48 h.

Optimization of ATBI Production in the Fermentation Flasks

Time Profile for the Production of ATBI

The production of the inhibitor at various time intervals was checked by removing samples at different time intervals and assaying for its anti-proteolytic activity.

The time course of production of ATBI and the effect of various additives was estimated in terms of the percentage inhibition against pepsin activity taking equal volume of the charcoal treated culture broth for the assay.

Carbon Sources

The effect of various carbon sources on the production of ATBI was determined by supplementing lactose, sorbitol, xylan, glucose, fructose, maltose and sucrose, all at a concentration of 1% in the production flasks.

Nitrogen Sources

The medium was formulated for the maximum production of the inhibitor using 1% w/v of soyameal, casein, casamino acids, urea, tryptone, peptone, beef extract, skimmed milk and yeast extract as the nitrogen sources in the fermentation flasks.

Addition of Amino Acids

The fermentation medium was supplemented with various amino acids and the effect on the production of the inhibitor was monitored. The amino acids used in the production flasks were alanine, arginine, asparagine, cysteine, glutamic acid, glycine, histidine, proline, and serine all at a final concentration of 0.5%.

Purification of ATBI

The cells and the residual soyameal from the extracellular culture broth of the extremophilic *Bacillus* sp were separated by centrifugation at 6000 rpm, at 4°C, for 20 min in a Sorvall RC 5C super speed centrifuge. The resulting extracellular culture filtrate (1000 ml) was treated with activated charcoal (65 g) and incubated at 4°C overnight. The charcoal was removed by filtration through Whatmann no. 3 filter paper. The colorless filtrate thus obtained was subjected to membrane filtration through amicon-UM10 (molecular weight cut off 10,000) and subsequently through amicon-UM2 (molecular weight cut off 2,000). The resulting inhibitor sample was concentrated to 50 ml by lyophilization. The residual concentrated inhibitor was further purified by reverse phase high performance liquid chromatography (rp-HPLC). The concentrated inhibitor sample (100 µl) was loaded onto a prepacked UltroPac column (Lichrosorb RP-18, LKB, 4 x 250 mm), which was pre-equilibrated with 10% acetonitrile (CH_3CN) and 0.1% trifluoroacetate (TFA). The fractions were eluted on a linear gradient of 0-50% CH_3CN with H_2O containing 0.01% TFA at a flow rate of 0.5 ml/min and monitored at a wavelength of 210 nm. The fractions detected were collected manually and checked for their anti-proteolytic activity. The fractions showing the inhibitory activity were pooled and the eluate was evaporated and lyophilized. The residual matter

was dissolved in distilled H_2O and was re-chromatographed on rp-HPLC under similar experimental conditions as described above.

Biochemical Properties of ATBI

The amino acid composition analysis of the purified ATBI was carried out on a Pharmacia LKB alpha plus amino acid analyzer. Samples were hydrolyzed by standard acid hydrolysis conditions using 6 N HCl at 110 °C for 22 h.

Isoelectric point of ATBI was determined by the modified straight tube method using ampholines in the range of pH 3.0-11.0 (Sathivel et al., 1995). Initially a broad range of ampholines were used to locate the approximate value of the pI, further the pH range was narrowed down to determine the exact pI of ATBI using appropriate ampholines.

Molecular mass of the purified ATBI was determined on a VG Biotek Platform-II quadrupole electrospray mass spectrometer (ES-MS) using CH_3CN-H_2O (1:1) as the mobile phase.

The amino acid sequence of the purified peptide was determined with a protein sequencer (Applied Biosystems Model 476A) based on the Edman degradation principle.

The sequence homology of ATBI with other peptidic inhibitor was carried out manually after retrieving the peptide sequences from the data bank.

pH and Thermal Stability of ATBI

The pH stability of ATBI was determined by pre-incubating ATBI (25 μM) in a range of pH values in appropriate buffers for 1 h and estimating the anti-proteolytic activity. For the temperature stability experiments, ATBI (25 μM) was incubated at temperatures 25-100°C for 24 h and by estimating its inhibitory activity against pepsin at different intervals of time.

Protease Inhibition Assay of ATBI

Pepsin assay

The inhibitory activity of ATBI was determined by estimating the anti-pepsin activity in 0.05 M KCl-HCl buffer, pH 2.0 using casein (0.6%) as the substrate. The detailed assay conditions for pepsin assay has been described in chapter 4. The inhibitory activity of ATBI towards HIV-1 protease and F-prot was determined as described in chapter 3, and 4 respectively.

All the following assays were carried out at 37° for 30 min and stopped by the addition of trichloroacetic acid (TCA). The proteolytic activities of the enzymes were measured by estimating the optical absorption of the acid soluble products at 280 nm.

Chymotrypsin Assay

The inhibitory activity of ATBI against chymotrypsin, was determined by assaying the proteolytic activity of 25 µl of chymotrypsin (1 mg/ml) in 0.05 M Borax-Boric acid buffer, pH 8.0, in the presence of 0.1 M $CaCl_2$, using casein (1%) as the substrate in the presence or absence of ATBI.

Trypsin Assay

The anti-trypsin activity of ATBI was determined by incubating 5 µl of trypsin (1 mg/ml) in the presence and absence of ATBI in a reaction mixture containing 0.05 M phosphate buffer pH 7.5 using casein (1%) as the substrate.

Subtilisin Assay

The inhibitory activity of ATBI against subtilisin was determined by assaying the proteolytic activity of 15 µl of subtilisin (0.5 mg/ml) in 0.05 M carbonate-bicarbonate buffer, pH 10.0, using casein (1%) as the substrate, in the presence or absence of ATBI.

Papain Assay

The anti-papain activity of ATBI was determined by incubating 25 µl of papain (0.5 mg/ml), in the presence or absence of ATBI in a reaction mixture containing 0.05 M Tris-HCl buffer, pH 7.5, 20 µl dithiothritol (1 M), using casein (1%) as the substrate.

Results

After extensive screening of various classes of microorganisms, we have identified an extremophilic *Bacillus* sp., which produces an aspartic protease inhibitor. The crude extracellular filtrate showed anti-pepsin activity. The aspartic protease inhibitor was named as ATBI, referring to the alkalo-thermophilic *Bacillus* inhibitor.

Production of ATBI

An assortment of various carbon, nitrogen sources, amino acids and the time profile for the maximum production of ATBI was evaluated. As revealed from figure 1A, among the different carbon sources supplemented, glucose induced maximum production of ATBI. In case of nitrogen sources, although after 48 hours a maximum production of the inhibitor was obtained in the presence of beef extract and soyameal alone, the production was considerably high when beef extract and soyameal were used in combination (Figure 1B). Arginine was found to be the most suitable amino acid, which induced the maximum production of ATBI (Figure 1C). From the time course of fermentation, it was evident that the production of ATBI was increased exponentially until 40 h and reached maximum at 48 h of growth (Figure 1D).

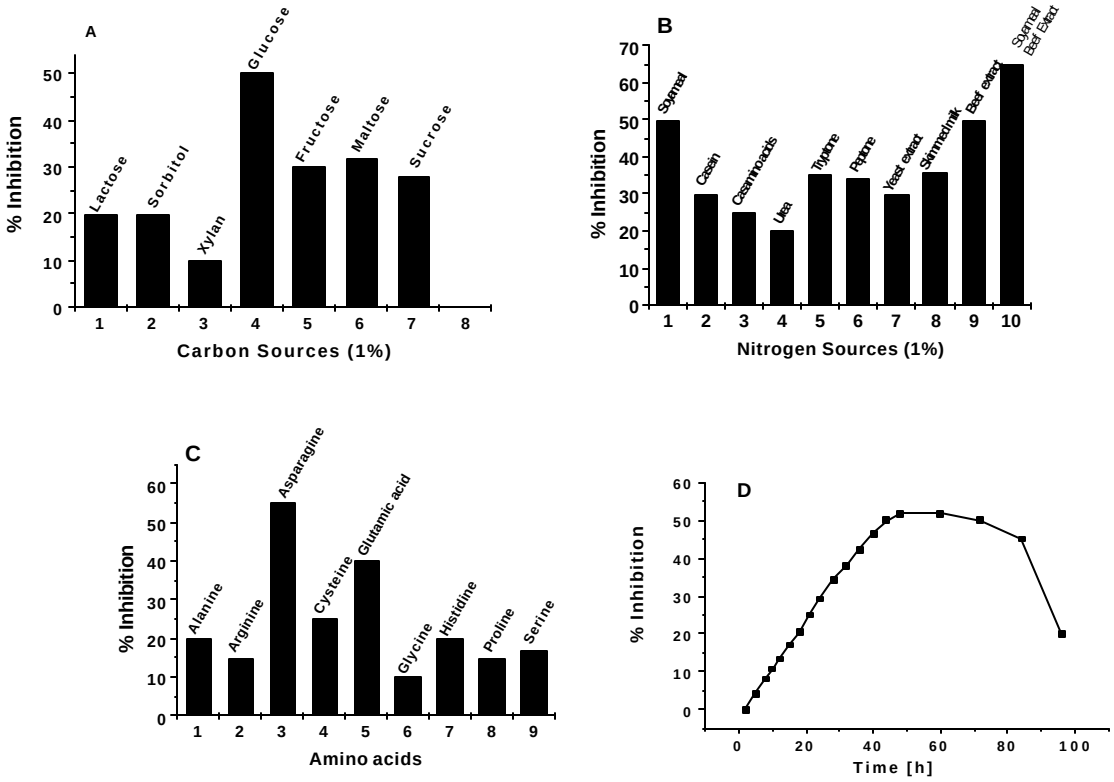

Figure 1. Optimization of Production of ATBI.

Production of ATBI in the presence of carbon sources (A), nitrogen sources (B), amino acids (C), and the production profile of ATBI as a function of time (D).

Purification of ATBI

The extracellular culture filtrate of the extremophilic *Bacillus* sp. was subjected to activated charcoal treatment and ultra filtration to remove the high molecular weight impurities. The inhibitor sample was concentrated by lyophilization. This concentrated inhibitor sample was further purified by rp-HPLC. The anti-asparitc protease activity was associated with the peak A, having a retention time of 2.553 min (Fig. 2a) and other eluted peaks, B and C, with retention times 3.268, and 3.853 min, respectively, showed no inhibitory activity. The fractions showing the inhibitory activity were pooled and lyophilized. Homogeneity of the active fractions containing peak A was indicated by the single peak as analyzed on rp-HPLC with the retention time of 2.560 (Fig. 2b). Further, the purified ATBI showed a single band on an analytical iso-electric focusing gel unit with a pI of 10.0.

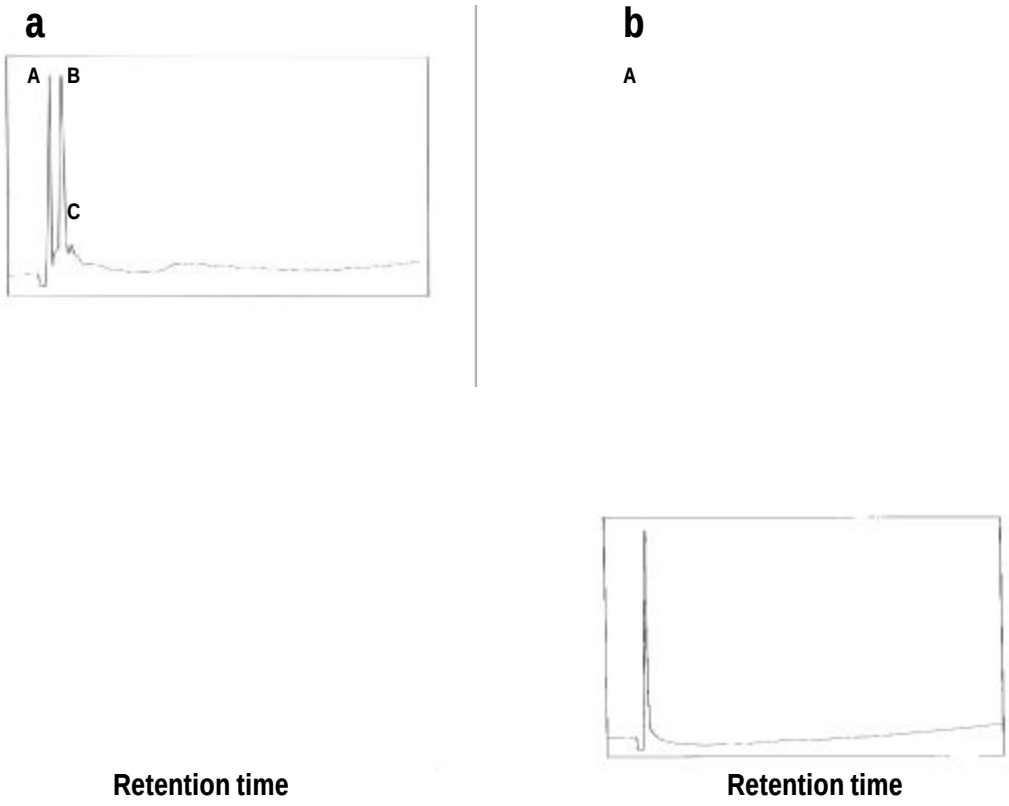

Figure 2. Reverse phase-HPLC purification of ATBI.

a) 100 µl of the lyophilized ATBI sample was loaded on a linear gradient of 0-50% acetonitrile with water containing 0.01% triflouroacetate for 15 min at a flow rate of 0.5 ml/min and monitored at 210 nm. The fractions containing the peaks A, B, and C were collected manually and assayed for the anti-proteolytic activity. b) 10 µl of the pooled fractions containing the peak A (associated with the anti-proteolytic activity) was reloaded onto the reverse-phase HPLC system under similar experimental conditions. The peak detected showed a retention time of 2.560 min.

Biochemical Properties of ATBI

The positive ninhydrin test with the purified ATBI revealed its peptidic nature. Amino acid composition data showed the predominance of aspartic acid in the inhibitor. The molar composition of different amino acids present in the inhibitor is given in Table-1. The amino acid composition data was corroborated by the amino acid sequencing data of the inhibitor. ATBI has an amino acid sequence of Ala-Gly-Lys-Lys-Asp-Asp-Asp-Asp-Pro-Pro-Glu as determined by a protein sequencer. The amino acid sequence of the inhibitor was distinctly different from the sequence of the other reported peptidic inhibitors of aspartic proteases. The predominance of the charged amino acid residues in the inhibitor sequence indicated its hydrophilic nature. The net charge per molecule calculated from the amino acid composition was negative indicating that ATBI is an anionic peptide. The molecular mass (M_r) of ATBI as determined from ES-MS was 1147 Da (Fig. 3a). The schematic representation of chemical structure of ATBI is shown in Figure 3b.

Table 1. Molar composition of amino acids in ATBI

Samples were hydrolyzed by standard acid hydrolysis conditions using 6 N HCl at 110°C for 22 h.

Amino acids	*Concentration (nM)*
Asp	*6.228*
Lys	*3.163*
Pro	*3.235*
Glu	*1.623*
Ala	*1.558*
Gly	*1.557*

a

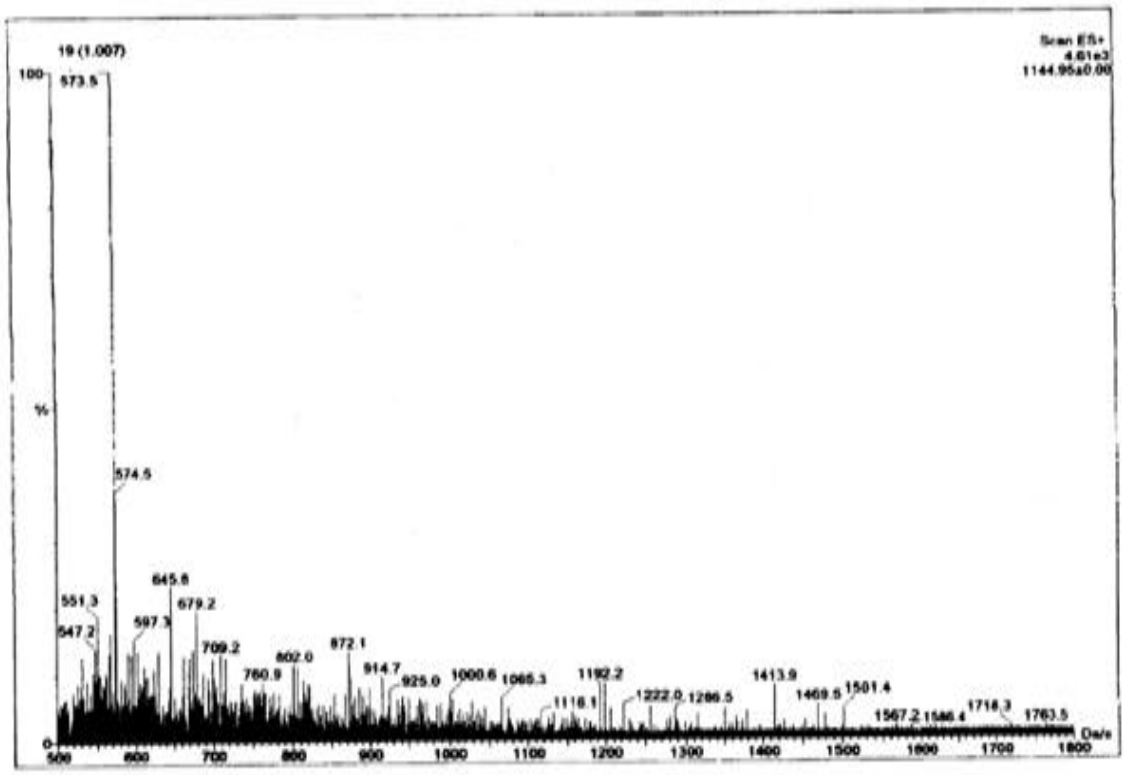

b

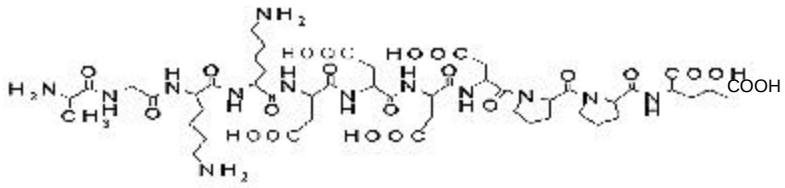

Figure 3. a) Molecular mass of ATBI. The purified ATBI was analyzed for the determination of the molecular mass using

acetonitrile-water (1:1) system as the mobile phase on a quadrupole electrospray mass spectrometer.

b) Schematic representation of the chemical structure of ATBI.

Stability of ATBI

ATBI was stable in a broad range of pH (2-10) (Fig. 4a). However, at pH 11 it looses its anti-proteolytic activity substantially (~55 %). The temperature stability of ATBI revealed a range of 28 - 70°C, where the inhibitor does not loose its inhibitory activity until 24 h (Fig. 4b). At 90 °C, ATBI was stable for 1 h and at 100 °C for 10 min.

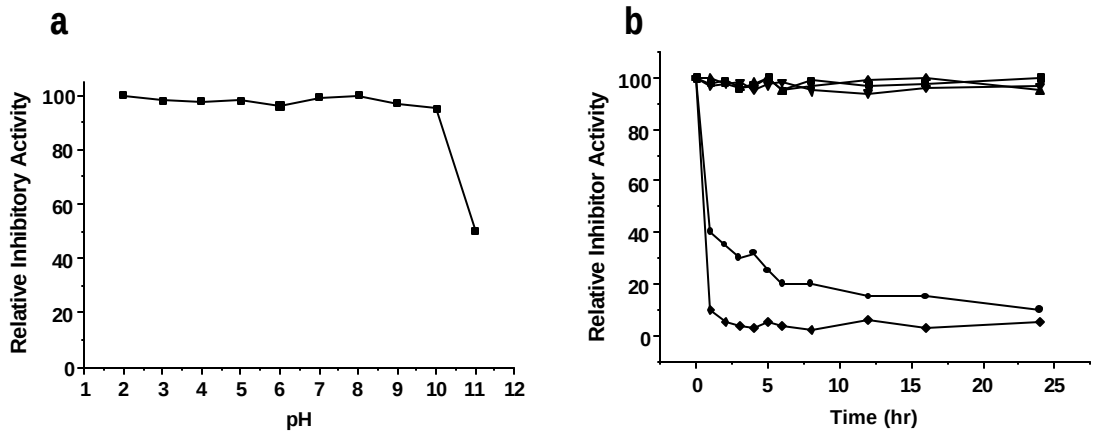

Figure 4. Stability of ATBI.

a) pH stability of ATBI. ATBI was treated with various buffers of different pH and its anti-proteolytic activity was determined by anti-pepsin activity. b) Temperature stability of ATBI. ATBI was incubated at 50 (■), 60 (▲), 70 (▼), 90 (●), and 100 °C (♦), for the time specified and the anti-proteolytic activity was determined at 37°C using pepsin.

Potency of ATBI towards other Classes of Proteases

ATBI when tested for its anti-proteolytic potency towards proteases belonging from other classes, such as trypsin, chymotrypsin, subtilisin, and papain, did not show any inhibitory activity. These results indicated the selectivity of ATBI towards only the aspartic protease class.

Discussion

In pharmacological research, enzyme inhibitors are used to inactivate specific enzymes or group of enzymes, leading to the treatment of many diseases. In order for an enzyme inhibitor to be an effective drug, it not only has to be potent inhibitor for its specific target enzyme but must also have good bioavailability, enabling the inhibitor to reach its target of inhibition in effective therapeutic concentrations. Computer-aided inhibitor design is a relatively new and powerful approach for the development of novel, potentially potent, nonsubstrate-analogue enzyme inhibitors. In concert with biological screening, computer-aided drug design can focus the search for inhibitors, thereby circumventing much of the time-consuming synthetic and natural product purification procedures of those compounds they find unlikely to function as inhibitors. Inhibitors of aspartic proteases have tremendous applications in biomedical research, because they are responsible for the physiological regulation of proteases, which are involved in biochemical regulation of cellular functions. There have been numerous reports of synthetic inhibitors of aspartic proteases over past few decades. However, there is a paucity of inhibitors from natural resources. To our knowledge, there have been no reports of aspartic protease inhibitors from extremophilic microorganisms. Exploiting the biodiversity of the soil sample, we have selected an extremophilic *Bacillus sp.*, which produced an aspartic protease inhibitor, ATBI. ATBI was determined to be an efficient inhibitor of aspartic proteases such as pepsin, F-prot and HIV-1 PR. The inhibitor was purified to homogeneity and was stable over a pH range of 2-10 and at 90°C for 1 h. Amino acid composition and the sequence data revealed the abundance of charged amino acid residues in the peptide, and homology search with other peptidic inhibitors of aspartic proteases revealed no similarity. The inhibitor has a molecular mass of 1147 Da, thus belonged to low-molecular weight class of inhibitors. ATBI was highly specific towards inhibiting the aspartic protease class of enzyme, as it failed to inhibit the representative enzymes of other classes of proteases. Being a low molecular weight hydrophilic peptide, and produced from a bacteria source, ATBI possess tremendous potential for the economical and effective production.

References

Abu-Erreish, G. M., and Peanasky, R. J. (1974) *J. Biol. Chem.* **249**, 1566-1578.

Bennet, B. D., Babu-Khan, S., Leoloff, R., Louis, J.-C., Curran, E., Citron, M., and Vassar, R. (2000) *J. Biol. Chem.* **275**, 20647-20651.

Dey, D., Hinge, J., Shendye, A., and Rao. M. (1991) *Can. J. Microbiol.* **38**, 436-442.

Dunn, B., Lewwitt, M., and Pham. C. (1983) *Biochem. J.* **209**, 355-362.

Harboe, M., Andersen, P. M., Foltman, B., Kay, J., and Kassell, B. (1984) *J. Biol. Chem.* **249**, 4487-4494.

Kay, J., Valler, M. J., and Dunn, B. N. (1983) In *"Proteinase Inhibitors Medical and Biological Aspects"* (Katunuma, N., Umezawa, H., and Holzer, H., Eds.), pp 201-210, Japan Scientific Societies Press, Tokyo.

Phylip, L. H., Lees, W. E., Brownsey, B. G., Bur, D., Dunn, B. M., Winther, J. R., Gustchina, A., Li, M., Copeland, T., Wlodawer, A., and Kay, J. (2001) *J. Biol. Chem.* **276**, 2023-2030.

Sathivel, C., Lachke, A., and Radhakrishnan, S. (1995) *J. Chromatogr.* **705**, 400-402.

Vassar, R., Bennet, B. D., Babu-Khan, S., Kahn, S., Mendiaz, E. A., Denis, P., Teplow, B. D., Ross, S., Amarante, P., Leoloff, R., Luo, Y., Fisher, S., Fuller, J., Edenson, S., Lile, J., Jaronsinski, M. A., Biere, A. L., Curran, E., Burgess, T., Louis, J.-C., Collins, F., Treanor, J., Roger, G., and Citron, M. (1999) *Science* **286**, 735-741.

Chapter 3

Interaction of ATBI with HIV-1 Protease, Implications in the Mechanism of Inactivation

Summary

HIV produces a small dimeric aspartyl proteases, which specifically cleaves the polyprotein precursors. This proteolytic activity is absolutely required for the production of mature, infectious virions and is therefore an attractive target for therapeutic. The active site cleft of the HIV-1 protease (PR) is bound by two identical conformationally mobile loops known as flaps, which are important for substrate binding and catalysis. ATBI, being an aspartic protease inhibitor has been tested for its potency towards the recombinant HIV-1 PR. Investigation of the kinetics of the enzyme-inhibitor interactions revealed that ATBI is a non-competitive inhibitor with the IC_{50} and K_i values 18.0 nM and 17.8 nM respectively. The non-dissociative nature of HIV-1 PR-ATBI complex with multiple dilutions prompted us to apply a model of tight binding inhibition for the determination of the kinetic parameters of HIV-1 PR inhibition. Sequence homology exhibited no similarity with the reported peptidic inhibitors of HIV-1 PR. The binding of the inhibitor with the enzyme and the subsequent induction of the localized conformational changes in the flap-region of the HIV-1 PR were monitored by exploiting the intrinsic fluorescence of the surface exposed Trp-42 residues, which are present at the proximity of the flaps. We have demonstrated by fluorescence and circular dichroism studies that ATBI binds in the active site of the HIV-1 PR. The localized conformational changes induced in the HIV-1 PR due to the interaction with ATBI were investigated by fluorescence spectroscopic studies. The titration of the enzyme with increasing concentrations of ATBI resulted in a concentration dependent quenching of the tryptophan fluorescence. A comparative analysis in the fluorescence spectra of the HIV-1 PR upon binding of the substrate or the known active site directed inhibitors was found to be similar to that of ATBI, suggesting that ATBI binds in the active site of the enzyme. To evaluate the effects of the inhibitor on the secondary structure of the enzyme, we have analyzed the CD spectra of HIV-1 PR-ATBI complex. Interestingly, the HIV-1 PR-ATBI complex and HIV-1 PR-substrate complex exhibited a similar pattern of negative ellipticity in the far-UV region, suggesting that the inhibitor causes similar structural changes in the enzyme as that of the substrate. Based on our results, we propose that the inactivation is due to the reorganization of the flaps impairing its flexibility leading towards inaccessibility of the substrate to the active site of the enzyme.

Introduction

The human immunodeficiency virus (HIV) has been identified as the etiological agent responsible for the development of the acquired immunodeficiency syndrome (AIDS) (Barre-Sinoussi et al., 1983). The elucidation of the type-1 (HIV-1) genomic sequence (Muessing et al., 1985; Ratner et al., 1985; Sanchez-Pescador et al., 1985; Wain-Hobson et al., 1985) provided momentum to an effervescence of research activities aimed at exploring and exploiting several viral gene products as targets for random compound screening and/or rational drug design (Mitsuya et al., 1991). The superb orchestration of efforts in molecular genetics, protein biochemistry, enzymology, medicinal chemistry, virology, X-ray crystallography, and molecular modeling have established the rational discovery of novel antivirals by targeting the HIV-1 PR. Plethora's of literature are available on the structural and functional aspects of the HIV-1 PR (Hellen et al., 1989; Davies, 1990; Debouck and Metcalf, 1990; Kay and Dunn, 1990; Meek et al., 1990; Oroszlan and Luftig, 1991; Fitzgerald and Springer, 1991; Rao et al., 1991; Tomasselli et al., 1991). HIV-1 exhibit the same 5'-LTR-*gag*-*pol*-*env*-LTR-3' genomic organization, which encodes for a handful of proteins. The *gag* and *pol* regions are initially translated by the host cell ribosomes into large polyprotein precursors that are later processed to yield the mature structural and catalytic proteins found in the virion. Translation of the HIV-1 *gag* open reading frame results in a 55 kD precursor, $Pr55^{gag}$, which contains the virion structural proteins arranged contiguously as NH_2-p17-p24(p25)-p7-p6-COOH. The HIV-1 *pol* open reading frame is translated as a *gag-pol* fusion polyprotein, $Pr160^{gag\text{-}pol}$, as a result of a ribosomal frame shift from the *gag* to the *pol* frames at a specific site positioned before the *gag* termination codon (Jacks et al., 1988). $Pr160^{gag\text{-}pol}$ contains the *gag* structural proteins followed by the protease (PR), reverse transcriptase (RT)/ribonuclease H (H), and integrase (IN) in the order NH_2-p17-p24(p25)-p7-p6-PR-RT(H)-IN-COOH. The proteolytic cleavage of the $Pr160^{gag\text{-}pol}$ is essential for the successful completion of the retroviral life cycle and the production of infectious virions. This polyprotein processing is not carried out by host cell proteases, but by a unique protease encoded by the virus itself. Mutation in the retroviral protease (Kohl et al., 1988; Adachi et al., 1991) or blocking its activity by inhibitors resulted in non-infectious viral particles with immature morphology and dramatically reduced reverse transcriptase activity. The essential nature and unique specificity of the HIV-1 PR made this enzyme an attractive target. However, the major problems to be addressed for the discovery of protease inhibitors by random compound screening and/or rational drug design are i) the identification of a sufficient and safe source of authentic HIV-1 PR, ii) the development of *in vitro* proteolytic assays, and iii) the mechanistic and structural characterization of the enzyme.

Although the HIV-1 PR was isolated from viral particles, it is a scarce and unsafe source of very poorly active enzyme (Copeland and Oroszlan, 1988; Lillehoj et al., 1988). Therefore, HIV-1 PR was initially produced using either recombinant DNA technology (Debouck et al., 1987) or total chemical synthesis (Schneider and Kent, 1988). Mature HIV-1 PR is 99-amino acid long and the recombinant enzyme was purified to homogeneity using a variety of purification strategies, such as ligand-affinity chromatography (Heimbach et al., 1989; Rittenhouse et

al., 1990; Wondrak et al., 1991), size exclusion chromatography (Strickler et al., 1989) or recovery from inclusion bodies (Tomasselli et al., 1990; [a]Cheng et al., 1990). The second important factor was the development of assays capable of reproducibility *in vitro*. The natural processing of HIV-1 $Pr55^{gag}$, and $Pr160^{gagpol}$ by HIV-1 PR seems to be limited to eight discrete sites. The activity of recombinant HIV-1 PR was demonstrated in *E. coli* cells. The protease was found to accurately process HIV-1 *gag* and *pol* precursors when coexpressed in the same cells (Debouck et al., 1987; Mizrahi et al., 1989; Farmerie et al., 1987). These microbial assays have been overweighed by high throughput biochemical assays in which purified HIV-1 PR carries out cleavage of oligopeptide substrates (Dunn et al., 1994 and references thereof). In such assays, purified recombinant HIV-1 PR and short peptide substrates comprising six or more amino acids derived from HIV-1 *gag-pol* cleavage sites, most generally the p17-p24 *gag* junction, -Ser-Gln-Asn-Tyr*Pro-Ile- are used. These assays have been adapted for high throughput in various formats including, radiometric (Wondrak et al., 1990; Hyland et al., 1990), spectrophotometric (Nashed et al., 1989; Tomaszek et al., 1990; Richards et al., 1990; Tamburini et al., 1990; Broadhurst et al., 1991), resonance energy transfer (Matoyoshi, 1990; Geoghegan et al., 1990; Toth and Marshall, 1990; Wang et al., 1990) and high performance liquid chromatography (Schneider and Kent, 1988; Darke et al., 1988; Billich et al., 1988; Moore et al., 1989; Krausslich et al., 1989), analysis of the reaction products. These rapid and facile peptidolytic assays were most attractive as they provide the starting point for the mechanistic studies on the enzyme and for the *de novo* design of protease inhibitors by transition state mimicry.

HIV-1 PR has been classified as an aspartic protease that functions as a homodimer, based on its primary amino acid sequence, its inhibition by pepstatin, and its crystal structure (Muessing et al., 1985; Ratner et al., 1985; Sanchez-Pescador et al., 1985). The HIV-1 PR as well as all retroviral proteases comprises a highly conserved domain, Aspartyl-Threonine-Glycine (DTG), which is found (in two copies) within cellular and fungal aspartyl proteases (Toh et al., 1985). Molecular modeling studies proposed that the retroviral proteases would resemble other aspartyl proteases functionally and structurally if they existed as homodimers of the 99 amino acid (Pearl and Taylor, 1987). The dimeric structure of HIV-1 PR was demonstrated experimentally by biochemical approaches (Meek et al., 1980; Darke et al., 1989) and by X-ray diffraction studies (Wlodawer et al., 1989; Lapatto et al., 1989; Navia et al., 1989; Weber, 1989). The three dimensional structure of HIV-1 PR revealed that the enzyme is C_2-symmetric homodimer whose amino acid carboxyl termini interact intimately at the dimer interface. The “roof” of the active site cleft is formed by two flexible glycine-rich β-strands called the flaps and the “floor” of the active site as shown biochemically (Hyland et al., 1991; Meek et al., 1980) and by mutagenesis (Kohl et al., 1988; Seelmeier et al., 1988; Le Grice et al., 1988; Loeb et al., 1989[a]; Loeb et al., 1989[b]). Understanding the mechanism of HIV-1 PR and the knowledge of it three-dimensional structure has been pivotal in the rational design of protease inhibitors. The crystallographic structures of HIV-1 PR-inhibitor complexes demonstrated that, the binding of a peptide analogue inhibitor or a peptide substrate involves numerous hydrogen-bonding interactions with the highly mobile flaps (Miller et al., 1989). Movement of these flaps apparently accompanies the

binding of the peptide analogue or substrate, which binds in an extended *b*-sheet, such that hydrogen bonds are established between the complementary carbonyl oxygens and the amide protons of the peptide within the flaps. The presumed function of the flap-peptide interactions is to entrap and align the scissile peptide sequence in the HIV-1 PR active site (Rodriguez et al., 1993).

The sequence data indicated the presence of four Trp residues A-6, A-42, B-6, and B-42, two on each monomer of the HIV-1 PR (Blundell and Pearl, 1989). Fluorescence intensity and anisotropy decays of protein-intrinsic tryptophan and tyrosine residues are valuable tools for studying protein conformation and their molecular dynamics (Eftink, 1991). Local motions, such as side chain and backbone fluctuations, occur in pico- and nano-second time scale, which can be monitored using time-resolved fluorescence spectroscopy. These motions can therefore influence the transient emission profiles of intrinsic chromophores if there is a basic photophysical interaction mode. This may be quenching of the fluorescence by a variety of mechanisms such as excited-state collisions, electron, or proton transfer, and also the radiationless transfer of electronic excitation energy (Lakowicz, 1983). In addition, the fluorescence anisotropy decay is the result of the fluorophore dynamics and the overall rotation of the macromolecule (Steiner et al., 1991). Structural and dynamic details of chromophore(s) and its environment are therefore reflected in the fluorescence intensity and anisotropy decays. Thus, the two tryptophan residues per HIV-1 PR monomer A6/B6 and A42/B42 can be used as sensors to investigate the local and global structural dynamics of the protease with further emphasis on conformational and dynamic changes upon binding of high-affinity inhibitors (Kungl et al., 1998). One might expect that if the flap regions of the HIV-1 PR were the only mobile portions of the enzyme and contained a Trp or Tyr residue, then the conformational changes in the flap regions that occur upon peptide binding would give rise to changes in protein fluorescence that specifically reflect movements of flaps (Rodriguez et al., 1993).

Rational Design of HIV-1 PR Inhibitors

The close functional relationship between renin and HIV-1 PR prompted several investigators to screen their renin inhibitors for anti-HIV-1 PR activity. Furthermore, the knowledge of renin inhibition (Greenlee, 1990; Kleinen et al., 1991; Ocain and Gharbia, 1991), accumulated over more than one decade in major pharmaceutical companies, served as the starting point for the discovery of potent inhibitors of HIV-1 PR, based on the transition-state mimetics. The first compound in this category to be subjected to clinical trials was Ro31-8959 (Williams, et al., 1992; Shaw et al., 1992; Muirhead et al., 1992). The concept of transition state analogs have been applied for the development of inhibitors, by preparing minimum peptide substrates in which the amide bond normally cleaved by HIV-1 PR is replaced by a nonhydrolyzable surrogate that mimics the tetrahedral transition state motif (Wolfenden, 1976). The structure and activity of the transition state cassettes introduced in the HIV-1 PR substrate are discussed below.

Aminomethyelene Isosteres

Aminomethylene or reduced amide isosteres ($\Psi[CH_2NH]$ or $\Psi[CH_2N]$) are known to inhibit renin (Szelke et al., 1982). Such isosteres were inserted into HIV-1 PR substrates (Tomasselli et al., 1990; Billich et al., 1988; Moore et al., 1989; Miller et al., 1989; Dreyer et al., 1989; Cushman et al., 1990; Rich et al., 1990). However, in contrast to their high affinity towards renin, these peptidomimetics were poor inhibitors of the HIV-1 PR (K_i in the range of 1-10 μM).

Statine Analogs

Naturally occurring pepstatin (isovaleryl-Val-Val-Sta-Ala-Sta-, with Sta (statine) = (4S, 3S)-4-amino-3-hydroxy-6-methylheptanoic acid) is a potent inhibitor of all aspartyl proteases (Umezawa et al., 1970). HIV-1 PR is inhibited moderately by the generic pepstatin (K_i ~1 μM). Design of inhibitors by substituting a statine like residue for the scissile bond within an HIV-1 PR oligopeptide substrate have resulted in compounds with moderate inhibition against HIV-1 PR (K_i in the range of 0.1-50 μM) (Tomasselli et al., 1990, Billich et al., 1988; Moore et al., 1989; Dreyer et al., 1989; Rich et al., 1990; Hui et al., 1991).

Phosphinic Acid Isosteres

Phosphinic acids were reported to be the inhibitors of pepsin (Barlett and Kezer, 1984). Incorporation of the tetrahedral phosphinic acid motif (Ψ[PO{OH}CH_2]) into HIV-1 PR peptide substrates attained modest to highly potent inhibition of retroviral enzyme (K_i ranging from 1 nM to 10 μM) (Dreyer et al., 1989; Grobeiny et al., 1990).

α,α-Difluoroketones

These transition state mimics resulted in very potent inhibitors of renin (Thaisrivongs et al., 1985) and pepsin (Gelb and Abeles, 1985), and when introduced in the substrate of HIV-1 PR, inhibited HIV-1 PR with K_i range 1 to 100 nM (Dreyer et al., 1989; Sham et al., 1991).

Dihydroxyethylene, Hydroxyethylene, and Hydroxyethylamine Isosteres

These three motifs also have shown to afford potent inhibition against renin (Thaisrivongs et al., 1987; Szelke, 1985; Dann et al., 1986), thus these nonhydrolyzable surrogates have been incorporated into HIV-1 PR substrates. Dihydroxyethylene {Ψ[CH[OH]CH[OH]}-containing peptidomimetics resulted in highly potent inhibitors of HIV-1 PR with K_i values ranging from 1-25 nM (Thaisrivongs et al., 1991; Ashorn et al., 1990). Incorporation of hydroxyethylene isosteres {Ψ[CH[OH]CH_2]} into HIV-1 PR peptide substrates also led to very potent inhibitors (K_i 0.1-10 nM) (Tomasselli et al., 1990; Richards et al., 1989; Dreyer et al., 1989; McQuade et al., 1990; Vacca et al., 1991; Lyle, 1991). Similarly, peptide analogs with hydroxyethylamine isostere {Ψ[CH[OH]CH_2N]} possess similar potency with the K_i values in the subnanomolar range (Rich et al., 1990; Roberts et al., 1990; Rich et al., 1991).

Structure Based Inhibitors of HIV-1 PR

X-ray crystallographic structure determination of HIV-1 PR (Wlodawer et al., 1989; Lapatto et al., 1989; Navia et al., 1989; Weber et al., 1989), and its complex with the inhibitors, revealed the hydrogen bonding interactions between the inhibitor and enzyme residues near the active site DTG triads and in the flaps (Miller et al., 1989; Fitzgerald et al., 1990; Swain et al., 1990; Jaskolski et al., 1991). In conjunction with molecular modeling, the detailed structural information has been very useful in the design of novel and more potent peptidomimetic inhibitors of the enzyme (Thaisrivongs et al., 1991; Rich et al., 1991). The C_2 dimeric structure of HIV-1 PR has been applied for the identification of compounds with inhibitor activity against HIV-1 PR, including symmetric inhibitors, inhibitors of dimerization, and compounds with steric complementarity to the active site.

Symmetric Inhibitors

The two fold rational symmetry of the active site of HIV-1 PR has been utilized to design novel inhibitors with a C_2 axis of symmetry positioned on or near the carbonyl carbon of the scissile amide bond and superimposed on the axis of symmetry of the enzyme. Pseudosymmetric (diamino alcohols) and symmetric (diaminodiols) inhibitors were synthesized and showed to exhibit highly potent inhibition towards HIV-1 PR with K_i in the 10^{-10} to 10^{-8}M range.

Inhibitors of Dimerization

HIV-1 PR is active in its homodimeric form ([b]Cheng et al., 1990; Dilanni et al., 1990; Babe et al., 1991), thus prevention of self-association of protomers or dissociation of dimers represents another approach to protease inhibition. The X-ray crystallography studies have revealed that the dimer interface consists of a four-stranded antiparallel β-sheet in which the N-termini (residues 1-4 and 101-104) and C-termini (residues 95-99 and 195-199) are linked by a network of hydrogen bonds (Wlodawer et al., 1989). Thus, short peptides consisting of the N-terminal or C-terminal sequence of HIV-1 PR were predicted to form similar interactions with their respective partner within the enzyme, thereby leading to subunit dissociation and enzyme inhibition (Weber, 1990). However, this strategy resulted in weak inhibition of the HIV-1 PR (Zhang et al., 1991; Schramm et al., 1991).

Inhibitors Sterically Complementary to the Active Site

Molecular modeling techniques have been used to search for molecules that fits in the pocket delimited by the active site cleft and the flaps (DesJarlais et al., 1990). Haloperidol, a compound closely related to one of the molecules identified (bromperidol), was found to block HIV-1 PR with a K_i ~ 100 μM. Currently used efforts on molecular modeling approach with the help of medicinal chemistry to search various specialized and proprietary three-dimensional databases, will certainly help in discovering novel nonpeptidic HIV-1 PR inhibitors.

Natural Products as HIV-1 PR Inhibitors

Natural products are a continuous and proven source of new lead compounds to drug discovery programs. For the screening of natural products as inhibitors for the HIV-1 PR, from microbial, marine, and vegetal origin, high throughput biochemical assays have been developed and being applied (Sarubbi et al., 1991). Besides pepstatin the antifungal antibiotic cerulenin, isolated from *Cephalosporium caerulens* (Onsura, 1976), has been characterized as an HIV-1 PR inhibitor (Pal et al., 1983; Blumenstein et al., 1989; Moelling et al., 1990) and exhibits antiretroviral activity (Goldfine et al., 1978; Ikuta and Luftig, 1986; Katoh et al., 1986). Cerulenin contains a critical epoxide residue, which appears to be responsible for the inactivation of the enzyme. Several synthetic derivatives of cerulenin have been prepared which inhibits the HIV-1 PR, but are less cytotoxic than cerulenin (Blumenstein et al., 1989). In another report Zn^{2+}, was found to be an effective inhibitor of human renin and HIV-1 PR (K_i ~ 10-20 μM) (Zhang et al., 1991). The inhibitory effect of Zn^{2+} is due to the binding at or

near the active site carboxyl groups. Semocochliodinol A and B isolated from the fungus *Chrysosporium merdarium* were reported to have anti-HIV-1 PR activity (Fredenhagen et al., 1996). During screening activities it was observed that penicillin derivatives which after optimization, were fairly active HIV-1 PR inhibitors (IC_{50} ~ 1-10 nM) (Humber et al., 1992; Holmes et al., 1993). Cytochalasin derivative L-696 474, which discovered in the extracts of fungal cultures showed less potency towards HIV- 1 PR (Lingham et al., 1992; Chen et al., 1993). Further, inhibitors of HIV-1 PR were found within flavone (Brinkworth et al., 1992), polyacetulenic acid (Patil et al., 1992), and tetronic acid (Roggo et al., 1994; Dolak et al., 1993) types of compound.

In the last decade, there have been enormous reports on synthetic compounds as inhibitors of HIV-1 protease, and tremendous efforts have been expended in finding inhibitors that could combine high activity and specificity with optimal bioavailability and pharmacological properties. However, the vast biodiversity prevalent, which have been the source of various novel, and effective natural products, remains unexplored. This chapter describes the interaction and kinetics of inactivation of HIV-1 PR with the natural peptidic inhibitor, ATBI, and the investigations of the conformational changes in the enzyme-inhibitor complex.

Materials and Methods

Materials

Ampicillin, Tetracyclin, Sodium Acetate, EDTA, β-mercaptoethanol, and the HIV-1 PR substrate Lys-Ala-Arg-Val-Nle-p-Nitro-Phe-Glu-Ala-Nle-Amide were from Sigma Chemicals. Na_2CO_3, Glucose, are from Qualigens, Glaxo India, Acetonitrile is from E-Merck. All other chemicals are of analytical grade.

Bacterial Strains, Growth Condition, and Plasmids

The *Escherichia coli* strain harboring the recombinant plasmid pTΔN containing the HIV-1 PR gene was grown in M9 media supplemented with ampicillin (40 μg/ml), thiamine hydrochloride (25 μg/ml), and glucose as the carbon source at 30°C. In analytical scale cultures, transformants were grown to mid-log phase and the temperature was then shifted to 42°C, and aliquots were withdrawn at appropriate time intervals and lysed by sonication. The supernatant obtained after centrifugation at 15, 000 x *g* for 15 min at 4 °C was assayed for HIV-1 PR activity as described (Graves et al., 1990). Preparative cultures of *E. coli* cells were grown in M9 medium supplemented with 0.2% casamino acids and 40 μg/ml ampicillin. Seed cultures (100 ml) were grown overnight at 30°C and used to inoculate 1-liter flasks containing 450 ml of the same medium. Cultures were grown at 30°C until mid-log phase before raising the growth temperature to 42°C for 90 min. Cells were pelleted by centrifugation at 6, 000 x *g* for 10 min, washed once with ice-cold phosphate buffered saline, and stored at -70°C. The recombinant *p*TΔN was constructed as described (Griffith et al., 1994) and was a kind gift from Prof. J. Kay (Dept. of Biochemistry, Univ. of Wales College of Cardiff, Wales, UK), Drs. N. Roberts, and A. D. Broadhurst (Dept. of Virology, Roche, Welwyn Garden City, UK).

Enzyme Purification

Cell pellets were thawed, resuspended in 10 mM Tris-HCl buffer, pH 8.0, 50 mM NaCl, 5 mM EDTA containing 1 mg/ml lysozyme (5 ml of buffer/liter of original culture volume), and left on ice for 20 min. Tween 20 was added to 0.2%, and the extract was incubated on ice until the cells were lysed. The cells were then sonicated for 1 min on ice. Cell extracts were centrifuged at 10, 000 rpm for 20 min at 4 °C. Solid streptomycin sulfate was added to a final concentration of 1% v/v while stirring at 4°C. The precipitated material was removed by centrifugation at 10, 000 rpm for 20 min at 4°C and the supernatant was dialyzed overnight against 10 mM potassium phosphate buffer, pH 7. 0. Solid ammonium sulfate was added to 30% saturation and the suspensions were stirred for 3 h and centrifuged at 10, 000 rpm for 20 min at 4°C. The pellet was resuspended in 10 mM potassium phosphate buffer, pH 7. 0 and dialyzed overnight against the same buffer. The resulted dialyzed sample was applied to a hydroxylapatite column (5 x 15 cm), equilibrated with 10 mM potassium phosphate buffer, pH 7. 0, containing 0.1 % Tween 20 and the enzyme was eluted on a linear gradient of 25-250 mM potassium phosphate buffer, pH 7. 0. The fractions were dialyzed and concentrated by lyophilization. The resulting concentrated enzyme was further purified by Sephadex G-75 column (3 x 150 cm) in 10 mM potassium

phosphate buffer, pH 7. 0, containing 100 mM NaCl, 5 mM β-mercaptoethanol. Fractions containing protease activity were pooled and concentrated, and the preparation was stored at -70 °C.

Enzyme Assay

The HIV-1 PR activity was assayed using the synthetic substrate Lys-Ala-Arg-Val-Nle-pNitro-Phe-Glu-Ala-Nle-Amide (Richards et al., 1990; Phylip et al., 1990). The HIV-1 PR was incubated at 37°C at different concentrations of the substrate in a reaction mixture containing 100 mM NaCl, 5 mM β-mercaptoethanol, 5 mM EDTA and 50 mM sodium acetate buffer, pH 5.6. After 15 min, the reaction was stopped by the addition of equal volume of 5% trichloroacetate and followed by 30 min incubation at 28°C. The hydrolysis of the peptide substrate was monitored either by reverse phase-high performance liquid chromatography (rp-HPLC) or by monitoring the decrease in optical abosorbance at 300 nm spectrophotometrically. HPLC analysis was carried out with a prepacked UltroPac column (Lichrosorb RP-18, LKB, 4 x 250 mm), eluting with a linear gradient of 0-30% acetonitrile in 0.1% trifluoroacetate (TFA) over a period of 30 min at a flow rate of 1.0 ml/min.

Kinetics of HIV-1 PR Inhibition

The inhibition constant K_i, for the HIV-1 PR inhibition was determined as described by Dixon (Dixon, 1953) and by Lineweaver-Burk's equation. In Dixon's method, proteolytic activity of the recombinant HIV-1 PR was measured at two different concentrations of substrate as a function of inhibitor concentration. The kinetic constants were determined by incubating the HIV-1 PR in the absence and presence of ATBI with increasing concentrations of the substrate for 15 min at 37°C. The inhibition was also analyzed by the double reciprocal plot. The kinetics of the HIV-1 PR inhibition was analyzed by a model for tight binding inhibition (Cha, 1976). Kinetic determinations of enzyme interaction with the inhibitor in the absence of substrate were determined at short intervals by assaying the residual protease activity. In these experiments, the residual enzymatic activity was measured after the HIV-1 PR and the inhibitor were mixed and the samples were sub-sampled at increasing time intervals and assayed with the substrate. In all the experiments, the inhibition of the HIV-1 PR was too rapid to measure under first order conditions. Rates of the HIV-1 PR were therefore determined in all cases by second order association rate kinetics. The association rate constants were calculated according to the integrated second order rate equation (Gigli et al., 1970).

$$k'' t = \frac{1}{[I] - [E]} \ln \left(\frac{[E]([I] - [EI])}{[I]([E] - [EI])} \right)$$

Where [E] is the enzyme concentration, [I] is the inhibitor concentration, [EI] is the concentration of enzyme-inhibitor complex. The residual values (free enzyme) at 60 s were subtracted from that of the total enzyme, and this gives the concentration of the enzyme-inhibitor complex. The dissociation rate constant (k' or a) were determined from the formula $a = b$ [I] by plotting the slope of the rate of inhibition (b) or association rate constant

(k'') in each reaction versus time multiplied by the inhibitor concentration. The slopes of the values were fitted by linear regression. Substrate protection studies were carried out by incubating the HIV-1 PR with different concentrations of substrate and then assaying the proteolytic activity at increased concentration of the inhibitor.

Fluorescence Analysis

Fluorescence measurements were performed on a Perkin-Elmer LS50 Luminscence spectrometer connected to a Julabo F20 water bath. Protein fluorescence was excited at 295 nm and the emission was recorded from 300-500 nm at 25°C. The slit widths on both the excitation and emission were set at 5 nm and the spectra were obtained at 500 nm/min. Fluorescence data were corrected by running control samples of buffer and smoothened. For binding studies, the HIV-1 PR (25 μg/ml) was dissolved in 50 mM sodium acetate buffer (pH 5.6) containing 100 mM NaCl, 5 mM EDTA, 5 mM β-mercaptoethanol. Titration of the enzyme with ATBI was performed by the addition of different concentrations of the inhibitor to the enzyme solution. For each inhibitor concentration on the titration curve a new enzyme solution was used. All the data on the titration curve were corrected for dilutions. Further, the emission spectra of the HIV-1 PR were recorded in the presence of the substrate and the active site based inhibitors a) N-Acetyl-Leu-Val-Phe-Al and b) Pepstatin at 25°C. Accessibility calculations and visualization of Trp residues were performed by Insight-II version 1995 MSI (*Biosym/Molecular Simulations Release* 95.0, 1995, San Diego, CA) from the crystallographic structure of the HIV-1 PR as described (Rutenber et al., 1993).

Circular Dichroism Analysis

CD spectra were recorded in a Jasco-J715 spectropolarimeter at ambient temperature using a cell of 1 mm path length. Replicate scans were obtained at 0.1 nm resolution, 0.1 nm bandwidth and a scan speed of 50 nm/min. Spectra were average of 6 scans with the baseline subtracted spanning from 280 nm-200 nm in 0.1 nm increment. The CD spectrum of the HIV-1 PR (25 μg/ml) was recorded in 50 mM sodium phosphate buffer (pH 5.6) containing 100 mM NaCl, 5 mM EDTA, 5 mM β-mercaptoethanol, in the absence/presence of substrate (40 μM) or ATBI (20 nM). Secondary structure content of the HIV-1 PR, the HIV-1 PR-substrate complex and the HIV-1 PR-ATBI complex was calculated using the algorithm of the K2d program (Andrade et al., 1993; Merelo et al., 1994).

Results

Kinetics of Inactivation of the Recombinant HIV-1 PR by ATBI

Based on our results obtained from the inhibitory activity of ATBI against pepsin, we have evaluated its potency towards HIV-1 PR. Interestingly ATBI was found to inhibit the purified recombinant HIV-1 PR with an IC_{50} value (50% inhibitory concentration) of 18 nM (Figure 1a). As revealed from figure 1a, the inhibition of the HIV-1 PR followed a sigmoidal pattern with increasing concentrations of the inhibitor. However, the secondary plot (the slope of inhibition graph versus inhibitor concentration) was not linear suggesting that the application of Michaelis-Menten inhibition kinetics was not appropriate in this study. The inhibition constant, K_i for the enzyme inhibitor interaction, determined by the Dixon plot was 17.8 nM (Figure 1b), which is almost equal to the IC_{50} value of the inhibitor. The Lineweaver-Burk's reciprocal plot (Figure 1c) showed that, ATBI was a non-competitive inhibitor of the HIV-1 PR and the K_i value determined from this analysis corroborated that obtained by the Dixon method.

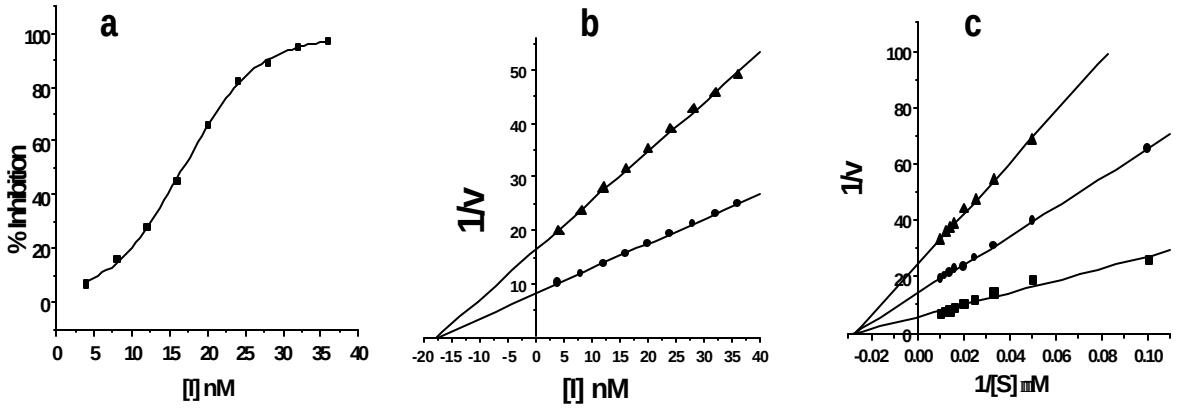

Figure 1. Binding of ATBI to the HIV-1 PR and inhibition kinetics analyses.

a) The percent inhibition of the HIV-1 PR activity was calculated from the residual enzymatic activity. The sigmoidal curve indicates the best fit for the percent inhibition data obtained and the IC_{50} value was calculated from the graph. b) Enzymatic activity of the HIV-1 PR (25 μg/ml) was estimated using the substrate [40 μM (▲), 80 μM (●)] at different concentrations of ATBI. The straight lines indicated the best fit of the data obtained. c) The HIV-1 PR (25 μg/ml) was incubated, without (■) or with the inhibitor at 10 nM (●), and 20 nM (▲) and assayed at increasing concentrations of the substrate. K_i was determined from the double reciprocal plot as per the non-competitive type of inhibition.

For the inhibition kinetic studies, the HIV-1 PR activity was monitored in the presence of various concentrations of inhibitor and substrate, as a function of time. A very rapid inhibition of the HIV-1 PR was observed which necessitated measuring all the kinetic parameters at second order association conditions. The dissociation rate constant, a-values obtained for ATBI were reasonably constant (Table I) and the average calculated value of a in the presence of substrate is $8.25 \pm 0.50 \times 10^{-4}$ s^{-1}. The association rate constants, b in the presence and absence of substrate were calculated from the plot of the HIV-1 PR inhibition versus time. The values of b (Table I) were not affected by the presence of the substrate indicating that the presence of substrate had no implication on the interaction of the inhibitor and enzyme. The non-competitive inhibition of HIV-1 PR was determined by plotting the reciprocal of the values of b as a function of the substrate concentration (Figure 2a). The plotted line did not fit a linear plot but was a good fit for a rectangular hyperbola, which confirmed the non-competitive inhibition. The mechanism of inhibition of the HIV-1 PR was further deciphered by the plot of Δb versus substrate concentration (Figure 2b). This plot is analogues to the diagnostic plot of slope versus substrate concentration (Henderson, 1972). Non-competitive inhibition was represented by the straight line with a slope = 0.

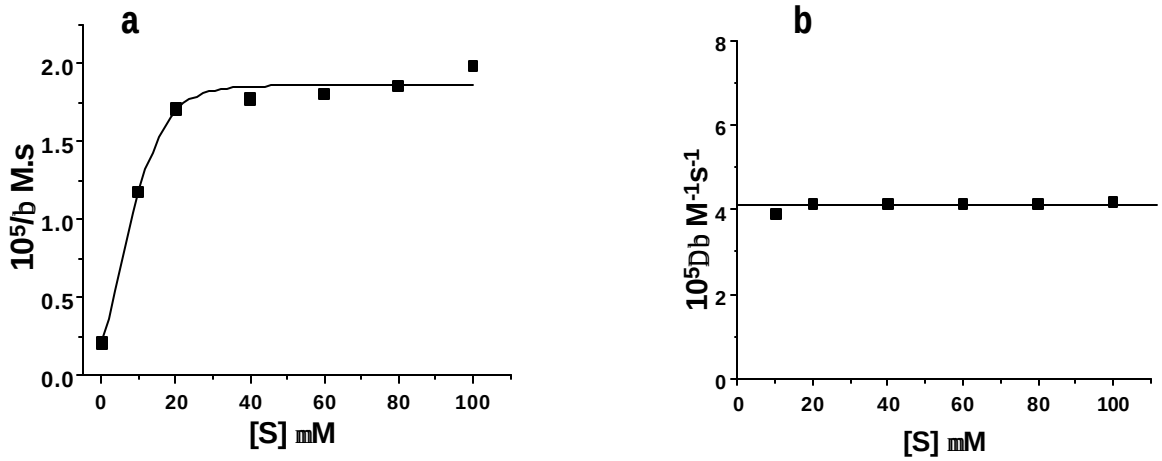

Figure 2. Determination of the binding constants of the HIV-1 PR and ATBI interactions.

a) The HIV-1 PR and ATBI were mixed and the samples removed at different time intervals were assayed to determine the residual activity of the enzyme. The rate constants were determined by the second order association kinetics. The hyperbola indicated the best fit of the data obtained by plotting the reciprocal of the association rate constant (b) *versus* the substrate concentration. b) Henderson plot of the change in the slope of Δb for the inhibition of the HIV-1 PR by ATBI, as a function of substrate. The straight line represents the best fit for the data generated for the values of Δb.

Table I

Kinetic parameters associated with the inhibition of HIV-1 PR by ATBI.

The table enlists the estimated kinetic values (means ± S. E. M.) for the inhibition of HIV-1 PR by ATBI, where S is the substrate, n is the number of determinations, $a = k'$, b is the association rate constant and Δb is the change in the association rate constant as influenced by the contribution of substrate.

[S] (μM)	n	10^{-4} x a (s^{-1})	10^{4} x b (M^{-1} s^{-1})	$10^{5}/b$ (M s)	10^{5} x Δb (M^{-1} s^{-1})	$10^{-6}/\Delta b$ (M s)
0	10	75.352±0.666	47.169±0.666	0.212±0.173	0	∞
10	5	8.503±0.968	8.510±0.273	1.175±0.135	3.886±0.453	2.573±0.184
20	5	8.482±1.122	5.851±0.198	1.709±0.257	4.132±0.325	2.420±0.151
40	5	8.655±0.975	5.637±0.252	1.774±0.332	4.138±0.381	2.421±0.138
60	5	8.237±0.996	5.531±0.235	1.808±0.277	4.135±0.434	2.418±0.134
80	5	8.108±1.677	5.396±0.262	1.853±0.248	4.144±0.516	2.413±0.173
100	5	7.233±0.987	5.032±0.255	1.987±0.274	4.174±0.457	2.395±0.162

Fluoremetric Analysis of Enzyme Inhibitor Interactions

From the crystallographic data (Wlodawer et al., 1989; Miller et al., 1989; Erickson et al., 1990; Fitzerald et al., 1990), it is clear that a large conformational change in the substrate-binding flap region of HIV-1 PR attends due to the binding of a peptide-analogue inhibitor. These flaps consist of two identical, symmetrical peptide loops of the sequence $Met_{(1)47}$-$Gly_{(1)48}$-$Gly_{(1)49}$-$Ile_{(1)50}$-$Gly_{(1)51}$-$Gly_{(1)52}$-$Phe_{(1)53}$ and are contributed by each of the two monomers of the protease. Binding of a substrate analogue to HIV-1 PR effects the movement of atoms by as much as 7 Å in this region of the protein, while other domains of the enzymes are relatively immobile (Miller et al., 1989). The sequence data of the HIV-1 PR indicated the presence of four Trp residues A-6, A-42, B-6, and B-42, two on each monomer of the enzyme (Rutenber et al., 1993). The visualization and accessibility calculations of these Trp residues revealed that they are present on the surface of the enzyme and thus are excellent probes to monitor the changes in the tertiary structure due to ligand binding. Therefore, the conformational changes induced in the HIV-1 PR upon binding of ATBI, were monitored by exploiting the intrinsic fluorescence by excitation of the π - π^* transition in the Trp residues. The fluorescence emission spectra of the HIV-1 PR exhibited an emission maxima (λ_{max}) at ~342 nm as a result of the radiative decay of the π - π^* transition from the Trp residues confirming the hydrophilic nature of the Trp environment. The titration of the native enzyme with increasing concentrations of ATBI resulted in a concentration dependent quenching of the tryptophanyl fluorescence (Figure 3a). However, the λ_{max} of the fluorescence profile indicated no blue or red shift revealing

that the ligand binding caused reduction in the intrinsic protein fluorescence without disturbing the gross three dimensional structure.

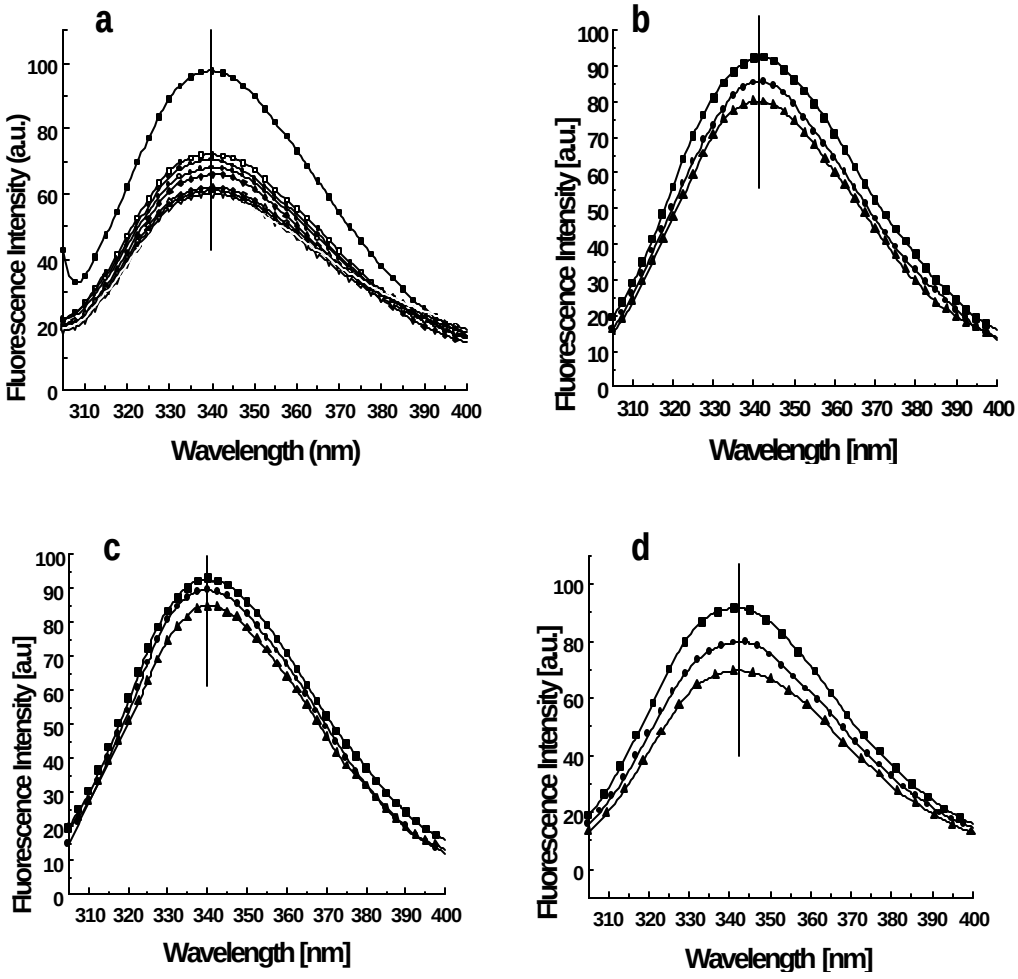

Figure 3. Fluorescence emission spectra of the purified HIV-1 PR

a) The HIV-1 PR (25 μg/ml) was dissolved in 50 mM sodium acetate buffer (pH 5.6) containing 100 mM NaCl, 5 mM EDTA, 5 mM β-mercaptoethanol. The concentrations of ATBI were 0 nM (■), 10 nM (□), 15 nM (●), 20 nM (○), 25 nM (◆), 40 nM (◇), 45 nM (▲), and 50 nM (△). b) Fluorescence spectra of HIV-1 PR in the absence (■) or presence of the synthetic substrate at concentrations, 25 μM (●) and 50 μM (▲). c) Fluorescence quenching spectra of HIV-1 PR in the absence (■) or presence of the 25 μM (●) and 50 μM (▲) of the inhibitor, N-Acetyl-Leu-Val-Phe-Al. d) Effect of Pepstatin on the fluorescence spectra of HIV-1 PR at concentrations, 0 μM (■), 25 μM (●), and 50 μM (▲)

Further to throw light into the mechanism of inactivation of the HIV-1 PR by ATBI, we have analyzed the interaction of two representative competitive inhibitors, N-Acetyl-Leu-Val-Phe-Al (Sarubbi et al., 1993) (Fig. 3c) and Pepstatin (Richards et al., 1989) (Fig. 3d), by steady-state intrinsic fluorescence measurements. These inhibitors are known to bind at the active site of the enzyme and inhibit its proteolytic activity. The binding of the competitive inhibitors led to the decrease in the quantum yield of the tryptophanyl fluorescence as indicated by the quenching of the emission spectra of the HIV-1 PR (Fig 3 c & d). Further, binding of the substrate (Lys-Ala-Arg-Val-Nle-p-Nitro-Phe-Glu-Ala-Nle-Amide) to the HIV-1 PR also resulted in concentration dependent quenching

of the tryptophanyl fluorescence (Fig. 3b). Comparative analysis of the fluorescence spectra of the active site based inhibitors and the substrate revealed the similar changes in the fluorescence spectra of the HIV-1 PR, which suggested that ATBI binds in the active site of the enzyme.

Secondary Structural Analysis of Enzyme Substrate/Inhibitor Complexes

In order to evaluate the effects of the inhibitor on the secondary structure of the enzyme we have analyzed the CD spectra of HIV-1 PR-ATBI complex. The secondary structure contents of the HIV-1 PR as determined from the crystallographic data were 4.04% a-helix, 47.47% b-sheet, and 48.49% of aperiodic conformation (Rutenber et al., 1993). The estimated secondary structure contents from the CD analysis were 5% a-helix, 48% b-sheet, and 47% aperiodic structure, which are in total agreement with the crystallographic data. The circular dichroism spectrum of the HIV-1 PR-ATBI complex showed a pronounced shift in the negative band at 220 nm of the native enzyme to 225 nm (Figure 4). This shift reveals a subtle change in the secondary structure of the enzyme upon ligand binding. To elucidate the changes in the secondary structure of the enzyme-inhibitor complex we have compared this data with that of the HIV-1 PR-substrate complex. Interestingly, the changes induced in the secondary structure of HIV-1 PR due to the substrate binding, showed a similar pattern of negative ellipticity in the far-UV region as that of the HIV-1 PR-ATBI complex. These structural changes brought

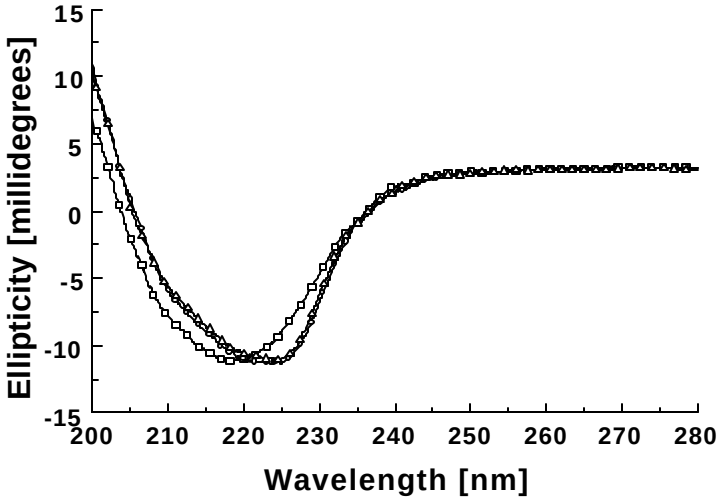

in the enzyme due to the binding of ATBI or the substrate was distinctly different from the unliganded form.

Figure 4. Effect of the secondary structure of the HIV-1 PR upon binding of the substrate or ATBI.

Far-UV circular dichroism spectra of the unliganded HIV-1 PR and its complexes with the substrate and ATBI. The HIV-1 PR (25 μg/ml) dissolved in the buffer (as described in the methods) and the CD spectra were recorded in the absence (□) or in the presence of the substrate 40 μM (○) or ATBI 20 nM (△) from 280-200 nm at 25°C. Each spectrum represents the average of six scans.

Discussions

The development of a new generation of protease inhibitors that effectively addresses the issue of resistance requires a better understanding of the interactions between the protease and inhibitors. Originally, the highly peptidic nature of these HIV PR inhibitors resulted in poor oral bioavailability and short half-lives *in vivo*, thus jeopardizing their use as therapeutic agents (De Clercq, 1995). However, manipulations of physicochemical properties (hydrophobicity/hydrophilicity, charge), reduction in size, elimination of peptide bonds, and formulation have led to compounds with enhanced oral absorption, allowing their advancement into clinical trials.

In the present chapter, we have described a spectrofluorometric approach towards investigating the interaction of the enzyme-inhibitor complex and the localized conformational changes induced in the HIV-1 PR upon binding of the non-competitive inhibitor ATBI. We have shown by analyzing the kinetic parameters of the interactions of the HIV-1 PR and the inhibitor that Michaelis-Menten kinetics cannot be applied for this inhibition study. The failure of substrate protection against HIV-1 PR inhibition by ATBI and the non-dissociative nature of the HIV-1 PR-ATBI complex with multiple dilutions and washings led us to apply tight binding inhibition kinetics. The short time observed for the inhibition, mandated performance of the kinetics under second-order rate conditions. Observed a and b values for ATBI were independent of the substrate concentration and relatively constant inferring that the binding of the inhibitor was not influenced by the presence of the substrate. However, a typical rectangular hyperbola resulted in a reciprocal plot of $1/b$ versus [S]. We have concluded by using a diagnostic plot of Δb versus [S], that the inactivation of the HIV-1 PR by ATBI was non-competitive.

Deciphering the crystal structure of the HIV-1 PR and its inhibitor complexes has gained immense interest amongst the crystallographers in the last decade. From the available crystallographic data, it is deduced that binding of substrate or peptide-analogue inhibitors in the substrate-binding site of HIV-1 PR induces conformational changes in the flaps (Pearl and Taylor, 1987; Rodriguez et al., 1993; Erickson et al., 1990). The crystal structure of the HIV-1 PR also suggested that the interaction between the backbone and side chain involving the flap contribute to the protease activity (Miller et al., 1989; Wlodawer and Erickson, 1993; Jaskolski et al., 1991). It must move away from the active site to allow the entry of substrate and the exit of products. In the down position, interacting with substrate, the two flaps of the dimer PR coordinate a water molecule that helps position the substrate for catalysis. The apparent function of these flaps is to force the peptide substrate into a b-sheet in the active site and to correctly position its scissile bond between the two catalytic aspartyl residues. The flaps accomplish this by the establishment of a series of hydrogen-bonding interactions between amide nitrogens and carbonyl oxygens of the peptide substrate, glycine residues in the flaps, and a water molecule which bridges, by formation of a hydrogen-bonding tetrahedron involving two carbonyl oxygens of the peptide (inhibitor or substrate) to the amide nitrogens of Ile-50 and Ile-150. Our interpretation for the changes observed in the secondary structure of the HIV-1 PR due to the binding of the substrate to the active site can be correlated to the inward movement of the flaps. It is significant to note that, the secondary structure of the HIV-1 PR undergoes

almost similar pattern of changes upon binding of the substrate or inhibitor. Thus, we have attributed the observed secondary structure changes in the HIV-1 PR-ATBI complex to the inward movement of the flaps of the HIV-1 PR. The non-competitive nature of the inhibitor may be addressed due to the better binding affinity of the inhibitor to the active site than the substrate. This however does not exclude the possibility of the differential binding pockets for the inhibitor and the substrate in the active site of the enzyme.

The tryptophanyl fluorescence appears to be uniquely sensitive to shielding by a variety of ligands because of the propensity of the excited indole nucleus to emit energy in the excited state. This phenomenon can be gainfully exploited to study the changes in the environment of the tryptophan residues of proteins. The Trp residues (A-42 and B-42) of the HIV-1 PR are present next to the Lys-43, the first residue of the flap region, which extends from Lys-43 to Arg-57 (Fig. 5). There have been reports of introducing Trp residue, which would act as a highly specific reporter in order to monitor the structural changes in the flap regions by substrate/inhibitor binding (Rodriguez et al., 1993). However, the site directed mutagenesis studies of the HIV-1 PR have revealed that the enzymatic activity is extremely sensitive to mutations in the flap-regions ([a]Loeb et al., 1989). The inhibitors that bind to the active site also bind to the inner face of the flaps of the HIV-1 PR. The binding of the inhibitor/substrate and the subsequent movement of the flaps may have influence on the intrinsic fluorescence of the Trp-42 residues. Based on the above assumption we have exploited these two Trp residues of the HIV-1 PR to investigate the localized conformational changes induced upon substrate or inhibitor binding. Our foregoing results have suggested that ATBI binds in the active site of the enzyme and is a unique example where the conformational changes in the flaps were investigated by monitoring the radiative decay of the π - π^* transition from the Trp residues without mutating any of the residue in the flaps. The fluorescence quenching of the HIV-1 PR by ATBI revealed that the binding of the inhibitor reduces the quantum yield of the Trp emission. These results were further corroborated by the quenching studies of the HIV-1 PR in the presence of the substrate and the known competitive inhibitors. The inhibition of the HIV-1 PR by N-Acetyl-Leu-Val-Phe-Al and Pepstatin is well documented. The quenching of the tryptophanyl fluorescence upon binding of the substrate or the active site inhibitors can be very well explained by the shielding effect of the Trp residues due to the inward movement of the flaps. The comparison of the emission spectra of the HIV-1 PR upon binding of ATBI with that of the substrate or the active site inhibitors led us to conclude that ATBI binds to the active site of the enzyme and induces the inward movement of the flaps thereby reduces the radiative decay of the intrinsic Trp fluorescence. The concentration dependent quenching of Trp fluorescence showed that, λ_{max} did not undergo any red or blue shift, wherein the quenching of fluorescence was considerably high. These findings indicated that the polarity of the Trp environment was negligibly altered after binding of the inhibitor, suggesting minimal conformational changes in the tertiary structure of the HIV-1 PR.

Majority of the inhibitors of HIV-1 PR are of hydrophobic in nature. There is a scarcity of hydrophilic peptidic inhibitors of HIV-1 PR, which will have significant importance for the bioavailability of the drug. Inhibition

of the HIV-1 PR by the hydrophilic peptides derived from the transframe region (TFR) of *gag-pol* has been reported (Louis et al., 1998). The transframe octapeptide (TFP) Phe-Leu-Arg-Glu-Asp-Leu-Ala-Phe, the N-terminus of the TFR and its analogues are competitive inhibitors of the mature HIV-1 PR. The smallest and most potent analogues are the tripeptides Glu-Asp-Leu and Glu-Asp-Phe, with the K_i values ~50 and ~20 μM respectively. Substitution of the acidic amino acids in the TFP by neutral amino acids and D or retro-D configurations of Glu-Asp-Leu resulted in >40-fold increase in K_i. Glu-Asp-Leu is extremely soluble in water, and its binding affinity decreases with increasing concentration of NaCl. The potency of this tripeptide is comparable to that of pepstatin A and its analogues, the best-known inhibitors of aspartic proteases (Tropea et al. 1992; Huff, 1991; Rich, 1985). The X-ray crystallographic studies showed the interactions of Glu at P2 and Leu at P1 of Glu-Asp-Leu with residues of the active site of the HIV-1 PR. As a hydrophilic inhibitor containing residues Asp, Ala, and Glu, ATBI may have similar mode of interactions with the residues in the active site of the HIV-1 PR as that of the TFP but it is not feasible to understand the interactions in atomic level at present. However, the crystal structure will impart light to understand the mechanism of inactivation of the HIV-1 PR by ATBI. With the existing experimental evidences we visualize that the charged side chains of the amino acids, the amide nitrogens and the carbonyl oxygen groups of ATBI could form many inter molecular hydrogen bonds and other weak interactions (van der Waals, ionic, etc.) with the β-sheet of the flaps and with the other residues present in or near the active site. Further, we propose that the tight binding and non-competitive nature of ATBI in conjunction with the multiple non-bonded interactions may be sufficient to cause the loss of the dynamic flexibility of the flaps, which is crucial for the substrate binding and catalysis of the enzyme. A schematic diagram representing the proposed mechanism is depicted in the Fig. 5. The non-competitive nature of the ATBI indicated that the inhibitor-complexed form of the HIV-1 PR loses its binding ability to the substrate, as the flaps can no more open up for the substrate to be aligned in the active site of the HIV-1 PR which subsequently results in the inactivation of the enzyme. These observations are in variance with the binding of the substrate to the enzyme in the absence of ATBI, where the flexibility of the flaps can be regained after catalysis.

Inhibitors directed towards the active site of the HIV-1 PR are well documented (Swain et al., 1990; Jaskolski et al., 1991). The substrate based inhibitors of HIV-1 PR face the acute problem of HIV drug resistance caused by active site mutations, a problem which prevents the long-term use of PR inhibitors as anti-HIV drugs (West and Feirlie, 1995; Deeks et al., 1997; Erickson and Burt, 1996). Despite, their loss in potency due to the spontaneous mutations occurring in the active site (Ermolief et al., 1997; Gulnik et al., 1995) leading towards the drug resistance behavior of the virus, there is a paucity of literature on non-competitive inhibitors. A constant search for the new class of HIV-1 PR inhibitors with high potency is a frontier area of biomedical research. The side chains of the peptidic inhibitor ATBI, which are capable of forming many non-bonded interactions (hydrogen bonding, van der Waals interactions, etc.) with the enzyme, might result in superior resistance characteristics in comparison to the competitive inhibitors. ATBI as proposed could interact with the backbone of the *b*-sheet of the

flaps of the HIV-1 PR thus eliminates the probability of drug resistance by single mutation. ATBI by virtue of its unique sequence and non-competitive mode of inhibition may represent a new class of inhibitors of the HIV-1 PR and could open up a new horizon for the development of lead molecules.

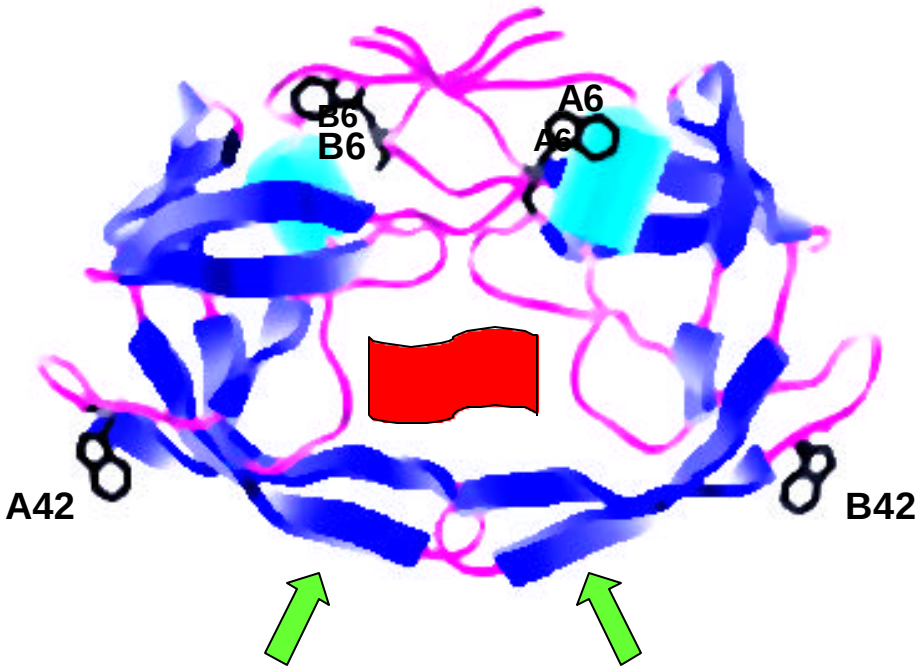

Figure 5. Schematic representation of the proposed mechanism of inhibition of the HIV-1 PR by ATBI.

Secondary structure of the HIV-1 PR as shown by the stereo-view ribbon diagram. The Trp residues A-42 and B-42 are adjacent to the flap region whereas the Trp residues A-6 and B-6 are far from the flap region. The HIV-1 PR and other retroviral proteases have the structural feature called "flap region" (shown in front of the arrows) which is important for the substrate binding and catalysis. The binding of the inhibitor (as indicated by the solid block) in the active site induces inward movement of the flaps (as indicated by the arrows). Further, we propose that the non-competitive nature of ATBI along with its multiple nonbonded interactions with the flaps is responsible for the loss of the dynamic flexibility of the flaps resulting in the inactivation of the HIV-1 PR. The structure of the HIV-1 PR is as described in the PDB ID 1 AID.

References

Adachi, A., Ono, N., Sakai, H., Ogawa, K., Shibata, R., Kiyomasu, T., Masuike, H., and Ueda, S. (1991) *Arch. Virol.* **117**, 45-58.

Andrade, M. A., Chacón, P., Merelo, J. J., and Morán, F. (1993) *Prot. Eng.* **6**, 383-390.

Ashorn, P., McQuade, T. J., Thaisrivong, S., Tomasselli, A. G., Tarpley, W. G., and Moss, B. (1990) *Proc. Natl. Acad. Sci. U. S. A.* **87**, 7472-7476.

Babe, L. M., Pichuantes, S., and Craik, C. S. (1991) *Biochemistry* **30**, 106-111.

Barlett, P. A., and Kezer, W. B. (1984) *J. Am. Chem. Soc.* **106**, 4282-4283.

Barre-Sinoussi, F., Cherman, J., Rey, J., Nurgerye, R., Chamaret, M., Gruest, S., Dauget, J., Axler-Blin, C., Fouzioux, F., Rosenbaum, C., and Montagnieer, L. (1983) *Science* **220**, 868-871.

Billich, S., Knoop, M.-T., Hansen, J., Strop, P., Sedlacek, J., Mertz, R., and Moelling, K. (1988) *J. Biol. Chem.* **263**, 17905-17908.

Blumenstein, J. J., Copeland, T. D., Oroszlan, S., and Michejda, C. J. (1989) *Biochem. Biophys. Res. Commun.* **163**, 980-987.

Blundell, T., and Pearl, L. A. (1989) *Nature* **337**, 596-597.

Braodhurst, A. V., Roberts, N. A., Ritchie, A. J., Handa, B. K., and Kay, J. (1991) *Anal. Biochem.* **193**, 280-286.

Brinkworth, R. I., Stoermer, M. J., and Fairlie, D. P. (1992) *Biochem. Biophys. Res. Com.* **188**, 631-637.

Cha, S. (1976) *Biochem. Pharmacol*. **25**, 2695-2702.

Chen, T. S., Doss, G. A., Hsu, A., Lingham, R. B., White, R. F., and Monaghan, R. L. (1993) *J. Nat. Prod.* **56**, 755-761.

[a]Cheng, Y.-S. E., Yin, F. H., Foundling, S., Blomstrom, D., and Kettner, C. A. (1990) *Proc. Natl. Acad. Sci. U. S. A.* **87**, 9660-9664.

[b]Cheng, Y.-S., McGowan, M. H., Kettner, C. A., Schloss, J. V., Erickson-Viitanen, S. and Yin, F. H. (1990) *Gene* **87**, 243-248.

Copeland, T. D, and Oroszlan, S. (1988) *Gene Anal. Technol.* **5**, 109-115.

Crowl, R., Seamans, C., Lomedico, P., and McAndrew, S. (1985) *Gene (Amst.)*, **38**, 31-38.

Cushman, M., Oh, Y.-I., Copeland, T. D., Snyder, S. W., and Oroszlan, S. (1990) *Ann. NY. Acad. Sci.* **616**, 503-507.

Dann, J. G., Stammers, D. K., Harris, C. J., Arrowsmith, R. J., Davies, D. E., Hardy, G. W., and Morton, J. A. (1986) *Biochem. Biophys. Res. Commun.* **134**, 71-77.

Darke, P. L., Leu, C. T., Davis, L. J., Heimbach, J. C., Diehl, R. E., Hill, W. S., Dixon, R. A., and Sigal, I. (1989) *J. Biol. Chem.* **264**, 2307-2312.

Darke, P. L., Nutt, R. F., Brady, S. F., Garsky, V. M., Ciccarone, T. M., Leu, C. T., Lumma, P. K., Freidinger, R. M., Veber, D. F., and Sigal, I. S. (1988) *Biochem. Biophys. Res. Commun.* **156**, 297-303.

Davies, D. R. (1990) *Annu. Rev. Biophys. Biophys. Chem*. **19**, 189-215.

De Clercq, E. (1995) *J. Med. Chem.* **38**, 2491-2517.

Debouck, C., and Metcalf, B. W. (1990) *Drug Des. Res*. **21**, 1-17.

Debouck, C., Gorniak, J. G., Strickler, J. E., Meek, T. D., Metcalf, B. W., and Rosenberg, M. (1987) *Proc. Natl. Acad. Sci. U. S. A.* **84**, 8903-8906.

Deeks, S. G., Smith, M., Holodniy, M., and Kahn, J. O. (1997) *J. Am. Med. Assoc.* **277**, 145-153.

DesJarlais, R. L., Seibel, G. L., Kuntz, I. D., Furth, P. S., Alavrez, J. C., Ortiz de Montellano, P. R., Decamp, D. L., Babe, L. M., and Craik, C. S. (1990) *Proc. Natl. Acad. Sci. U. S. A.* **87**, 6644-6648.

Dilanni, C. L., Davis, L. J., Holloway, M. K., Herber, W. K., Darke, P. L., Kohl, N. E., and Dixon, R. A. F. (1990) *J. Biol. Chem.* **265**, 17348-17354.

Dixon, M. (1953) *Biochem. J*. **55**, 170-171.

Dolak, L. A., Seest, E. P., Ciadella, J. I., and Bohanon, M. J. (1993) *Chem. Abstr.* **118**, 232376k.

Dreyer, G. B., Metcalf, B. W., Tomaszek, T. A., Carr, T. J., Chandler, A. C., Hyland, L., Fakhoury, S. A., Magaard, V. W., Moore, M. L., Strickler, H., Debouck, C., and Meek, T. D. (1989) *Proc. Natl. Acad. Sci. U. S. A.* **86**, 9752-9756.

Eftink, M. R. (1991) *Methods Biochem. Anal.* **35**, 127-205.

Dunn, B. M., Kay, J., Gutschina, A., and Wlodawer, A. (1994) *Methods Enzymol.* **241**, 254-278.

Erickson, J. W., and Burt, S. K. (1996) *Annu. Rev. Pharmacol. Toxicol.* **36**, 545-571.

Erickson, J., Neidhart, D. J., VanDrie, J., Kempf, D. J., Wang, X. C., Norbek, W., Platner, J. J., Rittenhouse, J. W., Toron, M., Wideburg, N., Kohlbrenner, W. E., Simmer, R., Helfrich, R., Paul, D. A., and Knigge, M. (1990) *Science* **49**, 527-533.

Ermolief, J., Lin, X., and Tang, J. (1997) *Biochemistry* **36**, 12364-12370

Farmerie, W. G., Loeb, D. D., Casavant, N. C., Hutchinson III, C. A., Edgell, M. H., and Swanstrom, R. (1987) *Science* **236**, 305-308.

Fitzgerald, P. M. D., and Springer, J. P. (1991) *Annu. Rev. Biophys. Biophys. Chem*. **20**, 299-320.

Fitzgerald, P. M., McKeever, B. M., VanMiddlesworth, J. F., Springer, J. P., Heimbach, J. C., Leu, C. T., Herber, W. K., Dixon, R. A., and Darke, P. L. (1990) *J. Biol. Chem.* **265**, 14209-14219.

Fredenhagen, A., Petersen, F. F., Tintelnot-Blomley, M., Rosel, J., Mett, H., and Hug, P. (1996) *J. Antibiot.* **50**, 395-401.

Gelb, M. H., and Abeles, R. H. (1985) *Biochemistry* **24**, 1813-1817.

Geoghegan, K. F., Spencer, R. W., Danley, D. E., Contillo Jr., L. G., and Andrews, G. C. (1990) *FEBS Lett.* **262**, 119-122.

Gigli, I., Mason, J. W., Colman, R. W., and Austen, K. F. (1970) *J. Immunol*. **104**, 574-581.

Goldfine, H., Harley, J. B., and Wake, J. A. (1978) *Biochim. Biophys. Acta.* **512**, 229-240.

Graves, M. C., Meidel, M. C., Pan, Y.-C., Manneberg, M., Lahm, H.-W., and Gruninger-Leitch, F. (1990) *Biochem. Biophys. Res. Commun.* **168**, 30-36.

Greenlee, W. J. (1990) *Med. Res. Rev.* **10**, 173-236.

Griffiths, J. T., Tomchak, L. A., Mills, J. S., Graves, M. C., Cook, N. D., Dunn, B. M., and Kay, J. (1994) *J. Biol. Chem*. **269**, 4787-4793.

Grobeiny, D., Wondrak, E. M., Galardy, R. E., and Orozslan, S. (1990) *Biochem. Biophys. Res. Commun.* **169**, 1111-1116.

Gulnik, S. V., Suvorov, L. I., Liu, B., Yu, B., Anderson, B., Mitsuya, H., and Erickson, J. W. (1995) *Biochemistry* **34**, 9282-9287.

Heimbach, J. C., Garsky, V. M., Michelson, S. R., Dixon, R. A., Sigal, I. S., and Darke, P. L. (1989) *Biochem. Biophys. Res. Commun.* **164**, 955-960.

Hellen, C. U. T., Krausslich, H.-G., and Wimmer, E. (1989) *Biochemistry* **28**, 9881-9890.

Henderson, P. J. F. (1972) *Biochem. J.* **127**, 321-333.

Holmes, D. S., Clemens, K. N., Cobley, K. N., Humber, D. C., Kitchin, J., Orr, D. C., Patel, B., Paternoster, I. L., and Storer, R. (1993) *Biomed. Chem. Lett.* **3**, 503-508.

Huff, J. R. (1991) *J. Med. Chem.* **34**, 2305-2314.

Hui, K. Y., Manetta, J. V., Gygi, T., Bowdom, B. J., Keith, K. A., Shannon, W. M., and Lai, M.-H. T. (1991) *FASEB J.* **5**, 259-262.

Humber, D. C., Cammack, N., Coates, J. A. V., Cobley, K. N., Orr, D. C., Storer, R., Weingrten, G. G., and Weir, M. P. (1992) *J. Med. Chem.* **35**, 3080-3081.

Hyland, L. J., Dayton, B. D., Moore, M. L., Shu, A. Y., Heys, J. R., and Meek, T. D. (1990) *Anal. Biochem.* **188**, 405-415.

Hyland, L. J., Tomaszek, T. A., and Meek, T. D. (1991) *Biochemistry* **30**, 8454-8463.

Ikuta, K., and Luftig R. B. (1986) *Virology* **154**, 195-206.

Jacks, T., Power, M. D., Masiarz, F. R., Luciw, P. A., Barr, P. J., and Varmus, H. E. (1988) *Nature*, **331**, 280-283.

James, M. N. G., Hsu, I.-N., and Delbaere, L. T. J. (1977) *Nature* **267**, 808-813.

Jaskolski, M., Tomasselli, A. G., Sawyer, T. K., Staples, D. G., Heinrikson, R. L., Schneider, J., Kent, S. B. H., and Wlodawer, A. (1991) *Biochemistry* **30**, 1600-1609.

Katoh, I., Yoshinaka, Y., and Luftig, R. B. (1986) *Virus Res.* **5**, 265-276.

Kay, J., and Dunn, B. M. (1990) *Biochim. Biophys. Acta*, **1048**, 1-18.

Kleinert, H. D., Baker, W. R., and Stein, H. H. (1991) *Adv. Pharmacol.* **22**, 207-250.

Kohl, N. E., Emini, E. A., Schleif, W. A., Davis, L. J., Heimbach, J. C., Dixon, R. A., Scolnick, E. M., and Sigal, I. (1988) *Proc. Natl. Acad. Sci. U. S. A.* **85**, 4686-4690.

Krausslich, H. G., Ingraham, R. H., Skoog, M. T., Wimmer, E., Pallai, P. V., and Carter, C. A., (1989) *Proc. Natl. Acad. Sci. U. S. A.* **85**, 807-811.

Kungl, A. J., Visser, N. V., van Hock, A., Visser, A. J. W. G., Billich, A., Schlilk, A., Gstach, H., and Auer, M. (1998) *Biochemistry* **37**, 2778-2786.

Lakowicz, J. R. (1983) In *"Principles of Fluorescence Spectroscopy 2"*, Plenum Press, New York/London.

Lapatto, R., Blundell, T., Hemmings, A., Overington, J., Wilderspin, A., Wood, S., Merson, J. K., Lee, S. E., Scheld, K. G., and Hobart, P. M. (1989) *Nature* **342**, 299-302.

Le Grice, S. J. F., Millis, J., and Mous, J. (1988) *EMBO J.* **7**, 2547-2553.

Lillehoj, E. P., Salazer, F. H. R., Mervis, R. J., Raum, M. G., Chan, H. W., Ahmad, N., and Venkatasan, S. (1988) *J. Virol.* **62**, 3053-3058.

Lingham, R. L., Hsu, A. H., Silverman, K. C., Bills, G. F., Dombrovski, A., Goldman, M. E., Darke, P. L., Huang, L., Koch, G., Ondeyka, J. G., and Goetz, M. A. (1992) *J. Antibiot.* **45**, 686-691.

[a]Loeb, D. D., Hutchison III, C. A., Edgell, M. H., Farmerie, W. G., and Swanstrom, R. (1989) *J. Virol.* **63**, 111-121.

[b]Loeb, D. D., Swanstrom, R., Everitt, L., Manchester, M., Stamper, S. E., and Hutchison III, C. A. (1989) *Nature* **340**, 397-400.

Louis, J. M., Dyda, F., Nashed, N. T., Kimmel, A. R., and Davies, D. R. (1998) *Biochemistry* **37**, 2105-2110.

Lyle, T. A., Wiscount, C. M., Guare, J. P., Thompson, W. J., Anderson, P. S., Darke, P. L., Zugay, J. A., Emini, E. A., Schleif, W. A., Quintero, J. C., Dixon, R. A. F., Sigal, I. S., and Huff, J. R. (1991) *J. Med. Chem.* **34**, 1228-1230.

Matoyoshi, E. D., Wang, G. T., Kraft, G. A., and Erickson, J. (1990) *Science* **247**, 954-958.

McQuade, T. J., Tomasselli, A. G., Liu, L., Karacostas, V., Moss, B., Sawyer, T. K., Heinrikson, R. L., and Tarpley, W. G. (1990) *Science* **247**, 454-456.

Meek, T. D., Dayton, B. D., Metcalf, B. W., Drayer, G. B., Strickeler, J. E., Gorniak, J. G., Rosenberge, M., Moore, M. L., Magaard, V. W., and Debouck, C. (1980) *Proc. Natl. Acad. Sci. U. S. A.* **86**, 1841-1845

Meek, T. D., Lambert, D. M., Metcalf, B. W., Petteway Jr., S. R., and Dreyer, G. H. (1990) In *"Design of Anti-AIDS Drugs"* (E. DeClereq, Eds.), Elsevier, Amsterdam, pp 225-256.

Merelo, J. J., Andrade, M. A., Prieto, A., and Morán, F. (1994) *Neurocomputing* **6**, 443-454.

Miller, M., Schneider, J., Sathyanarayan, B. K., Toth, M. V., Marshall, G. R., Clawson, L., Selk, L., Kent, S. B., and Wlodawer, A. (1989) *Science* **246**, 1149-1152.

Mizrahi, V., Lazarus, G. M., Miles, L. M., Meyres, C. A., and Debouck, C. (1989) *Arch. Biochem. Biophys.* **273**, 347-358.

Mitsuya, H., Yarchoan, R., Kageyama, S., and Broder, S. (1991) *FASEB J.* **5**, 2369-2381.

Moelling, K., Schulze, T., Knoop, M.-T., Kay, J., Jupp, R., Nicolaou, G., and Pearl, L. (1990) *FEBS Lett.* **261**, 373-377.

Moore, M. L., Bryan, W. M., Fakhoury, S. A., Magaard, V. W., Huffman, W, F., Dayton, B. D., Meek, T. D., Hyland, L., Dreyer, G. B., Metcalf, B. W., Strickler, J. E., Gorniak, J. G., and Debouck, C. (1989) *Biochem. Biophys. Res. Commun.* **159**, 420-425.

Muessing, M. A., Smith, D. H., Cabradilla, C. D., Benton, C. V., Lasky, L. A., and Capon, D. J. (1985) *Nature* **313**, 450-458.

Muirhead, G. J., Shaw, T., Williams, P. E. O., Madigan, A. M., Mitchell, A. C., and Houston, A. C. (1992) *Brit. J. Clin. Pharmacol.* **34**, 170P-171P.

Nashed, N. T., Louis, J. M., Sayer, J. M., Wondrak, E. M., Mora, P. T., Oroszlan, S., and Jerina, D. M. (1989) *Biochem. Biophys. Res. Commun.* **163**, 1079-1085.

Navia, M. A., Filtzgerald, P. M., McKeever, B. M., Leu, C. T., Heimbach, J. C., Herber, W. K., Sigal, I. S., Darke, P. L., and Springer, J. P. (1989) *Nature* **337**, 615-620.

Ocain, T. D., and Abou-Gharbia, M. (1991) *Drugs Future* **16**, 37-51.

Onsura, S. (1976) *Bacteriol. Rev.* **40**, 681-697.

Oroszlan, S., and Luftig, R. B. (1991) *Curr. Top. Microbiol. Immunol.* **157**, 153-185.

Pal, S. R., Gallo, R. C., and Sarmagadharan, M. G. (1988) *Proc. Natl. Acad. Sci. U. S. A.* **85**, 9283-9286.

Patil, A. D., Kokke, W. C., Cochran, S., Francis, T. A., Tomaszek, T., and Westley, J. W. (1992) *J. Nat. Prod.* **55**, 1170-1177.

Pearl, L. H., and Taylor, W. R. (1987) *Nature* **329**, 351-354.

Phylip, L. H., Richards, A. D., Kay, J., Konvolinka, J., Strap, P., Blaha, I., Velek, J., Kostka, V., Ritchia, A. J., Farmerie, W. G., Scarborough, P. E., and Dunn, B. M. (1990) *Biochem. Biophys. Res. Com*. **171**, 439-444.

Rao, J. K. M., Erickson, J. W., and Wlodawer, A. (1991) *Biochemistry* **30**, 4663-4671.

Ratner, L., Haseltine, W., Patarca, R., Livak, K. J., Starcich, B., Josephs, S. F., Doran, E. R., Rafalski, J. A., Whitehorn, E. A., Baumeister, K., Ivonoff, L., Petteway, S. R. Jr., Pearson, M. L., Lautenberger, J. A., Papas, T. S., Ghrayeb, J., Chang, N. T., Gallo, R. C., and Wong-Stall, F. (1985) *Nature* **313**, 277-284.

Rich, D. (1985) *J. Med. Chem.* **28**, 263-273.

Rich, D. H., Sun, C.-Q., Prasad, V. J. V. N., Pathiasseril, A., Toth, M. V., Marshall, G. R., Clare, M., Mueller, R. A., and Houseman, K. (1991) *J. Med. Chem.* **34**, 1222-1225.

Rich, D., Green, J. Toth, M. W., Marshal, G. R., and Kent, S. B. H. (1990) *J. Med. Chem.* **33**, 1285-1288.

Richards, A. D., Phylip, L. H., Farmerie, W. G., Scarborough, P. E., Alvarez, A., Dunn, B. M., Hirel, P., Pavlickova, L., Kostka, V., and Kay, J. (1990) *J. Biol. Chem*. **265**, 7733-7736.

Richards, A. D., Roberts, R., Dunn, B. M., Graves, M. C., and Kay, J. (1989) *FEBS Lett.* **247**, 113-117.

Rittenhouse, J., Turon, M. C., Helfrich, R. J., Albrecht, K. S., Weigel, D., Simmer, R. L., Mordinin, F., Erickson, J., and Kohlbrener, W. E. (1990) *Biochem. Biophys. Res. Commun.***171**, 60-66.

Roberts, N. A., Martin, J. A., Kinchington, C., Broadhurst, A. V., Craig, J. C., Duncan, I. B., Galpin, S. A., Handa, K., Kay, J., Krohm, A., Lambert, R. W., Merrett, J. H., Mills, J. S., Parkes, K. E. B\\., Redshaw, S., Ritchie, A. J., Taylor, D. L., Thomas, G. J., and Machin, P. J. (1990) *Science* **248**, 358-361.

Rodriguez, E. J., Debouck, C., Deckmann, I. C., Abu-Soud, H., Raushel, F. M., and Meek, T. D. (1993) *Biochemistry* **32**, 3557-3563.

Roggo, B. E., Peterson, F., Delmendo, R., Jenny, H. B., Peter, H. H., and Roesel, J. (1994) *J. Antibiot.* **47**, 136-142.

Rutenber, E., Fauman, E. B., Keenan, R. J., Fong, S., Furth, P. S., Ortiz de Montellano, P. R., Meng, E., Kuntz, I. D., DeCamp, D. L., Salto, R., Rose, J. R., Craik, C. S., and Stroud, R. M. (1993) *J. Biol. Chem*. **268**, 15343-15346, and Sec. structure as given by RCSB PDB home page: http://www.rcsb.org/pdb/ of HIV-1 PR as in PDB ID. 1AID.

Sanchez-Pescador, R., Power, M. D., Barr, P. J., Steimer, K. J., Stempien, M. M., Brown-Shimers, S. L., Gee, W. W., Renard, A., Randolph, A., Levy, J. A., Dina, D., and Luciw, P. A. (1985) *Science* **277**, 484-492.

Sarubbi, E., Nolli, M. L., Andronico, F., Stella, S., Saddler, G., Selva, E., Siccardi, A., and Denaro, M. (1991) *FEBS Lett.* **2**, 265-269.

Sarubbi, E., Seneci, P. F., Angelastro, M. R., Peet, N. P., Denaro, M., and Islam, K. (1993) *FEBS Lett*. **319**, 253-256

Schneider, J., and Kent, S. (1988) *Cell* **54**, 363-368.

Schramm, H. J., Nakashima, H., Scramm, W., Wakayama, H., and Yamamoto, N. (1991) *Biochem. Biophys. Res. Commun.* **179**, 847-851.

Seelmeier, S., Schmidt, H., Turk, V., and von der Helm, K. (1988) *Proc. Natl. Acad. Sci. U. S. A.* **85**, 6612-6616.

Sham, H. L., Betebenner, D. A., Wideburg, N. E., Saldivar, A. C., Kohlbrenner, W. E., Vasavanonda, S., Kempf, D. J., Norbeck, D. W., Zhao, C., Clement, J. J., Erickson, J. E., and Plattner, J. J. (1991) *Biochem. Biophys. Res. Commun.* **175**, 914-919.

Shaw, T., Muirhead, G. J., Parish, N., McClelland, G. R., and Houston, A. C. (1992) *Brit. J. Clin. Pharmacol.* **34**, 166P-167P.

Steiner, R. F. (1991) in *"Topics in Fluorescence Spectroscopy 2 "*(Lakowicz, J. R. Eds.) Plenum Press, New York/London.

Strickler, J. E., Gorniak, J. G., Dayton, B., Meek, T. D., Moore, M., Magaard, V. Malinowski, J. and Debouck, C. (1989) *Proteins* **6**, 139-154.

Swain, A. L., Miller, M. M., Green, J., Rich, D. H., Schneider, J., Kent, S. B., and Wlodawer, A. (1990) *Proc. Natl. Acad. Sci. U. S. A.* **87**, 8805-8809.

Szelke, M. (1985) In *"Aspartic Proteinases and Their Inhibitors"* (de Gruyter Eds.) Berlin, pp 421-441.

Szelke, M., Leekie, B., Hallet, A., Jones, D. M., Suetras, J., Atrash, B., and Lever, A. F. (1982) *Nature* **299**, 555-557.

Tamburini, P. P., Dreyer, R. N., Hansen, J., Letsinger, J., Elting, J., Gore-Willse, A., Dally, R., Hanko, R., Osterman, D., Kamarck, M. E., and You-Waren, H. (1990) *Anal. Biochem.* **186**, 363-368.

Thaisrivong, S., Tomasselli, A. G., Moon, J. B., Hui, J., McQuade, T. J., Turner, S. R., Strohback, J. W., Howe, W. J., Tarpley, W. G., and Heinrikson, R. L. (1991) *J. Med. Chem.* **34**, 2344-2356.

Thaisrivongs, S., Pals, D. T., Kati, W. M., Turner, S. R., and Thomasco, L. M. (1985) *J. Med. Chem.* **28**, 1553-1555.

Thaisrivongs, S., Pals, D. T., Kroll, L. T., Turner, S. R., and Hans, F.-S. (1987) *J. Med. Chem.* **30**, 976-982.

Toh, H., Ono, M., Saigo, K., and Miyata, T. (1985) *Nature* **245**, 626-621.

Tomasselli, A. G., Howe, W. J., Sawer, T. K., Wlodawer, A., and Heinrickson, R. L. (1991) *Chem. Today* **9**, 6-27.

Tomasselli, A. G., Olsen, M. K., Hui, J. O., Staples, D. J., Sawyer, T. K., Heinrickson, R. L., and Tomich, C. S. (1990) *Biochemistry* **29**, 243-248.

Tomaszek, T. A., Magaard, V. W., Bryan, H. G., Moore, M. L., and Meek, T. D. (1990) *Biochem. Biophys. Res. Commun.* **168**, 274-280.

Toth, M. V., and Marshall, G. (1990) *Int. J. Peptide Protein Res.* **36**, 544-550.

Tropea, J. D., Nashed, N. T., Louis, J. M., Sayer, J. M., and Jerina, D. M. (1992) *Bioorg. Chem.* **20**, 67-76.

Umezawa, H., Aoyagi, T., Morishima, H., Matsuzaki, M., Hamada, M., and Takeuchi, T. (1970) *J. Antibiot.* **3**, 259-262.

Vacca, J. P., Guare, J. P., deSolms, S. J., Sanders, W. M., Gruhani, E. A., Young, S. D., Darke, P. L., Zugay, J., Sigal, I. S., Schleif, W. A., Quintero, J. C., Emini, E. A., Anderson, P. S., and Huff, J. R. (1991) *J. Med. Chem.* **34**, 1225-1228.

Wain-Hobson, S., Sonigo, P., Danos, O., Cole, S., and Alizon, M. (1985) *Cell* **40**, 9-17.

Wang, G. T., Matayoshi, E., Huffaker, H. J., and Kraft, G. A. (1990) *Tetrahedron Lett.* **45**, 6493-6496.

Weber, I. T. (1990) *J. Biol. Chem.* **265**, 10492-10496.

Weber, I. T., Miller, M., Jaskolski, M., Leis, J., Skalka, A. M., and Wlodawer, A. (1989) *Science* **243**, 928-931.

West, M. L., and Fairlie, D. P. (1995) *Trends Pharm. Sci.* **16**, 67-75.

Williams, P. E. O., Muirhead, G. J., Madigan, M. J., Mitchel, A. M., and Shaw, T. (1992) *Brit. J. Clin. Pharmacol.* **34**, 155P-156P.

Wlodawer, A., and Erickson, J. W. (1993) *Annu. Rev. Biochem.* **62**, 543-585.

Wlodawer, A., Miller, M., Jaskolski, M., Sathyanarayan, B. K., Baldwin, E., Weber, I. T., Selk, L. M., Clawson, L., Schneider, J., and Kent, S. B. (1989) *Science* **245**, 616-621.

Wolfenden, R. (1976) *Annu. Rev. Biophys. Bioeng.* **5**, 271-306.

Wondrak, E. M., Copeland, T. D., Louis, J. M., and Oroszlan, S. (1990) *Anal. Biochem.* **188**, 82-85.

Wondrak, E. M., Louis, J. M., Mora, P. T., and Oroszlan, S. (1991) *FEBS Lett.* **280**, 347-350.

Zhang, Z.-Y., Poorman, R. A., Maggiora, L. L., Heinrikson, R. L., and Kezdy, F. J. (1991) *J. Biol. Chem.* **266**, 15591-15594.

Zhang. Z.-Y., Reardon, I. M., Hui, J. O., O'Connell, K. l., Poorman, R. A., Tomasselli, A. G., and Heinrikson, R. L. (1991) *Biochemistry* **30**, 8717-8721.

Chapter 4

Structural and Mechanistic Insight into the Inhibition of Aspartic Proteases by ATBI

Summary

ATBI exhibited two-step inhibition mechanism against the aspartic proteases, pepsin and F-prot. The evaluation of kinetic parameters displayed competitive inhibition for pepsin and F-prot by ATBI. The progress-curves for the degree of inhibition are time-dependent and consistent with a two-step, slow-tight binding inhibition mechanism:

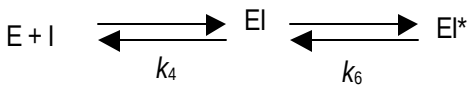

The K_i values associated with the formation of the first reversible complex (EI) of ATBI with pepsin and F-prot, were 17±0.5 x 10^{-9} M and 3.2±0.6 x 10^{-6} M, whereas the overall inhibition constant K_i* values were 55±0.5 x 10^{-12} M and 5.2±0.6 x 10^{-8} M, respectively. The rate constant k_5, determining the slow inhibition revealed a faster isomerization rate of the initial reversible enzyme-inhibitor complex, EI, for F-prot (2.3±0.4 x 10^{-3} sec^{-1}) than pepsin (7.7±0.3 x 10^{-4} sec^{-1}). However, ATBI dissociated from the tight enzyme-inhibitor complex (EI*) of F-prot faster (3.8±0.5 x 10^{-5} sec^{-1}) than pepsin (2.5±0.4 x 10^{-6} sec^{-1}). Comparative analysis of the kinetic parameters with pepstatin, the known inhibitor of pepsin, revealed a higher value of k_5/k_6 for ATBI. The binding of the inhibitor with the aspartic proteases and the subsequent conformational changes induced, were monitored by exploiting the intrinsic tryptophanyl fluorescence. The rate constants derived from the fluorescence data were in agreement with those obtained from the kinetic analysis, therefore the induced conformational changes were correlated to the isomerization of EI to EI*. Chemical modification of the Asp or Glu by WRK and Lys residues by TNBS abolished the anti-proteolytic activity and revealed the involvement of two carboxyl and one amine group of ATBI in the enzymatic inactivation.

Introduction

Enzyme inhibitors with specificity for a target enzyme are of interest for two general reasons. On one hand, they are useful probes of the kinetic and chemical mechanisms of enzyme-catalyzed reactions. On the other hand, their action provides background information for the development of specific bioactive compounds whose action may be beneficial to patients as chemotherapeutic agents. Of particular importance in these connections are compounds that act as inhibitory analogs of substrates and have high affinities for enzymes with K_i values in nanomolar range and less. The classification of inhibitors depends on the reversibility, strength, and rates of their interaction with enzyme. The four categories of reversible inhibitors are classical, tight-binding, slow-binding, and slow, tight-binding inhibitors (Morrison, 1982). The categories are generally differentiable based on the ratio of total inhibitor (I_t) to total enzyme (E_t) under experimental conditions and the qualitative time required for attainment of the equilibrium between the enzyme, inhibitor, and enzyme-inhibitor complex. The classification is essentially for inhibitors whose actions cannot be described by Michaelis-Menten kinetics. For classical reversible inhibitors, the affinity for the inhibitor is sufficiently low that $I_t >> E_t$ and the rates at which the inhibitor associate and dissociate from the enzyme are relatively high. When the affinity of an enzyme for the inhibitor is very high, tight-binding situations arise, then the experiment would be performed in concentration regimes where $I_t \cong E_t$. Under such conditions steady-state treatments are inadequate and incorrect, even though the net binding and release of inhibitors may be described by fast steps (Morrison, 1969; Henderson, 1972; Cha, 1975; Cha 1976).

There have been some development of the kinetic theory for tight-binding inhibitors (Goldstein, 1944; Strauss and Goldstein, 1943; Ackermann and Potter, 1949; Reiner, 1959; Eason and Stedman, 1936), but few studies have been undertaken in sufficient detail to test the theoretical predictions. The future development of tight-biding inhibitors for chemotherapeutic purpose will undoubtedly depend on application of kinetic techniques that yield quantitative information about the behavior of the inhibitors. When the structure of tight-binding inhibitor can be correlated with the dissociation constants for the enzyme-inhibitor complexes, a systematic approach can be made towards the synthesis of more effective inhibitors for a particular enzyme. Delineating the inhibition mechanism and understanding of the binding efficiency will thus provide further insight into their *in vivo* efficacy.

While classical and tight-binding inhibitors have been recognized for a very long time, awareness of compounds that cause inhibition of enzymes in a time-dependent manner is much more recent (Morrison, 1982; Cha et al., 1975; Cha, 1976; Williams and Morrison, 1979). A number of enzymatic reactions do not respond to the presence of competitive inhibitors instantly, but rather display a slow-onset of the inhibition. In some cases the inhibitor interacts slowly with the enzyme, in others the formation of the enzyme-inhibitor complex takes place in a very short time. Such inhibition is called slow-binding inhibition and the inhibitor is refereed to as slow-binding inhibitor (Williams and Morrison, 1979; Szedlacsek and Duggleby, 1995; Sculley et al., 1996). From the kinetic

point of view, the possible mechanisms for the slow-binding inhibition phenomena are described in Scheme I. Scheme 1 a assumes that the formation of an EI complex is a single slow step and the magnitude of k_3I is quite small relative to the rate constants for the conversion of substrate to product. However, scheme I b demonstrates the two-step slow-binding inhibition, where the first step involves the rapid formation of a reversible EI complex, which undergoes slow isomerization to a stable, tightly bound enzyme-inhibitor complex, EI* in the second step. The two-step mechanism of inhibition can be considered as the prototype of slow-binding inhibition on a steady-state time scale. The ratio between the kinetic constants of k_5/k_6 can be taken as an index of the accumulation of E.I* and the energetic of its formation. The higher the values of k_5/k_6 ratio, the longer-lived is the E.I* and the more likely the inhibitor is to have a useful *in vivo* lifetime. The weakness in the use of classical enzyme inhibitors as drugs of clinical condition is that enzyme inhibition results in the upstream accumulation of the substrate for the enzyme, which has an impact on the isomerization of E.I* to E.I and hence reversal of the inhibition which will be of immense value in clinical applications. Inhibitors, which inhibit the enzyme-catalyzed reactions at concentrations comparable to that of the enzyme and under conditions where the equilibria are set up rapidly, are referred as tight binding inhibitors. The establishment of the equilibria between enzyme, inhibitor, and enzyme-inhibitor complexes, in slow binding inhibition occurs slowly on the steady-state time scale (Morrison, 1982), which has been thoroughly reviewed (Morisson and Walsh, 1988; Yiallouros et al., 1999; Ploux et al., 1999; Merker et al., 1990; Pegg and Itzstein, 1994; Kati, et al., 1998). As yet, no general paradigm has emerged for relating inhibitor and/or enzyme structure which allows the predictions to be made about the design of compounds that would give rise to slow-binding inhibition. However, understanding the basis of the isomerization of EI complex to EI* complex could lead to design inhibitors that allow titration of the lifetime of the EI* complex. Early investigations of pepsin and the fungal aspartic proteases gave rise to a variety of mechanistic proposals, which were resolved in favor of the mechanisms shown in Scheme I (Suguna et al., 1987; James et al., 1992). The future development of slow-tight binding inhibitors will undoubtedly depend on application of kinetic techniques that yield quantitative information about the properties of the inhibitors.

An efficient inhibitor *in vivo* is characterized not only by its tight-binding but also by the rapid binding to prevent undesirable degradation of biological substrates during the formation of inhibitor complex. Considering the physiological importance of the aspartic proteases and their role in various diseases, there is a lacuna in the studies of slow binding inhibitors, which could provide greater insight into the inhibition mechanism and their *in vivo* efficacies. Investigations of the inhibition mechanism have generated enormous attention to unravel the interaction between potent inhibitors and the target enzymes. The best-known slow-biding inhibitor of pepsin is pepstatin (Umezawa et al., 1978), with the $t_{1/2}$ for the dissociation of pepstatin from pepsin is 2.5 h. This lifetime is long enough for medicinal chemists to proceed to incorporate the statyl group into design of inhibitors for other proteases such as renin. Several analogs of pepstatin have been prepared to analyze the structural features required to express slow, time-dependent onset of enzyme inhibition (Rich and Sun, 1980). There have been also

reports where two approaches have been combined in protease inhibitor design, by the use of a statyl-type residue along with a group that could accumulate as a stabilized tetrahedral (Gelb et al., 1985). However, the hydrophobic nature of pepstatin holds a disadvantage for its poor oral bioavailability.

Scheme I.

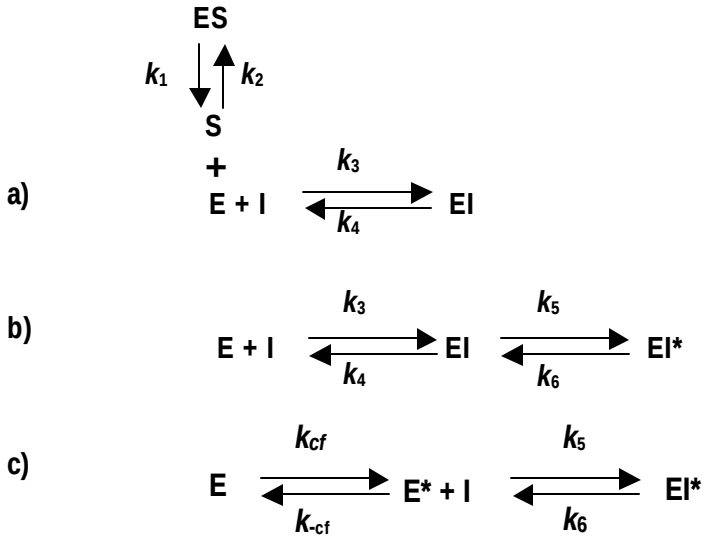

Where E stands for free enzyme, I is free inhibitor, EI is a rapidly forming pre-equilibrium complex and EI* is the final enzyme inhibitor complex. Binding between enzyme and inhibitor may either involve a single step, having a slow association and dissociation rates (Scheme I a) or have an initial fast binding step, followed by a slow reversible transformation of EI to another entity EI* (Scheme 1 b), or have an initial slow inter conversion of the enzym e E into another form E* which binds to the inhibitor by a fast step (Scheme 1 c).

`This chapter deals with the evaluation of the kinetic parameters of the slow-tight binding inhibition of the aspartic proteases pepsin from porcine gastric mucosa, and F-prot from the fungus *Aspergillus saitoi* by ATBI. ATBI exhibited time-dependent inhibition against both the enzymes with a two-step binding mechanism. The fluorescence studies revealed that the binding of ATBI induced localized conformational changes in the proteases, as reflected during the isomerization of the EI complex to EI* complex. Further, by chemical modification, we have assigned the residues of the inhibitor responsible for the enzyme inactivation

Materials and Methods

Materials

Pepsin, the F-prot, the aspartic protease from *Aspergillus saitoi*, and hemoglobin were from Sigma Chemical Co. U. S. A. N-Acetyl-L-pheneylalanyl-L-3,5-di-iodotyrosine, was form Aldrich Chemicals. All other buffer components and chemicals used were of analytical grade.

Enzyme assays

Pepsin Assay

Pepsin, 75 nM (porcine gastric mucosa) was incubated at 37°C for 30 min in KCl-HCl buffer, 0.02 M, and pH 2.0, with casein (6 mg/ml) or hemoglobin (5 mg/ml) in a reaction volume of 2 ml. The reaction was stopped with equal volume of 1.7 M perchloric acid (PCA), the mixture was centrifuged (10,000 g, 5 min) and filtered, and the optical absorbance of the filtrate was measured at 280 nm. The enzyme activity was also determined by the Folin-phenol reagent method by estimating the amount of tyrosine released at 660 nm from the standard graph. In the presence of the synthetic substrate, N-Acetyl-L-pheneylalanyl-L-3,5-di-iodotyrosine, pepsin was assayed as described by (Chiang et al., 1966), in incubation mixture containing a range of substrate concentrations.

Fungal Protease Assay

Proteolytic activity of the purified aspartic protease from *Aspergillus saitoi* (F-prot) was measured by assaying the enzyme activity using hemoglobin. 1.5 μM of F-prot was dissolved in Glycine-HCl buffer, 0.05 M, pH 3.0, was incubated with the inhibitor (20 μM) for 5 min. The reaction was started by the addition of 1 ml of hemoglobin (5 mg/ml) at 37°C for 30 min. The reaction was quenched by the addition of 2 ml of PCA (1.7 M) followed by centrifugation (10,000 g, 5 min) and filtration. The optical absorbance of the PCA soluble products in the filtrate was read at 280 nm.

For initial kinetic analysis, the kinetic parameters for the substrate hydrolysis were determined by measuring the initial rate of enzymatic activity. The inhibition constant K_i, was determined as described (Dixon et al., 1953) and by Lineweaver-Burk's equation and the K_m values were calculated from the double-reciprocal plots. In Dixon's method, proteolytic activity of the enzymes was measured at two different concentrations of substrate as a function of inhibitor concentration. The kinetic constants were determined by incubating the enzymes in the absence and presence of ATBI with increasing concentrations of the substrate. The inhibition of initial rate of enzyme activity was analyzed by the double reciprocal plot. One unit of protease activity is defined by an increase of 0.001 at Δ280 nm per min at pH 3.0 at 37°C measured as PCA soluble products using hemoglobin/casein as the substrate.

For the progress curve analysis, assays were carried out with 2 ml solutions containing the enzyme, substrate, and inhibitor at various concentrations. Five to six assays were performed in each slow-binding inhibition experiment: one without inhibitor and others with different inhibitor concentrations. At different time

intervals, aliquots were removed and the residual proteolytic activity was measured. Further details of the experiments are given in the respective figure legends. For the kinetic analysis and rate constant determinations, the assays were carried out in triplicates and the average value was considered throughout this work.

Evaluation of Kinetic Parameters

Initial rate studies that resulted reversible, competitive inhibition were analyzed according to the equation

$$v = \frac{K_m(1+I/K_i) + S}{V_{max}\,S} \qquad (1)$$

where K_m is the Michaelis constant, V_{max} is the maximal catalytic rate at saturating substrate concentration [S], K_i is the dissociation constant for the enzyme-inhibitor complex, and I is the inhibitor concentration (Cleland, 1979).

The progress curves for the interactions between ATBI and aspartic protease as per Scheme 1b were analyzed using the following equation (Beith, 1995; Morison and Stone, 1985):

$$[P] = v_s t + \frac{v_0 - v_s}{k}(1 - e^{-kt}) \qquad (2)$$

Where, [*P*] is the product concentration at any time t, v_0 and v_s are the initial and final steady-state rates and *k* is the apparent first-order rate constant for the establishment of the final steady-state equilibrium. For Scheme 1b, the relationship between *k*, the rate, and the kinetic constants is given by eq 3.

$$k = k_6 + k_5 \left[\frac{I / K_i}{1 + S / K_m + I / K_i} \right] \qquad (3)$$

The progress curves were fitted to eqs 2 and 3 using non-linear least-square parameter estimation to determine the best-fit values. The overall inhibition constant for Scheme 1b is defined as

$$K_i^* = \frac{[E][I]}{[EI] + [EI^*]} = K_i \left[\frac{k_6}{k_5 + k_6} \right] \qquad (4)$$

where $K_i = k_4 / k_3$.

For the time-dependent inhibition, there exists a time range in the progress curves in which formation of EI* is small (e.g., see Figure 3). Within this time range, it is possible to directly measure the effect of the inhibitor on v_0, i.e., to measure K_i directly. Values for K_i were obtained from Dixon analysis at a constant substrate concentration (eq 5).

$$\frac{1}{\quad} \qquad \frac{1}{\quad} \qquad \frac{K_m}{\quad}$$

$$\frac{}{v} = \frac{}{V_{max}} + \frac{}{V_{max}} (1 + I / K_i) \qquad (5)$$

The rate of enzyme-inhibitor dissociation, k_6, was measured directly for the time-dependent inhibition. Small volumes of concentrated enzyme and inhibitor were incubated to reach equilibrium, followed by large dilutions in assay mixtures containing near-saturating substrate. The rate of enzymatic activity regain was measured by rate of product formation.

Fluorescence Analysis

Fluorescence measurements were performed on a Perkin-Elmer LS50 Luminescence spectrometer connected to a Julabo F20 water bath. Protein fluorescence was excited at 295 nm and the emission was recorded from 300-500 nm at 25°C. The slit widths on both the excitation and emission were set at 5 nm and the spectra were obtained at 500 nm/min. Fluorescence data were corrected by running control samples of buffer and smoothened.

For inhibitor binding studies, pepsin and F-prot were dissolved in respective buffer systems. Titration of the enzyme with ATBI was performed by the addition of different concentrations of the inhibitor to the enzyme solution. For each inhibitor concentration on the titration curve a new enzyme solution was used. All the data on the titration curve were corrected for dilutions. The magnitude of the rapid fluorescence decrease ($F_0 - F$) occurring at each ATBI concentration was computer fitted to the equation $(F_0 - F) = \Delta F_{max}/\{1+ (K_I/[I])\}$ to determine the calculated value of K_I and ΔF_{max}. The first order rate constants for the slow loss of fluorescence k_{obs}, at each inhibitor concentration [I] were computer fitted to the equation, $k_{obs} = k_5[I]/\{K_i + [I]\}$, for the determination of k_5 under the assumption that, for a tight binding inhibitor, k_6 can be considered negligible at the onset of the slow loss of fluorescence.

Time course of the protein fluorescence following the addition of inhibitor were measured for up to 10 min with excitation and emission wavelengths fixed at 295 and 340 nm, respectively. Data points were collected at 0.5 s intervals during time courses. Corrections for the inner filter effect were performed as described by the following formula (Lakowicz, 1983).

$$F_c = F \text{ antilog } [(A_{ex} + A_{em})/2]$$

where F_c and F are the corrected and measured fluorescence intensities, respectively, and A_{ex} and A_{em} are the solution absorbances at the excitation and emission wavelengths, respectively. Background buffer spectra were subtracted to remove the contribution from Raman scattering.

Circular Dichroism Analysis

CD spectra were recorded in a Jasco-J715 spectropolarimeter at ambient temperature using a cell of 1 mm path length. Replicate scans were obtained at 0.1 nm resolution, 0.1 nm bandwidth and a scan speed of 50 nm/min. Spectra were average of 6 scans with the baseline subtracted spanning from 280 nm-200 nm in 0.1 nm

increment. The CD spectrum of the pepsin (50 nM) and F-prot (10 μM) was recorded in respective buffer system, in the absence/presence of substrate (40 μM) or ATBI (20 nM).

Chemical modification of ATBI with 2,4,6-trinitrobenzenesulfonic acid and N-ethyl-5-phenylisoxazolium-3'-sulfonic acid

N-ethyl-5-phenylisoxazolium-3'-sulfonic acid (Woodward's reagent K, WRK) has been known to react with the carboxyl group of aspartate and glutamate residues (Arana and Vallejos, 1981; Sinha and Brewer, 1985). To modify the carboxylic groups, ATBI (50 μM) was incubated in the absence or presence of different concentrations of WRK at 28°C for 1 h. Aliquots were removed at different time intervals and the reaction was quenched by the addition of sodium acetate buffer pH 5.0 to a final concentration of 100 mM. Excess reagent was then removed by gel filtration on a Bio-gel P2 column, equilibrated with sodium phosphate buffer, 0.05 M pH 6.0. The fractions were eluted at a flow rate of 12 ml/h. The active fractions were detected by the differential absorption at 210/340 nm and concentrated by lyophilization and the residual activity of the inhibitor was determined by assaying for the anti-proteolytic activity.

ATBI (50 μM) and 0.25 ml of 4% sodium bicarbonate was incubated with varying concentrations of 2,4,6-trinitrobenzenesulfonic acid (TNBS), a lysine group modifier (Okuyama and Satake, 1960), at 37°C in a reaction mixture of 0.5 ml in dark. Aliquots were withdrawn at suitable intervals and the reaction was terminated by adjusting the pH to 4.6. A control without the modifier was routinely included and the residual activity at any given time was calculated relative to the control. The extent of inactivation of pepsin was determined with the modified inhibitor as described before.

Results

Kinetic Analysis of the Inhibition of Pepsin and F-prot

In an attempt to delineate the mechanism of inhibition of the aspartic proteases by ATBI, we have determined the kinetic parameters for the enzyme inhibitor interactions using pepsin, the enzyme responsible for peptic ulcer and F-prot, from the fungus *Aspergillus saitoi*. Initial assessment of the potency and selectivity of ATBI with respect to the inhibition of pepsin and F-prot were determined from the IC_{50} values expressed as the concentration of compound required to inhibit 50% of the initial rate of the enzymatic activity. The IC_{50} values of ATBI for pepsin and F-prot were 22 nM and 5 μM, respectively (Figure 1). The reaction rates obtained after the addition of pepsin and F-prot to the reaction mixture containing ATBI and various concentrations of respective substrate were consistent with competitive inhibition and demonstrated little or no contribution occurred from auto-inactivation. The inhibition constant K_i associated with the formation of the reversible enzyme inhibitor complex (AP-ATBI), determined from the negative x-intercept of the Dixon plot analysis was $17 \pm 0.5 \times 10^{-9}$ and

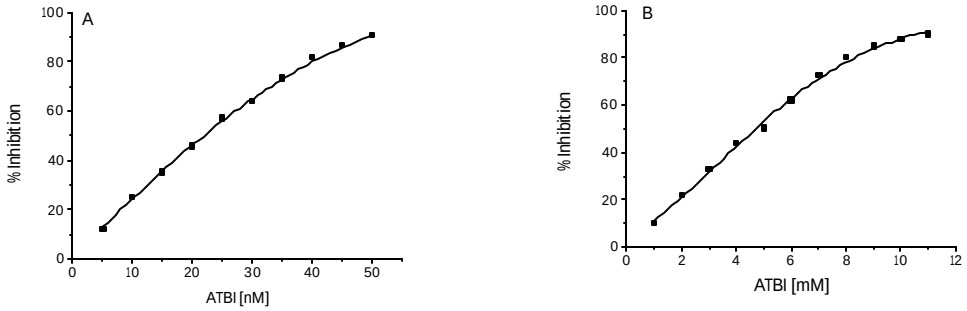

$3.25 \pm 0.6 \times 10^{-6}$ (Figure 2).

Figure1. Determination of IC_{50} value of ATBI against pepsin and F-prot.

Proteolytic activities of pepsin (A) and F-prot (B) were determined in the presence of increasing concentrations of ATBI. The percent inhibition of the proteolytic activity was calculated from the residual

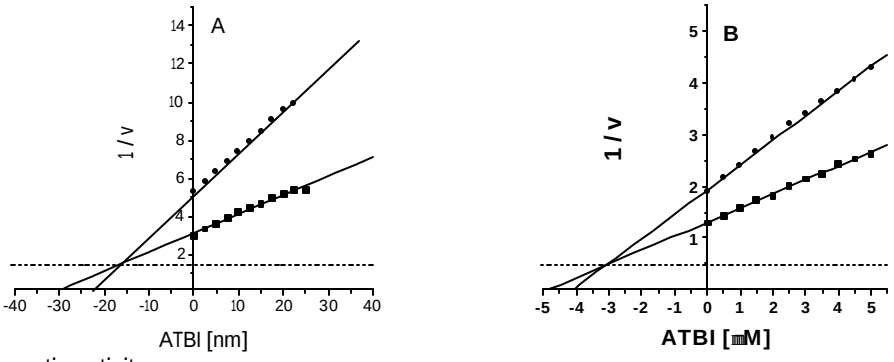

enzymatic activity.

Figure 2.Dixon Plots for the determination of K_i values.

Enzymatic activity of pepsin was estimated using casein at (■) 6 mg/ml, (●) 4 mg/ml, and hemoglobin at (■) 5 mg/ml, (●) 3 mg/ml, respectively, at different concentrations of ATBI. The reciprocal of

substrate hydrolysis by pepsin and F-prot (1/v) were plotted as a function of inhibitor concentration. The straight lines indicated the best fits for the data obtained.

In the absence of ATBI, the steady state rate of proteolytic activity of pepsin and F-prot reached rapidly whereas, in its presence a time dependent decrease in the steady state rate as a function of inhibitor was observed (Figure 3). The time dependent inhibition of ATBI with respect to the proteolytic activity of pepsin and F-prot indicated the slow-binding nature of ATBI. Examination of the progress curves revealed a time range where the initial rate of reaction did not deviate from linearity and the conversion of EI to EI* was minimal. For a low concentration of ATBI, the range was 0-3 and 0-4 min for pepsin and F-prot, respectively. Within this time range, classical competitive inhibition experiments can be used to determine k_4/k_3, which is the K_i value for a competitive inhibitor. From such experiments, K_i, associated with the formation of the reversible enzyme inhibitor complex (AP-ATBI) for ATBI was determined to be 17±0.8 x 10^{-9} M for pepsin and 3.2±0.5 x 10^{-6} M for F-prot (Figure 4), which are in total agreement with those obtained from the Dixon plot. The progress curves implicated an initial burst of the reaction rates followed by its dependence on the inhibitor concentration and time. The apparent rate of reaction *k*, from the progress curves when plotted *versus* the inhibitor concentration followed a hyperbolic function (Figure 3), indicating a two-step inhibition mechanism. The hyperbolic dependence of *k* suggested that a fast equilibrium precedes the formation of the final slow dissociating enzyme-inhibitor complex (AP-ATBI*), indicating a two-step inhibition mechanism by ATBI. Indeed, the data could be fitted to eq 3 by non-linear regression analysis, which yielded the best estimate of the overall inhibition constant, K_i* i.e., 55±0.5 x 10^{-12} M for pepsin and 5.2±0.6 x 10^{-8} M for F-prot.

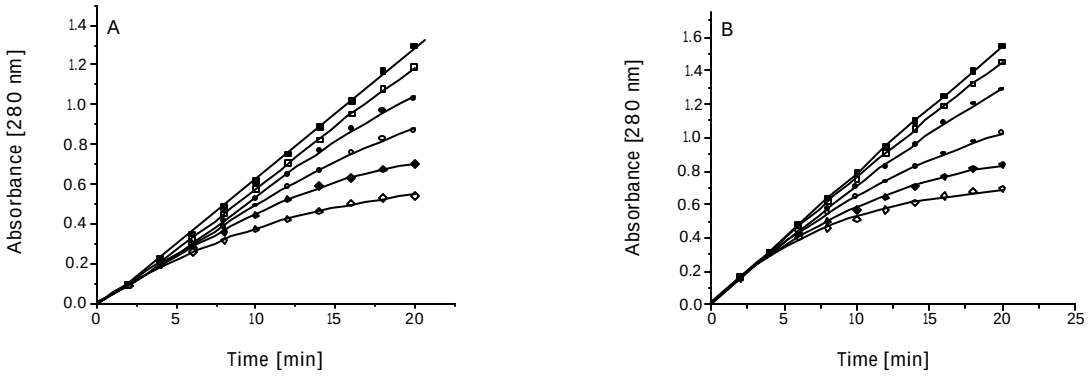

Figure 3. Time dependent inhibition of pepsin and F-prot by ATBI.
Reaction solution contained pepsin (50 pM, A) and F-prot (15 nM, B) in respective buffers at increasing concentrations of ATBI using casein (6 mg/ml) or hemoglobin (5 mg/ml). Reactions were initiated by the addition of the enzymes at 37°C. The points represent the hydrolysis of substrate as a function of time at 37°C. The lines indicate the best fits of data obtained from eq 2 and 3. Concentrations of ATBI were 0

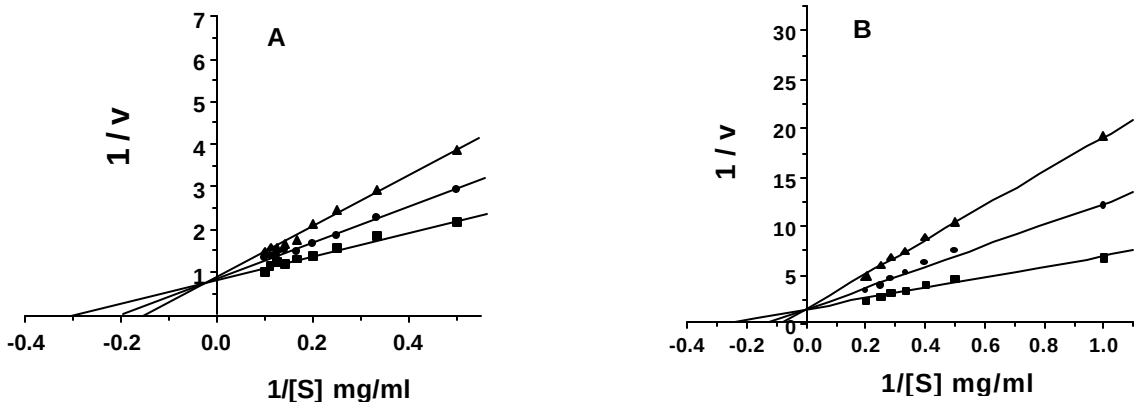

nM (■), 10 nM (□), 20 nM (●), 30 nM (○), 40 nM (◆), and 50 nM (◇) in A, and 0 μM (■), 1 μM (□), 2.5 μM (●), 5 μM (○), 10 μM (◆), and 15 μM (◇) in B.

Figure 4. Initial rate of reaction in the presence of ATBI.

Initial rate of proteolysis by pepsin (A) and F-prot (B). The enzymes were incubated (■) without or with the inhibitor at (●) 15 nM, (▲) 25 nM in A, and at (●) 5 μM, (▲) 10 μM in B, and assayed at increasing concentrations of substrate. The straight lines obtained indicated the best fit for the data obtained as analyzed by the Lineweaver-Burk's reciprocal equation and the K_i values were determined from the graphs.

An independent method to determine k_6, the rate constant for the conversion of AP-ATBI* to AP-ATBI, involves pre-incubating relatively high concentrations of enzyme and inhibitor for sufficient time to allow the system to reach equilibrium. Further, the enzyme inhibitor mixture was diluted 10,000 fold and assayed at saturating substrate concentration (100 K_m), which resulted in the dissociation and regeneration of enzymatic activity. Under these conditions, v_0 and the effective inhibitor concentration have been considered approximately equal to zero and the k_6 was determined from the rate of activity regenerated. The values of k_6 determined for pepsin and F-prot were $2.5\pm0.4 \times 10^{-6}$ sec^{-1} and $3.8\pm0.5 \times 10^{-5}$ sec^{-1}, respectively, by least-squares minimization of eq 2 (Figure 4). The final steady-state rate, v_s, was from the control containing pre-incubated enzyme without the inhibitor. The half time $t_{1/2}$, for reactivation of AP-ATBI*, determined from the k_6 values were 77 and 5 h, for pepsin and F-prot, respectively. The values of k_5, the rate constant for the isomerization of AP-ATBI to AP-ATBI*, were obtained from fits of eq 3 to the onset of inhibition data, using the experimentally determined values of K_i and k_6 (Table I).

Table-I

Inhibition constants of ATBI and Pepstatin against pepsin

Inhibition constants	$ATBI_a$	$Pepstatin_b$

K_i (M)	17±0.5 x 10^{-9}	1.3 x 10^{-8}
K_i*(M)	55±0.5 x 10^{-12}	4.5 x 10^{-11}
k_5 (sec^{-1})	7.7±0.3 x 10^{-4}	2.3±0.4 x 10^{-3}
k_6 (sec^{-1})	2.5±0.4 x 10^{-6}	3.8±0.5 x 10^{-5}
k_5 / k_6	310	290
$t_{1/2}$ (h)	77	2.5

[a]The K_i values for competitive inhibition were obtained from the steady state time range.
[b]Values obtained from Rich *et. al.* (21).

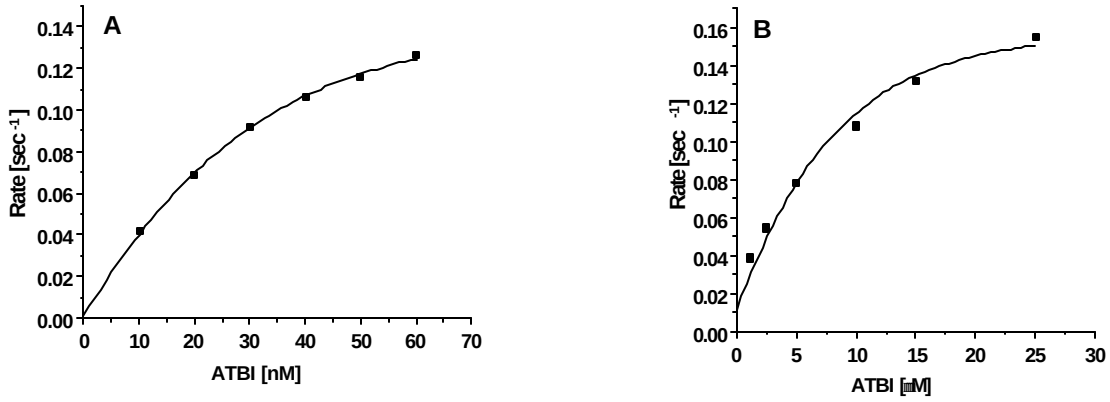

Figure 5. Effect of ATBI on the rate of reaction (*k*) of the proteolytic activity of pepsin and F-prot.
The rate constants *k* were calculated from the progress curves recorded following addition of pepsin (A) or F-prot (B) to the reaction mixture containing appropriate buffer and substrate. The solid line indicates the best fit of the data obtained.

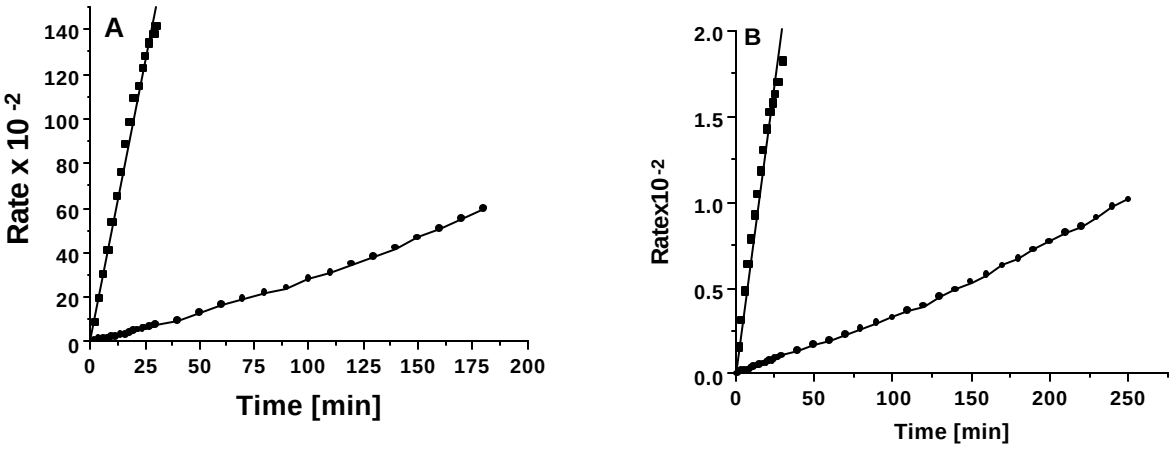

Figure 6. Dissociation rate (k_6) for pepsin- and F-prot-ATBI complexes.
Pepsin (1 μM, A) and F-prot (100 μM, B) were pre-incubated without (■) or with (●) equimolar concentrations of ATBI for 120 min on ice. The enzyme inhibitor mixture was diluted 10,000 fold into the assay mixture containing the substrate at 100 K_m. After pre-incubation, 2 μl of sample was removed and diluted to 20 ml in the same buffer. At the specified time, aliquots were removed and assayed for the proteolytic activity using casein or hemoglobin. The effective rate (k_6) was determined as described in the text.

There are two alternative models for the time-dependent inhibition by Scheme I (Beith, 1995; Erion and Walsh, 1987). An inhibition model in which the binding of the inhibitor to the enzyme is slow and tight, but occurs in a single step (Scheme I a) is eliminated based on the data of Table-I, because the inhibitor have measurable effect on the initial rates before the onset of slow-tight binding inhibition. An inhibition model where the inhibitor binds only to the free enzyme that has slowly adopted the transition-state configuration (Scheme I c) can also be

eliminated by the observed rates of onset of inhibition. From the observed results, we have concluded that the inhibition of the aspartic proteases followed slow-tight binding mechanism as described in Scheme 1b.

Fluorometric Analysis of Enzyme Inhibitor Interactions

The kinetic analysis of the enzyme-inhibitor interaction revealed that the two-step inhibition mechanism of pepsin and F-prot by ATBI followed Scheme 1b, where the initial enzyme-inhibitor complex AP-ATBI undergoes isomerization to AP-ATBI*. This isomerization is characterized by the induction of conformational changes in the enzymes due to the binding of the inhibitor. To delineate the conformational changes induced in the aspartic proteases due to the binding of ATBI, the fluorescence spectra of the enzyme-inhibitor complexes were monitored. The sequence data of pepsin indicated the presence of five Trp residues in its primary structure (Cooper et al., 1990; Sielecki et al., 1990). Although the sequence data of F-prot is not available, the tryptophanyl fluorescence revealed the presence of Trp residues. Therefore, the conformational changes induced in the proteases upon binding of ATBI were monitored by exploiting the intrinsic fluorescence by excitation of the π-π^* transition in the Trp residues. The tryptophanyl fluorescence spectra of pepsin and F-prot exhibited an emission maxima (λ_{max}) at ~342 nm, as a result of the radiative decay of the π - π^* transition from the Trp residues. The titration of the native enzymes with increasing concentration of ATBI resulted in a concentration dependent progressive quenching of the emission spectra of the enzymes (Figure 7). However, λ_{max} of proteases indicated the absence of blue or red shift in the intrinsic fluorescence, negating any drastic gross conformational changes in the three-dimension structure of the enzymes.

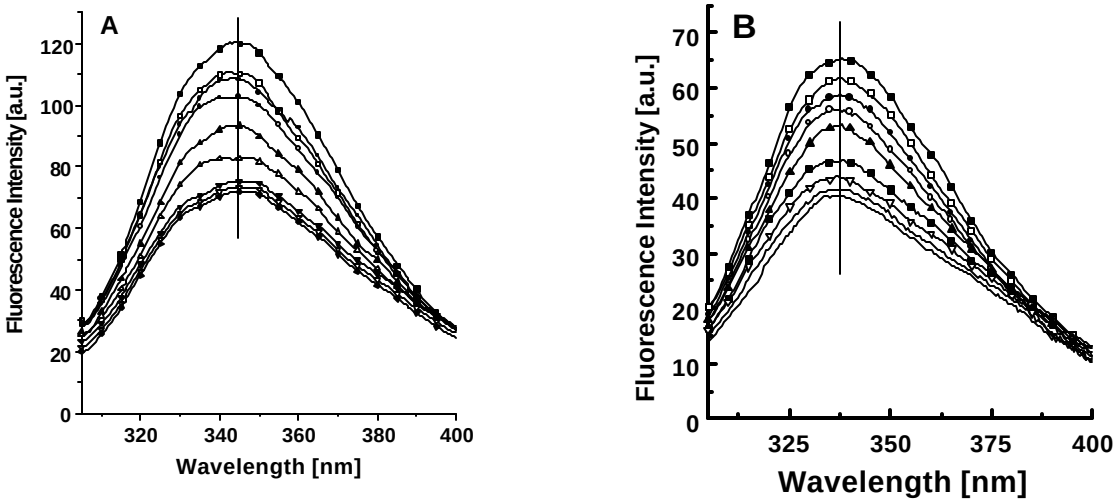

Figure 7. Fluorescence emission spectra of pepsin and F-prot.

The Fluorescence intensity spectra of pepsin (100 nM, A) and F-prot (20 μM, B) as a function of the inhibitor. Titration of the enzymes was performed by the addition of different concentrations of the inhibitor to the enzyme solutions. Pepsin and F-prot were dissolved in respective buffers. The

concentrations of ATBI were 0 nM (■), 10 nM (□), 15 nM (●), 25 nM (○), 35 nM (▲), 50 nM (△), 60 nM (▼), 65 nM (▽), 70 nM (◆) in A, and 0 μM (■), 1 μM (□), 2 μM (●), 3 μM (○), 4 μM (▲), 7.5 μM (△), 8 μM (▼), 9 μM (▽), 10 μM (◆) in B.

Further, to monitor the isomerization of AP-ATBI to AP-ATBI*, we have followed the intrinsic tryptophanyl fluorescence of the enzyme-inhibitor complexes as a function of time. Upon the addition of ATBI, a rapid decrease in the quantum yield of fluorescence was observed, followed by a slow decline to a final stable value over a period of 60 and 25 s for pepsin and F-prot, respectively (Figure 8), indicating an exponential decay of the fluorescence intensity. Once the stable value of the fluorescence had been reached, time had no further effect on the tryptophanyl fluorescence intensity. The magnitude of the rapid fluorescence decrease as a function of time was found to be similar to the total fluorescence quenching observed at a specific ATBI concentration. Thus we have concluded that both AP-ATBI and AP-ATBI* complexes have the same intrinsic fluorescence. Further, titration was performed in which an increasing concentrations of ATBI were added to the enzymes. The magnitude of the initial rapid fluorescence loss ($F_0 - F$) increased hyperbolically (Figure 9) corroborating the two-step, slow-tight binding inhibition of the aspartic proteases by ATBI. The estimated value of K_i determined by fitting the data for the magnitude of the rapid fluorescence decrease ($F_0 - F$) was 18.9 ±0.5 x 10^{-9} M and the k_5 value determined from the data derived from the slow decrease in fluorescence was 8.3 ±0.5 x 10^{-4} sec^{-1} for pepsin. These rate constants are in good agreement with that obtained from the kinetic analysis of pepsin, therefore, the initial rapid fluorescence decrease can be correlated to the formation of the reversible complex AP-ATBI, while the slow, time dependent decrease reflected the accumulation of the tight bound slow dissociating complex AP-ATBI*.

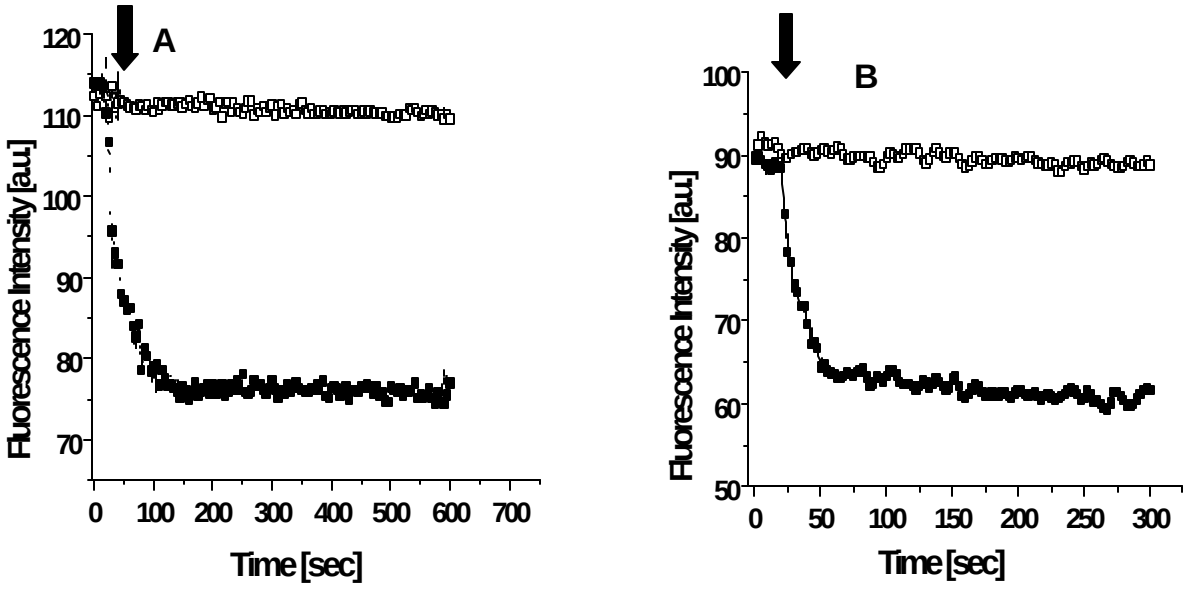

Figure 8. Time dependent effect of ATBI on the fluorescence quenching of the aspartic proteases. Pepsin (100 nM, A) and F-prot (20 μM, B) were treated at time indicated by the arrows and the fluorescence emission was followed for 10 min at a data acquisition time of 0.5 s. The excitation wavelength was fixed at 295 nm, where as the emission wavelength was 342 nm. The data were the

average of five scans with the correction for buffer and dilutions. (□) indicate absence of the inhibitor, whereas (■) indicate ATBI at 35 nM in A and 15 μM in B.

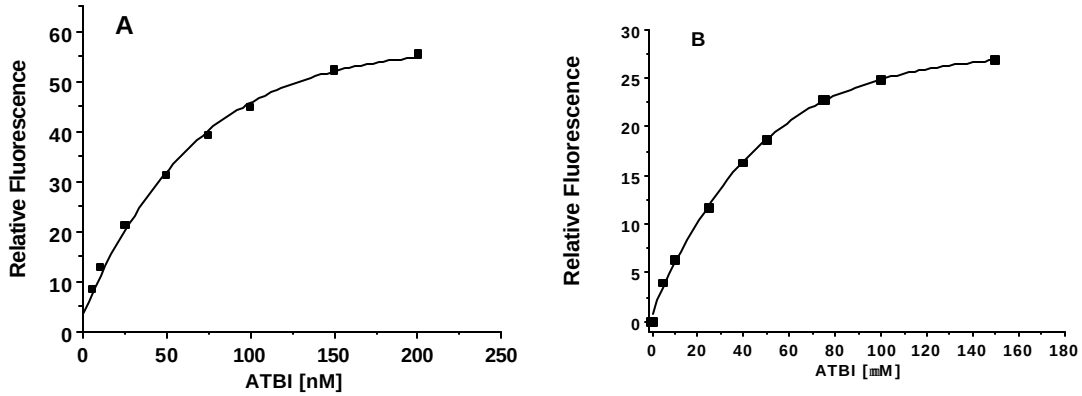

Figure 9. Effect of ATBI concentration on the tryptophan fluorescence of the aspartic proteases.
A constant amount of pepsin (100 nM, A) and F-prot (20 μM, B) were treated with increasing concentrations of ATBI and the fluorescence changes were measured at 28°C (excitation 295 and emission 342 nm). Each measurement was repeated five times and the average values of the fluorescence intensity at 342 nm were recorded. Control experiments with the buffer and inhibitor were performed under identical conditions. The fluorescence changes ($F - F_0$) were plotted against the inhibitor concentrations. The hyperbola indicates the best fit of the data obtained.

Secondary Structural Analysis of Enzyme-Inhibitor Complexes

In order to evaluate the effect of the inhibitor binding on the secondary structure of the aspartic proteases during the isomerization of AP-ATBI to AP-ATBI*, we have analyzed the CD spectra of pepsin- and F-prot-ATBI complexes. The circular dichroism spectra of the pepsin- and F-prot-ATBI complexes showed a typical *b*-sheet structure. Interestingly, the native enzyme and the enzyme-inhibitor complexes exhibited a similar pattern of negative ellipticity in the far-UV region indicating a little or no change in the secondary structure of the enzyme-

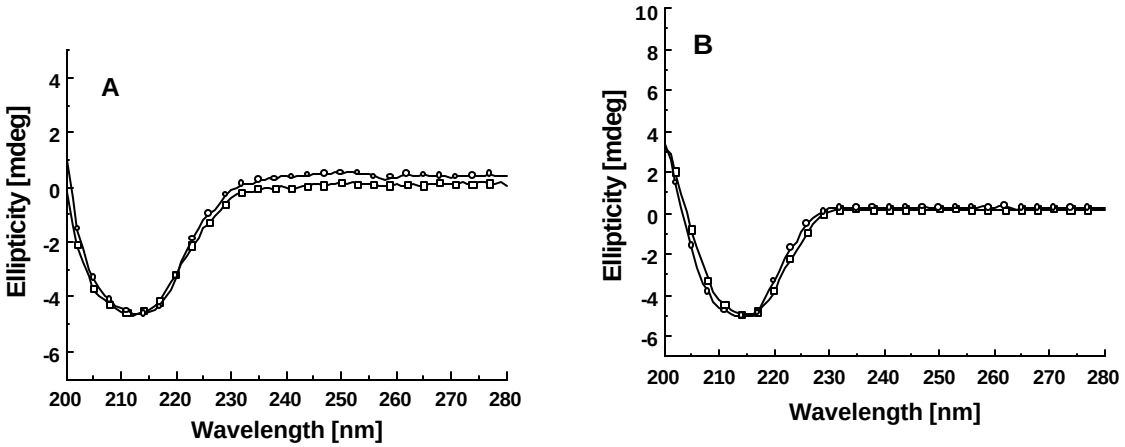

inhibitor complex (Figure 10).

Figure 10. Effect of the secondary structure of pepsin and F-prot upon binding of ATBI.

Far-UV circular dichroism spectra of the unliganded pepsin and F-prot and its complexes with ATBI. The CD spectra Pepsin (50 nM, A) and F-prot (10 μM, B) were recorded in the absence (□) or presence (○) of ATBI at 20 nM in A and 5 μM in B. Each spectrum represents the average of six scans with the baseline subtracted.

Identification of Functional Residues of ATBI

The role of functional groups involved in the inhibitory activity of ATBI was elucidated by employing chemical modifiers with specific reactivity. The amino acid sequence of ATBI, revealed the presence of Lys, Asp, and Glu residues with ionizable side chains. The involvement of these groups in the mechanistic pathway was investigated using WRK, a carboxyl group modifier, and TNBS, an amine group modifier of lysine. Semi-logarithmic plots of residual inhibitory activity against pepsin as a function of time were linear (Figure 11), signifying that the inactivation process obeys pseudo-first order kinetics. The modification of the carboxyl groups of ATBI by WRK was monitored by the differential absorption at 210/340 nm. Analysis of the order of reaction (Levy et al., 1963) for pepsin yielded a slope of 1.67 (Inset of Figure 11a), thus suggested the involvement of two carboxyl groups in enzyme inactivation. TNBS caused time- and concentration-dependent loss of the inhibitory activity of ATBI. A reaction order of 0.75 (Inset of Figure 11b) for pepsin was determined from the slope of the double logarithmic plot, indicated the involvement of a single amine group of ATBI in the enzyme inactivation.

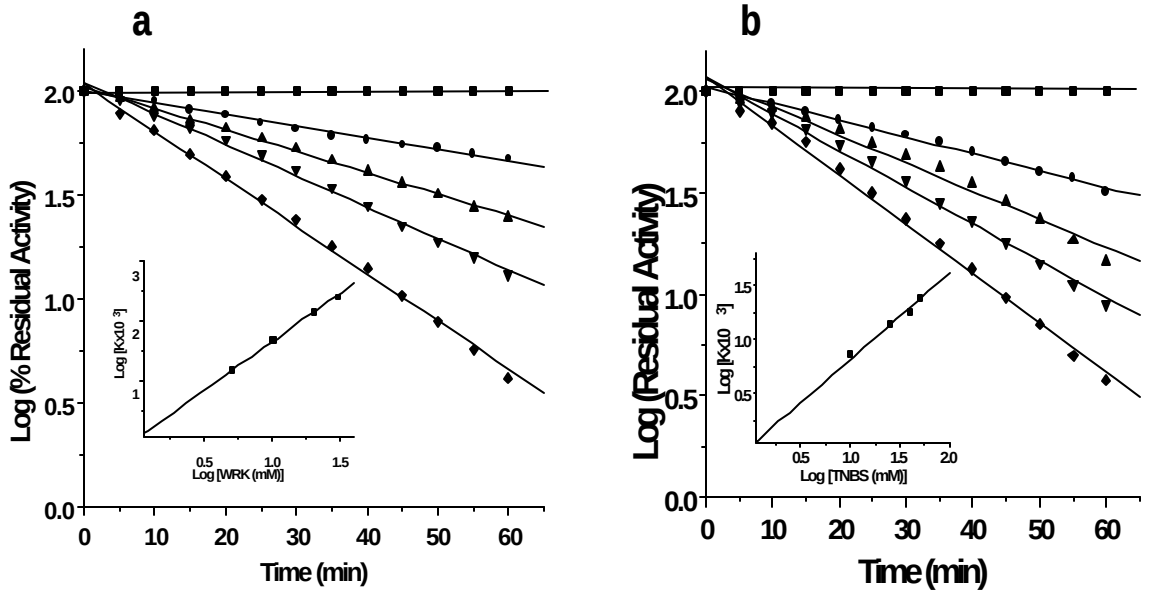

Figure 11. Differential labeling of the ionizable groups of ATBI with WRK and TNBS.

a) Inactivation of ATBI by WRK. ATBI (50 μM) was treated with 0 mM (■), 5 mM (●), 10 mM (▲), 20 mM (▼), and 30 mM (◆) of WRK at 28°C for 1 h. Aliquots of the reaction mixture were removed at times indicated and the reaction was quenched with the addition of sodium acetate buffer to a final concentration of 100 mM. b) Effect of TNBS on the inactivation of ATBI. ATBI (50 μM) was incubated without (■) or with 10 mM (●), 25 mM (▲), 40 mM (▼), and 50 mM (◆) of TNBS at 37°C in dark for 1 h. The lines represent the best fit for the data obtained as the natural logarithm of percent of residual inhibitory activity *versus* time. Inset represents the double logarithmic plots for the pseudo first-order rate constants *versus* the concentration of the modifiers.

Discussion

Several of enzymes are important targets physiologically and slow-binding inhibitors are pharmacologically or agriculturally consequential in principle and in practice. Even E.I* complexes with lifetimes of minutes can be of great utility. The existence of slow-binding inhibitors for given enzymes can provide useful probes of enzyme mechanism in the sense that isomerizations to high-affinity, slowly reverting complexes can shed light on the structures of reaction intermediates or proposed transition state structures.

The kinetic and fluorometric analysis of the aspartic proteases and inhibitor interactions revealed that ATBI is a slow, tight binding inhibitor of pepsin and F-prot. Pepsin is known to be responsible for the proteolytic digestion of proteinaceous food, excess secretion of which has harmful effects on the stomach as it damages the digestive tract and causes stomach or duodenal ulcer. Some of the species of *Aspergillus* are known to cause pulmonary infection, are characterized by the secretion of aspartic protease and thus, a potent inhibitor of that will have significant therapeutic value. For the development of effective drugs, the primary prerequisite is to assess the kinetic parameters associated with the enzyme-inhibitor interactions. During our initial kinetic analysis of inhibition studies, we noted that the inhibitor showed exceptional potency against pepsin and F-prot *in vitro* and indicated a 1:1 molar ratio of interaction with the target enzyme, thus ATBI belongs to the "tight-binding inhibitor" class (Williams and Morrison, 1979; Wolfenden, 1976). These results were reinforced by the equilibrium binding studies of the enzyme and inhibitor and further estimating the residual proteolytic activity.

The slow-binding inhibition of enzymes can be illustrated kinetically by three mechanisms as described in Scheme I. Simple second-order interaction between enzyme (E) and inhibitor (I) could result in slow-binding inhibition where the rate of complex formation is slow. Kinetically when an inhibitor has a low K_i value and the concentration of I varies in the region of K_i, both k_3I, and k_4 values would be low. These low rates of association and dissociation would lead to slow-binding inhibition. These low rates of association and dissociation would lead to slow-binding inhibition (Scheme 1a). In this case the product of the true second-order rate constant k_3 and the inhibitor concentration, I determine the rate of EI formation. Alternatively, binding may also involve two-steps, where there is a rapid formation of an initial collisional complex EI, that subsequently undergoes slow isomerization to form the final tight complex EI* (Scheme 1b). The nature of these changes has been discussed (Szedlacsek and Duggleby, 1995; Jencks, 1975). The extent of EI* formation depends on the affinity of the EI complex and the relative rates of formation of EI* and its relaxation to EI. Slow binding inhibitor can also arise due to an initial slow inter conversion of the enzyme E into another form E* which binds the inhibitor by a fast step (Scheme 1c). Kinetically, these mechanisms can be differentiated by investigating the behavior of the enzyme-inhibitor system at varying concentrations of the inhibitor. Scheme I a would predict that in the presence of substrate the initial rate of substrate hydrolysis will be independent of inhibitor concentrations as the concentration of EI would be significantly low. However, in Scheme I b, the inhibitor will inhibit the enzyme competitively at the onset of the reaction and at increasing concentration of inhibitor, the initial rate of substrate

hydrolysis will decrease hyperbolically. The kinetic properties of the aspartic proteases studied in this report provide a unique opportunity to quantitate these rates and affinities.

As found in most of ground-state inhibitors, formation of the first reversible complex, AP-ATBI, was too rapid to be measured at steady-state kinetics and was likely to be near diffusion control. The rate of formation of the second enzyme inhibitor complex AP-ATBI*, was slow and relatively independent of the stability of the AP-ATBI complex or of the ability of the inhibitor to stabilize the AP-ATBI* complex. Thus the major variable for slow binding inhibition is k_6, the first-order rate at which AP-ATBI* relaxes to AP-ATBI. An equivalent statement is that the apparent inhibitor constant K_i*, depends on the ability of the inhibitor to stabilize the AP-ATBI* complex. The longer half-life of the AP-ATBI* signified better stability and slow dissociating nature of these complexes. With "classical" inhibitors, the attainment of equilibrium between enzyme, inhibitor, and the enzyme-inhibitor complexes is rapid and requires large excess of inhibitor to enzyme. In contrast, with tight-binding inhibitors, the attainment of equilibrium may be rapid, but the total concentration of inhibitor needed to inhibit the enzyme is similar to the total concentration of the enzyme (Morisson and Walsh, 1988).

It is interesting to comment on the kinetic data of ATBI in the light of the extensive kinetic analysis of pepstatin, the known tight binding inhibitor of pepsin. The values of K_i and K_i* for ATBI were observed to be much lower than those of pepstatin. ATBI has a longer half-life and a better k_5/k_6 ratio, the determinant of the kinetic behavior of AP-ATBI*. These comparative results clearly indicated the superiority of the ATBI-inhibition system to that of pepstatin. However, due to the unavailability of the X-ray crystallographic data of pepsin-ATBI complex, we are unable to comment on the structural comparison between both the inhibitors. It will be indeed intriguing to compare the X-ray crystallographic data for the identification of the important contacts between the enzyme and the inhibitors, which will facilitate the understanding of the mechanism of inactivation of pepsin by ATBI. With the existing results, ATBI certainly holds an added advantage over pepstatin because of its hydrophilic nature and longer half-life.

It is well characterized that the onset of slow-binding inhibition is caused by a normal conformational mode of the enzyme-inhibitor complex that attains the stable configuration. The effectiveness of the slow-binding inhibitor reflects in its ability to stabilize the enzyme-inhibitor complex and thus a slow return to the ground state. The slow binding inhibitors combine at the active site and induce conformational changes that causes the enzyme to clamp down in the inhibitor, resulting in the formation of a stable enzyme-inhibitor complex. The time dependent inhibition kinetics of pepsin and F-prot by ATBI followed a two-step mechanism, which was also reflected in the quenching pattern of the fluorescence. Based on our fluorescence studies, we propose that the rapid fluorescence loss was due to the formation of the reversible AP-ATBI complex, whereas the subsequent slower decrease was a result of the accumulation of the tightly bound AP-ATBI* complex. The kinetically observable isomerization of AP-ATBI to AP-ATBI*, does not involve a major alteration in the three dimensional structure of the enzymes as reflected in the absence of any shift in the tryptophanyl fluorescence. Further,

agreement of the rate constant values determined from kinetic and fluorescence analysis prompted us to correlate the localized conformational changes to the isomerization of the AP-ATBI to AP-ATBI*.

Any changes in the environment of individual tryptophan residues may result in an alternation of fluorescence characteristics such as emission wavelength, quantum yield, and susceptibility to quenching (Pawagi and Deber, 1990). Fluorescence quenching can also result from the energy transfer to an acceptor molecule having an overlapping absorption spectrum (Cheung, 1991). As the inhibitor has no absorption in the region of 290-450 nm, we ruled out the quenching of fluorescence due to the energy transfer between the inhibitor and the tryptophan residues. The possibility that can be considered for the above inhibitor-induced fluorescence decrease is due to the presence of multiple sites, binding at one induced rapid fluorescence change and at a second caused the slow fluorescence decrease. To verify this possibility, fixed concentration of the enzymes was titrated with increasing concentrations of ATBI. The proteolytic activity of pepsin and F-prot decreased linearly with increasing concentrations of ATBI yielding a stoichiometry close to 1:1 expected for the slow-tight binding inhibition. The effect of ATBI concentration on the fluorescence quenching of the enzymes was also consistent with a 1:1 molar ratio. These results are therefore inconsistent with the presence of multiple high-affinity sites. Irrespective of the physical explanation for the quenching process, it was apparent that the inhibitor induced fluorescence quenching followed the formation of both the complexes AP-ATBI to AP-ATBI*.

The localization and characterization of the amino acids comprising the active center and the correlation between these residues with the inhibitory function are essential for understanding the mechanism of action of the inhibitor. To determine the residues involved in the anti-proteolytic activity, we have modified the ionizable groups of Lys, and Asp/Glu of ATBI. Modification of the amine group of Lys or the carboxyl group of Asp/Glu residues of ATBI by specific modifiers TNBS or WRK resulted in the loss of its inhibitory activity. The kinetic analysis indicated the participation of one amine and two carboxyl groups of ATBI in the inhibition of pepsin and F-prot. It is well established that the catalytic site of the aspartic proteases consists of two carboxyl groups and an essential lytic water molecule (Rao et al., 1998) and follow a general acid-base catalysis mechanism. The probable explanation for the involvement of two carboxyl groups of ATBI is that they may form a network of hydrogen bonds with the catalytic water molecule and with the ionizable groups in the active site of the enzyme. The participation of the Lys residue may be explained by considering its ability to form hydrogen bonding with the catalytic carboxyl groups of the enzymes. These interactions may interfere in the native weak interactions between the carboxyl groups of the active site and the lytic water molecule leading towards the inactivation of the enzymes. However, the crystal structure of the enzyme-inhibitor complex will aid in understanding the mechanism of inactivation of the aspartic proteases in detail.

From the results of our investigation, we conclude that the inactivation of pepsin and F-prot by ATBI, followed slow-tight binding inhibition mechanism and can be conveniently monitored by the fluorescence spectroscopy. Concomitant with the kinetic characterization, the fluorescence spectroscopy will be useful for the

evaluation of inhibitor kinetic constants in the absence of enzyme turnover and also for the further characterization of the mechanism of inhibition of aspartic protease by slow-tight binding inhibitors. Tight-binding inhibitors of aspartic proteases have important implications in the development of new approaches to the treatment of disease. The tight-binding nature of ATBI inhibition represents a unique system to design therapeutics directed at the aspartic protease targets and perhaps more importantly the hydrophilic nature of ATBI will have considerable potential for better oral bioavailability.

By its nature, slow-binding inhibition describes the increase in inhibition or fall off in reaction velocity that occurs as a function of time on the steady-state scale. Thus, for an inhibition that conforms to the mechanism described in Scheme Ib, K_i^* must be lower than K_i and this condition can satisfied only when k_6 is < k_5. Furthermore, the values of k_5 and k_6 must be of a magnitude that allows observation of the attainment of the equilibrium involving enzyme and inhibitor. If the absolute values of both were relatively high, the equilibrium between E.I and E.I* would be established before measurement of reaction begins. No indication of an isomerization reaction could be obtained. By contrast, if the values for k_5 and k_6 were relatively low, the formation of E.I* would not observed within the time over which there was no significant substrate depletion. Slow-binding inhibition is not simply due to the slow conversion of E.I to E.I* but requires that the reverse isomerization rate (k_6) be less than the forward isomerization rate (k_5). In extreme situation where k_6 tends to be zero, a slow-binding inhibitor becomes an active-site-directed irreversible inhibitor.

Slow-binding inhibition of enzyme-catalyzed reactions is probably a more general phenomenon than previously realized although the relationship between hysteresis and slow-binding inhibition remains to be determined. A sharp line of demarcation cannot be drawn between slow-binding and slow, tight-binding inhibition. Whenever experiments can be performed at inhibitor concentrations, which are ten, or more times that of the enzyme, the tight-binding condition will be circumvented and studies on the slow-binding inhibition will be facilitated. The reason for the slow-binding inhibition has not yet been established. Perhaps slow-binding inhibitors are such good analogues of the substrate that they induce a conformational change in the enzyme which is analogous to that associated with the formation of the transition state in enzymic catalysis (Wolfenden, 1976). The forward isomerization reaction would then be slow because the inhibitor does not have all the essential structural features of the transition state of a substrate while the reverse isomerization reaction would be even slower because that rate is not enhanced through product formation. The net effect is that enzymes subject to slow-binding inhibition clamp down on the inhibitors so as to hinder the release from enzyme-inhibitor complexes. Further, it can be argued that such enzymes bring about the formation of transition-state analogues. However, it is possible that slow-binding inhibitors may not help us gain an insight into the transition-state structure of enzyme-substrate(s) complexes. The answer to this question represents a real challenge to enzymologists. As a starting point attention might be directed towards a comparison of the three-dimensional structures of enzyme-classical inhibitor, and enzyme-slow-binding inhibitor complexes.

The investigation of mechanism of slow-tight binding inhibition has prompted us to explain the non-competitive inhibition of ATBI towards the HIV-1 PR and the competitive inhibition against pepsin and F-prot. As revealed from our kinetic studies, ATBI acts as a slow tight binding inhibitor towards pepsin and F-prot, whereas it is an extremely tight binding inhibitor of HIV-1 PR. As apparent from the kinetic analysis of slow tight binding inhibitors, at conditions where the rate of reverse isomerization of EI* to EI tends to zero, the competitive inhibitor would behave as a non-competitive inhibitor. Therefore, we propose that the determinant for the differential

inhibition mechanism of ATBI towards HIV-1 PR, pepsin and F-prot, is the dissociation rate constant K_6. The non-competitive inhibition of HIV-1 PR may due to the inability of the enzyme-inhibitor complex to dissociate, thus resulting in the formation of an irreversible complex..

References

Ackermann, W. W., and Potter, V. R. (1949) *Proc. Soc. Exp. Biol. Med.* **72**, 1-9.

Arana, J. L., and Vallejos, R. H. (1981) *FEBS Lett*. **123**, 103-106.

Beith, J. G. (1995) *Methods Enzymol.* **248**, 59-84.

Cha, S. (1975) *Biochem. Pharmacol.* **24**, 2177-2185.

Cha, S. (1976) *Biochem. Pharmacol.* **25**, 1561-1569.

Cheung, H. C. (1991) in *"Topics in Fluorescence Spectroscopy, Vol. 2*: *Principles:* (Lakowicz, J. R., Ed.) pp127-176, Plenum Press, New York.

Chiang, L., Sanchez-Chiang, L., Wolf, S., and Tang, J. (1966) *Proc. Soc. Exptl. Biol. Med.* **122**, 700-710.

Cleland, W. W. (1979) *Methods Enzymol.* **63**, 103-138.

Cooper, J. B., Khan, G., Taylor, G., Tickle, I. J., and Blundell, T. L. (1990) *J. Mol. Biol.* **214**, 199-222.

Davies, D. R. (1990*) Annu. Rev. Biophys. Biophys. Chem*. **19**, 189-215.

Debouck, C., and Metcalf, B. W. (1990) *Drug Dev. Res.* **21**, 1-17.

Dixon, M. (1953) *Biochem. J*. **55**, 170-171.

Dunn, B. M. (1992) *Adv. Detailed React. Mech*. **2**, 213-241.

Eason, L. H., and Stedman, E. (1936) *Proc. R. Soc. London, Ser B.* **121**, 142-165.

Erion, M. D., and Walsh, C. T. (1987) *Biochemistry* **12**, 3417-3425.

Fruton, J. S. (1976) *Adv. Enzymol. Relat. Areas Mol. Biol.* **44**, 1-36.

Gelb, M., Svaren, J., and Abeles, R. (1985) *Biochemistry* **24**, 1813-1817.

Goldstein, A. J. (1944) *Gen. Physiol.* **27**, 529-580.

Henderson, P. (1972) *Biochem. J.* **127**, 321-333.

James, M. N. G., Sielecki, A. R., Hayakawa, K., and Gelb, M. H. (1992) *Biochemistry* **31**, 3872-3888.

Jencks, W. C. (1975) *Adv. Enzymol. Relat. Areas Mol. Biol.* **43**, 219-411.

Kati, W. M., Saldivar, A. S., Mohamadi, F., Sham, H. L., Laver, W. G., and Kohlbrenner, W. E. (1998) *Biochem. Biophys. Res. Com.* **244**, 408-413.

Lakowicz, J. R. (1983) *"Principles of Fluorescence Spectroscopy"*, Plenum Press, New York.

Levy, H. M., Leber, P. D., and Ryan, E. M. (1963) *J. Biol. Chem.* **238**, 3654-3659.

Merker, D. J., Brenowitz, M., and Schramm, V. L. (1990) *Biochemistry* **29**, 8358-8364.

Morison, J. F., and Stone, S. R. (1985) *Comments Mol. Cell. Biophys.* **2**, 347-368.

Morisson, J. F., and Walsh, C. T. (1988) *Adv. Enzymol. Relat. Areas Mol*. *Biol*. **61**, 201-301.

Morrison, J. F. (1969) *Biochim. Biophys. Acta* **185**, 269-?.

Morrison, J. F. (1982) *Trends Biochem. Sci.* **7**, 102-105.

Okuyama, T., and Satake, K. (1960) *J. Biochem. (Tokyo)* **47**, 454-466.

Pawagi, A. B., and Deber, C. M. (1990) *Biochemistry* **20**, 950-955.

Pegg, M. S., and Vonitzstein, M. (1994) *Biochem. Mol. Biol. Int.* **32**, 851-858.

Ploux, O., Breyne, O., Carillon, S., and Marquet, A. (1999) *Eur. J. Biochem.* **259**, 63-70.

Rao, M. B., Tanksale, A. M., Ghatge, M. S., and Deshpande, V. V. (1998) *Microbiol. Mol. Biol. Rev.* **62**, 597-635.

Reiner, J. M. (1959) in *"Behavor of Enzyme Systems"* Burgess, Minneappolis, Minnesota.

Rich, D., and Sun, E. (1980) *Biochem. Pharmacol.* **29**, 2205-2212.

Richardson, C. T. (1985) *Am. J. Med.* **79** (suppl **2C**), 1-7.

Rosenthal, P. J. (1998) *Emerging Infect. Diseases* **4**, 49-57.

Scarborough, P. E., Guruprasad, K., Topham, C., Richo, G. R., Conner, G. E., Blundell, T. L., and Dunn, B. M. (1993) *Protein Sci*. **2**, 264-276.

Sculley, M. J., Morrison, J. F., and Cleland, W. W. (1996) *Biochim. Biophys. Acta.* **1298**, 78-86.

Sielecki, A. R., Fedorov, A., Boodhoo, A., Andreeva, N. S., and James, M. N. (1990) *J. Mol. Biol.* **214**, 143-170.

Sinha, U., and Brewer, J. M. (1985) *Anal. Biochem.* **151**, 327-333.

Strauss, O. H., and Goldstein, A. J. (1943) *Gen. Physiol.* **26**, 559-585.

Suguna, K., Padlan, E. A., Smith, C. W., Catlson, W. D., and Davies, D. R. (1987) *Proc. Natl. Acad. Sci. U. S. A*. **84**, 7009-7013.

Szedlacsek, S. E., and Duggleby, R. G. (1995) *Methods Enzymol.* **249**, 144-180.

Thaisrivongs, S. (1989) *Drug News Perspect.* **1**, 11-16.

Umezawa, H., Takita, T., and Shiba, T. (1978) Eds., *"Bioactive Peptides Produced by Microorganisms"* Halsted, New York.

Ward, M., and Kodama, K. H. (1991) In *"Structure and Function of the Aspartic Proteinases-Genetics, Structure, and Mechanisms"* (Dunn, B. M., Ed.) pp149-160, Plenum Press, New York.

Williams, J. W., and Morrison, J. F. (1979) *Methods Enzymol.* **63**, 437-467.

Wolfenden, R. (1976) *Annu. Rev. Biophys. Bioeng.* **5**, 271-306.

Yiallouros, I., Vassiliou, S., Yiotakis, A., Zwilling, R., Stocker, W., and Dive, V. (1998) *Biochem. J.* **331**, 375-379.

Chapter 5

Bifunctional Role of ATBI, Implications in Fungal Growth Inhibition

Summary

ATBI exhibited anti-fungal activity against a broad spectrum of phytopathogenic fungi including *Alternaria*, *Aspergillus*, *Curvularia*, *Colletotricum*, *Fusarium*, *Phomopsis*, and the saprophytic fungus *Trichoderma*. During the purification of ATBI, the anti-fungal activity of the inhibitor was co-purified with the aspartic protease inhibitory activity. The concentration of ATBI required for the 50 % growth inhibition (IC_{50}) ranged from 0.30 to 5.9 μg/ml, whereas the minimum inhibitory concentration varied from 0.60 to 3.5 μg/ml. The amino acid sequence of ATBI, did not exhibit primary structural homology to any known anti-fungal peptides. The negative charge and the absence of periodic secondary structure in ATBI suggested an alternative mechanism of action for fungal growth inhibition. ATBI was found to inhibit xylanase and aspartic protease (F-prot) competitively with the K_i values 1.75 and 3.25 μM respectively, suggesting higher binding affinity of ATBI to xylanase than aspartic protease. Growth of representative fungi on selective media for the production of xylanase and aspartic protease and their growth inhibition by ATBI on synthetic media containing specified carbon source for the production of the enzymes, revealed the role of these enzymes in fungal growth. Rescue of the growth inhibition by the reaction products of xylanase and aspartic protease indicated the involvement of these enzymes in the cellular growth. The chemical modification of Asp/Glu or Lys residues of ATBI abolished its anti-fungal activity, indicating the crucial role of these amino acids for the functional aspects of ATBI. The kinetic analysis of the TNBS and WRK modified ATBI abolished its anti-xylanolytic and anti-proteolytic activity and subsequently its anti-fungal activity. Our results envisage a paradigm shift in the concept of fungal growth inhibition for the role of antixylanolytic activity. The structural and functional characteristics of ATBI indicated that, this is the first report of a novel class of anti-fungal peptide, exhibiting bifunctional inhibitory activity.

Introduction

The screening of large "collections" of known individual compounds from the diversity present in natural resources such as soil samples, marine waters, insects, and tropical plants (Blondelle and Houghten, 1992; Bostian and Silver, 1990), for which the modes of action are initially unknown represents the primary current means for the identification of new anti-microbial agents. The continuing improvement in the understanding of anti-microbial resistance enables inhibition targets and pathways to be explored (Neu, 1989). This in turn permits the synthetic design of modified versions of existing anti-microbial compounds. The need for safe and effective anti-fungal agents has triggered considerable interest in the isolation of new compounds from biological resources. The rapid emergence of fungal pathogens resistant to currently available antibiotics has further compounded the dearth of novel anti-fungal agents. Presently available synthetic anti-fungal compounds possess various drawbacks such as lack of specificity, environmental hazards, biodegradability, etc. It is therefore imperative to find molecules that are non-toxic, biodegradable and having less tendency towards the development of resistant fungal strains. The past decade has witnessed a dramatic growth in knowledge of natural peptides from plants, animals, and microorganisms. These peptides play an important role in the protection of plants from invasive infection, and could prove to be useful tools for the genetic engineering of fungal resistance in transgenic plants (Terras, 1993).

Opportunistic fungal infections have become increasingly important causes of morbidity and mortality in neutropenic and/or immunocompromised patients with the AIDS pandemic accounting for much of this increase (Swerdloff et al., 1993). Commensurate with the rise in fungal infections has been an increase in the use of systemic anti-fungal drugs worldwide and the introduction of new drugs with systemic activity. However, therapeutic failure in antifungal treatment is not uncommon in immunocompromised patients and this failure can be attributed to several host- and drug-related factors. One of the major factors is the emergence of drug-resistant fungi that results in progressive disease during therapy. Increasing attention is being focused on defining the mechanism involved in anti-fungal drug activities, resistance, and in evaluating the efficacy of therapeutic modalities (Stevens and Holmberg, 1999).

The biological activity of a large number of peptide toxins have been rationalized in terms of the peptides having the ability to adopt amphiphilic α-helical structures and associate with lipid components of membranes (DeGrado et al., 1981; DeGrado, 1988; Kaiser and Kezdy, 1987). Although peptides are not considered as effective systemic therapeutic agents owing to their lack of oral bioavailability and rapid enzymatic degradation, it appears that insects, amphibians, and mammals use peptides to counter bacterial infections as one of a number of primary host defense systems (Zasloff, 1992; Sai et al., 2001). Because they have different modes of action from classical antibiotics, peptides can be expected to have value as alternative agents in the fight against new resistant microbial strains. The characterization of such new anti-fungal and antimicrobial peptides and the design of analogues with improved activities have allowed better understanding of the structure-activity relationship of

these peptides (Saberwal and Nagaraj, 1994). Earlier studies directed towards understanding the structure-activity relationships of a number of antimicrobial peptides isolated from natural sources (Juretic et al., 1989; Fink et al., 1989), indicated that amphipathic structures, combined with the presence of positively charged residues, were required for their antimicrobial activities. These studies have led to the design of a large number of novel cationic peptides with potent antimicrobial activities, all of which were found to be capable of adopting an amphipathic α-helical structure in the presence of lipid/cell membranes (Blondelle and Houghten, 1992; Buttner et al., 1992; Nakamura et al., 1990; Fink et al., 1989). The continuing development in the understanding of the mechanism of fungal resistance have enabled in deciphering the inhibition targets and pathways.

Anti-fungal peptides are classified into two classes based on their mode of action (DeLucca and Walsh, 1999). The first group acts by lysis, which occurs via several mechanisms (Shai, 1995). Lytic peptides may be amphipathic, having two faces, with one being positively charged and the other being neutral and hydrophobic. Some amphipathic peptides bind only to the membrane structure without traversing the membrane. Others traverse membranes and interact specifically with certain molecules. Certain amphipathic peptides aggregate in a selective manner, forming aqueous pores of variable sizes, allowing passage of ions or other solutes. The second class of peptide interferes with the cell wall synthesis or the biosynthesis of essential cellular component such as glucan or chitin (Debono and Gordee, 1994). Antimicrobial peptides are typically 20-40 amino acids in length, with a folded size approximating the membrane thickness. All evidence indicates that antimicrobial peptides act by permiablizing the cell membranes of microorganisms (Boman et al., 1994), although in addition, receptor-mediated signaling activities of some peptides have been reported (Yang et al., 1999; Hoffmann et al., 1999). The first indications that the peptides target the membranes were their wide spectrum of activity, and their speed of action, often within minutes *in vitro*. Subsequently, all-D amino acid enantiomers of various peptides were synthesized and exhibited the same antimicrobial activities as their all-L native peptide counterparts (Wade et al., 1990; Bessalle et al., 1990; Lehrer et al., 1996; Cho et al., 1998). This implies that the action of antimicrobial peptides does not involve stereospecific protein receptors; rather, the action is the result of direct interaction with the lipid matrix of the membranes. However, such interaction is generally considered nonspecific. The most intriguing question remains that “how do the defense mechanisms distinguish species self from infectious nonself?” Specificity or selective interaction of a protein is usually referred to the differential binding affinities of the protein to its target. Likewise, the first step of interaction between an antimicrobial peptide to the membrane is the physical binding of the peptide to the membrane surface. In this process, the electrostatic attraction apparently plays an important role (Matzuxzaki et al., 1997; Lohner et al., 1997). It is well known that bacterial membranes contain negatively charged lipids on the outer leaflet, whereas the outer leaflets of eukaryotes are predominantly neutral (Gennis, 1989). Despite their diversity in structure, most antimicrobial peptides are positively charged. Thus, electrostatic interaction can be viewed as playing a regulatory role in target cell selectivity. However, there is at least one other regulatory step in the peptides’ antimicrobial activity that occurs

after binding to the membrane. One apparent reason to suspect that the charge on membrane is not he sole factor determining the peptides' efficacy is the fact that different peptides preferentially kill different pathogens (Steiner et al., 1988). This cannot be the result of one cationic peptide being preferentially attracted to one group of pathogens while another cationic peptide is preferentially attracted to another group. For a similar reason, transmembrane electric potential is not likely a significant factor affecting the selectivity of peptides' action. Furthermore, the peptides exhibit varying levels of lytic activity against different eukaryotic cells.

Antimicrobial synthesized, cationic peptides have been recognized only recently as an important part of innate immunity (Bevins, 1994; Boman, 1995; Hancock and Lehrer, 1998) found throughout the evolutionary tree. However, examination of these peptides has shown general trends but little sequence homology, and this suggests that each peptide has evolved (probably convergently) to act optimally in the environment in which it is produced and against local microorganims. Antimicrobial peptides are so widespread that they are likely to play an important protective role. Antifungal and antimicrobial peptides have been reported from a large number of sources including mammals, insects, amphibians, bacteria, fungi, etc, (Hancock et al., 1995; Kleinkauf and von Dohren, 1988;Perlman and Bodansky, 1971).

Mammalian Peptides

Antimicrobial peptides isolated from mammals can be present within the granules of neutrophils, in mucosal or skin secretions from epithelial cells, or as the degradation products of proteins (Boman, 1995). Mammalian antifungal peptides include defensins, protegrins and gallinacins, tritrpticin, lactoferricin, and BPI protein domain III anologs. Classic defensins present in many organisms are predominantly β-sheet structures stabilized by three disulfide bonds that distinguish them from other antimicrobial peptides that form amphipathic helices (White et al., 1995). They are small, variably cationic proteins, whose three-dimensional folds form highly amphipathic molecules (Ganz et al., 1990). Defensins electrostatically bond to membranes causing the formation of multimeric pores and the leakage of essential minerals and metabolites (Lehrer et al., 1989; Lehrer et al., 1985; Patterson-Delafield et al., 1981; White et al., 1995). The protegrins, are produced by porcine leukocytes. They are cationic, cysteine-rich molecules with two intermolecular, parallel, disulfide bridges, which stabilize an amphipathic β-sheet structure comprising two anti-parallel strands (Aumelas et al., 1996; Harwig et al., 1994; Kokryakov et al., 1993). Protegrins formed weakly selective ionic channels that anions and small cations permeated, indicating that the cysteine bridges are a prerequisite for membrane permeability alteration but not for antimicrobial activity (Magoni, et al. 1996). Precursors of many antimicrobial peptides of porcine, bovine, and rabbit origin share highly conserved regions with antifungal properties (Levy et al., 1993; Storici et al., 1992; Zanetti et al., 1993). Tritrpticin corresponds to 13 amino acids of the C-terminal portion of cathelin, a putative protease inhibitor from porcine blood leukocytes. Bovine lactoferrin, an iron-binding protein, had broad antimicrobial properties (Bullen, 1981; Reiter, 1983). Lactoferricin, an enzymatic product of lactoferrin, possessed greater antimicrobial properties than lactoferrin and corresponds to the 18 amino acid residues near the N

terminus of lactoferrin in a region distinct from its iron binding sites (Bellamy et al., 1992; Tomita et al., 1991). The bactericidal and permeability-increasing (BPI) protein is a cationic protein stored principally in the azurophilic granules of neutrophils (Elsbach and Weiss, 1997), from which several potent antifungal peptides were derived (Lim et al., 1996).

Insect Peptides

Cecropin, which form α-helices in solution, are linear peptides in the hemolymph of the giant silk moth (*Hylopora cecropia*) (Boman and Hultmark, 1987; Steiner et al., 1981). They are positively charged and form time-variant and voltage-dependent ion channels in planar lipid membranes (Christensen et al., 1988). Drosomycin produced by *Drosophila melanogaster*, is an insect defensin with significant homology with plant antifungal peptides isolated from seeds of members of the family *Brassicaceae* (Feulbaum et al., 1994). Insect peptides, which are antifungal include antifungal peptide (Ijima et al., 1993), holotricin 3 (Lee et al., 1995), and thanatin (Fehlbaum et al., 1996). Anti-fungal protein, a histidine-rich peptide that causes cellular leakage, was purified from the third instar larval hemolymph of *Sacrophaga peregrina*. Holotrocin 3, a glycine- and histidine-rich peptide was purified from the larval hemolymph of *Holotrichia diomphallia*. Thanatin, a nonhemolymph antifungal peptide was produced by *Podisus maculiventirs*.

Amphibian Derived Peptides

The isolation of bombinin (Haberman, 1977) and subsequently the megainins (Zasloff, 1987) led to the investigation and discovery peptides throughout the amphibian species. The African clawed from (*Xenopus laevis*) produces the magainins, which are α-helical ionophores that dissipate ions gradients in cell membranes causing lysis (Westerhoff et al., 1989). Their helical, amphiphilic structure was responsible for affinity to membranes (Chen et al., 1988). The South American arboreal frog (*Phyllomedusa sauvagii*) produces the dermaseptin family of nonhemolytic antifungal peptides (De Lucca et al., 1998; Mor et al., 1991). Dermaseptins are linear cationic, lysine-rich peptides and are believed to lyse microorganisms by interacting with lipid bilayers, leading to alterations in membrane functions responsible for osmotic balance (Hani et al., 1994; Mor et al., 1994; Pouny et al., 1992). Recently four broad-spectrum antimicrobial peptides, tigerinins have been reported from the adrenaline stimulated skin secretions of the Indian frog *Rana tigerina* (Sai et al. 2001). These peptides are characterized by an intramolecular disulfide bridge between two cysteine residues forming a nonapeptide ring. The peptides are β-turn structures, cationic and exert their activity by permeabilizing the membrane.

Bacterial Peptides

Antimicrobial peptides are secreted from both gram-positive and negative bacteria. These have been classified within bacteriocins. Various strains of *Bacillus subtilis* produce the iturin peptide family, which are small cyclic peptidolipids characterized by a lipid-soluble β-amino acid linked to a peptide containing D and L amino acids (Pergament and Carmelli, 1994). Iturins affected membrane surface tension, which caused pore formation and which resulted in leakage of K^+ and other vital ions, paralleling cell death (Latoud et al., 1987; Thimon et al., 1992). Members of the *Pseudomonas syringae* pv *syringae* group produce small cyclic lipodepsipeptides known as syringomycins (Segre et al., 1989), the major form being syringomycin E (SE). SE increased transmembrane K^+, H^+, and Ca^+ fluxes and the membrane potential in plasma membranes of plants and yeasts (Reidel and Takemoto, 1987; Takemoto et al., 1989; Takemoto et al., 1991; Zhang and Takemoto, 1987). Some peptide

bacteriocins, including the *E. coli* 7-amino acid peptide microcin C7, which inhibits protein synthesis, and the *Lactococcus* peptide mersacidin, which inhibits peptidoglycan biosynthesis, have specific mechanisms, which inhibit bacterial functions. However, most of these peptides, e. g., nisin and epidermin, are thought to perbialize target cell membranes (Baba and Schneewind, 1998; van Belkum et al., 1991).

Other Antifungal Peptides from Bacteria and Fungi

Other antifungal peptides include CB-1 produced by *Bacillus lichemiformis*, which is a chitin-binding peptide containing fatty acids bound to amino acids (Oita et al., 1996). A *Bacillus lichemiformis* isolate produces fungicin, a hydrophilic narrow spectrum antifungal peptide that is resistant to proteolytic enzymes and lipase (Lebbadi et al., 1994). A cyanobacterium, *Schizotrix*, produces schizotrin A, a cyclic undecapeptide (Pergament and Carmelli, 1994), which inhibits *C. albicans* and *C. tropicalis*, and also the radial growth of *Fusarium oxysporum*. Cepacidines are glycolipids that have similar structures and produced by *Burkholderia cepacia* (Lee et al., 1994; Lim et al., 1994). They display potent antifungal activity superior to those of amphotericin B (Lee et al., 1994), and inhibit *Candida* sp., *Aspergillus niger*, *F. oxysporum* (Lee et al., 1994). *Pseudomonas lilacinus* produces two antifungal peptides, 1907-II and 1907-VIII, consisting of several amino acids, a methylamine, and a fatty acid (Sato et al., 1980), which inhibits *C. albicans*. The leucinostatin-trichopolyn group is structurally related to 1907-II and 1907-VIII. Leucinostatins are produced by submerged cultures of *Penicillium lilacinum* (Arai et al., 1973; Fukushima et al., 1983). *Mycogone resea* produces helioferins, which are members of the leucinostatin-trichopolyn group, exhibit antifungal activity against *C. albicans* (Grafe et al., 1995).

Chitin Synthase Inhibitors

Inhibitors of chitin synthase, nikkomycins, and polyoxins produced by *Streptomyces* posses antifungal activities (Chapman et al., 1992; Hori et al., 1974; Hori et al., 1974; Isono et al., 1969; McCathy et al., 1985; McCathy et al., 1985; Moneton et. al., 1986; Suzuki et al., 1965; Tariq and Develin, 1996). Another chitin synthase inhibitor FR-900403 is also known to exhibit antifungal activity (Iwamoto et al., 1990).

Peptides Affecting Glucan Synthesis

Echinocardins, which consists of a diverse family of lipopeptides, are noncompetitive inhibitors of (1,3)-β-D-glucan synthase (Beaulieu et al., 1993; Mizoguchi et al., 1977; Perez et al., 1981; Sawistowska-Schroder et al., 1984). Their mode of action is similar to that of the papulacandins, the naturally occurring antifungal glycolipids (Aguly et al., 1979; Bartizal et al., 1992; Grunner and Traxler, 1977). The hemolytic property of the native echinocandins was greatly reduced by enzymatically created analogs (designed LY compounds) of echinocandins. *Zalerion arboricola* produces the pneumocandins, which were effective against certain fungal strains, and have greater potency and spectra activity than echinocandins (Fromtling and Abruzzo, 1989, Schmatz et al., 1990). Aculeacins (A through G) are produced by *Aspergillus aculeatus* (Mizuno et al., 1977) and showed antifungal activity against *Candida albicans* and *Saccharomyces cerevisae* but reduced the growth of only few filamentous fungi (Mizoguchi et al., 1977; Satoi et al., 1977). *Aspergillus syndowi* var *mundundensis*

produces the mulundocandnins, whose structures differ from those of the echinocandins by the replacement of one of the threonines with a serine residue, and the lipophilic side chain is 12-methylmyristoyl rather than linocoyl (Mukhopadhyay and Ganguli, 1986). Mulundocandin and related compounds were found to be active against *C. albicans* and *A. niger* (Roy et al., 1986). *Cleophoma empetri* F-11899 produces the water-soluble lipopeptides WF11899 A, B, and C. These peptides demonstrated potent *in vivo* anti-Candida activities in a murine model of systemic infection and were superior to eliofungin and fluconazoles (Iwamoto et al., 1994). Aureobasidins are produced by *Aureobasidium pullulans* (Takesako et al., 1991). This group has 18 members whose structures have eight lipophilic amino acid residues and an α-hydroxyacid (Ikai et al., 1991[a], Ikai et al., 1991[b]). Their mode of action and structures differ from those of the echinocandins in that they are believed to alter actin assembly and delocalize chitin cell walls, resulting in lysis by disruption of cell membranes (Endo et al., 1997). Another study indicated that sphingolipid synthesis is the target of aureobasidin A (Nagiec et al., 1997)

Plant Antifungal Peptides

Thionins were the first antimicrobial peptides to be isolated from plants (Fernadez de Calaya et al., 1972). They are toxic towards both gram-positive and negative bacteria, fungi, yeast, and various mammalian cell types (Broekaert et al., 1997). Other antimicrobial peptides isolated, found to be structurally related to insect and mammal defensins and are named as plant defensins. Whereas most antimicrobial peptides from animals and bacteria have antibacterial activity, plant defensins show high antifungal activity (Broekaert et al., 1997), reflecting the relative importance of fungal pathogens in the plant world. Plant defensins, which are not related to either the mammalian or the insect defensins, have eight disulfide-linked cysteines comprising a triple-stranded antiparellel β-sheet structure with only one α helix (Bruix et al., 1995; Bruix et al., 1993). Their mechanisms of action have not yet been elucidated, although the possibility of permeabilization through direct protein-lipid interactions has been eliminated (Thevssen et al., 1996). They reduced hyphal elongation without marked morphological distortions (Bruix et al., 1995; Bruix et al., 1993). Some plants produce lipid transfer proteins, a family of homologous peptides having eight disulfide-linked cysteines. Onion seeds produce the lipid transfer peptide, ACE-AMP_1, which inhibited *F. oxysporum* (Cammue et al., 1995). *Zea maize* seeds produce the peptide zeamatin, which belongs to a third class of plant antifungal compounds (Vigers et al., 1991). Zeamatin causes the release of cytoplasmic material from *C. albicans* and *N. crassa*, resulting in hyphal rupture. They appear to pearmeabilize the fungal plasma membrane and inhibit *C. albicans*. Members of the family *Rhamnaceae* and other plant families produce the basic cyclopeptides in which a 10- or 12-membered peptide-type bridge spans the 1,3 or 1,4 positions of a benzene ring (Gournelis et al., 1997). The antifungal properties of many members of the family have not yet been determined.

Viral Peptides

Viral peptides were first identified, through protein modeling, as two positively charged, highly amphipathic helices within the cytoplasmic tail of the envelope protein of HIV-1 (Eisenberg and Wesson, 1990).

Further studies have shown these peptides and peptides derived from other lentivirus transmembrance proteins to have antimicrobial and cytolytic activities (Stein et al., 1996). All these peptides have a high proportion of arginines and no lysines, but a difference in selectivity between the peptides has been observed (Stein et al., 1996).

Synthetic Peptides

To permit full exploitation of peptides as new antimicrobial agents, it is important to determine their mode of action. By basing a synthetic peptide on a naturally occurring peptide, it is possible to improve antimicrobial activity and at the same time give insight into the mechanism of action. Synthetic peptides can also be designed to improve factors such as specificity, stability, and toxicity. Peptides named as “modellins” of different lengths and hydrophobicities have been synthesized, which possess antibacterial and hemolytic activity (Bessalle et al., 1993). These studies have been based on naturally occurring peptides. It is also possible to discover potent antimicrobial peptides randomly. Combinatorial libraries allow the systematic examination of millions of peptides. D4E1 is a synthetic peptide that is active against germinated conidia of *Aspergillus* species (De Lucca et al., 1998).

The present chapter deals with the antifungal activity of ATBI against a number of fungal strains and its bifunctional role in the mechanism of fungal growth inhibition.

Materials and Methods

Materials

Potato dextrose, bactoagar and other microbiological media components were from Himedia, India. Xylan, DNSA, and xylose were from Sigma Chemical co. USA. Filter discs were from Whatman. All other chemicals were of analytical grade.

Fungal Strains

The fungal strains, *Alternaria solani* (NCIM 887), *Aspergillus flavus* (NCIM 535, 538, 542), *Aspergillus niger* (NCIM 773), *Aspergillus oryzae* (NCIM 637, 643, 649, 1032), *Claviceps purpurea* (NCIM 1046), *Colletotrichum* sp., *Curvularia fallax* (NCIM 714), *Curvularia lunata* (NCIM 716), *Curvularia cymbopogonis* (NCIM 695), *Fusarium oxysporum* (NCIM 1008, 1043, 1072), *Fusarium moniliforme* (NCIM 1099, 1100), *Helminthosporium* sp. (NCIM 1079), *Phomopsis* sp., *Penicilium fellulatum* (NCIM 1227), *Penicillium roqueforti* (NCIM 712), and *Trichoderma reesei* (NCIM 992, 1051, 1052, 1186) were from our in-house culture collection unit, National Collection of Industrial Micro-Organisms (NCIM), Pune, India.

Anti-Fungal Activity Assay

Anti-fungal activity of ATBI was assayed essentially by a) hyphal extension inhibition assay, b) spore suspension assay, and c) micro-spectrometric assay. The hyphal extension assay was carried out as described (Roberts and Selitrennikoff, 1986), with some modifications. Freshly grown fungal mycelium was spot inoculated at the center of a petriplate containing Potato Dextrose (PD) agar media and incubated at 28°C for 24-48 h. Sterile filter paper discs (5 mm diameter) impregnated with different concentrations of ATBI were placed in front of the growing fungal mycelium. The plates were further incubated at 28°C and the crescent zones of retarded mycelial growth were observed. The anti-fungal activity by the spore suspension assay was determined as described (Mauch, 1988). All manipulations were carried out under sterile conditions. Fungal spores were harvested from the freshly grown fungal culture and suspended in sterile water. The concentration of the spore suspension was adjusted to $1.0\text{-}2.5\times10^5$ spores/ml, depending on the fungus to be tested. To 1 ml of the freshly prepared spore suspension, 1 ml of half strength PD agar was added and was immediately overlaid on petridishes containing PD agar. To allow for spore germination and initial vegetative growth, plates were incubated at 28°C for 24-48 h. At this time, sterile filter discs were laid on the agar surface, and different concentrations of ATBI were applied to the discs. The plates were incubated at 28°C and photographed after 24-72 h. All test solutions were filtered through a 0.22 μm membrane prior to the application. Micro-spectrometric anti-fungal assay was performed for the quantitative demonstration of anti-fungal activity as described (Broekaert, 1990). Briefly, routine tests were performed with 20 μl of (0.22 μm filter sterilized) test solution and 80 μl of fungal spore suspension (10^5 spores/ml) in half strength PD broth. Control micro-culture contained 20 μl of sterile distilled water and 80 μl of the fungal spore suspension. Unless otherwise stated the incubation conditions for the

experiments were 28°C for 48 h. Anti-fungal activity is expressed in terms of percent inhibition as defined in (Cammue, 1992).

The purified ATBI was treated at 90°C for 5 min at pH 6.0 and the anti-fungal activity was determined by spore suspension assay. Similarly, the pH stability of ATBI was determined in the range from pH 2-10 at 40°C and its effect on the anti-fungal activity was checked as described before.

Minimum Inhibitory Concentration

The minimum inhibitory concentrations (MIC) of the inhibitor for the growth inhibition of the fungal strains were determined by broth dilution method (Amsterdam, 1991). Serial dilutions of ATBI were made in half-strength PD broth in micro titer plates. Each well was inoculated with 10 µl of 10^5 spores/ml of the test organism. The MIC was determined after overnight incubation of the plates and was taken as the lowest concentration of ATBI at which growth was inhibited.

Structural Studies and Homology Search

Circular dichroism (CD) spectra of ATBI (25 µg/ml) were recorded on a J-715 spectropolarimeter (Jasco) using a quartz cell of 1 mm path length. Measurements were made over a 250-190 nm range. All CD spectra were recorded at room temperature and obtained with a 1 nm band width, scan speed of 50 nm/min, and time constant of 5 s. The spectra obtained were the average of six scans to improve the signal to noise ratio. A base line was recorded and subtracted after each spectrum. The data were expressed in terms of ellipticity as measured in millidegrees. Sequence homology search was undertaken after retrieving the sequences of all the anti-fungal peptides from the databases and aligning them manually.

Production of Xylanase and Aspartic Protease from the Fungal Strains

Freshly grown *T. reesei* and *A. oryzae* were inoculated into a synthetic liquid media having the composition, KH_2PO_4 (2 g/l), $(NH_4)_2SO_4$ (7 g/l), Urea (1.5 g/l), $MgSO_4.7H_2O$ (0.3 g/l), $CaCl_2.2H_2O$ (0.3 g/l), $FeSO_4.7H_2O$ (5 mg/l), $MnSO_4.H_2O$ (1.56 mg/l), $ZnSO_4.7H_2O$ (1.4 mg/l), $CoCl_2$ (1 mg/l), Tween 80 (1 g/l) and containing oat spelt xylan (10 g/l) or soyameal (20 g/l) for the production of xylanase or aspartic protease respectively at 28ºC for 72 h. The fungal cells were separated by filtration and centrifugation and the extracellular culture filtrate was tested for the presence of xylanase and aspartic protease. The inhibition of the xylanase and acid protease in the culture filtrate was detected by plate assay. The above synthetic medium was also used in agar plates for the fungal growth inhibition assay of *T. reesei* and *A. oryzae*, in the presence xylan or casein at various concentrations of ATBI.

Xylanase Inhibition Assay

Xylanolytic activity of the purified xylanase from the extremophilic *Bacillus* sp. was determined at pH 6.0 and 50°C by measuring the amount of reducing sugar liberated following the hydrolysis of oat spelt xylan (1%), in a reaction volume of 1 ml. The reducing sugar released was determined by the Dinitrosalicylic acid (DNSA)

method as described (Miller, 1959) using D-xylose as the standard. One unit of xylanase activity is defined as the amount of enzyme, which produced 1 μmol of xylose equivalent per min from xylan under the assay conditions. Xylanase inhibition assay was carried out as described above in the presence of increasing concentrations of the inhibitor. Inhibition kinetics was analyzed by Lineweaver-Burk reciprocal plot.

Protease Inhibition Assay

Proteolytic activity of the purified aspartic protease from *Aspergillus saitoi* (F-Prot) was measured by assaying residual enzyme activity after incubating the enzyme and the inhibitor. F-Prot activity was measured in the absence or presence of inhibitor. 50 μl (100 μg/ml) of F-Prot in glycine-HCl buffer, 0.05 M, pH 3.0 was incubated with the inhibitor (25 μg/ml) for 5 min. The reaction was started by the addition of 1 ml of hemoglobin (5 mg/ml) and was allowed to proceed for 30 min at 37°C. The enzymatic activity was quenched by the addition of 2 ml of PCA (1.7 M) followed by 30 min incubation at 28°C. The precipitate formed was removed by centrifugation and filtration. The optical absorbance of the PCA soluble products in the filtrate was read at 280 nm. One unit of protease activity is defined by an increase of 0.001 at Δ280 nm per min at pH 3.0 at 37°C measured as PCA soluble products using hemoglobin as the substrate. The inhibition kinetics was performed by Lineweaver-Burk's double reciprocal plot.

Chemical Modification of ATBI with 2,4,6-Trinitrobenzenesulfonic Acid and *N*-ethyl-5-phenylisoxazolium-3'-sulfonic Acid

ATBI (25 μg) and 0.25 ml of 4% sodium bicarbonate was incubated with varying concentrations of 2,4,6-trinitrobenzenesulfonic acid (TNBS), a lysine group modifier (Okuyama 1960), at 37°C in a reaction mixture of 0.5 ml in dark. Aliquots were withdrawn at suitable intervals and the reaction was terminated by adjusting the pH to 4.6. A control without the modifier was routinely included and the residual activity at any given time was calculated relative to the control. The extent of inactivation of F-prot and xylanase was determined with the modified inhibitor as described before.

N-ethyl-5-phenylisoxazolium-3'-sulfonic acid (Woodward's reagent K, WRK) has been known to react with the carboxyl group of aspartate and glutamate residues (Arana and Vallejos, 1981; Sinha and Brewer, 1985). To modify the carboxylic groups, ATBI (25 μg) was incubated in the absence or presence of different concentrations of WRK at 28°C for 1 h. Aliquots were removed at different time intervals and the reaction was quenched by the addition of sodium acetate buffer pH 5.0 to a final concentration of 100 mM. Excess reagent was then removed by gel filtration on a Bio-gel P2 column, equilibrated with sodium phosphate buffer, 0.05 M pH 6.0. The fractions containing the modified ATBI were concentrated by lyophilization and the residual activity of the inhibitor was determined by assaying for the anti-xylanolytic and anti-proteolytic activity.

The TNBS and WRK modified ATBI was used in the experiments to determine the anti-fungal potency against *T. reesei* and *A. oryzae*. Control experiments with the chemical modifiers were performed to observe the impact of these compounds on the fungal growth inhibition.

Rescue of Fungal Growth Inhibition by the Enzymatic Reaction Products

Hydrolysis of Xylan

The hydrolysis of xylan (1%) was carried out in a 5 ml reaction mixture containing 500 units of xylanase in potassium phosphate buffer 0.05 M, pH 6.0 at 50°C for 1 h. The hydrolysis was monitored by estimating the reducing sugar formed by the DNSA method using xylose as the standard. The hydrolyzed products were separated from the reaction mixture by passing through amicon UM 10 membrane.

Hydrolysis of Casein

Casein (1%) was subjected to enzymatic hydrolysis by F-prot (100 μg/ml) in a reaction volume of 5 ml containing glycine-HCl buffer 0.05 M, pH 3.0 at 37°C for 1 h. The hydrolyzed products were separated by membrane filtration and centrifugation followed by monitoring at 280 nm.

The hydrolyzed products of xylan and casein were concentrated by lyophilisation and used for the rescue of the cellular growth inhibition by spore suspension assay on the synthetic agar media containing xylan or casein. ATBI was applied to the paper discs and the growth inhibition was observed after 12 h. To the inhibited mycelial growth of *T. reesei* and *A. oryzae*, the hydrolyzed products of xylan and casein were added and the plates were further incubated at 28°C for overnight and the vegetative growth of the fungi was monitored.

Results

Anti-fungal Activity of ATBI

The extracellular culture filtrate of the extremophilic *Bacillus* sp. was evaluated for its potency for the fungal growth inhibition. Aliquots of the sterile filtered culture filtrate were added to the filter discs on the agar plates containing germinating fungal spores. In the following 24 h, distinct inhibition zones developed around the filters treated with the culture filtrate. The culture filtrate exhibited anifungal activity against the saprophytic fungi *T. reesei*. To assess the anti-fungal activity of the compound we have purified the molecule (ATBI) from the culture filtrate. During the purification process, the anti-fungal property of ATBI was found to be co-purified with its aspartic protease inhibitory activity. The anti-fungal activity of the purified ATBI was assessed in a variety of standard biological assays against 16 fungal strains (Table-1). ATBI showed strong inhibitory activity against *A. flavus, A. oryzae*, *A. solani, F. oxysporum, F. moniliforme*, and *T. reesei*, and moderate activity against *A. niger, C. cymbopogonis, Phomopsis* sp., *C. falax, C. lunata*, *P. roqueforti*, *P. fellulatum*, *Helminthosporium* sp., and *Colletotrichum* sp.

Table-1

Antifungal potency of ATBI against the tested fungal strains and the comparison of their IC_{50} and MIC values.

Fungal Strains	IC_{50} (µg/ml)	MIC (µg/ml)
Aspergillus flavus	1.25	0.82
Aspergillus oryzae	2.12	1.12
Alternaria solani	1.00	0.60
Fusarium oxysporum	3.50	2.30
Fusarium moniliforme	2.52	1.84
Trichoderma reesei	0.52	0.30
Phomopsis sp.	ND	3.80
Curvularia lunata	ND	3.92
Curvularia lymbopogonis	ND	4.21
Colletotrichum sp.	ND	3.95
Helminthosporium sp.	ND	4.15
Curvularia falax	ND	4.03
Aspergillus niger	ND	3.85
Penicillium roqueforti	ND	5.68
Penicillium fellulatum	ND	5.90
Claviceps purpurea	NA	NA

ND stands for “Not Determined”, NA stands for “Not Active”

The anti-fungal activity of ATBI was indicated by the zone of inhibition developed around the paper discs against the vegetative growth after the spore germination (Figure 1). The diameter of the clearance zone observed was found to be proportional to the concentration of the inhibitor applied. Further, fungal growth inhibition was monitored microscopically, wherein the spores of different fungal strains were cultured in the presence of varied concentrations of the inhibitor. The morphological differences observed in the mycelial growth after 24 h at 28°C are shown in Figure 2. In the presence of the inhibitor, the germination of *T. reesei* spores was delayed whereas in *F. oxysporum, F. moniliforme, A. solani,* and *A. oryzae*, the rate of growth of the mycelia was slower. As revealed from the micrograph, there was no indication of lysis in mycelia in the presence of ATBI.

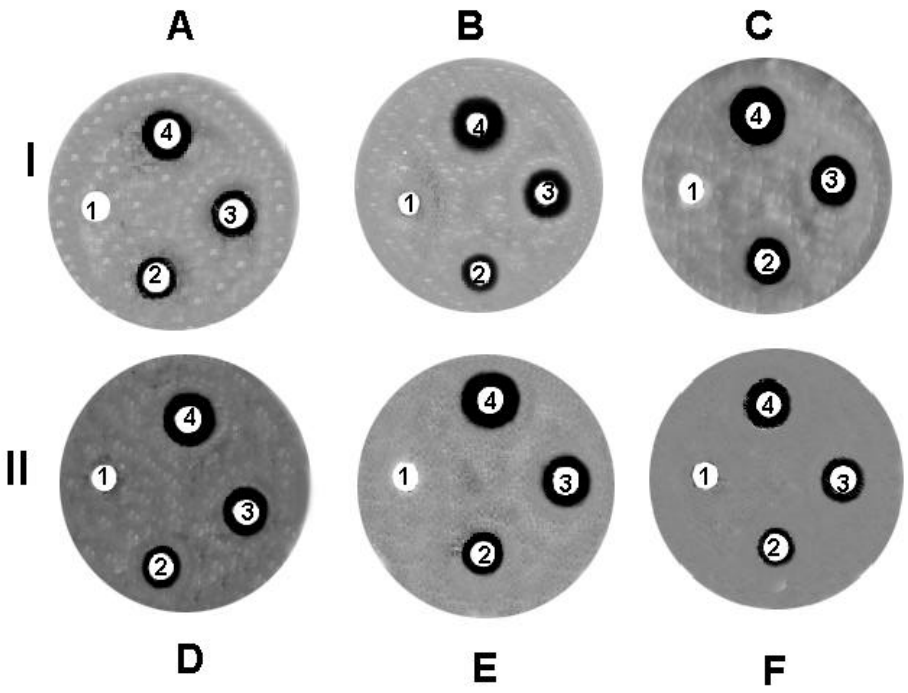

Figure 1. Inhibition of fungal growth by the purified ATBI.

Fungal spores were allowed to germinate on PD agar and grow for 24 h before the test solution was added. Subsequently filter discs were placed on the agar, 40 µl of test solutions were added on the discs, and the fungi were allowed to grow for 12 h. The test solution (40 µl) contained 0 µg (1), 1 µg (2),

2 µg (3), and 3 µg (4) of ATBI. Fungal strains tested were *T. reesei* (A), *F. oxysporum* (B), *A. solani* (C), *A. flavus* (D), *A. oryzae* (E), and *F. moniliforme* (F).

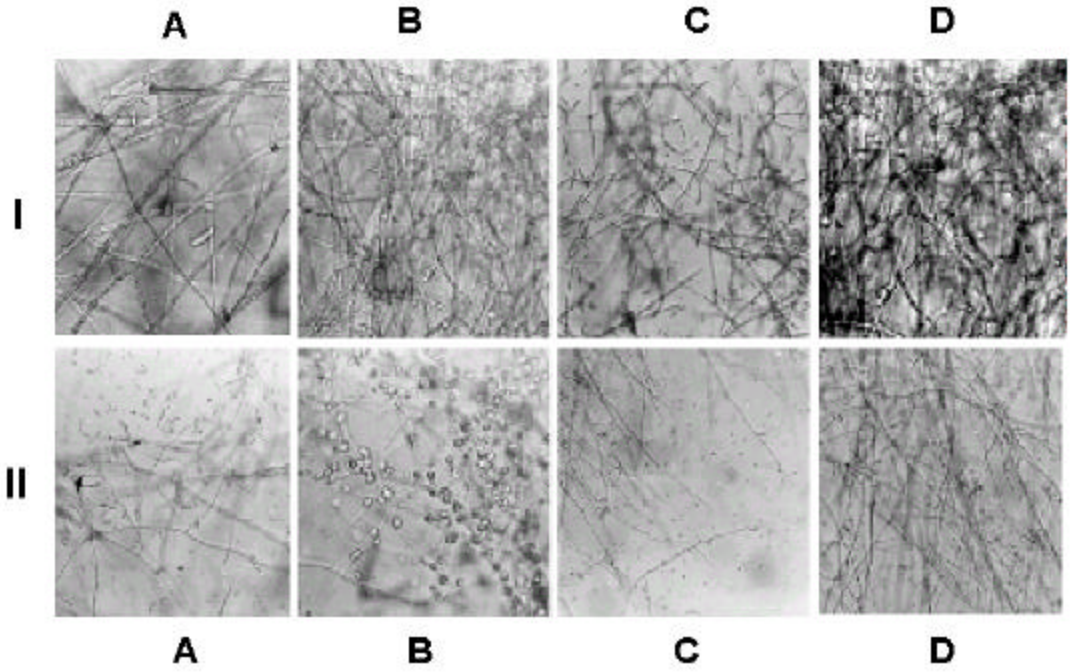

Figure 2. Morphological changes induced in the mycelia of the fungal strains in the presence of ATBI. Fungal spores were germinated in half strength PD broth in the absence (panel-I) or presence (panel-II) of ATBI and the growth was observed after 24 h. The fungal strains tested were *F. moniliforme* (A), *T. reesei* (B), *F. oxysporum* (C), and *A. oryzae* (D).

After 24 h, the concentration of ATBI required for 50% inhibition (IC_{50}) of fungal growth varied from 0.52 μg/ml for *T. reesei* to 3.5 μg/ml for *F. moniliforme*, whereas the minimum inhibitory concentration (MIC) ranged from 0.30 μg/ml for *T. reesei* to 5.90 μg/ml for *P. fellulatum*. The saprophytic fungus *T. reesei,* was found to be the most sensitive to ATBI whereas *C. purpurea* was the least sensitive strain. Figure 3 describes the time dependent dose response curves of *T. reesei*, *F. oxysporum, F. moniliforme*, *A. solani*, *A. oryzae*, and *A. flavus*. As revealed from the figure the extent of growth inhibition tended to decrease with the increase in the incubation time. For example, in case of *A. oryzae* the IC_{50} value of ATBI (after 24 h) was increased from 2.125 to 2.25 and 2.375 μg/ml after 48 and 72 h respectively. The time dependent decrease in potency of ATBI was less pronounced in *T. reesei* and *A. solani* as compared to *A. oryzae*, *A. flavus*, *F. oxysporum*, and *F. moniliforme*.

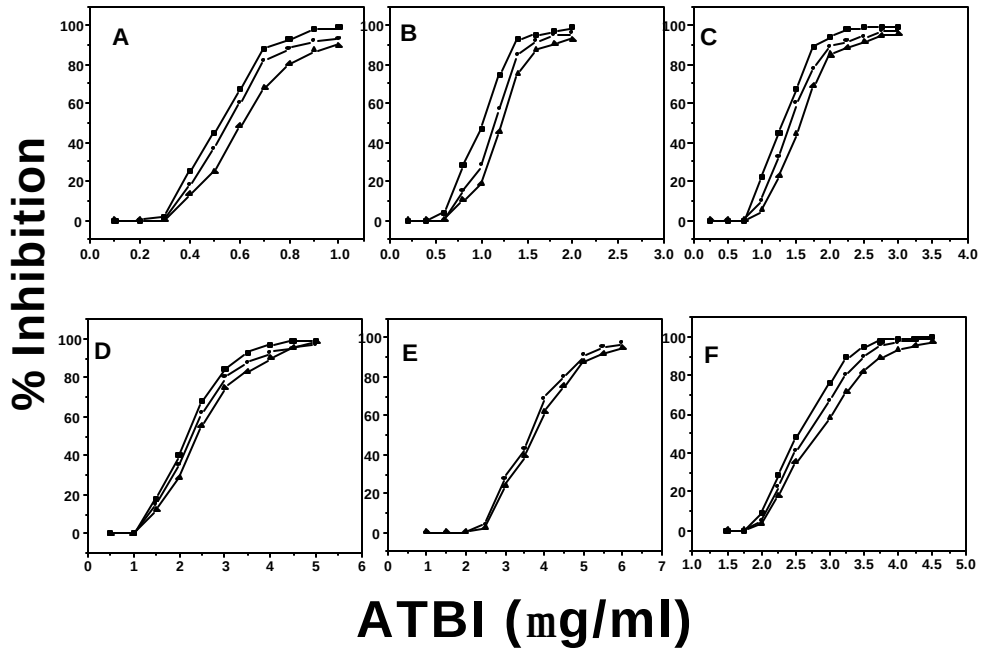

Fig.ure 3. Time-dependent dose response growth inhibition curves.

Growth inhibition of the fungal strains, *T. reesei* (A), *A. solani* (B), *A. flavus* (C), *A. oryzae* (D), *F. oxysporum* (E), and *F. moniliforme* (F) at different concentrations of ATBI, was recorded after 24 h (■), 48 h (●), and 72 h (▲). To 80 µl of spore suspension (10^5 spores/ml), 20 µl of test solution containing various concentrations of ATBI was added in a micro-culture plate. Control micro-culture plate contained 20 µl of distilled water and 80 µl of spore suspension. Anti-fungal activity of ATBI was estimated in terms of percent inhibition and the IC_{50} values were calculated from the curves.

The stability of the inhibitor towards fungal growth inhibition and aspartic protease inhibitory activity was checked with respect to temperature and pH. In similar tests, the anti-fungal and aspartic protease inhibitory activity of ATBI was resistant to heat treatment up to 90°C for 10 min and was stable over a pH range of 2-10.

Primary and Secondary Structure Analysis of ATBI

Searches of the protein databases have failed to identify any anti-fungal proteins with significant homology to ATBI. The primary structure also revealed an unusually high content of aspartic acid (4 residues per molecule). The net charge per molecule calculated from the amino acid composition was negative indicating that ATBI is an anionic peptide. The secondary structure of ATBI as revealed from the CD spectrum exhibited a negative band at approximately 203 nm, which is a characteristic feature of random coil conformation (Figure 4). Further, the secondary structure content calculated from the CD data by the algorithm of the K2d program (Andrade, et al., 1993; Merelo, et al., 1994), showed no periodic structure in the peptidic inhibitor. These results were corroborated by constructing the peptide according to the Brookhaven protein building method using SYBYL software, which also predicted a random coil structure of ATBI.

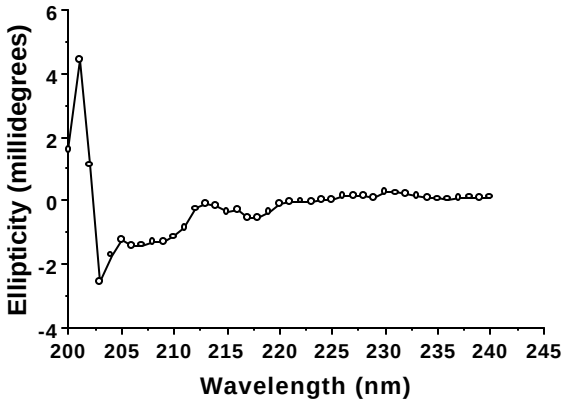

Figure 4. **Far-UV circular dichroism spectrum of ATBI**.

ATBI (25 μg/ml) was dissolved in KCl-HCl buffer, 0.05 M, pH 3.0 and the CD spectrum was recorded from 280-200 nm at 25°C. The spectrum shown is the average of six scans with the baseline subtracted. The data is expressed in terms of ellipticity as measured in millidegrees.

Role of Xylanase and Aspartic Protease in Fungal Growth Inhibition

To understand the mechanism of the fungal growth inhibition by ATBI, we have investigated the role of two essential hydrolytic enzymes, xylanase and aspartic protease, which are crucial for the growth of fungal strains, and thus, in their biosynthetic pathway. The production of xylanase and aspartic protease is well documented in *A. oryzae* (Christov et al., 1999, Tsujita et al., 1977) and in *T. reesei* (Zeilinger and Mach, 1998, Eneyskaya et al., 1999) hence, we have tested the anti-fungal potency of ATBI against these two fungi by growing them on selective media. As revealed from figure 5, the growth of *T. reesei* and *A. oryzae* on the synthetic agar medium containing xylan or casein was inhibited by ATBI.

To correlate the anti-xylanolytic and anti-proteolytic activity of ATBI to its anti-fungal property, the fungal strains were grown in a synthetic medium in shake flasks, containing xylan or soyameal as the sole carbon source and the production of xylanase and aspartic protease was estimated at 72 h. In the presence of xylan the fungal cultures produced considerable amount of xylanase whereas the production of aspartic protease was negligible. Similarly, the selective production of aspartic protease was observed in the culture broth when soyameal was used in the growth medium. To investigate the effect of ATBI on xylanase and aspartic protease activity, the culture filtrates were added in the central well of the agar plate containing xylan or casein. ATBI was added in the peripheral wells and the plates were incubated at 37°C. The xylanolytic or proteolytic activity was detected by the clearance zone observed around the central well and their inhibition was prominent by the crescent zone in front of the well containing ATBI (Figure 6). For the aspartic protease activity, the central well was equilibrated with glycine-HCl buffer, 0.05 M (pH 3), before addition of the culture broth. The retardation of the

mycelial growth and the inhibition of xylanase and aspartic protease activities by ATBI suggested the correlation between the inhibitions of these enzymatic activities to the fungal growth inhibition

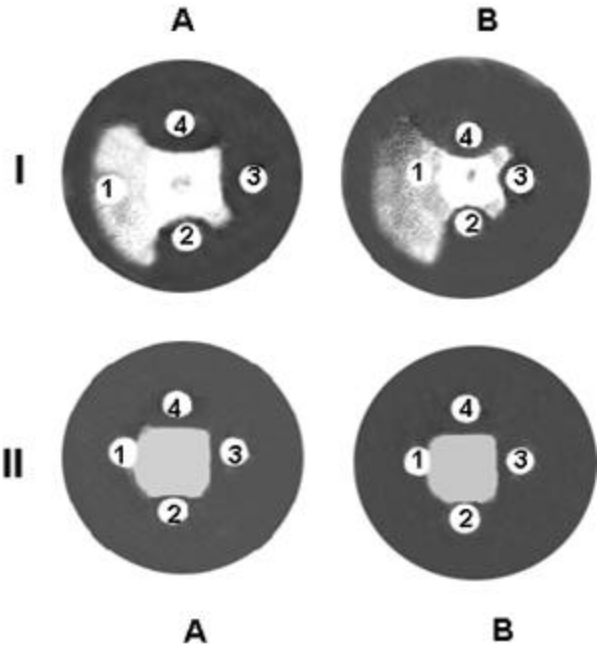

Figure 5. Plate assay for the growth inhibition and enzymatic activities.

Growth inhibition of *T. reesei* (panel-I) and *A. oryzae* (panel-II) on selective growth medium in the presence of ATBI. The fungal strains were spot inoculated on the synthetic agar media containing 0.5% of xylan (A) or soyameal (B) as the carbon source. The paper discs at the periphery of the advancing mycelia contained 0 μg (1), 1 μg (2), 2 μg (3), and 3 μg (4) of ATBI. After the inhibitor treatment, the plates were incubated for 12 h.

.

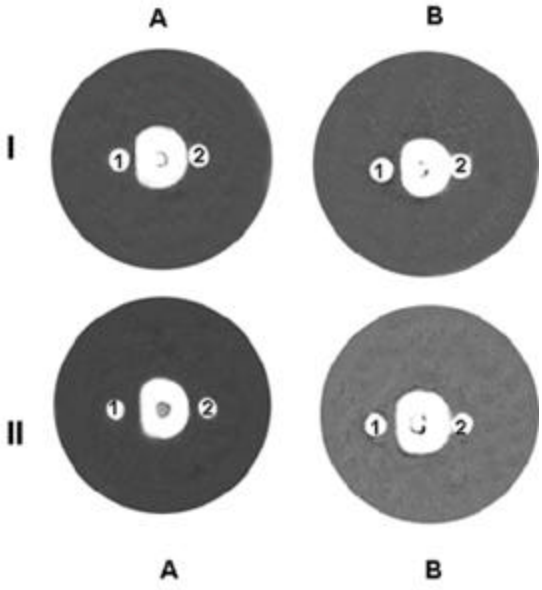

Figure 6. Anti-xylanolytic and anti-proteolytic activity of ATBI.

T. reesei, (panel-I) and *A. oryzae* (panel-II) were grown in the synthetic medium containing 0.5 % of xylan or casein. The culture filtrates were added in the central well of the agar plate containing 0.5% of xylan (A) or casein (B). The peripheral wells indicate the presence (1) or absence (2) of ATBI.

The role of xylanase and aspartic protease in fungal growth inhibition was further investigated by enriching the ATBI treated fungal strains with the enzymatic products of xylan and casein. On the synthetic medium containing xylan or casein the spore suspension of *T. reesei* and *A. oryzae* were inoculated and allowed to grow. ATBI was added to the discs and zone of inhibition was observed after 12 h. To the ATBI treated discs enzymatically hydrolyzed xylan or casein was added and the fungi were further allowed to grow for 24 h. As a control sterile distilled water was added to an ATBI treated disc. As observed from Figure 7, growth inhibition was rescued by the addition of hydrolyzed xylan or casein. The control did not show the revival of the growth. The rescue of the fungal growth inhibition by the enzymatic reaction products strengthened the role of xylanase and aspartic protease in the cellular growth inhibition.

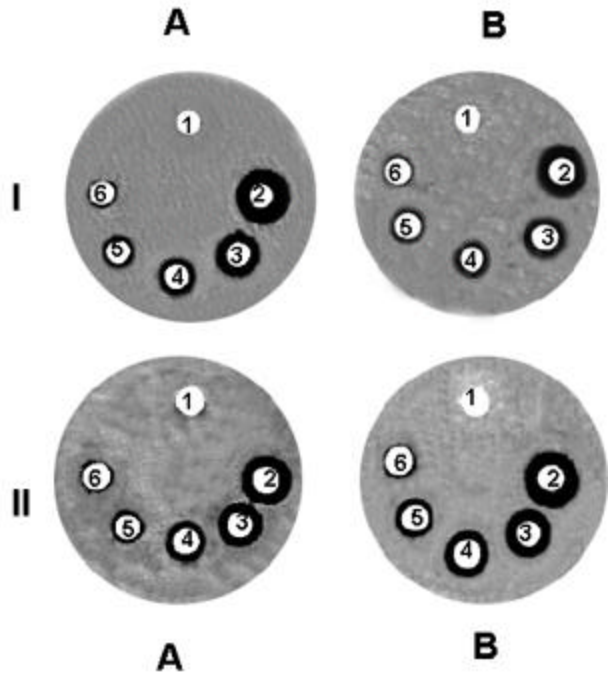

Figure 7. Rescue of fungal growth inhibition by the enzymatic reaction products.

Fungal spore (10^5 spores/ml) of *T. reesei* (panel-I) and *A. oryzae* (panel-II) were allowed to germinate on the synthetic agar media containing 0.5% of xylan (A) or casein (B). The filter discs on the agar contained 0 μg (1), 3 μg (2-6) of ATBI. After 24 h the hydrolyzed products of xylan (A) or casein (B) at a concentration of 0 μg, 0.5 μg, 1 μg, and 2 μg were added to the filter discs 3, 4, 5, and 6 respectively and the growth was observed after 12-24 h.

Chemical Modification of ATBI and Assessment of its Anti-fungal Activity

The role of functional groups for the inhibitory activity of ATBI was elucidated by employing chemical modifiers with specific reactivity. The amino acid sequence of ATBI revealed that Lys, Asp, and Glu are the amino acids containing ionizable side chains. The involvement of these groups in the mechanistic pathway was investigated using WRK, a carboxyl group modifier, and TNBS, an amine group modifier of lysine. The inhibitory activity of the WRK or TNBS modified ATBI was determined by assaying against xylanase and F-Prot, and the residual inhibitory activity at the given time was calculated relative to the control. Xylanase and F-Prot contained carboxyl group in the active site, thus it was essential to remove the excess WRK reagent completely to avoid enzyme inactivation by the modifier itself. Semi-logarithmic plots of residual inhibitory activity against xylanase and aspartic protease as a function of time were linear (Figure 8) signifying that the inactivation process obeys pseudo-first order kinetics. Loss of inhibitory activity was dependent on time and concentration of the reagent. The reaction of WRK is initiated by the formation of ketoketenimine, which modifies the carboxyl groups of the inhibitor to give an enol ester. The modification of the carboxyl groups of ATBI was monitored by the differential absorption at 210/340 nm. Analysis of the order of reaction for xylanase and F-Prot by the method described (Levy, 1963) yielded a slope of 1.67 and 1.64, respectively (Insets of Figure 8a), suggesting the involvement of two carboxyl groups of ATBI in the enzyme inactivation. The participation of the amine group of the lysine residues of ATBI was elucidated by lysine modifier TNBS. TNBS caused time- and concentration dependent loss of the inhibitory activity of ATBI. A reaction order of 0.75 and 0.79 for xylanase and F-Prot respectively with respect to the modifier was determined from the slope of the double logarithmic plots (Insets of Figure 8b) indicating the involvement of a single amine group of ATBI in the enzyme inactivation.

In order to elucidate the mechanism of action of ATBI in fungal growth inhibition, the carboxyl, and amine modified ATBI was tested for its potency towards the growth inhibition of *T. reesei* and *A. oryzae* on selective growth media. Figure 9 indicated that the TNBS or WRK modified ATBI did not inhibit the fungal growth indicating the involvement of the amine and carboxylic groups of the Lys and Asp/Glu residues respectively. Control experiments were carried out with the chemical modifiers WRK and TNBS using the synthetic agar medium. Interestingly, WRK inhibited the growth of *T. reesei* and *A. oryzae* as carboxyl group is known to present in the active site of xylanase and aspartic protease. TNBS failed to inhibit the fungal growth, which is may be due to the absence of Lys residue in the active site of these enzymes.

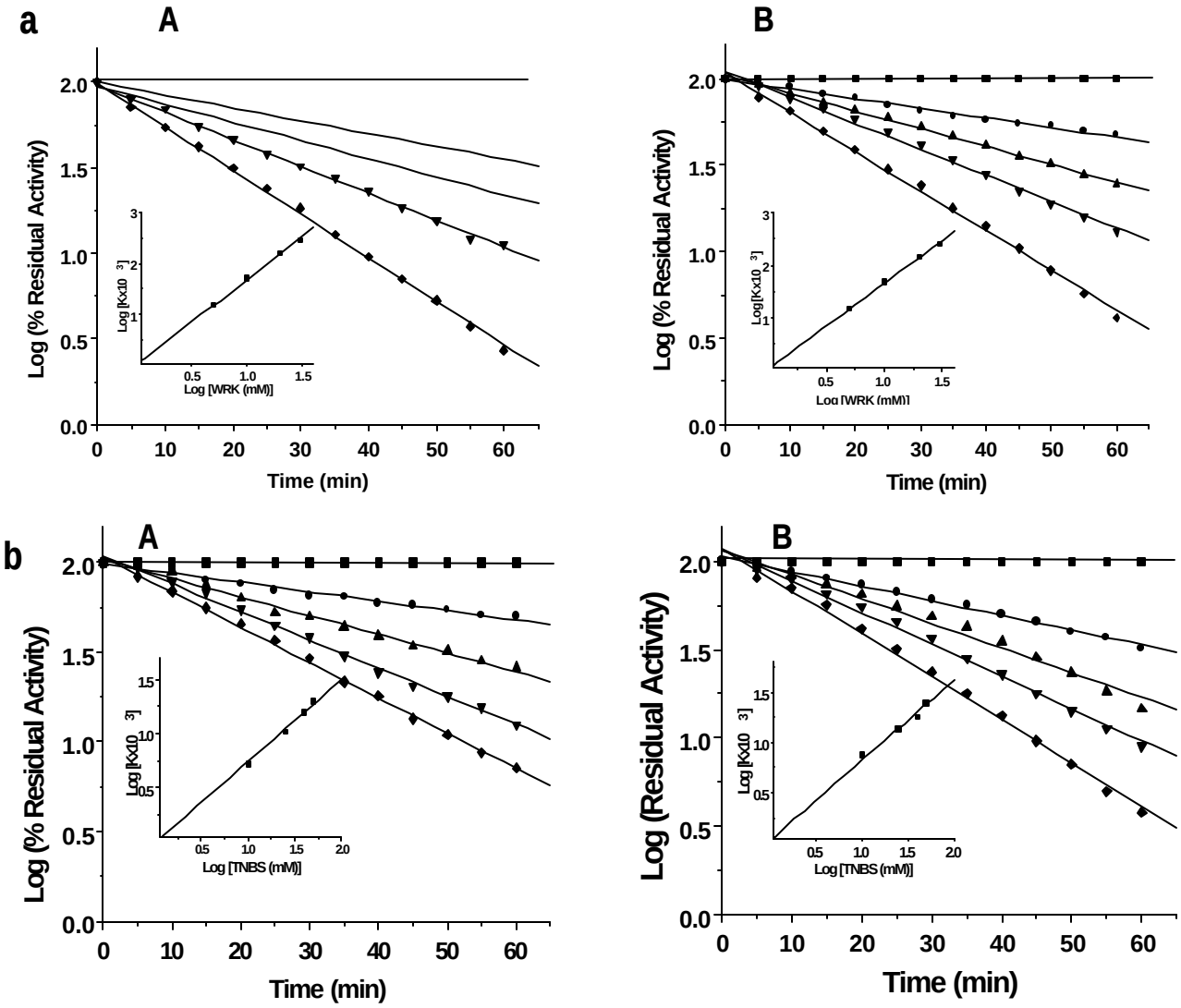

Figure 8. Differential labeling of the ionizable groups of ATBI with WRK and TNBS.

a) Inactivation of ATBI by WRK. ATBI (5 µg) was treated with 0 mM (■), 5 mM (●), 10 mM (▲), 20 mM (▼), and 30 mM (◆) of WRK at 28°C for 1 h. Aliquots of the reaction mixture were removed at times indicated and the reaction was quenched with the addition of sodium acetate buffer to a final concentration of 100 mM and assayed for the inhibitory activity. b) Effect of TNBS on the in-activation of ATBI. ATBI (5 µg) was incubated without (■) or with 10 mM (●), 25 mM (▲), 40 mM (▼), and 50 mM (◆) of TNBS at 37°C in dark for 1 h. Aliquots at specified time intervals were removed and the reaction was stopped by adjusting the pH to 4.6.

The inhibitory activity of the WRK or TNBS modified ATBI was determined by assaying against xylanase (A) and F-Prot (B) and the residual inhibitory activity at the given time was calculated relative to the control. The lines represent the best fit for the data obtained as the natural logarithm of percent of residual inhibitory activity *versus* time. Inset represents the double logarithmic plots for the pseudo first-order rate constants *versus* the concentration of the modifiers.

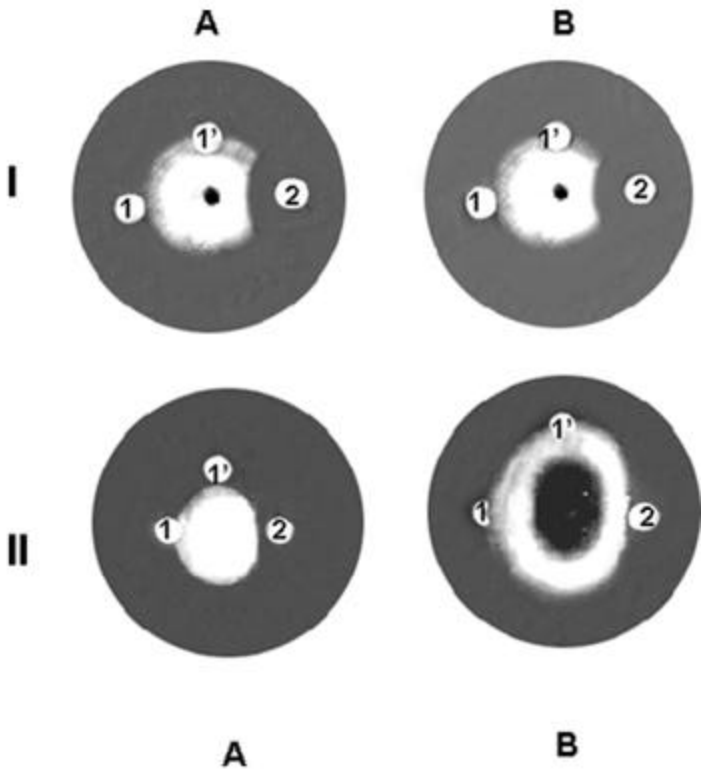

Figure 9. Effect of chemically modified ATBI and enzymatic hydrolyzed products of xylan and casein on the growth

Inhibition of *T. reesei* and *A. oryzae*.

Fungal growth inhibition in the presence of TNBS or WRK modified ATBI. *T. reesei* (panel-I) and *A. oryzae* (panel-II) were grown on the synthetic agar media containing 0.5% of xylan (A) or casein (B). The test solution containing TNBS modified (1), WRK modified (1'), or unmodified (2) ATBI was applied onto the paper discs at the periphery of the advancing mycelia and the fungal growth was observed after 12-24 h.

Inhibition Kinetics of Xylanase and Asparatic Protease by ATBI

To elucidate the mechanism of inhibition of xylanase and aspartic protease by ATBI we have investigated the kinetics of inactivation. For the inhibition studies, we have used the purified xylanase from the extremophilic *Bacillus* sp. and F-Prot from *Aspergillus saitoi* respectively as model systems. The enzyme activities were monitored in the presence of various concentrations of inhibitor and substrate, as a function of time. The double reciprocal plots of reaction velocity versus substrate concentration obtained for the enzymes demonstrated steady state kinetic behavior and competitive mode of inhibition (Fig. 10) suggesting the binding of ATBI to the active site of both the enzymes. The inhibition constant K_i, determined, for xylanase and F-Prot was 1.75 μM and 3.25 μM respectively revealing the higher binding affinity of ATBI to the active site of xylanase than the F-Prot.

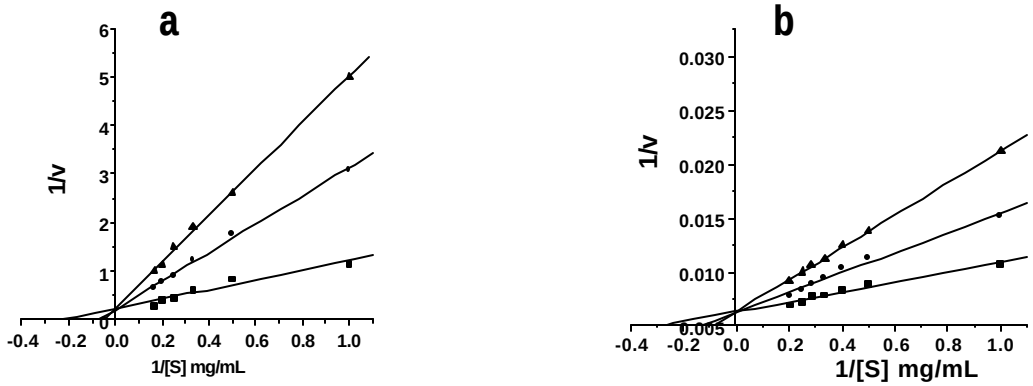

Figure 10. Lineweaver-Burk reciprocal plots for the inhibition of xylanase and F-Prot by ATBI.

a) Purified xylanase (25 μg/ml) in 50 mM potassium phosphate buffer, 0.05 M, pH 6.0, was incubated without (■) or with the inhibitor at 10 μg/ml (●), and 20 μg/ml (▲) and assayed at increasing concentrations of xylan. b) F-Prot (100 μg/ml) in glycine-HCl buffer, 0.05 M, pH 3.0, was assayed in the absence (■) or presence of 10 μg/ml (●), 20 μg/ml (▲) of ATBI at increasing concentrations of hemoglobin.

The reciprocals of the rate of the substrate hydrolysis by xylanase and aspartic protease (1/v) for each inhibitor concentration were plotted against the reciprocals of the substrate concentration (1/[S]). The straight lines indicated the best fit for the data obtained. Inhibition constant K_i was calculated from the formula for the competitive type of inhibition.

Discussion

Most common antibiotics are organic molecules that are synthesized by multienzyme pathways makes it difficult to devise ways to construct structural analogs that do not require laborious organic chemistry. Because of the ease with which analogs of antibiotic peptides can be made, they hold considerable promise as a general source of new antibiotics that can augment or supplant the current repertoire of antibiotics that is diminishing in the face of increasing antibiotic resistance among microbial populations. Discovery of novel antifungal pepides and elucidation of their mechanism of action will expand our understanding of intrinsic host defenses and will certainly provide new approaches to antifungal chemotherapy.

Protease inhibitors, in particular, have attracted lot of attention since they have been shown to inhibit proteases that present in many species of herbivorous insects and fungal pathogens (Ryan, 1990; Lorito et al., 1994). The protease inhibitors play an important role in the protection of plant tissue from pest and pathogen attack by virtue of anti-nutritional interactions. Reports on cysteine and serine protease inhibitors, chitinases, glucanases, ribosome-inactivating proteins, and permatins as anti-fungal agents are well documented (Wolfson, et al., 1995; Ryan, 1990; Mauch, et al., 1988). The present study is the first report of a bifunctional inhibitor, ATBI, which inactivates xylanase and aspartic protease as well as exhibits anti-fungal activity. It is noteworthy that many of the fungal strains inhibited by the inhibitor are plant pathogens of significant importance to agriculture. ATBI was found to be active against relatively a broad spectrum of filamentous fungi and its IC_{50} values indicated an exceptionally high potency. Significantly, in case of *T. reesei, A. solani,* and *A. flavus* the IC_{50} values were in nanomolar range. Our results documented that the specific activity of ATBI was decreased when the incubation time for the fungal growth was increased. A possible explanation for this phenomenon is that the germlings at the early stages of growth were more affected than the mycelium development at later stages. ATBI was found to inhibit spore germination at high concentration and at lower concentrations delayed growth of the hyphae, which subsequently exhibited abnormal morphology. Since the MIC and IC_{50} values of ATBI for the growth of certain fungal strains is sufficiently low, it could be promising for the possible development of anti-fungal drugs on the basis of this peptide.

Anti-fungal peptides usually target the cytoplasmic membrane by using the self-promoting pathway due to their α-helical and β-sheet structure (Sawyer, 1988; Ronish and Krimm, 1974). On association with the membranes, many of these peptides are presumed to form ion channels resulting in the alteration of permeability and consequently cell lysis (Nagaraj and Balaram, 1981; Bernhelmer and Rudy, 1986; Dempsey, 1990). To reach the target cytoplasmic membrane, antimicrobial peptides must overcome the barrier of the outer membrane, which they apparently do by utilizing the self-promoted uptake pathway (Sawyer, 1988; Piers, 1994). This involves displacement of divalent cations from their binding sites on surface lipopolysaccharides and consequent permeabilization of the outer membrane. To unravel the possible role of helicity of ATBI in the mechanism of fungal growth inhibition, we have investigated its secondary structure. Our results from the CD spectrum and from

the structure prediction by SYBYL software revealed the absence of any periodic structure in ATBI. Furthermore, the structural features of the inhibitor could not be correlated with the biological activity against fungal growth inhibition since lysis was not observed in the morphological changes in the hyphae growth. Moreover as an anionic peptide, ATBI cannot displace the divalent ions from the lipopolysaccharide of the cytoplasmic membrane. The primary structure of the anti-fungal peptide is completely different from those of any anti-fungal proteins so far isolated as indicated by the sequence homology studies. The structural novelty of ATBI probably depends on its high aspartic acid content and its unique sequence. The exceptional primary and secondary structure of ATBI suggested a different mechanism for fungal growth inhibition than the existing traditional anti-fungal compounds.

To colonize plants, fungal microorganisms have evolved strategies to invade plant tissues, to optimize growth in the plant, and to propagate. Bacteria and viruses, as well as some opportunistic fungal parasites, often depend on natural openings or wounds for invasion. In contrast, many true phytopathogenic fungi have evolved mechanisms to actively traverse the plants outer structural barriers, the cuticle, and the epidermal cell wall. To gain entrance, fungi generally secrete a cocktail of hydrolytic enzymes including cutinases, cellulases, pectinases, xylanases, and proteases (Knogge, 1996; Goodenough et al., 1991). The ability of some proteinaceous plant inhibitors to modulate the activity of hydrolytic enzymes from plant pathogens has led to the theory/understanding that they play a role in plant defense as well as in the control of intrinsic enzyme activity. The data documented so far were not pertaining to the role of aspartic protease inhibitors in fungal growth inhibition. The role of inhibitors of chitin synthase (Chapman et al., 1992; Hori et al., 1974), glucan synthase (Beaulieu et al., 1993; Schmatz et al., 1990;) and proteases (Lorito et al., 1994) as anti-fungal agents have been well established. However, there is a lacuna of literature on the inhibitors of xylanase, cellulase, and aspartic protease exhibiting anti-fungal activity, which could provide further insight into the understanding of host-pathogen interactions. In order to examine the contribution of the inhibition of xylanase and aspartic protease to the observed anti-fungal activity we have investigated the inhibition of these two enzymes by ATBI *in vitro*. The analysis of inhibition kinetics data revealed the binding of ATBI to the active site of xylanase and aspartic protease and a competitive mode of inhibition for both the enzymes. Further, to delineate the role of xylanase and aspartic protease in fungal growth inhibition, we have grown *T. reesei*, a saprophyte, and *A. oryzae*, a phytopathogen as model systems on a synthetic medium containing xylan or casein as the sole carbon source. The retardation of mycelial growth by ATBI in the presence of xylan or casein, where the selective production of xylanase and aspartic protease was observed implied the role of these enzyme activities in the fungal growth inhibition. The kinetic constant K_i revealed that ATBI binds more effectively to the active site of the xylanase than the aspartic protease indicating the major contribution of anti-xylanolytic activity in fungal growth inhibition. This concurs with our thinking that, when a pathogen invades a host, on contact with the hemicellulosic/cellulosic surface the secretion of xylanolytic/cellulolytic enzymes would be essential for its survival. Hence, we visualize

the functional role of a xylanase inhibitor in restricting the invasion of pathogens. There have been reports of bifunctional inhibitors of α-amylase and trypsin (Skordalakes et al., 1998; Strobl et al., 1995). However, a bifunctional inhibitor of xylanase and aspartic protease, which are active in distinctly different physiological conditions, is so far not reported. To our knowledge, ATBI represents the first report of a bifunctional aspartic protease inhibitor showing broad spectrum of anti-fungal activity.

The localization and characterization of the amino acids comprising the active center and the correlation between these residues with the inhibitory function are essential for understanding the mechanism of action of the inhibitor. To determine the residues involved in the anti-xylanolytic or proteolytic activity, we have modified the ionizable groups of Lys, and Asp/Glu of ATBI. Modification of the amine group of Lys or the carboxyl group of Asp/Glu residues of ATBI by specific modifiers TNBS or WRK resulted in the loss of its inhibitory activity. The kinetic analysis indicated the participation of one amine and two carboxyl groups of ATBI in the inhibition of xylanase and F-prot. It is well established that the catalytic site of xylanase and aspartic protease consists of two carboxyl groups and an essential lytic water molecule (Kulkarni et al., 1999; Rao, et al., 1998). Although both the enzymes are active in entirely different physiological conditions, the structural and kinetic studies have revealed a similar mechanism where the enzymatic reaction follows general acid-base catalysis with the direct participation of the lytic water molecule. The probable explanation for the involvement of two carboxyl groups of ATBI is that they may form a network of hydrogen bonds with the catalytic water molecule and with the ionizable groups in the active site of the enzyme. The participation of the Lys residue may be explained by considering its ability to form hydrogen bonding with the catalytic carboxyl groups of the enzymes. These interactions may interfere in the native weak interactions between the carboxyl groups of the active site and the lytic water molecule leading towards the inactivation of the enzymes. Further, to decipher the role of ionizable groups of ATBI in fungal growth inhibition the Lys, Asp/Glu modified ATBI was tested for its anti-fungal property on selective conditions. The modified ATBI failed to inhibit the growth of *T. reesei* and *A. oryzae* in the presence of xylan or casein indicating the involvement of carboxyl and amine groups in fungal growth inhibition. This can be explained by the fact that abolishing the inhibitory property of ATBI resulted in the recovery of the xylanase and aspartic protease activity in the fungal strains. These results were further corroborated by the rescue of the growth inhibition by the addition of enzymatic products. Enrichment by the hydrolyzed products of xylan and casein to the ATBI treated *T. reesei* and *A. oryzae* had substantially enhanced the growth. The rescue of fungal growth on the selective media containing xylan and casein has prompted us to propose the essential role of xylanase and aspartic protease in the cellular growth of fungal strains.

The bifunctional inhibitor, ATBI, was stable over a wide range of pH and temperature. Therefore, the direct application of ATBI as a biocontrol agent for the protection of plants against phytopathogenic fungi by encapsulation for surface application or by spray would be very useful. For more effective results, the seeds could be treated with the formulated preparation of ATBI, thus can be protected from fungal pathogenesis during

germination. Moreover, being of microbial origin and an extracellular product, ATBI offers an attractive and economical process for commercial production. T here have been reports where the inhibition of the fungal growth was due to the inhibition of a single hydrolytic enzyme. However, as a bifunctional inhibitor, ATBI may act in concert to circumvent host invasion and make it difficult for the pathogens to acquire resistance. Because of its small size, unique composition, and potentially different secondary structure, ATBI may open a new horizon for the synthesis of potent anti-fungal compounds.

References

Aguly, B. C., Rommele, G., Grunner, J., and Wehrlli, W. (1979) *Eur. J. Biochem.* **97**, 345-351.

Amsterdam, D. (1991) In *"Antibiotics in Laboratory Medicine"* (Lorain, V., Eds.) pp-72-778, Williams & Wilkins, Baltimore.

Andrade, M. A., Chacón, P., Merelo J. J., and Morán, F. (1993) *Prot. Eng.* **6**, 383-390.

Arai, T ., Mikami, Y., Fukushima, T., Utsumi, T., and Yazawa, K. (1973) *J. Antibiot.* **26**, 1606-1612.

Arana, J. L., and Vallejos, R. H. (1981) *FEBS Lett*. **123**, 103-106.

Aumelas, A., Mangoni, M., Roumestand, C., Chiche, E., Despaux, E., Grassy, G., Calas, B., and Chavanieu, A. (1996) *Eur. J. Biochem.* **237**, 575-583.

Baba, T., and Schneewind, O. (1998) *Trends Microbiol.* **6**, 66-71.

Bartizal, K., Abruzzo, G., Trainor, C., Frupa, D., Nollstadt, K., Schmatz, R., Schwartz, R., Hammond, M., Balkovec, J., and Vanmiddlesworth, F. (1992) *Antimicrobiol. Agents Chemother.* **36**, 1648-1657.

Beaulieu, K., Tang, J., Zeckner, D. J., and Parr, T. R. (1993) *FEMS Microbiol. Lett.* **108**, 133-138.

Bellamy, W., Takase, M., Yamauchi, H., Wakabayashi, H., Kawase, K. and Tomita, M., (1991) *Biochim. Biophys. Acta.* **1121**, 130-136.

Bernhelmer, A. W., and Rudy, B. (1986) *Biochim. Biophys. Acta* **864**, 123-141.

Bessalle, R., Gorea, A., Shalit, I., Metzger, J. W., Dass, C., and Desiderio, D. M. (1993) *J. Med. Chem.* **36**, 151-155.

Bessalle, R., Kapitkovsky, A., Gorea, A., Shalit, I., and Fridkin, M. (1993) *FEBS Lett.* **274**, 151-155.

Besson, F., Peypoux, J., Quentin, J., and Michel, G. (1984) *J. Antibiot.* **37**, 172-177.

Bevins, C. (1994) *Ciba Found. Symp.* **186**, 250-269.

Blondelle, S. E., and Houghten, R. A. (1992) *Annu. Rep. Med. Chem.* **27**, 159-168.

Blondelle, S. E., and Houghten, R. A. (1992) *Biochemistry* **31**, 12688-12694.

Boman, H. G. (1995) *Annu. Rev. Immunol.* **13**, 61-92.

Boman, H. G., and Hultmark, D. (1987) *Annu. Rev. Microbiol.* **41**, 103-126.

Boman, H. G., Marsh, J., and Goode, J. A., Eds. (1994) *Antimicrobial Peptides*, Ciba Foundation Symposium 186, pp1-272, John Wiley & Sons, Chichester, U. K.

Bostian, K., and Silver, L. (1990) *Eur. J. Clin. Microbiol. Infect. Dis.* **9**, 455-461.

Broekaert, W. F., Cammue, B. P. A., De Bolle, M. F. C., Thevissen, K., Desamblanx, G. W., and Osborn, R. W. (1997) *Crit. Rev. Plant. Sci.* **16**, 297-323.

Broekaert, W. F., Franky, R. G., Cammue, B. P. A., and Vanderleyden, J. (1990) *FEMS Microbiol. Letts.* **69**, 55-60.

Bruix, M. C., Gonzales, C., Santoro, J., Sariano, F., Rocher, A., Mendez, F., and Rico, M. (1995) *Biopolymers* **36**, 751-763.

Bruix, M. C., Jimenez, M. A., Santoro, J., Gonzales, J., Colilla, F. J., Mendez, F., and Rico, M. (1993) *Biochemistry* **132**, 715-763

Bullen, J. J. (1981) *Rev. Infect. Dis.* **3**, 1127-1138.

Buttner, K., Blondelle, S. E., Ostresh, J. M., and Houghten, R. A. (1992) *Biopolymers* **32**, 575-583.

Cammue, B. P. A., De Bolle, M. F. C., Terras, F. R. G., Proost, P., Damme, J. V., Rees, S. B., Vanderleyden, J., and Broekaert, W. F. (1992) *J. Biol. Chem.* **267**, 2228-2232.

Cammue, B. P., A., Thevissen, K., Hendricks, M., Eggrmont, K., Goderis, I. J., Proost, P., Van Damme, J., Osborn, R. W., Guerbette, F., Kader, J.-C., and Boreckaert, W. F. (1995) *Plant Pathol.* **109**, 445-455.

Chapman, T., Kinsman, O., and Houston, J. (1992) *Antimicrob. Agents Chemother.* **36**, 1909-1914.

Chen, H.-C., Roman, J. H., Morell, J. I., and Huang, C. M. (1988) *FEBS Lett*. **236**, 462-466.

Cho, Y., Turner, J. S., Dinh, N., and Lehrer, R. I. (1998) *Infect. Immun.* **66**, 2486-2493.

Christensen, B., Fink, R. J., Merrifield, R. B., and Mauzerall, D. (1988) *Proc. Natl. Acad. Sci.* **85**, 5072-5076.

Christov, L. P., Szakacs, G., and Balakrishnan, H. (1999) *Process Biochem*. **34**, 511-517.

De Lucca, A. J., Bland, J. M., Grimm, C., Jacks, T. J., Cary, J. W., Jaynes, J. M., Cleveland, T. E., and Walsh, T. J. (1998) *Can. J. Microbiol.* **44**, 514-520.

De Lucca, A. J., Bland, J. M., Jacks, T. J., Grimm, C., Cleveland, T. E., and Walsh, T. J. (1998) *Med. Mycol.* **36**, 291-298.

Debono, M., and Gordee. R. S. (1994) *Annu. Rev. Microbiol.* **48**, 471-497.

DeGrado, W. F. (1988). *Adv. Protein Chem.* **39**, 51-124.

DeGrado, W. F., Kezdy, F. J., and Kaiser, E. T. (1981) *J. Am. Chem. Soc.* **103**, 679-681.

DeLucca, A. J., and Walsh, T. J. (1999) *Antimicrob. Agents Chemother.* **43**, 1-11.

Dempsey, E. C. (1990) *Biochim. Biophys. Acta* **1031**, 143-161.

Denning, D. W., and Stevens. D. A. (1990) *Rev. Infect. Dis.* **12**, 1147-1201.

Eisenberg, D., and Wesson, M. (1990) *Biopolymers* **41**, 171-177.

Elsbach, P., and Weiss, J. (1997) *Immunbiology* **187**, 417-429.

Endo, M., Takesake, K., Kato, I., and Yamaguchi, H. (1997) *Antimicrob. Agents Chemother.* **41**, 672-676.

Eneyskaya, E. V., Kulminskaya, A. A., Savel'ev, A. N., Savel'eva, N. V., Shabalin, K. A., and Neustroev, K. N. (1999) *Appl. Microbiol. Biotechnol*. **52**, 226-231.

Fehlbaum, P., Bulet, P., Chernych, S., Briand, J.-P., Rousel, L., Letellier, L., Hetru, C., and Hoffinman, J. A. (1996) *Proc. Natl. Acad. Sci. U. S. A.* **93**, 1221-1225.

Fehlbaum, P., Bulet, P., Michuat, L., Laguex, N., Broackaert, W. F., Hetru, C., and Hoffinman, J. A. (1994) *J. Biol. Chem.* **269**, 33159-33163.

Fernadez de Calaya, R., Gonzalez-Pascual, B., Garcia-Olmedo, F., and Carbonero, P. (1972) *Appl. Microbiol.* **23**, 998-1000.

Fink, J., Boman, A., Boman, H. G. and Merrifield, R. B. (1989) *Int. J. Peptide Res.* **33**, 412-421.

Fink, J., Merrifield, R. B., Boman, A., and Boman, H. G. (1989) *J. Biol. Chem.* 6260-6267.

Fromtling, R., and Abruzzo, G. K. (1989) *J. Antibiot.* **42**, 174-178.

Fukushima, K., Arai, T., Mori, Y., Tsuboi, M., and Suzuki, M. (1983) *J. Antibiot.* **36**, 1606-1612.

Ganz, T., Selsted, M. E., and Lehere, R. I. (1990) *Eur. J. Hematol.* **44**, 1-8.

Gennis, R. B. (1989) In *"Biomembranes"*, pp 151-158, Springer Verlag, New York.

Goodenough, P. W., Clark, D. C., Durrant, A. J., Gilbert, H. J., Hazlewood, G. P., and Waksman, G. (1991) *FEBS Lett.* **282**, 355-358.

Gournelis, D. C., Laskaris, G. G., and Verpoorte, R. (1992) *Nat. Prod. Rep.* **14**, 75-82.

Grafe, U., Ihn, W., Titzan, M., Schade, W., Stengel, C., Schlegel, B., Fleek, W. F., Kunkel, W., Hartle, A., and Gutsche, W. (1995) *J. Antibiot.* **48**, 126-133.

Grunner, J., and Traxler, P. (1977) *Experentia* **33**, 137.

Haberman, E. (1977) *Science* **177**, 314-322.

Hancock, R. E. W., and Lehrer, R. (1998) *Trends Biotechnol.* **16**, 82-88.

Hancock, R. E. W., Falla, T., and Brown, M. H. (1995) *Adv. Microbiol. Physiol.* **37**, 135-175.

Hani, K., Nicolas, P., and Mor. A. (1994) In *"Proceedings of the 23rd European Peptide Symposium"* (H. L. S. Maia Eds.), Escom. Leiden, The Netherlands.

Harwig, S. S. L., Swiderek, K. M., Lee, T. D., and Lehrer, R. I. (1995) *J. Pep. Res.* **3**, 207-215.

Hoffmann, J. A., Kafatos, F. C., Janeway, C. A., and Ezekowitz, R. A. B. (1999) *Science* **248**, 1313-1318.

[a]Hori, M., Eguchi, J., Kakiki, K., and Misato, T. (1974) *Agric. Biol. Chem.* **38**, 690-266.

[b]Hori, M., Eguchi, J., Kakiki, K., and Misato, T. (1974) *J. Antibiot.* **27**, 260-266.

Ijima, R., Kurata, S., and Natori, S. (1993) *J. Biol. Chem.* **268**, 12055-12061.

Ikai, K., Shiomi, K., Takesako, K., Mizutanis, S., Yamamoto, J., Ogawa, Y., Ueno, M., and Kato, I. (1991) *J. Antibiot.* **44**, 1187-1198. (a)

Ikai, K., Takesako, K., Shiomi, K., Moriguchi, M., Yamamoto, J., Kato, I., and Naganawa, H. (1991) *J. Antibiot.* **44**, 1187-1198.(b)

Isono, K., Asahl, K., and Suzuku, S. (1969) *J. Am. Chem. Soc.* **61**, 490-7505.

Iwamoto, T., Fujiie, A., Nitta, K., Hashimoto, S., Okuhara, M., and Kohsaka, M. (1994) *J. Antibiot.* **47**, 1092-1097.

Iwamoto, T., Fujiie, A., Tsurumi, Y., Nanbata, K., and Shibuya, K. (1990) *J. Antibiot.* **43**, 1183-1185.

Juretic, D., Chemn, H.-C., Brown, J. H., Morell, J. L., Hendler, R. W., and Wester, H. V. (1989) *FEBS Lett*. **249**, 219-223.

Kaiser, E. T., and. Kezdy, F. J (1987) *Annu. Rev. Biophys. Biophys. Chem.* **16**, 561-581.

Kleinkauf, H., and von Dohren, H. (1988) *Crit. Rev. Biotechnol.* **8**, 1-32.

Knogge, W. (1996) *Plant Cell* **8**, 1711-1722.

Kokryakov, V. N., Harwig, S. S. L., Panyutich, A. A., Shevechenko, A. A., Aleshina, G. M., Shanova, O. V., Korneva, H. A., and Lehrer, R. I. (1993) *FEBS Lett.* **327**, 231-236.

Kulkarni, N., Shendye, A., and Rao, M. (1999) *FEMS Microbiol. Rev.* **23**, 411-456.

Latoud, C., Peypoux, F., and Michel, G. (1987) *J. Antibiot.* **40**, 1588-1595.

Lebbadi, M., Galvez, A., Maqueda, M., Martinez-Bueno, M., and Valdivia, E. (1994) *J. Appl. Bacteriol.* **77**, 49-53.

Lee, C. H., Kim, S. H., Hyun, B. C., Suh, J. W., Yon, C., Kim, C. O., Lim, Y. A., and Kim, C. S. (1994) *J. Antibiot.* **47**, 1402-1405.

Lee, S. Y., Moon, H.-J., Kurata, S., Natori, S., and Lee, B. L. (1995) *Biol. Pharm. Bull.* **18**, 1049-1052.

Lehrer, R. I., Ganz, T., Szklarek, D., and Selsted, M. E. (1985) *J. Clin. Invest.* **81**, 1829-1835.

Lehrer, R. I., Harwig, S. S. L., and Wagar, E. A. (1996) *Infect. Immun.* **64**, 4863-4866.

Lehrer, R. I., Raton, A., Daher, A., Harwig, S. S., Ganz, T., and Sested, M. E. (1989) *J. Clin. Invest.* **84**, 553-561.

Levy, H. M., Leber, P. D., and Ryan, E. M. (1963) *J. Biol. Chem.* **238**, 3654-3659.

Levy, O., Weiss, J., Zaramber, K., Ooi, C. E., and Elsbach, P. (1993) *J. Biol. Chem.* **268**, 6058-6063.

Lim, E., Wong, P., Fadem, M., Motchinik, P., Bakalinsky, M., and Little, R. (1996) In *"Program and abstracts of the 36th Interscience Conference on Antimicrogial Agents and Chemotherapy",* American Society for Microbiology, Washington, D. C.

Lim, Y., Suh, J. W., Kim, S., Hyun, B., Kim, C., and Lee, C. H. (1994) *J. Antibiot.* **47**, 1406-1416.

Lohner, K., Latal, A., Lehrer, R. I., and Ganz, T. (1997) *Biochemsitry* **36**, 1525-1531.

Lorito, M., Broadway, R. M., Joes, C. M. K., Woo, S. L., Novell, C., Williams, D. L., and Herman, G. E. E. (1994) *Mol. Plant Microbe Interact.* **7**, 525-527.

Mangoni, M., Aumelas, A., Chamet, P., Roumestand, C., Chiche, E., Despaux, E., Grassy, G., Calas, B., and Chavanieu, A. (1996) *FEBS Lett.* **383**, 93-98.

Matzuxzaki, K., Sugishita, K., Harada, M., Fugii, N., ad Miyajima, K. (1997)*Biochim. Biophys. Acta* **1327**, 119-130.

Mauch, F., Mauch-Mani, B., and Boller, T. (1988) *Plant Physiol.* **88**, 936-942.

McCathy, P. J., Troke, P. F., and Gull, K. (1985) *J. Gen. Microbiol.* **131**, 775-780.

McCathy, P., Newman, D. J., Nishet, L. J., and Kingsbury, W. D. (1985) *Antimicrob. Agents Chemother.* **28**, 494-499.

Merelo, J. J., Andrade, M. A., Prieto, A., and Morán, F. (1994) *Neurocomputing* **6**, 443-454.

Miller, G. L. (1959) *Anal. Chem.* **31**, 426-428.

Mizoguchi, J., Saito, T., Mizono, K., and Hayano, K. (1977) *J. Antibiot.* **30**, 308-313.

Mizuno, K., Yagi, A., Satoi, S., Takada, M., Hayasi, M., Asano, K., and Matsuda, T. (1977) *J. Antibiot.* **30**, 297--302.

Moneton, P., Sarthou, P., and Le Goffic, F. (1986) *J. Gen. Microbiol.* **132**, 2147-2153.

[a]Mor. A., Hani, K., and Nicolas, P. (1994) *J. Biol. Chem.* **269**, 31635-31641.

[b]Mor. A., Nguyen, V. H., Delfour, A., Migliore-Samour, D., and Nicolas, P. (1994) *Biochemistry* **30**, 8824-8830.

Mukhopadhyay, T., and Ganguli, B. N. (1986) *J. Antibiot.* **40**, 281-289.

Nagaraj, R., and Balaram, P. (1981) *Acc. Chem. Res.* **14**, 356-362.

Nagiec, M. N., Nagiec, E. E., Baltisburger, J. A., Well, G. R., Lester, R. L., and Dickson, R. L. (1997) *J. Biol. Chem.* **272**, 9809-9817.

Nakamura, H., Ayogi, H., Lee, S., Ono, S., Kato, T., Murata, Y., and Sugihara, (1990) *Bull. Chem. Soc. Jpn.* **63**, 1180-1184.

Neu, H. C. (1989) *Diagno. Microbiol. Infect. Dis.* **12**, 109S-116S.

Oita, S., Horita, M., and Yanagi, S. O. (1996) *Biosci. Biotech. Biochem.* **60**, 481-483.

Okuyama, T., and Satake, K. (1960) *J. Biochem.* (Tokyo) **47**, 454-466.

Patterson-Delafield, J. D., Szklarek, D., Martinez, R. J. and Lehrer, R. I. (1981) *Infect. Immun.* **31**, 723-731.

Perlman, D., and Bodansky, M. (1971) *Annu. Rev. Biochem.* **40**, 449-464.

Perez, P., Varona, R., Garcia-Acha, L., and Duran, A. (1981) *FEBS Lett.* **129**, 249-252.

Pergament, I., and Carmelli, S. (1994) *Tetrahedron Lett.* **35**, 8473-8476.

Piers, K. L., and Hancock, R. E. W. (1994) *Mol. Microbiol.* **12**, 951-958.

Pouny, Y., Rapaport, D., Mor, A., Nicolas, P., and Shai, Y. (1992) *Biochemistry* **31**, 12416-12423.

Rao, M. B., Tanksale, A. M., Ghatge, M. S., and Deshpande, V. V. (1998) *Microbiol. Mol. Biol. Rev.* **62**, 597-635.

Reidel, H. H., and Takemoto, J. Y. (1987) *Biophys. Biochim. Acta* **898**, 56-59.

Reiter, B. (1983) *Int. J. Tissue React.* **5**, 87-96.

Ronish, E. W., and Krimm, S. (1974) *Biopolymers* **13**, 1635-1651.

Roy, K., Mukhopadhyay, T., Reddy, G. C. S., Desikan, K. R., and Ganguli, B. N. (1986) *J. Antibiot.* **40**, 275-280.

Ryan, C. A. (1990) *Annu. Rev. Phytopahol.* **28**, 415-449.

Saberwal, G., and Nagaraj, R. (1994) *Biochim. Biophys. Acta* **1197**, 109-131.

Sai, K. P., Jagannadham, M. V., Vairamani, M., Raju, N. P., Devi, A. S., Nagaraj, R., and Sitaram. N. (2001) *J. Biol. Chem.* **276**, 2701-2707.

Sato, M., Beppu, T., and Arima, K. (1980) *Agric. Biol. Chem.* **44**, 3037-3040.

Satoi, S., Yagi, A., Asano, K., Mizuno, K., and Watanbe, T. (1977) *J. Antihbiot.* **30**, 303-307.

Sawistowska-Schroder, E. T., Kerridge, D., and Perry, H. (1984) *FEBS Lett.* **173**, 134-138.

Sawyer, J. G., Martin, N. L., and Hancock, R. E. W. (1988) *Infect. Immun.* **56**, 693-698.

Schmatz, D. M., Romancheck, M. A., Pittarelli, L. A., Schwartz, R. E., and Fromtling, R. (1990) *Proc. Natl. Acad. Sci. U.S.A.* **87**, 5950-5954.

Segre, A., Bachman, R. C., Ballio, A., Bossa, F., Grgurina, L., Iacobellis, N. S., Marino, G., Pucci, P., Simmaco, M., and Takemoto, J. Y. (1989) *FEBS Lett.* **255**, 27-31.

Shai, Y. (1995) *TIBS* **20**, 460-464.

Sinha, U., and Brewer, J. M. (1985) *Anal. Biochem.* **151**, 327-333.

Skordalakes, E., Elgendy, S., Goodwin, C. A., Green, D., Sculty, M. F., Kakkar, V. V., Freyssinet, J. M., Dodson, G., and Deadman, J. J. (1998) *Biochemistry* **37**, 14420-14427.

Steiner, H., Andreu, D., and Merrifield, R. B. (1988) *Biochim. Biophys. Acta* **939**, 260-266.

Steiner, H., Hultmark, D., Engstrong, H., Bennich, H., and Boman, H. G. (1981) *Nature* **292**, 246-248.

Stevens, D. A., and. Holmberg. K., (1999) *Curr. Opin. Anti-Infect. Invest. Drugs* **1**, 306-317.

Storici, P., Del Sal, G., Schneider, C., and Romeo, D. (1992) *FEBS Lett.* **314**, 187-190.

Strobl, S., Muehlhahn, P., Bernstein, R., Wiltscheck, R., Maskos, K., Wunderlich, M., Huber, R., Glockshuber, R., and Holak, T . A. (1995) *Biochemistry* **34**, 8281-8293.

Suzuki, S., Isono, K., Nagatsu, J., Mizutani, T., Kawashima, Y., and Mizuno, T. (1965) *J. Antibiot.* **18**, 131-136.

Swerdloff, J. N., Filler, S. G., and Edwards Jr., J. E. (1993) *Clin. Infect. Dis.* **17**(suppl. 2), 457-467.

Takemoto, J. Y., Giannini, J. L., Vassey, T., and Biskin, D. P. (1989) In *"Phytotoxins and Pathogenesis"* (Graniti, A., Durbin, R. D., and Ballio, A. Eds.), pp 167-175, Springer-Verlag, Berlin, Germany.

Takemoto, J. Y., Zhang, Y. L., Taguchi, N., Tachikawa, T., and Miyakawa, T. (1991) *J. Gen. Microbiol.* **137**, 653-659.

Takesako, K., Ikai, K., Haruna, F., Endo, M., Shimanaka, K., Sono, E., Nakamura, T., Kato, I., and Yamagachi, H. (1991) *J. Antibiot.* **44**, 919-924.

Tariq, V. N., and Develin, P. L. (1996) *Fungal Gent. Biol.* **20**, 4-11.

Tencza, S. B., Douglas, J. P., Creighton, D. J., Montelaro, R. C., and Mietzner, T. A. (1997) *Antimicrob. Agents Chemother.* **41**, 2394-2398.

Terras, F. R. G., Eggermont, K., Kovaleva, V., Raikhel, N. V., Osborn, R. W., Kester, A., Rees, S. B., Torrekens, S., Van Leuven, F., Vanderleyden, J., Cammue, B. P. A., and Broekaert, W. F. (1993) *Plant Cell* **7**, 573-588.

Thevssen, K., Ghazi, A., De Samblanx, G. W., Brownlee, C., Osborn, R. W., and Broekaert, W. F. (1996) *J. Biol Chem.* **271**, 15018-15025.

Thimon, L., Peypoux, F., Maget-Dana, R., and Michel, G. (1992) *J. Am. Oil Chem. Soc.* **69**, 92-93.

Tomita, M., Bellamy, W., Takase, M., Yamauchi, H., Wakabayashi, H., and Kawase, K. (1991) *J. Dairy Sci.* **74**, 4137-4142.

Tsujita, Y., and Endo, A. (1977) *J. Bacteriol*. **130**, 48-56.

van Belkum, M. J., Kok, J., Venema, G., Holo, H., Nes, I. F., Konings, W. N., and Abee, T. (1991) *J. Bacteriol.***173**, 7934-7941.

Vigers, A. J., Roberts, W. K., and Selitrennikoff, C. P. (1991) *Mol. Plant-Microbe Interact.* **4**, 315-323.

Wade, D., Boman, A., Wahlin, B., Drain, C. M., Andreu, D., Boman, H. G., and Merrifield, R. B. (1990) *Proc. Natl. Acad. Sci. U. S. A.* **87**, 4761-4765.

Westerhoff, H. V., Juretic, V. D., Hendler, R. W., and Zasloff, M. (1989) *Proc. Natl. Acad. Sci. U. S. A.* **86**, 6597-6601.

White, S. H., Wimley, W. C., and Selsted, M. E. (1995) *Curr. Opin. Struct. Biol.* **5**, 521-527.

Wolfson, J. L., and Murdock, L. L. (1995) *Environ. Entomol.* **24**, 52-57.

Yang, D., Chertov, O., bykovskaia, S. N., chen, Q., Buffo, M. J., Shogan, J, Anderson, M., Schroder, J. M., Wang, J. M., Howard, O. M. Z., and Oppenheim, J. J. (1999) *Science* **286**, 525-528.

Zanetti, M., Del Sal, G., Storici, P., Schneider, C., and Romeo, D. (1993) *J. Biol. Chem.* **268**, 522-526.

Zasloff, M. (1987) *Proc. Natl. Acad. Sci. U. S. A.* **84**, 5449-5454.

Zasloff, M. (1992) *Curr. Opin. Immunol.* **4**, 3-7.

Zeilinger, S., and Mach, R. (1998) *Curr. Top. Cereal Chem*. **1**, 27-35.

Zhang, L., and Takemoto, J. Y. (1987) *Phytopathology* **77**, 297-303.

Chapter 6

Unfolding and Chaperone Mediated Refolding of the Aspartic Proteases

Introduction

An important challenge in molecular biology is finding the rules that determine how a nascent polypeptide chain acquires its three-dimensional and functional structure. Indeed, the rapid progress in genome sequencing including that of the human genome, which has aroused great interest in medical circles, makes the solution of the protein folding problem all the more urgent. Sequencing the gene is only the first step; it is essential to know the nature, the structure, and the function of the protein that is coded by the gene. To diagnose the true cause of a disease, and for an approach to a rational treatment, not only it is necessary to locate the gene responsible for a disease, but also it is essential to know the structure of the protein for which it codes. Protein folding, the second translation of the genetic message, completes the information transfer from DNA to the active protein product. For a complete understanding of this process, it is necessary to decipher the folding code, the second part of the genetic message DNA→RNA→Polypeptide Chain→?→Functional Protein.

The Fundamentals of Protein Folding from the Anfinsen Postulate to the New View

The Anfinsen postulate and the Levinthal paradox

The remarkable achievement of Anfinsen and his group in refolding of denatured and reduced ribonuclease into a fully active enzyme marked the beginning of the modern era of the protein-folding problem. The fundamental principle stated by Anfinsen was that "all the information of a protein in a given native conformation is contained in its amino acid sequence" (Anfinsen et al., 1968; Anfinsen, 1973). The question of how an unstructured (random coil) polypeptide can rapidly and efficiently find its appropriate fold from countless alternatives is, however, a problem that has perplexed the scientific community for many years. Considerable progress in understanding this remarkable process has been made recently through a combination of theoretical and experimental advances. The thermodynamic control of protein folding is a corollary to the Anfinsen postulate; it means that the native structure is at a minimum of the Gibbs free energy. This statement was discussed by Levinthal in a consideration of the short time required for the folding process in vitro as well as in vivo. Indeed, for a 100-amino acid polypeptide chain, if we assume only two possible conformations for each residue there are 10^{30} possible conformations for the chain as a whole. If only 10^{-11} second is required to convert one conformation into another, a random search of all conformations would require 10^{11} years, an unrealistic time in a biological context where the folding time is of the order of seconds or minutes. Thus, it is clear that evolution has found an effective solution to this combinatorial problem, which is termed as the Levinthal Paradox.

Folding Models and Pathways of Protein Folding

In order to understand how the polypeptide chain could overcome the Levinthal paradox, different folding models arising from theoretical considerations (Karplus and Sali, 1985, and references there in), folding simulations, or experimental observations (Kim and Baldwin, 1990, and references there in) have been proposed. These models include the classical nucleation-propagation model and the recent nucleation-condensation model (Fersht, 1997), the stepwise sequential and hierarchical folding model (Kim and Baldwin, 1990; Janicke 1987), the

modular model (Wetlaufer, 1981; Chotia, 1984), the diffusion-collision model (Karplus and Weaver, 1994), the hydrophobic collapse model (Dill, 1985), and the jigsaw puzzle model (Harrison and Durbin, 1985).

Detection and Characterization of Intermediates in Protein Folding

The unfolding-refolding transition under equilibrium has often been described as a two-state process in which only the unfolded and the native species are significantly populated. The intermediates are generally unstable and poorly populated under equilibrium conditions. The existence of intermediates has been shown from kinetic studies for most proteins even when the two-state approximation describes the overall denaturation process. Two major impediments to characterize these species are the high cooperativity and the rapidity of the process, especially in the early events of protein folding. In spite of these inherent difficulties, much effort has been devoted to characterize these transient species. Kinetic trapping of intermediates during the refolding of disulfide-bridged proteins was developed for lysozyme (Wetlaufer and Ristow, 1973) and used for bovine pancreatic trypsin inhibitor (BPTI) (Creighton, 1974; Weissman and Kim, 1992). An elegant method using differential chemical labeling has been elaborated (Ghelis, 1980) and applied to the refolding of elastase. In the past decade, several methods have been developed allowing some of the intermediates to be characterized, particularly stopped-flow mixing devices coupled to circular dichroism, and NMR using rapid hydrogen-deuterium exchange associated with a mixing system allowing for the pulse labeling of transient species. This method is very informative, yielding residue-specific information (Roder et al., 1988; Baldwin, 1993; Dobson, 1991). Protein engineering has also been successfully employed to stabilize intermediates or to probe particular regions of a protein during folding process (Matouschek and Fersht, 1991; Ballery et al., 1993; Garcia et al., 1995). Another approach frequently used to investigate the function of intermediates is the study of protein fragments (Wetlaufer, 1981; Pecorari, et al., 1993).

The formation of secondary structures in the early steps of proteins has been observed for many proteins (Ballery et al., 1993; Ptitsyn, 1995) and such early species with a high content of secondary structures were named "the molten globule" (Ohgushi and Wada, 1983). The literature being rather confusing concerning the structural characteristics of the molten globule state, Goldberg and colleagues (Chaffote et al., 1992) have introduced the term "specific molten globule" and defined its characteristics. The specific molten globule is a compact intermediate with high content of native secondary structure, but a fluctuating tertiary structure. Since tertiary structure is not stabilized, the aromatic residues can rotate in a symmetrical environment and are accessible to the solvent as assessed by the absence of near UV circular dichroism. It contains an accessible hydrophobic surface susceptible to binding to the hydrophobic dye, aniline naphthalene sulfonate. The formation of a molten globule as an early folding intermediate has been reported for proteins such as xylose reductase, α-lactalbumin, carbonic anhydrase, β-lactamase, the α- and β_2-subunits of tryptophan synthase, bovine growth hormone, and phosphoglycerate kinase (Rawat and Rao, 1998; Ballery, 1993; Ptitsyn, 1995; Chaffote et al., 1992). However, the secondary structures observed in the early stages of the folding process is not always identical to those observed in the native structure (Chaffote et al., 1992; Shiraki et al., 1995; Alexandrescu et al., 1993; Radford, 1992). There are also

reports of an intermediate preceding the molten globule state (Ptitsyn, 1995; Uversky and Ptitsyn, 1996). This species, less compact than that of a molten globule, has a significant secondary structure content but lesser than that of a molten globule, and displays hydrophobic regions accessible to a solvent, thus has been called a "pre-molten globule" (Jeng and Englander, 1991). Its occurrence has been observed during the cold denaturation of β-lactamase and carbonic anhydrase, and also during the refolding of several other proteins (Fink, 1995). The rapid formation of transient intermediates, either molten or pre-molten, or both, with a high content of secondary structure and a small amount of fluctuating tertiary structure have been supported by a great number of observations (Dobson, 1991; Fink, 1995).

The New View: the Energy Landscape and the Folding Funnel

Many phenomenological models have been proposed over the years, more recently a unified model of protein folding based on the effective energy surface of the polypeptide chain has emerged. This so-called new view of protein folding arises from theoretical studies. Several models have been proposed to overcome the Levinthal paradox by simulation of folding from random coil to the native structure. There are essentially two approaches, lattice models, and molecular dynamics simulations. In the lattice models, the protein chain is represented as a string of beads on a two dimensional square lattice, or on a three-dimensional cubic lattice. The interactions between residues (the beads) provide energy function for Monte Carlo simulation. In such models, the aim is not to examine the folding of a particular amino acid sequence. Instead, the idea is to include the most essential features of proteins, i.e., the heterogeneous character of interactions (hydrophobic and polar) and the existence of long-range interactions to explore the general characteristics of the possible folds (Dill et al., 1995; Dobson et al., 1998).

The "new view" has evolved during the past few years from both experiment and theory using simplified mechanical models illustrated by the concept of folding funnel (Wolynes et al., 1995). The model has been represented by an energy landscape and describes the thermodynamic and kinetic behavior of the transformation of an ensemble of unfolded molecules to a predominantly native state. As underlined by Wolynes et al. "to fold, a protein navigates with remarkable ease through a complicated energy landscape". A wide variety of folding behaviors emerges from the energy landscape depending on the energetic parameters and conditions. The energy landscape metaphor provides a conceptual framework for understanding both two-state and multi-state kinetics, protein mis-folding and subsequent aggregation. There is an increasing amount of evidence showing that the initially extended polypeptide chain folds through a heterogeneous population of partially folded intermediate species in fluctuating equilibrium (Dobson et al., 1998; Pecorari et al., 1996).

Protein Misfolding and Aggregation: Implications in Human Diseases

It is interestingly clear that protein folding is not only an essential feature of the conversion of genetic information into biological activity, but also a key feature in the control and localization of this activity. This conclusion leads naturally to the idea that the failure of proteins to fold, or to fold into incorrect structure, can be

cause of disease. Cystic fibrosis is an example of a genetic disease where a variant protein (CFTR) is unable to fold correctly to a stable state in the endoplasmic reticulum and fails to reach the plasma membrane, eventually being degraded. Interestingly, even the wild type chains do not fold with high efficiency; only 30% of wild type chains survive the quality control mechanisms of the endoplasmic reticulum. It is perhaps not surprising that a wide range of mutations in different regions of the CFTR protein results in significantly reduced levels of activity in sufferers of this condition.

Protein aggregation is a widespread phenomenon that can occur under particular conditions or following certain mutations in the polypeptide chain (Yon, 1996). It occurs commonly when proteins are over expressed in foreign organisms with high concentration leading towards the formation of inclusion bodies. Another consequence of abnormal protein folding yields aggregates with the appearance of amyloid fibrils, leading to the spongiform encephalopathies. These severe pathologies include prion-associated diseases such as scrapie in sheep, mad cow disease in cattle and Creutzfeld-Jacob in humans (Prusiner, 1998). Alzheimer's disease is also characterized by the presence of amyloid fibrillar deposits in the brain tissue (Kelly, 1996).

The Need of Chaperones

There are several possible fates of the newly synthesized protein chains inside cells. The major distinction between these fates is whether the chains succeed in folding correctly, or they aggregate. Aggregation has commonly been regarded as a nuisance, which affects *in vitro* protein refolding studies, and is also a problem for cells. In the intracellular environment, the competition between folding, aggregation, and degradation determines whether a polypeptide chain can achieve its functional state with the efficiency required for successful cell growth, or whether it aggregates into a state that causes cellular damage and even death. It has been assumed for a long time that protein folding in the cell also occurs spontaneously, except for organellar exported proteins that require a cellular targeting, and translocation machinery to reach their proper destination. This concept has been challenged by the discovery of a cellular network of molecular chaperones and folding catalysts that assists a large variety of protein folding processes in virtually all compartments (Gething and Sambrook, 1992; Hartl, 1996). The activity of chaperones has been proposed to be essential for the folding of cytosolic proteins. In particular, the ubiquitous and abundant heat-shock protein 70 (Hsp70) chaperones, with their co-chaperones, have been proposed to be required for the co-translational folding of cytosolic proteins (Langer et al., 1992; Hartl, 1996; Mayhew and Hartl, 1996) in addition to their demonstrated roles in other folding processes, including protein translocation across membranes (Schatz and Dobberstein, 1996), assembly and disassembly of protein oligomers (Chappell et al., 1986; Alfano and McMacken, 1989), refolding of denatured proteins (Skowyra et al., 1990; Langer et al., 1992; Schroder et al., 1993; Freeman and Morimoto, 1996; Ehrnsperger et al., 1997), degradation of unstable proteins (Straus et al., 1990; Sherman and Goldberg, 1992) and control activity of regulatory proteins (Bohen and Yamamoto, 1994; Gamer et al., 1996). These roles of Hsp70 proteins rely on their ability to associate with short hydrophobic segments of unfolded substrate polypeptides in an ATP-controlled fashion (Rudiger et al., 1997; Bukau and Horowich, 1998).

The major classes of general chaperones are the Hsp40, Hsp60, Hsp70, Hsp90, 100 kDa heat shock proteins (Hsp100), and the small heat shock proteins (sHsp). Recent investigations have shown that not only do the major chaperones often function with protein cofactors, but also direct interactions between members of the Hsp40, Hsp70, and Hsp90 families may be frequent. The need for chaperones are mainly to prevent aggregation and misfolding of newly synthesized proteins, to prevent non-productive interactions with other cell components, to direct the assembly of larger proteins and multi-protein complexes, and to protect proteins from unfolding during exposure to stress.

The Small Heat Shock Proteins (sHsps)

sHsps represent an abundant and ubiquitous family of stress proteins and have been detected in virtually all types of organisms. While many different classes of sHsps co-exist in the cytosol, as well as in the organelles of plants (Vierling, 1991), yeast and mammalian cells possess only one or two members of the sHsp family (Ariggo and Landry, 1994). Interestingly, the eye lens protein α-crystallin is also considered to be a member of the sHsp family, as it displays similar structural and functional properties (Ingolia and Craig, 1982; Klemenz et al., 1991; Horwitz, 1992; Jakob et al., 1993; Merck et al., 1993). Although the overall homology between different sHsps is rather low, they are grouped together based on their (i) conserved regions of C-terminal half of the protein (Plesofsky-Vig et al., 1992; de Jong et al., 1993; Jakob and Buchner, 1994; Waters, 1995), (ii) increased expression upon heat shock (Lindquist et al., 1982; Welch, 1985; Landry et al., 1989; Inaguma et al., 1992; Klemenz et al., 1993) and (iii) monomeric size (15-30 kDa). Despite their low monomeric molecular masses, sHsps exist within the cell as large oligomeric complexes of 12-40 subunits with a mean M_r of 300-800 kDa (Chiesa et al. 1990; Behlke et al., 1991; Lee et al., 1995; Waters et al., 1996). Upon heat shock or under several other stress conditions, sHsps become phosphorylated and, in parallel, the oligomeric size undergoes significant dynamic changes leading to both smaller and larger complexes (Arrigo et al., 1998; Colleir et al., 1988; Nover et al., 1989; Kato et al., 1994; Mehlen et al., 1995).

The abundance of sHsps under physiological conditions varies significantly depending on the cell type and organisms studied. Except in the eye lens, the sHsps achieved a highest levels of ~0.1% of the total protein in heart muscle cells at physiological conditions (Bhat and Nagineni, 1989; Kato et al., 1991). Further more, sHsps expression varies depending on development, growth cycle, differentiation, and oncogenic status of the cell (Bond and Schlessinger, 1987; Gaestel et al., 1989; Crete and Landry, 1990; Pauli et al., 1990; Ciocca et al., 1993; Gernold et al., 1993; Klemenz et al., 1993). Under heat shock conditions, the level of sHsps increases drastically (10- to 20-fold), accounting to up to 1% of the total cellular protein (Arrigo and Landry, 1994). In mammalian cells, sHsps accumulate with kinetics similar to other Hsps but are synthesized for a longer time period stress (Arrigo and Wlech, 1987; Landry et al., 1991; Klemenz et al., 1993). Interestingly, over expression of virtually all mammalian as well as plant sHsps was shown to convey a significant thermoresistance to cells (Landry et al., 1989; Knauf et al., 1992; Aoyama et al., 1993; Schirmer et al., 1994; van den Ilssel et al., 1994), indicating a general thermoprotective function of these proteins. sHsps have been known to function in a number of different, seemingly unrelated processes ranging from RNA stabilization (Nover, et al., 1989) to elastase inhibition (Voorter et al., 1994) and interaction with the cytoskeleton (Miron et al., 1991; Lavoie et al., 1993; Benndorf et al., 1994; Nicholl and Quinlan, 1994). Experiments using well-established *in vitro* assays for chaperone function showed that sHsps possess chaperone properties similar to those of the model chaperone GroE (Jakob and Buchner, 1994; Buchner, 1996). sHsps, including α-crystallin, which was previously thought to play only a structural role in the eye lens, were shown to suppress aggregation of unfolding proteins and increase the yield of reactivation of denatured substrate

protein (Horowitz, 1992; Jakob et al., 1993; Merck et al., 1993; Lee et al., 1995). Interestingly, sHsps chaperone protein folding in an ATP-independent way (Horowitz, 1992; Jakob et al., 1993; Merck et al., 1993). This property is not altered significantly by sHsps phosphorylation (Knauf et al., 1994). Due to their subunit molecular weight and their recent addition to the chaperone family, sHsps and α-crystallin have been termed "junior chaperones" (Jaenicke and Creighton, 1993). However, little is known about the molecular mechanism of these chaperones and their integration into the chaperone system of the cell where only the coordinated function of several chaperone systems seems to guarantee survival under heat shock conditions.

The analysis of the molecular mechanism of Hsps has so far been focused mostly on the ATP-dependent Hsp70 and GroE families, whereas the function of the members of ATP-independent group of small Hsps is still poorly understood. While the expression of Hsps is still ubiquitous and a similar set of protein is produced from prokaryotes to mammals, the importance and apparent function of the different Hsps seem to vary in different organisms (Parsell and Lindquists, 1994). In yeast, thermo-tolerance is conveyed predominantly by Hsp104, whereas in *Drosophila* Hsp70 seems to be the important factor. Finally, GroE is essential for protein folding in prokaryotes and organelles, however, a functional counterpart seems to be lacking in the eukaryotic cytosol, since the structurally related TCp-1 complex appears to be restricted to actin and tubulin folding (Lewis et al., 1996). The question arises as to why the cell expends a considerable amount of energy on the expression of several distinct classes of Hsps under heat shock conditions. In this context, it is reasonable to assume that functional interactions between different "chaperone machinery" which provides optimal conditions for protein protection (Gething, 1991). Several studies have supported a structural and functional relationship between ATP and sHSPs. Equilibrium binding studies, intrinsic tryptophan fluorescence, and ^{31}P nuclear magnetic resonance spectroscopy demonstrated an interaction between ATP and bovine α-crystallin (Reddy et al., 1992). ATP is an abundant phosphorous metabolite present in high concentrations in lens cells from many species (Pirie, 1962). High concentrations of ATP are present in the skeletal muscle (Burt et al., 1976) in which high levels of α-crystallin are coexpressed (Bennardini et al., 1992). Although the role of ATP in the reaction cycles of protein folding by GroEL/Hsp60 and DnaK/Hsp70 is well characterized, a detailed understanding at the molecular level of the functional interactions between α-crystallin and ATP remains to be elucidated.

In an attempt to delineate the folding and unfolding mechanism of the aspartic proteases, we have studied the unfolding and refolding pathway of the aspartic proteases, HIV-1 PR (the key retroviral enzyme for the propagation of the virus), and F-prot (a fungal aspartic protease). The major findings incorporated in this chapter suggests that α-crystallin functions as an molecular chaperone in an ATP dependent manner not only in suppression of the unfolding and aggregation of HIV-1 PR but also mediating the proper refolding of the enzyme to a fully functional conformation. F-prot, a 47-kDa protein from the fungi *Aspergillus saitioi*. The genus *Aspergillus* possess few species, which are human pathogens, makes this protein an excellent model in understanding of the folding mechanism of aspartic protease.

Section I

Equilibrium Unfolding of HIV-1 PR, Evidence for an Alterative Conformation, which Resembles a Molten Globule

Summary

Elucidating the mechanistic details underlying the efficient refolding of proteins now appears to be an important consideration for defining how proteins fold to their native structure. Denaturation studies using the structure-perturbing agent guanidinium hydrochloride (GdmHCl) indicated that the HIV-1 PR folds through a partially folded molten-globule state. The molten globule state of the enzyme was characterized by its perturbed tertiary structure, intact secondary structure, and the exposure of the hydrophobic surfaces, as analyzed by the fluorescence and circular dichroism studies. The present work demonstrates the active participation of α-crystallin in the refolding of the HIV-1 PR. Fluorescence and light scattering experiments revealed that *α*-crystallin interacts with the molten-globule state of HIV-1 PR and prevents its aggregation. However, the enzyme failed to regain its functional integrity as revealed by the small recovery of enzymatic activity (8%) with the assistance of *α*-crystallin. Interestingly, in the presence of ATP and *α*-crystallin, reactivation of HIV-1 PR increased by five fold. Further, thermal denaturation of the enzyme at 50°C resulted in the rapid aggregation and loss of enzymatic activity. Although, *α*-crystallin prevented aggregation of thermally unfolded HIV-1 PR, there was no indication of reconstitution of the active enzyme. Addition of ATP along with *α*-crystallin, assisted further in preventing aggregation of thermally denatured HIV-1 PR. Consistent with these findings *in vitro*, *in vivo* experiments demonstrated that cell viability at 50°C, increased five fold in *Escherichia coli* expressing α-A and α-B crystalline, suggesting that α-crystallin protects cells against physiological stress *in vivo* by maintaining cytosolic proteins in their native and functional conformations. The experimental evidences presented here serve to conclude that HIV-1 PR refolds through a molten globule state and α-crystallin acts like a molecular chaperone *in vitro* and *in vivo*, in an ATP dependent manner.

Materials and Methods

Materials

ATP (adenosine 5'-triphosphate), IPTG, ANS, Ampicillin, Tetracycline, GdmHCl (Guanidinium hydrochloride), and α-crystallin were purchased from Sigma Chemical Co. All other chemicals used were of analytical grade.

In Vitro Folding Studies of HIV-1 PR

Denaturation/Reactivation Studies

All experiments described below were performed in the presence of 0.05 M sodium phosphate buffer, pH 6.0. For unfolding studies of HIV-1 PR, 25 μM of the enzyme was incubated with increasing concentrations of GdmHCl (1-6 M) for 2 h at 28°C. Unfolding of the enzyme was followed by fluorescence and circular dichroism, and by estimating the residual proteolytic activity. Renaturation was initiated by diluting 10 μl of the sample into 1 ml of 0.05 M sodium phosphate buffer pH 6.0. The enzyme was mixed vigorously for 6-8 h at 28°C. Renaturation was carried out i) in the absence of α-crystallin, ii) in the presence of α-crystallin (0.5 mg/ml), iii) in the presence of ATP (4 mM), and iv) in the presence of α-crystallin (0.5 mg/ml) + ATP (4 mM). Aliquots (100 μl) were withdrawn at various times of refolding and assayed for proteolytic activity of HIV-1 PR. Reactivation of chemically denatured HIV-1 PR was calculated as the percentage activity relative to a control sample of native HIV-1 PR tested under identical conditions.

Fluorescence Studies

Fluorescence measurements were performed on a Perkin-Elmer LS50 Luminescence spectrometer connected to a Julabo F20 water bath. Protein fluorescence was excited at 295 nm and the emission was recorded from 300-500 nm at 25°C. The slit widths on both the excitation and emission were set at 5 nm and the spectra were obtained at 100 nm/min. Fluorescence data were corrected by running control samples of buffer and smoothened. Emission spectra of the native and chemically denatured HIV-1 PR (25 μM), in 0.05 M phosphate buffer were recorded in the absence/presence of α-crystallin (0.5 mg/ml), ATP (4 mM) and α-crystallin (0.5 mg/ml) + ATP (4 mM) at similar experimental conditions.

Aggregation Assay

HIV-1 PR (25 μM) was incubated in 0.05 M phosphate buffer, pH 6.0 and thermally unfolded at 50°C as a function of time. The unfolding of the protein was followed by fluorescence. To monitor, the kinetics of thermal aggregation, light scattering was measured in a Perkin-Elmer luminescence spectrophotometer connected to a julabo water bath, in stirred and thermostatted quartz cells. Time course of the protein fluorescence were measured with the excitation and emission wavelengths fixed at 375 nm. Background buffer spectra were subtracted to remove the contribution from Raman scattering. Thermal aggregation was also monitored i) in the

absence of α-crystallin, ii) in the presence of α-crystallin, iii) in the presence of ATP, and iv) in the presence of α-crystallin + ATP.

Circular Dichroism Studies

CD spectra of HIV-1 PR were recorded in a Jasco-J715 spectropolarimeter at ambient temperature using a cell of 1-mm path length. Replicate scans were obtained at 0.1 nm resolution, 0.1 nm bandwidth and a scan speed of 50 nm/min. Spectra were average of 6 scans with the baseline subtracted spanning from 280 nm-200 nm in 0.1 nm increment. The CD spectrum of the HIV-1 PR (25 μM) was recorded in 50 mM sodium phosphate buffer (pH 6.0) in the absence/presence of increasing concentrations of GdmHCl (1-6 M).

ANS Binding Studies

HIV-1 PR (25 μM) was treated with varying concentrations of GdmHCl as described above. Further, the GdmHCl treated HIV-1 PR was incubated with ANS (10 μM) for 1 h in dark. The spectra of the ANS fluorescence were recorded with excitation at 375 nm and emission in the range of 400-600 nm with the slit widths on both the excitation and emission were set at 5 nm and at a scan speed of 100 nm/min. ANS was prepared in methanol at10 mg/ml final concentration.

In Vivo Studies of HIV-1 PR

Co-transformation of α-crystallin and HIV-1 PR into E. coli BL21

E. coli BL21 cells were transformed with the recombinant plasmids (pET 21a series, Novagen) containing α-A and α-B crystallin genes respectively by the calcium chloride method (Sambrook, et al., 1989). The recombinant cells were selected on LB plates containing ampicillin. The presences of the transformed plasmids in the recombinants were confirmed by selection of blue colonies by growing the cells in the presence of IPTG. The plasmids from the recombinant cells were isolated by alkali lysis method (Sambrook et al., 1989). These transformants were further transformed with the plasmid (pTΔN) containing the HIV-1 PR gene. The plasmid containing HIV-1 PR confers ampicillin as well as tetracycline resistance to the cells. The double transformed *E. coli* BL21 cells were selected on ampicillin, and tetracycline plates. These transformants were further confirmed by the isolation of plasmid DNA.

Induction of the α-crystallin and HIIV-1 protease in E. coli BL21

The double transformed *E. coli* BL21 cells in LB media containing ampicillin (50 μg/ml) and tetracycline (10 μg/ml) were incubated at 37°C until the growth of the cells reached OD_{600} of 0.5. IPTG (1 mM) was added to the liquid medium and the cells were grown further for 3 h, for the induction of α-crystallin. At this time, the growth temperature of the cells was increased to 50°C, which induces the expression of the HIV-1 PR, the model protein used to investigate the fate of the proteins in the cells after the growth at elevated temperature. During the growth of bacterial cells, samples were removed at different time intervals and the colony forming units were calculated by spreading the diluted cells on to LB plates. The percentage of CFUs was calculated relative to the CFUs counted from a control culture without the co-expression of α-crystallin and HIV-1 PR and also by taking another control culture without any plasmid.

Role of ATP on the Chaperone Activity of α-crystallin in vivo

The recombinant *E. coli* cells were grown in LB medium and were enriched with ATP (5 mM) to check the effect of ATP on the chaperone activity of α-crystallin after the induction of α-crystallin and HIV-1 PR as described before**.** ATP was added to the growing cells at different time intervals and also at different stages of differential expression of α-crystallin and HIV-1 PR. The effect of ATP on the chaperone activity of α-crystallin was estimated by the CFUs.

Results

In Vitro Studies of Folding Pathway of the HIV-1 PR

Spectroscopic Characterization of the Native and Molten Globule State of HIV-1 PR

For the unfolding studies, HIV-1 PR was incubated with increasing concentrations (1-6 M) of the denaturating reagent GdmHCl, and the changes in the secondary and tertiary structure of the enzyme were monitored by various spectroscopic methods. The changes in the tertiary structure of HIV-1 PR were analyzed by the tryptophanyl fluorescence. The fluorescence emission spectra of the native (N), molten globule like (MG), and the unfolded (U) state of HIV-1 PR were analyzed by exciting the protein at 295 nm. The N-form of HIV-1 PR exhibited an emission maxima (λ_{max}) at 340 nm, whereas in the presence of 1-2 M of GdmHCl, the fluorescence of the enzyme showed a decrease and pronounced red shift in the λ_{max} (Figure 1). However, there was no further shift in λ_{max} of the 3-6 M GdmHCl denatured enzyme, indicating the complete exposure of the tryptophan residues as a consequence of the total unfolding of the protein.

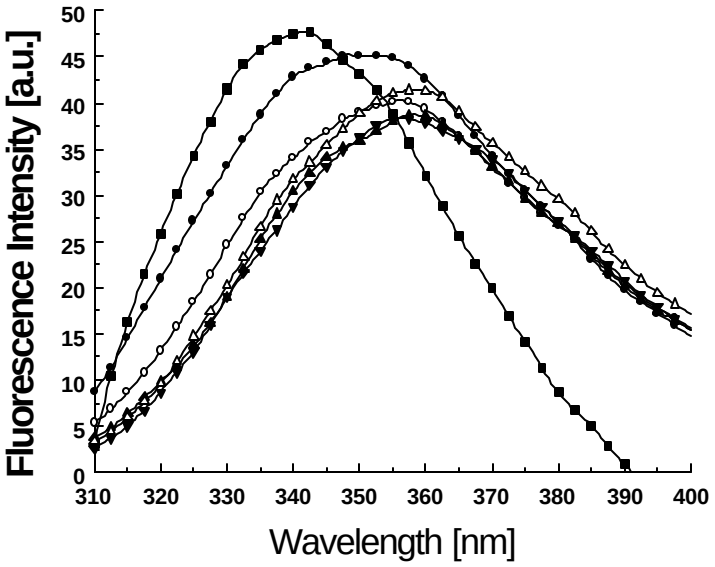

Figure 1. Fluorescence spectroscopic analysis of the unfolding of HIV-1 PR by GdmHCl.
Changes in the fluorescence of HIV-1 PR as a function of GdmHCl concentration. Tryptophanyl fluorescence of the HIV-1 PR (25 μM) in the absence (■) or presence of GdmHCl at (□) 1M, (●) 2 M, (○) 3 M, (▲) 4 M, (△) 5 M, and (▼) 6 M.

Effect of the denaturant on the secondary structure of the enzyme was monitored by circular dichroism spectroscopy. The mean negative ellipticities at 220 nm were normalized with respect to that in the absence of GdmHCl and plotted against the respective GdmHCl concentration (Figure 2). A decrease in the negative ellipticity in the CD spectra was observed with the increasing concentration of GdmHCl. At 2 M GdmHCl the mean residue ellipticity of HIV-1 PR decreased by almost 50% of that of in the absence of GdmHCl. Further increase in the denaturant concentration resulted in the reduction of negative ellipticity until there was a substantial loss of secondary structure of the HIV-1 PR in 6 M GdmHCl (Figure 2).

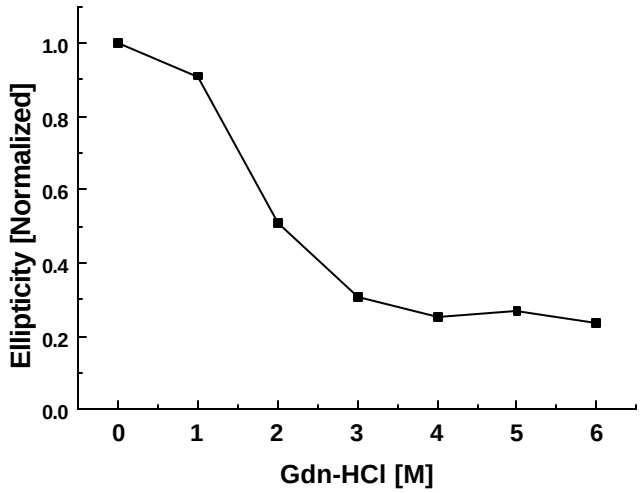

Figure 2. Circular dichroism spectra of HIV-1 PR as a function of GdmHCl.
Dependence of the mean residue ellipticity of HIV-1 PR at 220 nm as a function of GdmHCl concentration. HIV-1 PR (10 μM) was incubated with varying concentrations of GdmHCl for 2 h at 28 °C. The ellipticity values obtained were normalized with respect to that in the absence of GdmHCl.

ANS Binding

The fluorophore ANS (8-Anilinonapthalene-1-sulfonic acid), was used to determine the relative exposure of the hydrophobic environment in the folding intermediate of HIV-1 PR. ANS does not possess intrinsic fluorescence in aqueous solutions, however, its binding to the hydrophobic pockets of proteins results in the enhancement of its fluorescence. As shown in the Figure 3, the binding of ANS to the 2 M GdmHCl treated HIV-1 PR resulted in the maximum increase in its fluorescence intensity indicating the optimum exposure of the hydrophobic surface. The subsequent decrease in the fluorescence with increased concentration of GdmHCl indicated the progressive unfolding of the protein with total unfolding at 6 M. ANS has been widely used to detect the formation of molten globule-like intermediates in the folding pathways of several proteins (Ptitsyn et al. 1990). It was evident from the fluorescence, CD studies that at 2 M GdmHCl, HIV-1 PR retains substantial amount of

secondary structure although the tertiary structure was labile. Altogether, our spectroscopic and ANS binding studies revealed that at 2 M GdmHCl HIV-1 PR partially unfolded to its molten globule state.

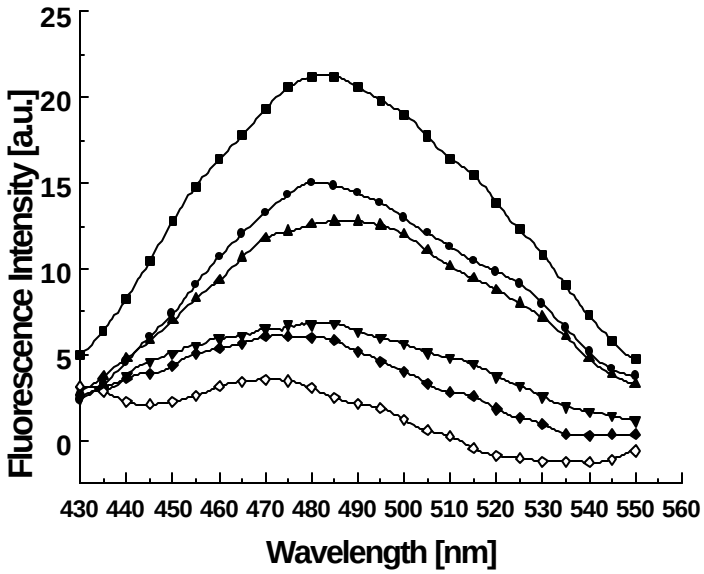

Figure 3. ANS binding of the hydrophobic surface of the chemically denatured HIV-1 PR.
HIV-1 PR was incubated with 1M (●), 2 M (■), 3 M (▲), 4 M (▼), 5 M (◆), and 6 M (◇) of GdmHCl for 2 h. Fluorescence intensity of HIV-1 PR (25 μM) excited at 375 nm after incubation with ANS (10 μM) in dark for 1 h.

Chaperone Assisted Refolding of the HIV-1 PR

The refolding of HIV-1 PR from its completely denatured state (U) was unsuccessful as revealed by the fluorescence spectra and the activity measurements. Similar results were also obtained for progressively less denatured HIV-1 PR with 3-5 M GdmHCl. The molecular chaperone α-crystallin failed to assist the enzyme to refold to its native state when it was denatured with 3-6 M of GdmHCl. Further investigations were carried out to study the influence of α-crystallin on the renaturation of the HIV-1 PR-MG state. The refolding of HIV-1 PR-MG was initiated in the absence/presence of α-crystallin. Aliquots removed at different time intervals were checked for the recovery of enzymatic activity. In the presence of α-crystallin the enzyme recovered 8% of activity after 3 h, although there was no measurable activity upto 30 min (Figure 4). Activity measurements revealed that, HIV-1 PR-MG lacked the ability to spontaneously reconstitute to the active enzyme. α-crystallin mediated reconstitution of active HIV-1 PR, only from its MG state, indicating that the chaperone probably traps the protease in a conformation resembling the molten globule. Evidence for this observation was provided by delay experiments wherein refolding of HIV-1 PR was initiated in the renaturation buffer in absence of α-crystallin. Concomitant decrease in the ability of α-crystallin to reconstitute active HIV-1 PR from the HIV-1 PR-MG state was observed with an increase in the time between the dilution of HIV-1 PR-MG and the addition of α-crystallin. The increase in

HIV-1 PR-MG concentration also resulted in a progressive decrease in the yield of reconstituted HIV-1 PR, indicating that the loss of recoverable HIV-1 PR is due to aggregation and not due to irreversible isomerization.

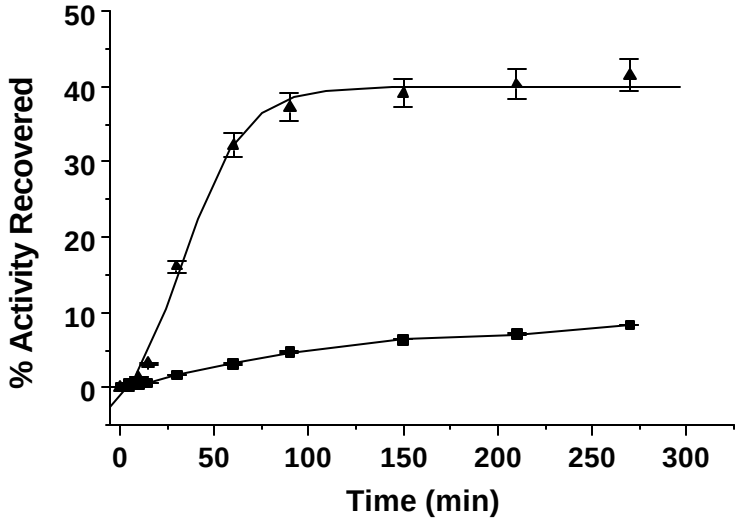

Figure 4. ATP enhances the effects of α-crystallin on the refolding and reactivation of chemically denatured HIV-1 PR.

Effects of α-crystallin on the reactivation of chemically denatured HIV-1 PR (25 μM) in the absence (■) or presence (●) of 4 mM ATP.

Enhancement of Chaperone Activity of α-crystallin by ATP

The poor yield of the active enzyme from the HIV-1 PR-MG state prompted us to evaluate the effects of ATP on α-crystallin assisted refolding and reactivation of HIV-1 PR. Dilution of the chemically denatured HIV-1 PR into the non-denaturation buffer resulted in the rapid aggregation of the enzyme. However, when chemically denatured HIV-1 PR was diluted into a non-denaturing solution containing α-crystallin, reactivation yields of enzymatically active HIV-1 PR was increased upto 10% (Figure4). Similar to GroEL and DnaK (Buchner et al., 1991; Ayling and Baneyx, 1996; Skowyra et al., 1990; Frydman et al., 1994; Martin et al., 1993), we have attempted to find out if ATP played any role in the chaperone function of α-crystallin. For this functional *in vitro* analysis, refolding of HIV-1 PR-MG was initiated in a buffer containing α-crystallin in the absence or presence of ATP. 4 mM ATP enhanced the effect of α-crystallin on refolding and reactivation of HIV-1 PR nearly five fold. It is interesting to note that 4 mM ATP alone displayed no effect on the refolding and reactivation of HIV-1 PR.

Unfolding and Aggregation of HIV-1 PR

In another approach, the role of α-crystallin in folding of HIV-1 PR was investigated at intermediate and higher temperatures. Aggregation of proteins was used as a criterion for misfolding in accordance with related studies (Gragerov et al., 1991; Horowich et al., 1993; Herrmann et al., 1994). Upon incubation at temperatures above 50°C, HIV-1 PR was rapidly inactivated as revealed by the loss of its proteolytic activity and aggregation assays. At this temperature, inactivation was accompanied by quantitative protein aggregation. Aggregation of HIV-1 PR starts 3 min after incubation at 50°C and reaches the plateau at ~ 12 min (Figure 4). However, α-crystallin was able to suppress aggregation of HIV-1 PR upto 70%. Interestingly, α-crystallin in the presence of ATP resulted in 100% suppression of aggregation of HIV-1 PR in solution at 50°C (Figure 5), although ATP alone had no effect on the aggregation of HIV-1 PR.

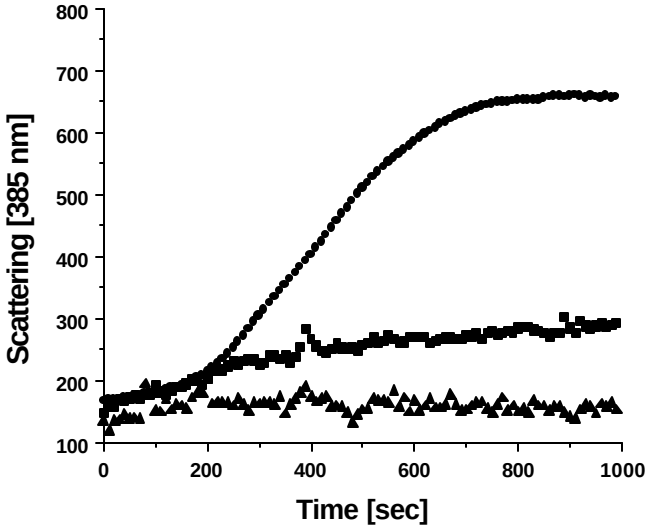

Figure 5. ATP enhances the suppression of HIV-1 PR aggregation by α-crystallin.
Effects of α-crystallin on the aggregation of HIV-1 PR (25 μM) at 50°C, in the absence (■) or presence (●) of α-crystallin (0.5 mg/ml), and α-crystallin with 4 mM ATP (▲).

***In Vivo* Folding Studies of the HIV-1 PR by Differential Expression**

The protective effect of α-crystallin was evaluated in cells exposed to thermal stress *in vivo*. The plasmid containing α-crystallin (A and B) gene was transformed into *E. coli* cells, and expressed by IPTG induction. To these cells, another plasmid containing the HIV-1 PR gene was transformed, whose expression was induced by the increase in temperature. The *E. coli* cells containing the plasmids were cultured at 37°C until the OD_{600} reaches 0.5. At this time expression of α-crystallin was induced by the addition of IPTG and the cells were allowed to grow for 3 h. Then the growth temperature was increased to 50°C, a temperature at which the

bacterial cells rapidly undergo autolysis and concomitant necrotic death. Cell viability was measured by counting the colony forming units (CFU) at selected time points during the course of heat shock. Upon shift to 50°C, un-induced control cultures rapidly underwent autolysis as measured by the decrease in the CFUs (Figure 6). Within 9 h of heat shock at 50 °C, no viable cells were observed in the un-induced control cultures, whereas cultures that overexpressed α-crystallin remained viable for 10 h. In order to investigate the role of ATP for the chaperone activity of α-crystallin *in vivo*, ATP (5 mM) was added to the culture medium after the induction of α-crystallin expression in the bacterial cells. Interestingly the CFU counts increased in presence of ATP, which clearly indicated a probable role of ATP for assisting α-crystallin in the refolding of proteins.

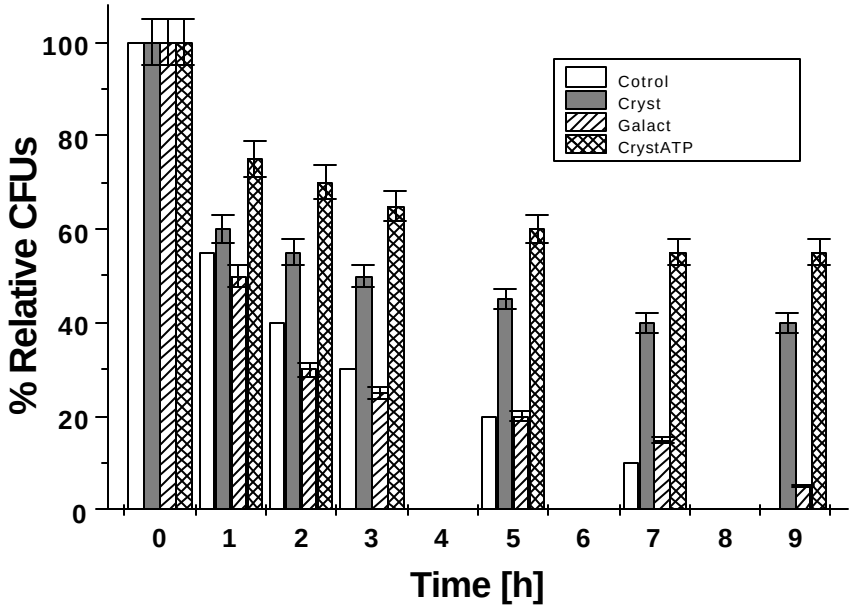

Function 6. Protective effect of a -crystallin expression on cell viability and enhancement of chaperone activity by ATP at 50 °C *in vivo*.

The protection of α-crystallin [cryst] expression vs. Control cultures 1 (uninduced [control]) and control culture 2 (over expressed β-galactosidase, [Galact]) and the role of ATP on CFUs at different time intervals after heat shock at 50°C.

Discussion

There have been considerable interests in the study of partly folded states that can be adopted by a polypeptide chain under equilibrium conditions (Baldwin, 1991; Dill and Shortle, 1991; Dobson, 1992). In part, the interest has arisen from the recognition that such states are similar to the partly folded kinetic intermediates observed in the folding pathway (Kim and Baldwin, 1990; Udgaonkar and Baldwin, 1988), but are difficult to study in detail because of their transient nature. Studying conformational states of proteins, which interact with chaperones is one of the important aspects in understanding the molecular mechanisms of chaperone-target protein interactions. The chaperone-substrate interaction appears to be non-specific with respect to the substrate proteins but specific in terms of the conformational states of the substrate, which interact with the chaperone molecules (Martin and Hartl, 1997).

Our results demonstrated for the first time the presence of a molten globule-like structure in the folding pathway of the HIV-1 PR. HIV-1 PR is an indispensable enzyme for the replication of the virus particles and thus a useful target for therapeutics. Although the kinetic and x-ray crystallographic studies have helped in understanding a great detail about the functional and structural aspects of the enzyme, the unfolding and folding pathways of HIV-1 PR remains still unexplored. We present the experimental evidences that the molecular chaperone, α-crystallin suppressed the unfolding and aggregation of HIV-1 PR and actively participated in the refolding and reactivation of HIV-1 PR, in an ATP dependent manner. The tertiary structure of HIV-1 PR collapsed in the presence of GdmHCl in a concentration dependent manner. When HIV-1 PR was unfolded at higher concentrations of GdmHCl, it lost its ability to refold and regain its proteolytic activity. However, at 2 M GdmHCl or below, it retained the ability to refold and reconstitute to active form although not spontaneously. Fluorescence and CD spectra revealed that the enzyme unfolded at 2 M GdmHCl, lacked in a rigid tertiary structure, but retained substantial secondary structure. ANS, a hydrophobic fluorophore has been widely used to detect the presence of exposed hydrophobic surfaces on the molten globule-like intermediates in the folding pathways of several proteins (Ptitsyn, 1990). A maximum increase in the ANS fluorescence was observed at 2 M indicating the optimum exposure of hydrophobic surfaces in this state of HIV-1 PR. The molten globule state is characterized to be as compact as the native protein with solvent-accessible hydrophobic regions and appreciable amount of secondary structure but lacking rigid tertiary structure (Fink, 1995; Ptitsyn, 1995). The spectroscopic investigations along with the ANS binding studies revealed that HIV-1 PR unfolds through an intermediate, which resembles the molten globule state. The action of α-crystallin as a molecular chaperone *in vitro* also tested in an assay measuring the unfolding and aggregation of HIV-1 PR at higher temperature. As revealed from the aggregation experiments, α-crystallin protected HIV-1 PR from aggregation. Although ATP alone did not influence the kinetics of HIV-1 PR aggregation, with α-crystallin, ATP assisted the chaperone to

suppress aggregation completely and in the refolding of the enzyme to its native state with a recovery of 60%. These results demonstrated the role of ATP in the chaperone activity of α-crystallin.

A functional relationship between ATP and chaperone-like activity for α-crystallin has been suggested by equilibrium binding studies, intrinsic tryptophan fluorescence, and ^{31}P nuclear magnetic resonance spectroscopy that demonstrated an interaction between ATP and total bovine α-crystallin (Palsimo, et al., 1995; Reddy, et al., 1992). Conformational changes have been proposed to play a major role in the binding of folding intermediates and in the discharge of polypeptides from molecular chaperones. One of the signals for inducing such structural changes is the hydrolysis of ATP as reported in case of the chaperone DnaK (Liberek et al., 1991) and GroEL (Mendoza et al., 1991; Goboubinoff et al., 1989). However, reports are also available wherein the chaperones GroEL (Schmidt and Buchner, 1992) and BiP (Kassenbrock and Kelly, 1989) do not require ATP hydrolysis. Instead, the mere binding of the adenine nucleotide to the chaperone induces a typological change in the chaperone that weakens its interaction with the bound protein. This acts to release the protein, further allowing it to assume its native state. Thus, we propose the assistance of ATP towards the chaperone activity of α-crystallin, however, future experiments will be necessary to determine the specificity of the interaction between α-crystallin and ATP and to investigate the effect of ATP on the conformation of α-crystallin in great detail.

Expression of the sHsp, α-crystallin in bacterial cells was associated directly with maintenance of cell viability under conditions of thermal stress. An association between cytosolic proteins and α-crystallin under conditions of thermal stress may prevent both protein denaturation and degradation *in vivo*, and may be responsible for the protection against cell death. Of the interest, ATP levels in the lens of the eye are among the highest of any cells in the body (Pirie, 1962; Greiner, et al., 1985; Greiner, et al., 1981; Klethi, and Mandel, 1965). The high level of ATP associated with chaperone activity *in vitro* may indicate that large lenticular pools of ATP participate in chaperone activity of α-crystallin in the folding of normal lens proteins during development and protection against unfolding and aggregation, a primary cause of lens cell opacification and the leading cause of blindness in the world. This action of ATP is consistent with the concept of a functional relationship between common cell metabolites and molecular chaperones (Clark and Huang, 1996). Although the molecular nature of the reaction cycle that α-crystallin uses in the refolding of proteins remains to be determined, it is possible that α-crystallin may share similar mechanisms with GroEL and/or other molecular chaperones. It has been suggested that sHsps are a class of ATP-independent chaperones (Buchner, 1996); however, the sHsps are the least well characterized among the Hsps. The reaction mechanism that GroEL uses in the folding of proteins, originally determined by biochemical approaches, has been substantiated by the recent solutions of its crystal structures (Braig, et al., 1994; Xu et al., 1997). In contrast, the atomic structure of α-crystallin has not been accomplished. Future experiments will be required to define the reaction mechanism of α-crystallin in the refolding of proteins and to determine whether the chaperone functions of α-crystallin are unique among sHsps in the use of ATP.

Section II

Interaction of α-Crystallin with the Molten Globule State of F-prot

Summary

Denaturation studies of F-prot using the structure-perturbing agent (GdmHCl) were carried out. The protein completely unfolded in the presence of 4-6 M GdmHCl as revealed by the loss in the tertiary structure, secondary structure, and enzymatic activity. However, at 3 M GdmHCl, although the tertiary structure of F-prot was perturbed, the secondary structure of the protein was substantial. Binding of the hydrophobic fluorophore, ANS, to this state of the protein resulted in the maximum increase in the fluorescence, suggesting the presence of a molten globule state. Complete unfolding of F-prot as achieved at 6 M GdmHCl failed to refold and rapidly aggregated leading towards the inactivation of the enzyme. Thermal aggregation of the protein as reflected by the light scattering experiments revealed that F-prot aggregates at 60°C. α-crystallin, are group of structural proteins which share both sequence and structural homology with small heat shock proteins, whose chaperone like activity has been described in suppressing protein unfolding and aggregation in response to thermal or chemical stress. Refolding of F-prot in the presence of α-crystallin prevented aggregation, however it failed to reconstitute the enzyme to its active form as revealed by the activity data. To investigate the role of ATP on the chaperone activity of α-crystallin, renaturation of the denatured F-prot at 3 M GdmHCl, was initiated in the presence of α-crystallin and ATP. The chaperone activity was found to be enhanced by 5 fold in the presence of ATP. Based on our above results we propose the enhanced chaperone activity of α-crystallin in the presence of ATP for the refolding of chemically denatured F-prot.

Materials and Methods

Materials

The Fungal Protease (VIII) from *Aspergillus saitoi* (F-prot), ATP (adenosine 5'-triphosphate), ANS, GdmHCl (Guanidinium hydrochloride), and α-crystallin were purchased from Sigma Chemical Co. All other chemicals used were of analytical grade.

Denaturation and Renaturation Studies of F-prot

For unfolding studies of F-prot (50 μM) was incubated with 6 M GdmHCl for 2 h at 28 °C in 0.05 M Glycine-HCl buffer, pH 3.0. Unfolding of the enzyme was followed by fluorescence and circular dichroism, and by estimating the residual proteolytic activity. Renaturation was initiated by diluting 10 μl of the sample into 1 ml of 0.05 M Glycine-HCl buffer, pH 3.0. The enzyme was mixed vigorously for 6-8 h at 28 °C. Renaturation was carried out i) in the absence of α-crystallin, ii) in the presence of α-crystallin (0.5 mg/ml), iii) in the presence of ATP (4 mM), and iv) in the presence of α-crystallin (0.5 mg/ml) + ATP (4 mM). Aliquots (100 μl) were withdrawn at various times of refolding and assayed for proteolytic activity of F-prot. To investigate the dependence of renaturation on the order of addition of ATP and α-crystallin, the renaturation of F-prot was initiated in the presence of a) α-crystallin followed by addition of ATP after 1 h, b) α-crystallin preincubated with ATP for 1 h. Reactivation of chemically denatured F-prot was calculated as the percentage activity relative to a control sample of native F-prot tested under identical conditions.

Fluorescence Studies

Fluorescence measurements were performed on a Perkin-Elmer LS50 Luminescence spectrometer connected to a Julabo F20 water bath. Protein fluorescence was excited at 295 nm and the emission was recorded from 300-500 nm at 25°C. The slit widths on both the excitation and emission were set at 5 nm and the spectra were obtained at 100 nm/min. Fluorescence data were corrected by running control samples of buffer and smoothened. Emission spectra of the native and chemically denatured F-prot (50 μM), in 0.05 M Glycine-HCl buffer, pH 3.0, were recorded. Emission spectra of the enzyme were also recorded in the absence/presence of α-crystallin (0.5 mg/ml), ATP (4 mM) and α-crystallin + ATP (4 mM) at similar experimental conditions.

Aggregation Assay

F-prot (50 μM) was incubated in 0.05 M Glycine-HCl buffer, pH 3.0, and thermally unfolded at 60 °C as a function of time. To monitor, the kinetics of thermal aggregation, light scattering was measured in a Perkin-Elmer luminescence spectrophotometer connected to a julabo water bath, in stirred and thermostatted quartz cells. Time course of the protein fluorescence were measured with the excitation and emission wavelengths fixed at 375 nm. Background buffer spectra were subtracted to remove the contribution from Raman scattering.

Circular Dichroism Studies

CD spectra of F-prot were recorded in a Jasco-J715 spectropolarimeter at ambient temperature using a cell of 1-mm path length. Replicate scans were obtained at 0.1 nm resolution, 0.1 nm bandwidth and a scan speed of 50 nm/min. Spectra were average of 6 scans with the baseline subtracted spanning from 280 nm-200 nm in 0.1 nm increment. The CD spectrum of the F-prot (50 μM) was recorded in 0.05 mM Glycine-HCl buffer, pH 3.0 in the absence/presence of increasing concentrations of GdmHCl (1-6 M).

ANS Binding Studies

The chemically denatured F-prot was incubated with ANS (10 μM) for 1 h in dark. The spectra of the ANS fluorescence were recorded with emission in the range of 400-600 nm and excitation at 375 nm with the slit widths on both the excitation and emission were set at 5 nm and at a speed of 100 nm/min.

Results

In an extension to our work on the unfolding and refolding studies on HIV-1 PR, we have further extended our investigations to another model aspartic protease F-prot from a fungal source.

Unfolding Studies of F-prot

F-prot was chemically denatured with increasing concentrations of the GdmHCl. F-prot exhibited an emission maxima (λ_{max}) at 340 nm in its native form (N), whereas in denaturating conditions there was a decrease in the fluorescence intensity with a pronounced red shift λ_{max} (Figure 1a). The increase in the intensity of λ_{max} of the unfolded F-prot with increasing concentration of the denaturant indicated the complete exposure of the buried tryptophan residues to the aqueous environment. These results were corroborated by the circular dichroism studies of the unfolded and partially folded states. The mean residue ellipticity of F-prot at 3 M GdmHCl decreased by almost 50%, and at 6 M GdmHCl, the protease lost its secondary structure considerably indicating the complete unfolding of the protein (Figure 1b).

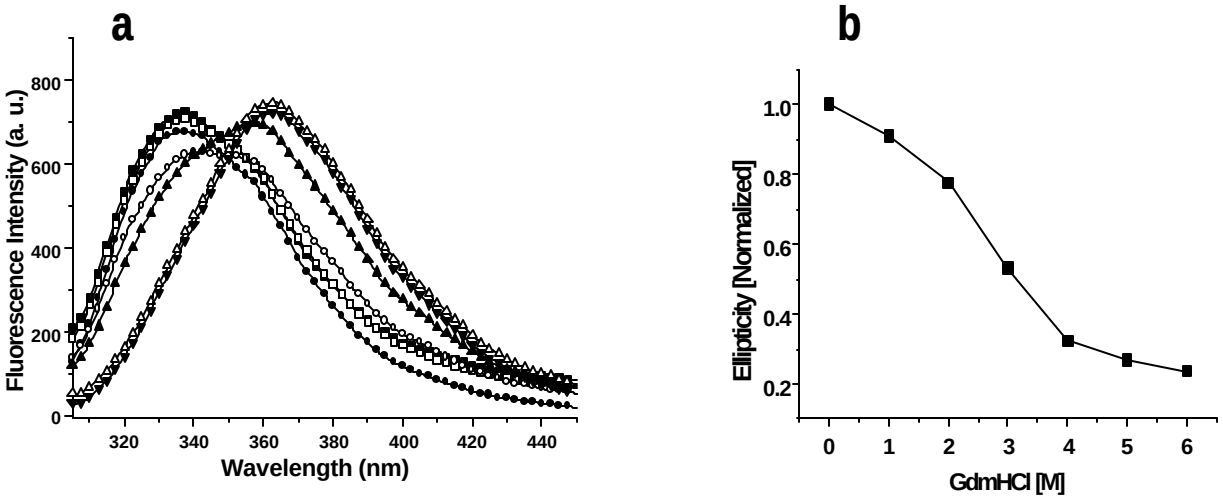

Figure 1. Spectroscopic analysis of the unfolding of F-prot by GdmHCl.

a) Changes in the fluorescence of F-prot as a function of GdmHCl concentration. Tryptophanyl fluorescence of the F-prot (50 μM) in the absence (■) or presence of GdmHCl at (□) 1 M, (●) 2 M, (○) 3 M, (▲) 4 M, (△) 5 M, and (▼) 6 M. b) Dependence of mean residue ellipticity of F-prot at 220 nm as a function of GdmHCl concentration. F-prot (10 μM) was incubated with varying concentrations of GdmHCl for 2 h at 28 °C. The ellipticity values obtained were normalized with respect to that in the absence of GdmHCl.

ANS Binding

Intermediate emission of tryotophanyl fluorescence can be observed with certain collapsed folding states containing a fluctuating hydrophobic core that adsorbs the fluorescent compound ANS. ANS was used to determine the relative amount of exposed hydrophobic surface on the folding intermediate of F-prot. As observed from the

Figure 2, the ANS fluorescence of F-prot-ANS complex increased consistently upto 3 M GdmHCl, which was followed by a sharp decline with further increase in the denaturant to 4-6 M GdmHCl. The ANS fluorescence increased in a concentration dependent manner indicating the progressive exposure of the buried hydrophobic pockets. From the spectroscopic analysis of the unfolding of F-prot it was apparent that at 3 M GdmHCl, the protease possess a fluctuating tertiary structure and a considerable secondary structure. Further, binding of ANS to this state of the protease indicated a molten globule like structure in the unfolding pathway of F-prot.

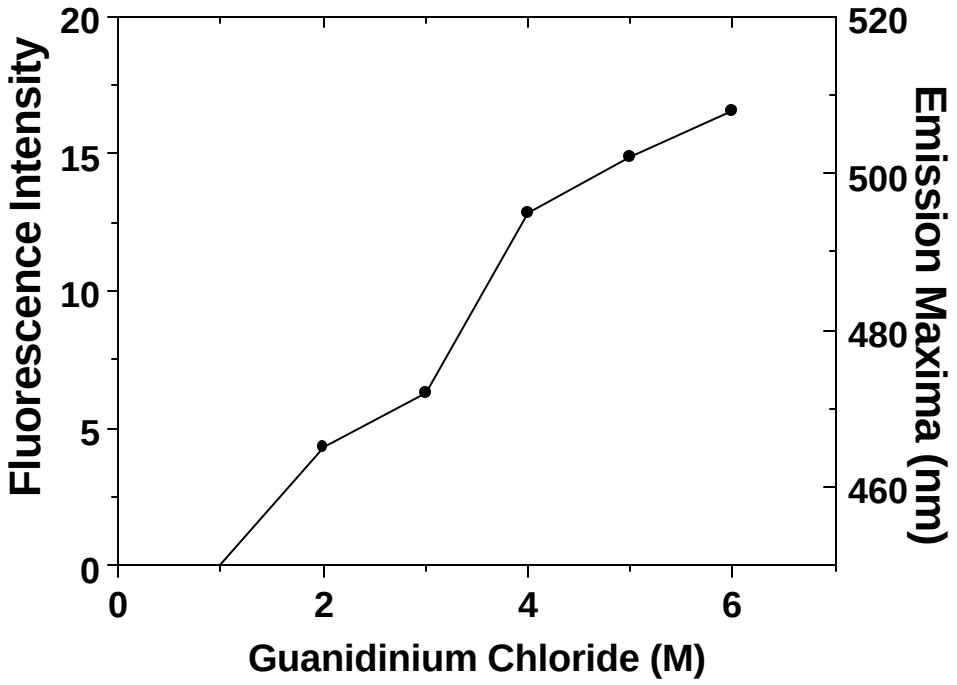

Figure 2. Exposure of hydrophobic surfaces of chemically denatured F-prot by GdmHCl measured by ANS fluorescene.

ANS fluorescence intensity (□) and the emission maxima (●) of F-prot (25 μM). F-prot was treated with varying concentration of GdmHCl for 2 h, and then incubated with ANS (10 μM) for 1 h in dark. The data shown are the resulting spectra after subtraction of the respective blanks.

Chaperone Assisted Refolding of F-Prot and Role of ATP in Protein Folding

The chemically denatured F-prot at 4-6 M GdmHCl failed to reconstitute in the absence/presence of α-crystallin. However, at 3 M GdmHCl, the enzyme recovered 10 % of activity in the presence of α-crystallin (Figure 3). The effects of α-crystallin on the refolding and reactivation of F-prot in the presence of ATP were determined *in vitro*. Addition of 5 mM ATP to the renaturation mixture containing α-crystallin enhanced the refolding and reactivation of F-prot nearly five fold as revealed by the recovery of 80% enzymatic activity. However, 4 mM ATP

alone displayed no effect on the refolding and reactivation of F-prot (Figure 3). These results corroborated our previous findings about the role of ATP in the chaperone function of α-crystallin.

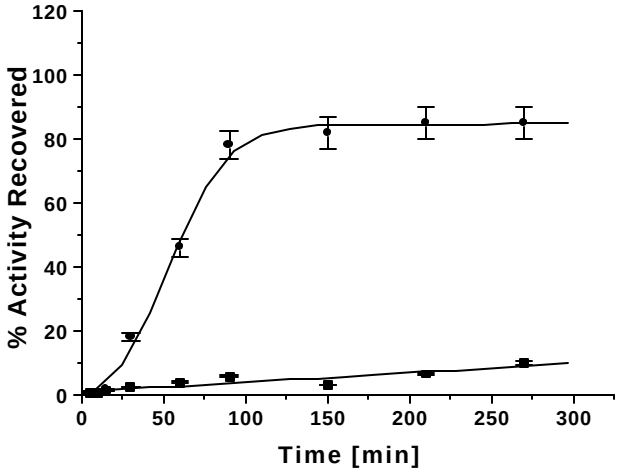

Figure 3. ATP enhances the effects of α-crystallin on the refolding and reactivation of chemically denatured F-prot.

Effects of α-crystallin on the reactivation of 50 μM chemically denatured F-prot in the absence (■) or presence (●) of 4 mM ATP.

Thermal Unfolding and Aggregation of F-prot

The ability of α-crystallin to prevent the aggregation of proteins in heat shock conditions may be a prerequisite for their refolding under permissive conditions. This was tested by unfolding the F-prot at different temperatures and following the extent of aggregation in the absence/presence of α-crystallin. F-prot denatured and aggregated rapidly in solution at temperature, 60°C and above. α-crystallin alone suppressed aggregation upto 40%, however, in the presence of ATP the percentage of suppression of aggregation increased to almost 70%, in solution at 60°C (Figure 4).

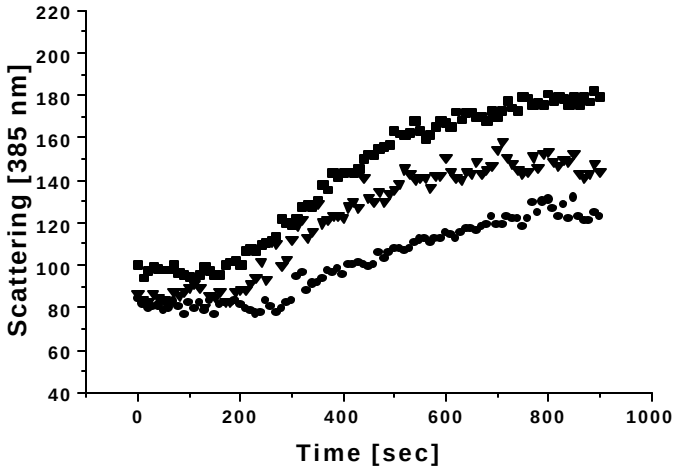

Figure 4. Role of ATP in enhancing the suppression of F-prot aggregation by a -crystallin.
Effects of α-crystallin on the aggregation at 50° C of 50 μM F-prot in the absence (■) or presence of α-crystallin (0.5 mg/ml) (●), and α-crystallin with 4 mM ATP (▲).

Discussion

The present investigation was carried out to gain some insight into the conformation of F-prot interacting with the chaperone α-crystallin and the mechanistic details underlying the reconstitution of active enzyme. The conditions for the unfolding of native F-prot were sought in the belief that the unfolded enzyme or its folding intermediates would serve as a substrate for the α-crystallin mediated reconstitution of active F-prot. Our results demonstrated the refolding and reactivation of F-prot via a molten globule like intermediate. Although α-crystallin alone failed to reconstitute the active enzyme, presence of ATP was necessary for the recovery of the active enzyme, which corroborated our findings in the folding pathway of HIV-1 PR.

The existence of molten-globule like intermediates has been demonstrated with several proteins and are known to be involved in various cellular functions such as membrane translocation of proteins (Bychkova et al., 1988; van der Goot et al., 1991), chaperone-assisted protein folding (Hendrick & Hartl, 1993) and also in various genetic diseases (Tanford, 1968; Pace, 1986). Interest in such intermediates is strong since they have been proposed to be an obligatory intermediate formed early in the folding pathway (Kim & Baldwin, 1990). A common feature of the molten-globule state is the exposure of hydrophobic surfaces that lead to aggregation of proteins during folding. Our *in vitro* studies using F-prot revealed that the chaperone α-crystallin operated by interacting with the hydrophobic regions that appear on the surface of molten-globule state of F-prot. This reduces the concentration of the free partially folded F-prot (F-prot-MG) during renaturation and thus prevents loss of enzyme activity due to their hydrophobic aggregation. Presence of ATP induced reconstitution of the active F-prot. It has been reported that α-crystallin binds to molten globule states of carbonic anhydrase (Rajaraman et al., 1996) and xylose reductase (Rawat and Rao, 1998). Our results do not completely rule out the possibility that F-prot is undergoing refolding while bound to the surface of α-crystallin, however, it seems more plausible that the folding of F-prot is initiated during the bound state and the functional activity is obtained during the free state of equilibrium. Das and Surewicz (1995) reported that the specificity of α-crystallin appears to be limited to specific conformational intermediates that occur on the denaturation pathway.

It has been reported that in *E.coli* a cascade of molecular chaperones mediate folding of proteins. The chaperone DnaK interacts with polypeptides in their extended conformation and prevents premature misfolding and aggregation after which GroEL stabilizes folding intermediates resembling the molten-globule and mediates proper folding. The transfer of DnaK/DnaJ-bound protein to GroEL requires GroE as the coupling factor (Langer et al., 1992). Such a mechanism is likely to exist in eukaryotes also (Langer et al., 1992; Ellis, 1990). Our investigations revealed that α-crystallin is able to reconstitute F-prot *via* interaction with its non-native conformer characterized by an increased surface hydrophobicity but at a remarkably low degree of unfolding. The inability of α-crystallin to reconstitute F-prot from its extended conformation implies that *in vivo*, other chaperones may be involved in binding to the unfolded polypeptides and prevent premature misfolding and aggregation, whereas the proper folding and assembly may depend on the subsequent transfer of the partially folded polypeptide to α-crystallin. Further

evidence is provided by the observation that α-crystallin prevents aggregation of lens proteins induced by oxidative stress and UV radiation. These conditions are not likely to unfold protein molecules completely but induce formation of partially folded state with hydrophobic surfaces that result in its aggregation (Das et al., 1996). For many years, α-crystallin was thought to be a lens specific structural protein where it played a role to facilitate proper transmission of light. However, recently α-crystallin has been demonstrated to be present in various non-lenticular tissues such as brain, spleen and heart and found in NIH 3T3 cells expressing Ha-*ras* and v-*mos* (Iwaki et al., 1989; Klemenz et al., 1991). α-Crystallin has been reported to be induced by thermal or hypertonic stress (Klemenz et al., 1991; Dasgupta et al., 1992) and its expression is markedly increased in a number of neurological diseases such as Creutzfeld-Jacob disease, Alexander disease and Lewy body disease (Iwaki et al., 1992; Dugid et al., 1988; Lowe et al., 1990). Our present investigation on α-crystallin adds to the information available on its chaperone function, which may assist to shed some light on its diverse roles *in vivo*.

References

Alexandrescu, A. T., Evans, P. A., Pitkeathly, M., Baum, J., and Dobson, C. M. (1993) *Biochemistry* **32** 1707-1718.

Alfano, C., and McMacken, R. (1989) *J. Biol. Chem.* **264**, 10709-10718.

Anfinsen, C. B. (1973) *Science* **181**, 223-230.

Anfinsen, C. B., Heber, E., Sela, M., and White Jr., F. W. (1961) *Proc. Natl. Acad. Sci. U. S. A.* **47**, 1309-1314.

Aoyama, A., Froehli, E., Scaefer, R., and Klemenz, R. (1993) *Mol. Cell Biol.* **13**, 1824-1835.

Arrigo, A.-P., and Landry, J. (1994) In Morimoto, R. I. (ed.), *"The Biology of Heat Shock Proteins and Molecular Chaperones"*, Cold Spring Harbor Laboratory Press, Cold Spring Harbor, NY, pp 335-373.

Arrigo, A.-P., and Welch, Y. J., (1987) *J. Biol. Chem.* **262**, 15359-15369.

Ayling, A., and Baneyx, F. (1996) *Prot. Sci.* **5**, 478-487.

Badcoe, I. G., Smith, C. J., Wood, S., Halsall, D. J., Holbrock J. J., Lund, P., and Clarke, A. R. (1991) *Biochemistry*, **3**, 9195-9201.

Baldwin, R. L. (1991) *Chemtracts* **2**, 379-389.

Baldwin, R. L. (1993) *Curr. Opin. Struct. Biol.* **3**, 84-91.

Ballery, N., Desmadril, M., Minard, P., and Yon, J. M. (1993) *Biochemistry* **32**, 708-714.

Ballew, R. M., Sabelko, J., and Gruebele, M. (1996) *Nature Struct. Biol.* **3**, 923-926.

Becker, J., and Craig, E. A. (1994) *Eur. J. Biochem.* **219**, 11-23.

Behlke, J., Lutsch, G., Gaestel, M., and Bielka, H. (1991) *FEBS Lett.* **288,** 119-122**.**

Benndorf, R., Hayess. K., Ryazantsev. S., Wieske, M., Behlke. J., and Lutsch, G. (1994) *J. Biol. Chem.* **269**, 20708-20784.

Bhat. S. P., and Nagineni, C. N. (1989) *Biochem. Biophys. Res. Commun.* **158**, 319-325.

Bohen, S. P., and Yamamoto, K. R. (1994) In *"The Biology of Heat Shock Proteins and Molecular Chaperones"* (Morimoto, R. I., Tissieres, A., and Georgopoulos, C. Eds.), Cold Spring Harbor Laboratory Press, Cold Spring Harbor, NY, pp 313-334.

Bond. U., and Schlesinger, M. J. (1987) *Adv. Genet.* **24**, 1-29.

Braig, K., Otwinowski, Z., Hegde, R., Biosvert, D. C., Joachimiak, A., Horwich, A. L., and Sigler, P. B. (1994) *Nature* **371**, 578-586.

Buchner, J. (1996) *FASEB J.* **10**, 10-19.

Buchner, J., Schmidt, M., Fuchs, M., Jaenicke, J., Rodulph, R., Schmid, F. X., and Kiefhaber, T. (1991) *Biochemistry* **30**, 1586-1591.

Bukau, B., and Horowich, A. I. (1998) *Cell* **92**, 351-366.

Bychkova, V. E., Berni, R., Rossi, G. L., Kutyshenko, V. P., and Ptitsyn, O. B. (1994) *Biochemistry* **31**, 7566-7571.

Caines, G. H., Schleich, T., Morgan, C. F., and Farnsworth, P. N. (1990) *Biochemistry* **29**, 7547-7557.

Chaffote, A. F., Cadieux, C., Guillou, Y., and Goldberg, M. E. (1992) *Biochemistry* **31**, 4303-4308.

Chappell, T. G., Welch, W. J., Schlossman, D. M., Palter, K. B., Schlesinger, M. J., and Rothman, J. E. (1986) *Cell* **45**, 3-13.

Chiesa, R., McDermott, M. J., and Spector, A. (1990) *FEBS Lett.* **268**, 222-226.

Chotia, C. (1984) *Annu. Rev. Biochem.* **53** 537-572.

Ciocca, D. R., Oesterreich, S., Chamness, G. C., McGuire, W. L., and Fuqua, S. A. (1993) *J. Natl. Cancer Inst.* **85**, 1558-1570.

Collier, N. C., Heuser. J., Levy. M.A., and Schlesinger, M. J. (1988) *J. Cell Biol.* **106**, 1131-1139.

Creighton, T. E. (1974) *Prog. Biophys. Mol. Biol.* **33**, 231-297.

Crete, P., and Landry, J. (1990) *Radiat. Res.* **121**, 320-327.

Csermely, P., and Kahn, C. R. (1991) *J. Biol. Chem.* .**266**, 4943-4950.

Das, K .P., and Surewicz, W.K. (1995) *J. Biol. Chem.* **270**, 1536-1542.

Das, K. P., and Surewicz, W. K. (1995) *FEBS Lett.* **369**, 321-325.

Das, K. P., Petrash, J. M., and Surewicz, W. K. (1996) *J. Biol. Chem.* **271**, 10449-10452.

Dasgupta, S., Hohman, T. C., and Carper, D. (1992) *Exp. Eye Res.* **54**, 461-470.

de Jong, W. W., Leeunissen, J. A., and Voorter, C. E. (1993) *Mol. Biol. Evol.* **10**, 103-126.

Dill, K. A. (1985) *Biochemistry* **24,** 650-668.

Dill, K. A., and Chan, H. S. (1997) *Nature Struct. Biol.* **4**, 10-19.

Dill, K. A., and Shortle, D. (1991) *Annu. Rev. Biochem.* **60**, 795-825.

Dill, K. A., Bromberg, S., Yue, K., Fiebing, K. M. Yee, D. P., Thomas, P. D., and Chan, H. S. (1995) *Protein Sci.* **4**, 561-602.

Dobson, C. M. (1991) *Curr. Opin. Struct. Biol.* **1**, 22-27.

Dobson, C. M. (1992) *Curr. Opin. Struct. Biol.* **2**, 6-12.

Dobson, C. M., Sali, A., and Karplus, M. (1998) *Angew. Chemie. Int.* **37**, 868-893.

Dobson, C., and Karplus, M. (1982) *Curr.Opin. Structural Biol.* **9**, 92-101.

Dugid, J. R., Rohwer, R. G., and Seed, B. (1988) *Proc. Natl. Acad. Sci. U. S. A.* **57**, 5738-5742.

Eaton, W. A., Munow, V., Thompson, P. A., Henry, E. R., and Hofrichter, J. (1998) *Accounts Chem. Res.* **31**, 745-753.

Ehrnsperger, M., Graber, S., Gaestel, M., and Buchner, J. (1997) *EMBO J.* **16**, 221-229.

Ellis, J. (1987) *Science* **250**, 954-959.

Ellis, R. J., and Hartl, F. U. (1999) *Curr. Opin. Structu. Biol.* **9**, 102-110.

Fersht, A. R. (1997) *Curr. Opin. Struct. Biol.* **7**, 3-9.

Fink, A. L. (1995) *Annu. Rev. Biophys. Biomol. Struct.* **24**, 495-522.

Freeman, B. C., and Morimoto, R. I. (1996) *EMBO J.* **15**, 2969-2979.

Frydman, J., Nimmesgern, E., Ohtsuka, K., and Hartl, F. U. (1994) *Nature (London)* **370**, 111-117.

Gaestel, M., Gross, B., Bendorf, R., Strauss, M., Schunk, W. N., Kraft, R., Orro, A., Boehm, H., Stahl, J. *et. al.* (1989) *Eur. J. Biochem.* **179**, 209-213.

Gamer, J., Multhaup, G., Tomoyasu, T., McCarty, J. S., Rudiger, S., Schonfeld, H.-J., Schirra, C., Bujard, H., and Bukau, B. (1996) *EMBO J.* **15**, 607-617.

Garcia, P., Desmadril, M., Minard, P., and Yon, J. M. (1995) *Biochemistry* **34**, 397-404.

Gernold, M., Knauf, U., Gaestel, M., Stahl, J., and Kloetzel, P. M. (1993) *Dev. Genet.* **14**, 103-111.

Gething, M. J. (1991) *Curr. Opin. Cell Biol.* **3**, 610-614.

Gething, M.-J., and Sambrook, J. (1992) *Nature* **355**, 33-45.

Ghelis, C. (1980) *Biophys. J.* **32**, 503-514.

Ghelis, C., and Yon, J. M. (1992) In *Protein Folding*. Academic Press, New York.

Goboubinoff, P., Christeller, J. T., Gatenby, A. A., and Lorimer, G. H. (1989) *Nature* **342**, 884-888.

Gragerov, A. L., Martin, E. S., Krupenko, M. A., Kashlev, M. V., and Nikiforov, V. G. (1991) *FEBS Lett.* **291**, 222-224.

Greiner, J. V., Kopp, S. J., and Gloenk, T. (1985) *Invest. Opthalmic Vis. Sci.* **26**, 537-544.

Greiner, J. V., Kopp, S. J., Sanders, D. R., and Gloenk, T. (1981) *Invest. Opthalmic Vis. Sci.* **21**, 700-713.

Hagen, S. J., Hofrichter, J., Szabo, A., and Eaton, W. A. (1996) *Proc. Natl. Acad. Sci. U. S. A.* **93**, 11615-11617.

Harrison, S. C., and Durbin, R. (1985) *Proc. Natl. Acad. Sci. U. S. A.* **82**, 4028-4030.

Hartl, F. U. (1996) *Nature* **381**, 571-580.

Hendrick, J. P., and Hartl, F. U. (1993) *Annu. Rev. Biochem.* **62**, 349-384.

Herrmann, J. M., Stuart, R. A., Craig, E. A., and Neupert, W. (1994) *J. Cell. Biol.* **127**, 893-902.

Horowich, A. L., Brooks Low, K., Fenton, W. A., Hirshfield, I. N., and Furtak, K. (1993) *Cell* **74**, 909-917.

Horwitz, J. (1992) *Proc. Natl. Acad. Sci. U. S. A.* **89**, 10499-10453.

Inaguma, Y., Shinohara, H., Goto, S., and Kato, K. (1992) *Biochem. Biophys. Res. Commun.* **182**, 844-850.

Ingolia, T. D., and Craig, E. A. (1982) *Proc. Natl. Acad. Sci. U. S. A.* **79**, 2360-2364.

Iwaki, T., Kumelwaki, A., Liem, R., and Goldman, J. E. (1989) *Cell* **57**, 71-78.

Iwaki, T., Wisniewski, T., and Iwaki, A. (1992) *Am. J. Pathol.* **140**, 345-356.

Jaenicke, R., and Creighton, T. E. (1993) *Curr. Biol.* **3**, 234-235.

Jakob, U., and Buchner, J. (1994) *Trends Bipchem. Sci.* **19**, 205-211.

Jakob, U., Gaestel, M., Engel, K., and Buchner, J. (1993) *J. Biol. Chem.* **268**, 1517-1520.

Janicke, R. (1987) *Prog. Biophys. Mol. Biol.* **49**, 117-237.

Jeng, M. F., and Englander, S. W. (1991) *J. Mol. Biol.* **221**, 1045-1061.

Kaenicke, R. (1999) *Prog. Biophys. Mol. Biol.* **71**, 155-1241.

Kantorow, M., and Piatigorsky, J. (1994) *Proc. Natl. Acad. Sci. U. S. A.* **91**, 3112-3116.

Kantorow, M., Horwitz, J., van Boekel, M. A., de Jong, W. W., and Piatigorsky, J. (1995) *J. Biol. Chem.* **270**, 17215-17220.

Karplus M., and Sali, A. (1985) *Curr. Opin. Struct. Biol.* **5**, 58-73.

Karplus, M., and Weaver, D. L. (1994) *Protein Sci.* **3**, 650-668.

Kassenbrock, C. K., and Kelly, R. B. (1989) *EMBO. J.* **8,** 1461-1467.

Kato, K., Hasegawa, K., Goto, S., and Inaguma, Y. (1994) *J. Biol. Chem.* **269**, 11274-1127?

Kato, K., Shinohara, H., Inaguma, Y., Shimizu, K., and Ohshima, K. (1991) *Biochim. Biophys. Acta* **1074**, 173-180.

Kelly, J. W. (1996) *Curr. Opin. Struct. Biol.* **6**, 11-17.

Kim, P. S., and Baldwin, R. L. (1990) *Annu. Rev. Biochem.* **59**, 631-660.

Klemenz, R., Froeli, E., Steiger, R. H., Schaefer, R., and Aoyama, A. (1991) *Proc. Natl. Acad. Sci. U. S. A.* **88**, 3652-3656.

Klemenz, R., Froeli, E., Steiger, R. H., Schaefer, R., and Aoyama, A. (1993) *J. Cell Biol.* **120**, 639-645.

Klethi, A. M., and Mandel, P. (1965) *Proc. Natl. Acad. Sci.* **93**, 15185-15189.

Knauf, U., Kielka, H., and Gaestel, M. (1992) *FEBS Lett.* **309**, 297-302.

Kuwajima, K. (1996) *FASEB J.***31**, 102-109.

Landry, J., Chretien, P., Lambert, H., Kickey, E., and Weber, I. A. (1989) *J. Cell Biol.* **109**, 7-15.

Landry, J., Chretien, P., Laszlo, A., and Lambert, H. (1991) *J. Cell Physiol.* **147**, 93-101.

Langer, T., Lu, C., Echols, H., Flanagan, J., Hayer, M. K., and Hartl, F. U. (1992) *Nature* **356**, 683-689.

Lavoie, J. N., Kickey, W., Weber, A., and Landry, J. (1993) *J. Biol. Chem.* **268**, 24210-24214.

Lee, J. G., Pokala, N., and Wierling, E. (1995) *J. Biol. Chem.* **270**, 10432-10438.

Lewis, S. A., Tian, G., Vainberg, I. E., and Cowan, N. J. (1996) *J. Cell Biol.* **132**, 1-4.

Liberek, K., Skowyra, D., Zylicz, M., Johnson, C., and Georgopoulos, C. (1991) *J. Biol. Chem.* **266**, 14491-14496.

Lindquist, S., DiDomenico, B. J., Bugaisky, G. E., Kurtz, S., and Petko, L., (1982) In *"Heat Shock from Bacteria to Man"* (Schlesinger, M. J., Asburner, M., and Tissieres, A. Eds), Cold Spring Harbor Laboratory Press, Cold Spring Harbor, NY, pp 167-176.

Lowe, J., Landon, M., Pike, I., Spendlove, I., McDeromtt, H., and Mayer, R. J. (1990) *Lancet.* **336**, 515-516.

Martin, J., and Hartl, F. U. (1997) *Curr. Opin. Struct. Biol.* **7**, 41-52.

Martin, J., Mayhew, M., Langer, T., and Hartl, F. U. (1993) *Nature* **366**, 228-233.

Matouschek, A., and Fersht, A. R. (1991) *Methods Enzymol.* **202**, 82-112.

Mayhew, M., and Hartl, F. U. (1996) In *"Escherichia coli and Salmonella typhimurium Cellular and Molecular Biology"* (Neidhardt, F. C. Eds.), ASM Press, Washington DC, pp 922-937.

McCammon, J. A. (1996) *Proc. Natl. Acad. Sci. U. S. A.* **93**, 11426-11427.

Mehlen, P., Mehlen, A., Guillet, D., Preville, X., and Arrigo, A.-P. (1995) *J. Cell Biol.* **58**, 248-259.

Mendoza, J. A., Rogers, E., Lorimer, G. H., and Horowitz, P. M. (1991) *J. Biol. Chem.* **266**, 13044-13049.

Merck, K. B., Gorenen, P. J., Voorter, C. E., de Haard-Hoekman, W. A., Horwitz, J., Bloemendal, H., and de Jong, W. W. (1993) *J. Biol. Chem.* **268**, 1046-1052.

Miron, T., Vancompernolle, K., Vandekerckhove, J., Wilchek, M., and Geiger, B. (1991) *J. Cell Biol.* **114**, 255-261.

Nicholl, I. D., and Quinlan, R. A. (1994) *EMBO J.* **13**, 945-953.

Nover, J., Sharf, K. D., and Neumann, D. (1989) *Mol. Cell Biol.* **9**, 1298-1308.

Ohgushi, M., and Wada, A. (1983) *FEBS Lett*. **164**, 21-24.

Palmisano, D. V., Groth-Vasselli, B., Farnsworth, P. N., and Reddy, M. C. (1995) *Biochim. Biophys. Acta* **1246**, 91-97.

Parsell, D. A., and Lindquist, S. (1994) In *"The Biology of Heat Shock Proteins and Molecular Chaperones"* Cold Spring Harbor Laboratory Press, Cold Spring Harbor, NY, pp 457-494.

Pauli, D., Tonka, C. H., Tissiers, A., and Arrigo, A. P. (1990) *J. Cell Biol.* **111**, 817-828.

Pecoran, F., Minard, P., Desmadril, M., and Yon, J. M. (1996) *J. Biol. Chem.***271**, 5270-5276.

Pecorari, F., Minard, P., Desmadril, M., and Yon, J. M. (1993) *Protein. Eng.* **6**, 313-325.

Pirie, A. (1962) *Exp. Eye Res.* **1**, 427-435.

Plaxo, K. W., and Dobson, C. M. (1996) *Curr. Opin. Struct. Biol.* **6**, 630-636.

Plesfsky-Vig, N., Big, J., and Brambl, R. (1992) *J. Mol. Evol.* **35**, 537-545.

Prusiner, S. B. (1998) *Proc. Natl. Acad. Sci. U. S. A.* **95**, 13363-13383.

Ptitsyn, O. B. (1995) A*dv. Protein Chem.* **47**, 83-229.

Ptitsyn, O. B., and Rashin, A. A. (1973) *Doklady Akademii Nauk SSSR @13**, 473-475.***

Ptitsyn, O. B., Pain, R. H., Semisotnov, G. V., Zerovnik, E., and Razgulyaev, O. I. (1990) *FEBS Lett.* **262**, 20-24.

Radford, S. E., Dobson, C. M., and Evans, P. A. (1992) *Nature* **358**, 302-307.

Rajaraman, K., Raman, B., and Rao. Ch. M. (1996) *J. Biol. Chem.* **271**, 27595-27600.

Raman, B., and Rao, Ch. M. (1994) *J. Biol. Chem.* **269**, 27264-27268.

Rawat, U., and Rao, M. (1998) *J. Biol. Chem*. **273**, 9415-9423.

Reddy, M. C., Palsimano, D. V., Groth-Vaseli, B., and Farnsworth, P. N. (1992) *Biochem. Biophys. Res. Cummun.* **189**, 1578-1584.

Roder, H., Elove, G. A., and Englander, S. W. (1988) *Nature* **335**, 700-704.

Rudiger, S., Buchberger, A., and Kukau, B. (1997) *Nature Struct. Biol.* **4**, 342-349.

Sambrook, J., Fritsch, E. F., and Maniatis, T. (1989) In *"Molecular Cloning, A Laboratory Manual"*, Cold Spring Harbor Laboratory Press, Cold Spring Harbor, NY.

Schatz, G., and Dobberstein, B. (1996) *Science* **271**, 1519-1526.

Schirmer, E. C., Lindquist, S., and Vierling, E. (1994) *Plant Cell* **6**, 1899-1909.

Schmidt, M. A., and Buchner, J. (1992) *J. Biol. Chem.* **267**, 16829-16833.

Schroder, H., Langer, T., Hard, F. U., and Bukau, B. (1993) *EMBO J.* **12**, 54-58.

Shastry, M. C. R., Sander, J. M., and Roder, H. (1998) *Accounts Chem. Res.* **31**, 717-725.

Sherman, M. Y., and Goldberg, A. I. (1992) *EMBO J.* **11**, 71-77.

Sherman, M. Yu., and Goldberg, A. L. (1992) *Nature* **357**, 167-169.

Shiraki, K., Nishikawa, K., and Goto, Y. (1995) *J. Mol. Biol.* **245**, 180-194.

Skowyra, D., Georgopoulos, C., and Zylicz, M. (1990) *Cell* **62**, 939-944.

Straus, D., Walter, W., and Gross, C. A. (1990) *Genes Dev.* **4**, 2202-2209.

Tissieres, A., Mitchell, K., and Tracy, V. M. (1974) *J. Mol. Biol.* **84**, 573-586.

Udgaonkar, J. B., and Baldwin, R. L. (1988) *Nature* **23**, 482-495.

Uversky, V. N., and Ptitsyn, O. B. (1996) *J. Mol. Biol.* **255**, 215-228.

van Boekel, M. A. M., Hoogakker, S. E. A., Harding, J. J., and de Jong, W. W. (1996) *Opthalmic Res.* **28**, Suppl. 1, 32-38.

van den Jissel, P. R. J. A., Overcamp, P., Knauf, U., Gastel, M., and de Jong, W. W. (1994) *FEBS Lett.* **355**, 54-56.

van der Goot, F. G., Gonzales-Manas, J. M., Lakey, J. H., and Pattus, F. (1991) *Nature* **354**, 408-448.

Vierling, E. (1991) *Annu. Rev. Plant Physiol.* **42**, 579-620.

Viitanen, P. V., Lubben, T. H., Reed, J., Goloubinoff, P., O'Keefe, D. P., and Lorimer, G. P. (1990) *Biochemistry* **29**, 5665-?

Voorter, C. E., de Haard-Hoekman, W., Merck, K. B., Bloemendal, H., and de Jong, W. W. (1994) *Biochim. Biophys. Acta* **1204**, 43-47.

Wang, J. D., and Weissman, J. S. (1999) *Nature Struct. Biol.* **6**, 597-600.

Wang, K., and Spector, A. (1996) *Eur. J. Biochem.* **242**, 56-66.

Waters, E. R., (19950 *Genetics* **141**, 785-795.

Waters, E. R., Lee, J. L., and Wierling, E. (1996) *J. Exp. Bot.* **47**, 325-338.

Weissman, J. A., and Kim, P. S. (1992) *Nature* **336**, 42-48.

Welaufer, D. B., and Ristow, S. (1973) *Annu. Rev. Biochem.* **42**, 135-158.

Welch, W. J. (1985) *J. Biol. Chem.* **260**, 3058-3062.

Wetlaufer, D. B. (1981) *Adv. Protein Chem.* **34**, 61-92.

Wolynes, P. G., Onuchic, J. N., and Thirumalai, D. (1995) *Science* **267**, 1619-1620.

Xu, Z., Horwich, A. L., and Sigler, P. B. (1997) *Nature (London)* **388**, 741-750.

Yon, J. M. (1996) In "*Encyclopedia of Molecular Biology and Molecular Medicine* V", VCH, Weinheim, pp 73-93.

Yon, J. M. (1997) *Cell. Mol. Life Sci.* **53**, 557-567.

Zylicz, M., LeBowitz, J. H., McMecken, R., and Georgopoulos, C. (1983) *Proc. Natl. Acad. Sci. U. S. A.* **80**, 6431-6435.

Chapter 7

Interaction of Aspartic Proteases with Lipids Matrix and Colloidal Gold

Section I

Interaction of Pepsin with Octadecyl Amine, Lipid Bilayers

Summary

The entrapment of proteins in different inert matrices with the aim of protection, retention of the native structure and accessibility of the encapsulated proteins to cofactors, and substrates has evoked considerable interest currently. The interaction of the aspartic protease, pepsin, with thermally evaporated lipid, octadecyl amine, has been demonstrated. The approach is based on diffusion of the enzyme from aqueous solution, driven primarily by attractive electrostatic interaction between charged groups on the enzyme surface and ionized lipid molecules in the film. The kinetics of pepsin diffusion into the amine films was followed using quartz crystal microgravimetry (QCM) measurements. The encapsulated pepsin showed catalytic activity comparable to that of the enzyme molecules in solution indicating facile access of biological analytes/reactants in solution to the entrapped enzyme. The time required for the biocomposite formation was less in comparison to some of the techniques currently in vogue, which demonstrated the commercial application of the protocol used. We propose that secondary interactions such as hydrophobic and hydrogen bonding could also be responsible for the diffusion process. The conformational integrity of the entrapped pepsin was investigated by the Fourier Transformed Infrared spectroscopy, UV-vis spectroscopy and by activity measurements. The presence of well distinct amide bands in the FTIR spectrum and the activity measurements of the encapsulated enzyme ruled out any significant distortion to the native structure of the enzyme.

Introduction

Lipid-protein interaction is probably the single most critical factor that determines the action of protein molecules in biological membranes (Mouritsen et al., 1984, Chapman, 1984) and is an area of fundamental interest. Techniques pertaining to the immobilization and encapsulation of proteins in different matrixes are continuously being developed, and such biocomposites have important applications in the food, chemical, pharmaceutical, and agriculture industries. The structural changes of proteins on their binding to a number of alkane derivatives has been studied in detail previously (Reynolds et al., 1970; Steinhardt et al., 1971). To understand some of these problems, researchers have immobilized proteins onto two-dimensional (2-D) supports such as supported lipid bilayers. Furthermore, issues such as protein orientation, biological activity, and effect of salts/ions and pH on the immobilization process have been addressed (May et al., 1999; Mouritsen et al., 1984; Himachi et al., 1994; Himachi et al. 1991; Himachi et al., 1990; Ramsdan, 1998; Hianik et al., 1996; Chen et al., 1999; Nassar 1997; Lu et al., 1997; Burgess 1998; Salamon 1996). From the technological and biomedical applications point of view, studies on protein-lipid interactions have played a significant role in developing protocols for drug delivery and immunosensing systems (Rui et al., 1998; Wink et al., 1998; Puu 2001). Till date proteins/enzymes have been immobilized onto/within 2-D supports such as phospholipid/synthetic bilayers (Himachi et al., 1994; Rusling, 1998), silicate sol-gels (Gill and Ballesteros, 1998; Avnir and Braun, 1996), cross-linked crystals (Tischer and Wedekind, 1999), monolayers attached to solid supports (Ostuni et al., 2001), Langmuir-Blodgett (LB) films (Boussaad et al., 1998), polymer matrices (Franchina et al., 1999; Zhu et al. 2000), galleries of α-zirconium phosphates (Kumar and Chaudhari, 2000), and antibody/antigen labelled surfaces (deWildt et al., 2000). Apart form a number of solid supports used for biomolecule immobilization, lipids in the form of monolayers and bilayers have proved to be a versatile matrix since it offers a better bio-friendly environment, flexibility and inertness. Commercial exploitation of such biocomposites in various fields can be achieved if the processes involved in making such biocomposites are relatively quick, inexpensive, protein-friendly, and applicable to a large range of biomolecules with high loading factors. An important requirement is that the matrix for immobilizing the proteins should be biocompatible and inert i.e., it should not interfere with the native structure of the protein and thereby compromise its catalytic activity. Lipids are more biocompatible than the conventional inorganic and sol-gel matrixes used by many workers in this area. The biocompatibility would reduce the matrix-mediated denaturation of the biomolecules and also would not interfere with the biological processes offering the protein its natural environment. Protection of the protein against microbial degradation, hydrolysis and deamidation and accessibility of the encapsulated proteins to cofactors, substrates and redox agents are important goals, especially in biosensing (Avnir and Braun, 1996) and catalytic (Shabat et al., 1997) applications. The use of immobilized biocatalysts results in additional advantages such as convenient handling, ease of separation from the product and possibility for reuse thereby lowering the effective cost of the enzymes dramatically ([a]Tischer et al., 1999; [b]Tischer et al. 1999).

This section of the chapter describes the encapsulation of pepsin into octadecyl amine films and further investigation on the structural and functional integrity of the enzyme in the lipid matrix.

Materials and Methods

Materials

Octadecylamine was from Aldrich Chemicals. All other chemicals and buffer salts were of the highest quality.

Deposition of Fatty Lipid Films

250 Å thick octadecylamine ($C_{18}H_{37}NH_2$; ODA; pK_b~10.5) films were deposited on gold coated AT cut quartz crystals (for QCM measurements) and Si (111) substrates (for FTIR, contact angle measurements and enzyme activity measurements). The deposition was done in an Edwards E308 vacuum coating unit at a pressure of 1 x 10^{-7} Torr, employing a liquid nitrogen trap. The film deposition rate and thickness was monitored *in-situ* using an Edwards FTM5 thickness monitor having a resolution of $\pm$ 1Hz. For the 6 MHz crystal used in this investigation, this translates into a mass resolution of 12 ng/cm^2.

Encapsulation Studies

10^{-5} M concentrated solution of pepsin was prepared in Glycine-HCl buffer, pH 3.0. The enzyme diffusion into the thermally evaporated ODA films was monitored by immersion of the ODA covered gold coated AT cut quartz crystals for different time intervals in the enzyme solution and measuring the frequency change of the crystals *ex-situ* after thorough washing and drying of the crystals. The frequency changes were converted to mass loading using the standard Sauerbrey formula (Sauerbrey, 1959; Buttry and Ward, 1992; Wang et al., 1992). The time obtained from the QCM measurements was used for the formation of pepsin-lipid biocomposites by simple immersion of Si (111) substrates in the enzyme solution.

Fourier Transform Infrared Spectroscopy

FTIR measurements of the enzyme-lipid biocomposite films on Si (111) substrates were made after immersion of 250 Å thick ODA films in the pepsin solution for 20 min and thereafter rinsing in deionized water and drying the films in flowing nitrogen for 5 minutes. A Shimadzu FTIR-8201 PC instrument operated in the diffuse reflectance mode at a resolution of 4cm^{-1} was used to obtain FTIR spectra of the enzyme-lipid biocomposite films. In order to obtain good signal to noise ratios, 256 scans were taken of the composite films in the range 400 – 4000 cm^{-1}.

Enzyme Activity Measurements

The biochemical activity of the enzyme-lipid biocomposite film on Si(111) substrate was determined by reaction with hemoglobin (5 mg/ml) (0.05 M glycine + HCl buffer). Si (111) substrates of known dimension coated with 250 Å thick ODA films were immersed in pepsin solution for 1 hour until the pepsin density in the films reached equilibrium values. These films were immersed in 1 ml of hemoglobin at 37^{o}C for 60 minutes and then

withdrawn. The reaction was quenched by addition of 1.7 M perchloric acid and the precipitate removed by centrifugation. The supernatant was analyzed for its optical absorbance at 280 nm. For comparison, control enzymatic activity of equivalent concentration of pepsin in solution was determined.

Results and Discussion.

The motivation for encapsulating an enzyme in a lipid matrix was two-fold. The utilization of enzymes in different areas of synthetic organic chemistry is now fairly well established (Lalonde et al., 1995; Zelinski and Waldmann, 1997; Gill et al., 1999; Bosley et al., 1994; Bastida et al., 1998) and the technique proposed would have immediate application in organic chemistry in addition to the more thoroughly studied biocatalytic applications. Secondly, the presence and accessibility of the enzyme in the AA matrix to biological analytes in solution may readily be determined by reaction with suitable proteins.

It has been shown earlier that thermally evaporated films of fatty acids and amines can be spontaneously organized via selective ionic interaction of ions by immersion of the film in a suitable electrolyte. This leads to an organized lamellar film structure similar to c-axis oriented Y-type Langmuir-Blodgett films (Ganguly et al., 1995; Pal, 1996). This approach has been extended for the formation of surface modified colloidal nanoparticles-fatty lipid composites (Patil and Sastry, 1997; Sastry et al., 1998; Patil et al., 1999; Sastry, 2000). A logical extention is the formation of enzyme-lipid biocomposites, and has been demonstrated here by the formation of pepsin-lipid composites. The amine groups in the lipid films are protonated at low pH (pH=3). At this pH, the net charge on the pepsin molecules is negative (pI of pepsin~1) leading to selective electrostatic interactions between the two entities. The enzyme molecules may be viewed as “giant anions”, and process of incorporation of the enzymes in fatty amine films as arising through *selective electrostatic binding* of the pepsin molecules in the amine matrix. This leads to the immobilization of pepsin into the lipid matrix.

Quartz Crystal Microgravimetry.

Quartz crystal microgravimetry (QCM) comprises a thin quartz crystal sandwiched between two metal electrodes that establish an alternating electric field across the crystal, causing vibrational motion of crystal at its resonant frequency. In 1850, Jacques and Pierre Curie discovered that a mechanical stress applied to the surface of various crystals like Rochelle salt, quartz and tourmaline, afforded a corresponding electrical potential across the crystal whose magnitude was proportional to the applied stress. Shortly after their initial discovery, converse piezoelectric effect was also verified, in which application of a voltage across these crystals afforded a corresponding mechanical strain. The inverse piezoelectric effect is the basis of QCM. AT -cut quartz resonator, in which thin quartz wafer is prepared by slicing a quartz rod at an angle of 35^0 with respect to the X-axis of the crystal, resonates in the thickness shear mode. Application of electric field across the crystal causes a vibrational motion of the quartz crystal, with amplitude parallel to the surface of the crystal (Buttry et al., 1992; Wang et al., 1992). The result of the vibrational motion of the quartz crystal is the establishment of a transverse acoustic wave that propagates across the thickness of the crystal, reflecting back into the crystal at the surfaces. When a uniform layer of foreign material is added to the surface of the quartz crystal, the acoustic wave will travel across

the interface, and will propagate through the layer. This leads to decrease in the frequency of the crystal. Frequency changes on deposition of the film can be converted to mass loading using the Saurbrey formula.

We have exploited the principle of QCM to determine the mass uptake of pepsin in the ODA films. As revealed by figure1, the QCM mass uptake data of pepsin diffusion into 250 Å thick ODA films during immersion in the pepsin solutions followed hyperbolic path. It can be seen from the curve that initially as more number of free ionized amine functional groups are available, the diffusion of the enzyme is faster, and then finally the saturation occurs. The time required for the formation of pepsin-lipid biocomposite is better than most of the reports available suggesting the applicability of the protocol for commercial purposes.

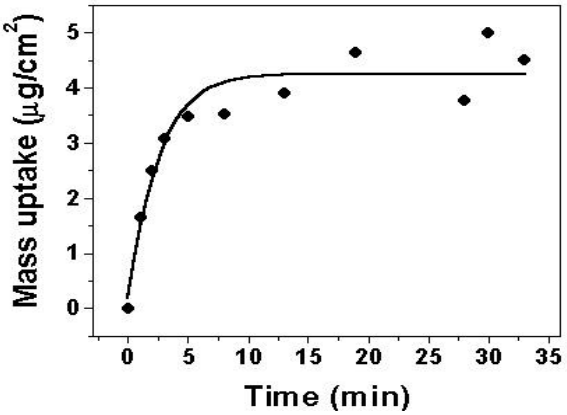

Figure 1. QCM mass uptake curves measured *ex-situ* as a function of time of immersion of 250 Å thick ODA films in 10^{-5} M pepsin solution at pH = 3.

Fourier Transform Infrared Spectroscopy

The amide linkages between amino acid residues in polypeptides and proteins give rise to well-known signatures in the infrared region of the electromagnetic spectrum. The position of the amide I and II bands in the FTIR spectra of proteins is a sensitive indicator of conformational changes in the protein secondary structure (Dong et al., 1992; Templeton et al., 1999; Kumar and McLendon, 1997) and have been used to study the pepsin molecules in the ODA matrix. Figure 2 shows the FTIR spectra recorded from a 250 Å thick as-deposited ODA film (curve 1) and the ODA film after immersion in 10^{-5} M pepsin solution for 60 min (curve 2). A number of vibrational modes can be observed for the films. The amide I band, which arises due to the C=O band in the amide bond occurs at 1647 cm^{-1} for the pepsin-ODA biocomposite film (feature a). While a small feature at this wavenumber does occur in the as-deposited ODA film, the intensity of this band increases in film 2 clearly showing that it originates in the pepsin molecules. The position of this band is close to that reported for native proteins in earlier reports (Dong et al., 1992; Templeton et al., 1999; Kumar and McLendon, 1997) and indicates that the secondary structure of the enzyme in the ODA environment is unperturbed. The amide II band, arising

due to the N-H mode in the amide bond which occurs at 1521 cm^{-1} (feature c) can also be clearly seen for the pepsin-ODA composite film (curve 2). Presence of this band corroborates that the secondary structure of the protein is maintained in the encapsulated form. The origin of the band at 1564 cm^{-1} (feature b, curve 1) is as yet not fully understood but its intensity is reduced on complexation of the ODA molecules with pepsin.

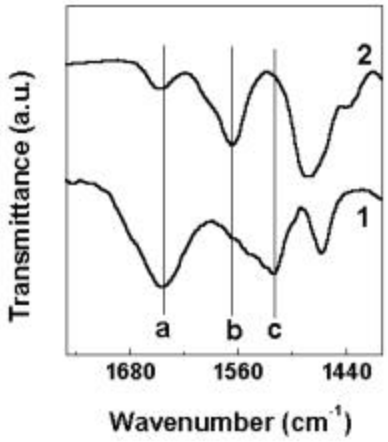

Figure 2. FTIR spectrum recorded from a 1000 Å thick ODA film before (curve 1) after immersion for 60 minutes
in pepsin solution at pH = 3 (curve 2). Features A-C are discussed in the text.

Enzymatic Activity Measurements of the Bioconjugate

The proteolytic activity of the biocomposite was determined and compared with that of the free enzyme in solution under similar conditions. The results obtained from these assay studies are given in Table 1. It is observed that the activity of pepsin in the ODA matrix is slightly less than that of the enzyme in solution. This may be a consequence of the orientation of the enzyme in the lipid matrix limiting the accessibility of the substrate hemoglobin to the active enzyme sites. Another possibility is that not all the enzyme molecules participate in catalysis during the first run, as revealed by the fact that one of the films showed enzymatic activity during three successive runs, albeit considerably reduced each time (Table 1).

Table 1

Details of the enzymatic activity studies of pepsin with hemoglobin.

System	Amount of pepsin (mg)	Optical density (OD) at 280 nm	Normalized OD at 280 nm#
Pepsin solution	2.0	0.458	0.229
Pepsin - ODA (film 1)	2.7	0.450	0.166
Pepsin – ODA (film 2, run	3.6	0.549	0.153

1)			
Pepsin – ODA (film 2, run 2)	3.6	0.041	0.011
Pepsin – ODA (film 2, run 3)	3.6	0.015	0.004

The normalized OD values are the ratios of the measured OD to the weight of pepsin in the film/solution.

Scheme I

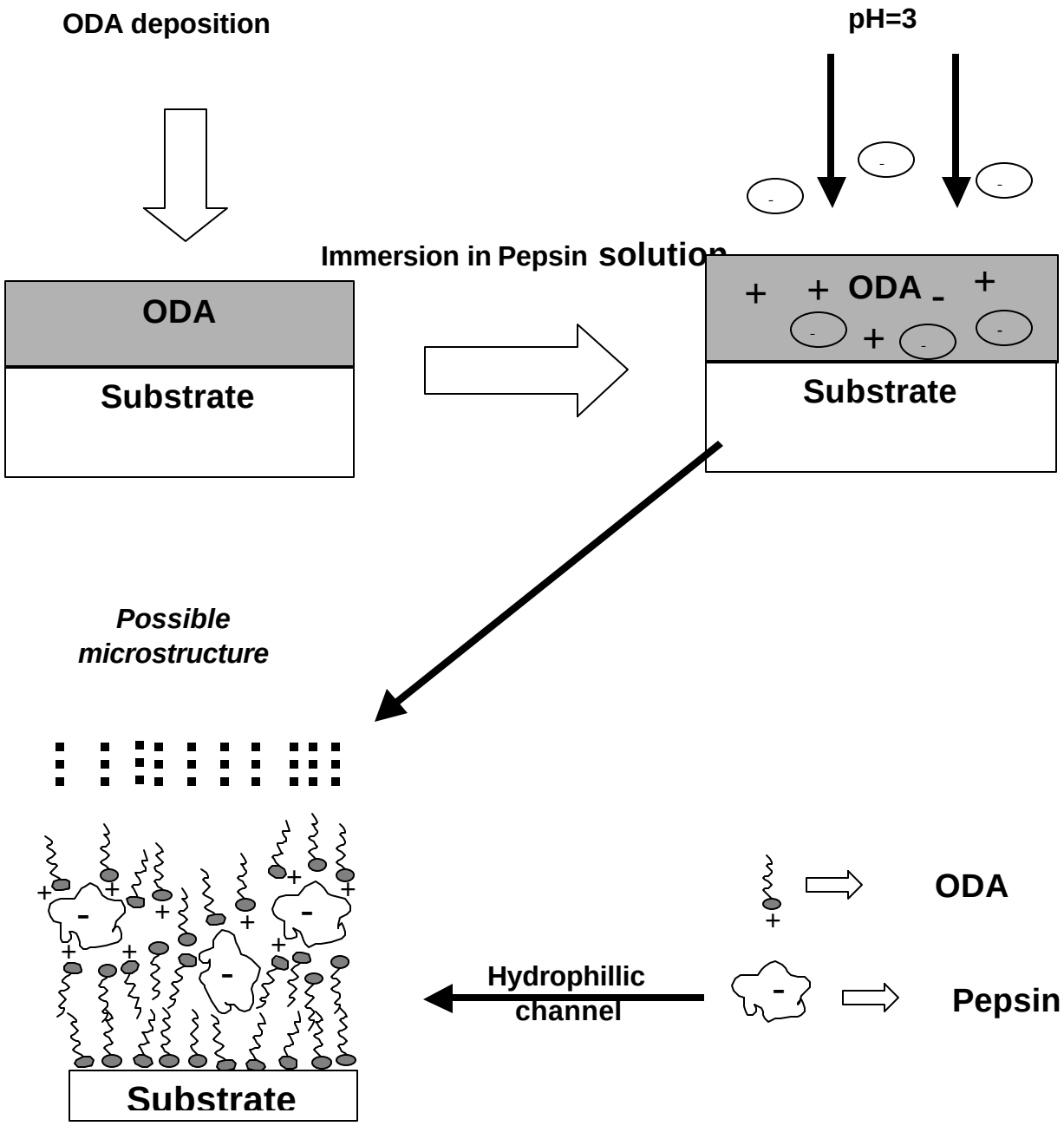
ODA deposition
pH=3
Immersion in Pepsin solution
ODA
Substrate
ODA
Substrate
Possible microstructure
Substrate
ODA
Hydrophillic channel
Pepsin

Conclusions

The different measurements on the pepsin-ODA composite films clearly establish the following. The electrostatically controlled diffusion of the enzyme molecules from the aqueous phase into the lipid matrix may be accomplished under conditions close to that where the enzyme shows maximum activity by suitable choice of the lipid (either cationic or anionic). The enzyme molecules are encapsulated within the ODA matrix without significant distortion to the native structure. Access of the enzyme molecules to substrate molecules in solution is possibly provided via hydrophilic channels in the films (Scheme 1). The elasticity of the bilayers may be primarily responsible for this and enables the matrix to adopt the contours of the enzyme molecule (Scheme 1). The reasonably fast time-scales for the synthesis of the enzyme-lipid composites and the enzyme-friendly encapsulation conditions are a major improvement over other techniques currently being investigated. The enzyme-loading factor can be easily controlled by depositing thicker lipid films with an additional degree of freedom provided by the chain length of the lipid amphiphiles.

Section II

Interaction of Pepsin with Colloidal Gold Nanoparticles

Summary

Pepsin-colloidal gold conjugates were prepared by a protein-friendly process and the structural and functional integrity of the bioconjugates have been investigated. The pepsin-gold conjugates were obtained by mixing colloidal gold and pepsin solutions at pH 3 and, thereafter, centrifugation, washing, and redispersion of the pepsin-gold conjugate material in water. Films of the bioconjugate obtained by solvent evaporation on suitable substrates were further analyzed by scanning electron microscopy (SEM), energy dispersive analysis of X-rays (EDAX), transmission electron spectroscopy (TEM), Fourier transform infrared spectroscopy (FTIR) and X-ray photoelectron spectroscopy (XPS). While TEM and SEM measurements showed aggregates of the enzyme/colloidal gold conjugates, the intactness of secondary and tertiary structures of the enzyme, as determined by FTIR, and fluorescence spectroscopies. The functional integrity of the bioconjugate was analyzed by the catalytic activity measurements, clearly indicates that the enzyme is stable in its natural state and is possibly stabilized by the colloidal gold particles. The enzyme in the pepsin-Au bioconjugate retained substantial biocatalytic activity and was more stable than the free enzyme in solution. In the case of pepsin-gold nanoparticle bioconjugates, we believe that cysteine residues present on the enzyme surface forms covalent linkage with the nanoparticles. It is also possible that amine residues in the enzyme will also bind to the metal surface.

Introduction

The interaction of biomolecules such as proteins/enzymes with three-dimensional (3-D) curved surfaces such as colloidal nanoparticles has also been receiving a fair amount of attraction. This is mainly due to the novel properties of such bioconjugates. The high surface-to-volume ratio offered by colloidal particles results in the concentration of the immobilized entity being considerably higher than that afforded by protocols based on immobilization on planar, 2-D surfaces. Polymer colloidal particles have largely been used as templates for the immobilization of proteins/enzymes/DNA (Caruso et al. 1999; Schmitt et al. 1997; Elgersma et al. 1990). Covalent and other secondary interactions are responsible for such an immobilization process. On the other hand, metal colloidal particles such as gold, silver and CdS have also been used as templates for the immobilization of biomolecules (Keating et al. 1998; Stonehuerner et al., 1992; Scouten et al. 1992). Furthermore, measurement of the catalytic activity of the enzyme in the bio-conjugate material would indirectly yield information on the orientation of the enzyme on the nanoparticle surface as well as the nature of interaction with the nanoparticles. Metal nparticles such as gold and silver are surface sensitive, which is advantageous, as any change in surface states of these nanoparticles by bioconjugation leads to a dramatic change in the optical properties. Mirkin and co-workers have extensively used gold nanoparticles for biosensing and biomedical applications (Mirkin, 2000; Storhoff et al. 2000). These advantages and its biocompatibility make gold nanoparticles an ideal 3-D template for such studies.

The use of colloidal particles as versatile and efficient templates for the immobilization of biomolecules has been recognized since the early 1980s (Rembaum and Dreyer, 1980) Examples of colloidal particle-biomolecule conjugates include immunomicrospheres that can be used to react in a very specific way with antibodies, target cells, or viruses, depending on the type of antigen adsorbed on the microspheres. A number of groups have studied the adsorption of proteins on colloidal particles. In making a shift to nanoscale curved or 3-D surfaces, Caruso et al. have successfully extended the layer-by-layer (l-b-l) technique to the assembly of protein layers on polystyrene (PS) latex particles (Caruso and Mohwald, 1999). By virtue of the high surface-to-volume ratio exhibited by colloidal particles, their use in the immobilization of enzymes and formation of bioconjugate materials would result in a concentration of the enzymes considerably higher than that afforded by protocols based on immobilization on planar, 2-D surfaces. Schmitt et al. (Schmitt et al., 1997) reported on the formation of a monomolecular layer of bovine serum albumin (BSA) on the surface of PS latex particles while Elgersma et al. have demonstrated the adsorption of BSA on positively and negatively charged polystyrene lattices (Elgersma et al., 1990). The interaction of colloidal metal particles such as gold and silver with proteins/enzymes as well as the study of the enzymatic activity of the nano-bioconjugates has also received attention. Natan and co-workers have studied cytochrome c: gold colloid conjugates in great detail as regards their stability, protein orientation on the colloidal particle surface as well as possible application in surface enhanced Raman scattering (SERS) (Keating et al., 1998). Macdonald and Smith have studied the orientation of cytochrome *c* adsorbed on citrate-

reduced silver colloidal particles (Macdonald and Smith, 1996). In an interesting recent report, single molecule spectroscopy (SMS) of hemoglobin molecules adsorbed on 100 nm sized citrate-reduced silver colloidal particles using SERS has been described (Xu et al., 1999). In the area of metal nanoparticle-enzyme conjugate materials, Crumbliss, Stonehuerner, and co-workers have studied the formation and enzymatic activity of gold nanoparticles complexed with horseradish peroxidase (Stonehuerner et al., 1992) and xanthine oxidase (Zhao 1996) as well as glucose oxidase and carbonic anhydrase molecules (Crumbliss et al., 1996) A salient feature of their work is the demonstration that enzyme molecules are bound tightly to gold colloidal particles and retain significant biocatalytic activity in the conjugated form while the enzyme molecules dentature on adsorption to planar surfaces of gold (Crumbliss et al., 1996).

Developing on our earlier work on the encapsulation and enzymatic activity of the digestive enzyme, pepsin, in fatty lipid films (Gole et al., 2000) we demonstrate in this section of the chapter, the functionalization of colloidal gold particles with pepsin under protein-friendly (pH 3) conditions at which the enzyme shows significant catalytic activity. The pepsin-gold conjugate material (hereafter referred to as pepsin-Au) has been characterized using a host of techniques and the catalytic activity.

Materials and Methods

Materials

Chloroauric acid and sodium borohydride were obtained from Aldrich. All buffer salts were from standard commercial sources and of the highest quality available.

Colloidal Gold Synthesis

100 ml of 1.25 x 10^{-4} M concentrated aqueous solution of chloroauric acid ($HAuCl_4$) was prepared in double distilled water. The as-prepared pH of the solution was ca 4. The chloroaurate ions were reduced by addition of 0.01 g of sodium borohydride ($NaBH_4$) at room temperature. The gold atoms start aggregating due to Van der Waals forces to yield 3.5 nm sized colloidal gold nanoparticles (Patil et al., 1999). Further aggregation is stopped possibly due to the electrostatic stabilization due to borate ions on the gold surface. UV-vis spectroscopy measurements of the gold solution yielded an absorbance maximum at 512 nm (Patil et al., 1999).

Formation of Pepsin-Colloidal Gold Conjugates

Pepsin (*pI*~1) at a concentration of10^{-6} M was prepared in Glycine-HCl (0.05 M, pH 3) buffer. Different effective concentrations of pepsin were added to a known volume of colloidal gold solution to yield an overall protein concentration in solution of 10^{-7} and 10^{-8} M. The pH of colloidal gold was adjusted to 3 prior to the addition of pepsin. The solution was stored for a period of 12 h at 4°C and centrifuged to remove uncoordinated pepsin in solution. The pellet obtained was rinsed several times with the buffer and then re-suspended in Gly-HCl buffer and stored at 4°C for further experimentation.

UV-vis Spectroscopy Studies

The pepsin-Au bio-conjugate solution was monitored by UV-vis spectroscopy using a Shimadzu dual-beam spectrophotometer (model UV-1601 PC) operated at a resolution of 1 nm. The surface plasmon resonance due to colloidal gold (ca. 520 nm) (Patil et al., 1999; Alvarez et al., 1997) and the π-π^* transitions due to the tryptophan and tyrosine residues in the enzyme were monitored immediately after addition of pepsin to the gold solution and after centrifugation/re-suspension of the bio-conjugate in water.

Scanning Electron Microscopy (SEM) and Energy Dispersive Analysis of X-rays (EDAX) Measurements

SEM and EDAX measurements of a pepsin-Au film obtained by placing a drop of the bio-conjugate solution on a Si (111) substrate and evaporation of water were performed on a Leica Stereoscan-440 scanning electron microscopy (SEM) equipped with a Phoenix EDAX attachment.

Transmission Electron Microscopy (TEM) Measurements

TEM measurements were performed on a JEOL Model 1200EX instrument operated at an accelerating voltage of 120 kV. Samples for TEM were prepared by placing a drop of centrifuged/re-suspended pepsin-Au

solution on a carbon-coated TEM copper grid. The mixtures were allowed to dry for 1 min and the extra solution was removed using a blotting paper.

Secondary and Tertiary Structure Studies

Fourier transform infrared spectroscopy (FTIR) was used to study the secondary structure of the enzyme in the bio-conjugate. A pepsin-Au film on a Si (111) substrate was prepared as mentioned above and FTIR spectra of the film were recorded on a Shimadzu FTIR-8201 PC instrument operated in the diffuse reflectance mode at a resolution of 4 cm^{-1}. To obtain good signal to noise ratios, 256 scans of the bio-conjugate film were taken in the range 400 – 4000 cm^{-1}.

Fluorescence measurements of the bioconjugate were performed on a Perkin-Elmer LS50 Luminescence spectrometer connected to a Julabo F20 water bath. Protein fluorescence was excited at 280 nm and the emission was recorded from 300-500 nm at 25°C. The slit widths on both the excitation and emission were set at 5 nm and the spectra were obtained at 500 nm/min. Fluorescence data were corrected by running control samples of buffer and smoothened.

Quantitative Estimation of Pepsin in the Bio-Conjugate System

The amount of pepsin in the pepsin-Au bio-conjugate system was determined by fluorescence spectroscopy. Fluorescence emission intensities at 340 nm from a known quantity of the pepsin:colloidal gold conjugate materials were compared with the intensity of standard pepsin solutions of different concentrations. From the calibration curve, the amount of pepsin in the bioconjugate solution was determined and used to calculate the specific activity of the enzyme.

Chemical Analysis by X-ray Photoelectron Spectroscopy (XPS)

A pepsin:colloidal gold bio-conjugate film on Si (111) substrate was further characterized by XPS. XPS measurements were carried out on a VG MicroTech ESCA 3000 spectrometer equipped with a multichanneltron hemispherical electron energy analyser at a pressure better than 1 x 10^{-9} Torr. The electrons were excited with un-monochromatized Mg K_α X-rays (energy = 1253.6 eV) and the spectra were collected in the constant analyzer energy mode at a pass energy of 50 eV. This leads to an overall resolution of ca. 1 eV for the measurements. Si 2p (substrate), C 1s, N 1s, Au 4f, S 2p, and O 1s core level spectra were recorded from the drop coated bio-conjugate film at an electron takeoff angle (ETOA, angle between the surface plane and electron emission direction) of 60^o. Prior to curve stripping by a non-linear least squares procedure, the inelastic electron background was removed by the Shirley algorithm (Shirley, 1972).

Enzymatic Activity Measurements

To estimate the proteolytic activity of pepsin in the bioconjugate solution, 100 µl of the pepsin-Au solution was reacted with 1 ml of hemoglobin (5 mg/ml) in a total reaction of 2 ml, and incubated at 37^oC for 30 minutes. Equal volume of 1.7 M perchloric acid was added to stop the reaction. The precipitate was removed by centrifugation and the optical absorbance of the filtrate measured at 280 nm. For comparison, the catalytic activity of an identical concentration of the free enzyme in solution was recorded. In order to determine the confidence

limits of the specific activity measurements for the pepsin-Au conjugate material, separate measurements of the specific activity were made as described above for 6 different pepsin-Au solutions. The stability of the pepsin-Au bio-conjugate in terms of its specific activity was determined over a period of 4 days and compared with the specific activity of an equal quantity of the free enzyme in solution.

Results and Discussion

In this study, we have chosen to study the immobilization of pepsin on colloidal gold particles. Measurement of the catalytic activity of the enzyme in the bioconjugate material would indirectly yield information on the orientation of the enzyme on the nanoparticle surface as well as the nature of the interaction with the gold surface. Moreover, the sensitivity of the optical properties of colloidal gold particles due to, for example, protein adsorption and its biocompatibility make it an ideal 3-D template for such studies.

Preparation of Pepsin-Au Conjugates

The pH of the as-prepared colloidal gold solution was ca. 9. Pepsin has a *pI* ~1 and shows significant catalytic activity at pH 3, and therefore, the pH of colloidal gold was lowered prior to addition of pepsin. A 10^{-6} M standard solution of pepsin was prepared in glycine-HCl (0.05 M, pH 3) buffer and added to colloidal gold solution, to form pepsin solutions of 10^{-7} and 10^{-8} M concentrations. At pH 3, both the gold colloidal particles and pepsin molecules are expected to be negatively charged, and therefore, electrostatic interactions between the two cannot explain the binding of the enzyme to the gold nanoparticles. The sequence analysis of the pepsin used in this study showed that the enzyme is composed of one lysine and five cysteine residues (Sielecki et al., 1990). While it is known that amine functional groups from primary amines bind to colloidal gold through weak covalent interactions (Leff et al., 1996), it is likely that in the case of pepsin-Au conjugates the enzyme molecules bind to the colloidal particle surface via thiolate linkages through the cysteine residues as well. Support for cysteine mediated binding of pepsin to the gold colloids also have been reported (Sasaki et al.,1997) wherein it was demonstrated that the functional protein, myosin subfragment 1, binds to gold thin film surfaces through a Au-S bond involving cysteine residues in the protein.

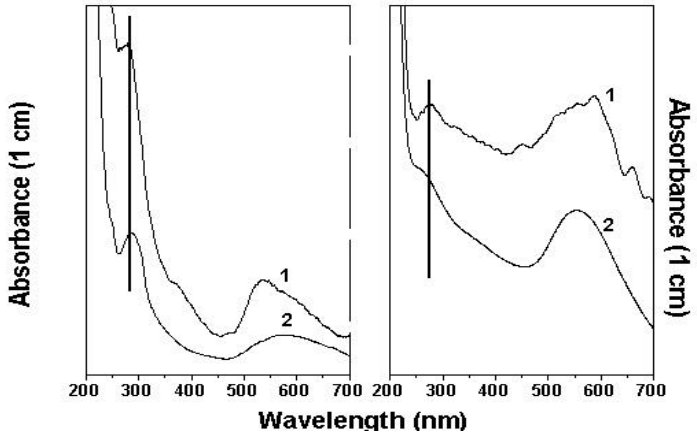

Figure 1. UV-vis spectra of pepsin-Au bio-conjugate solutions

a) UV-vis spectra of pepsin-Au bio-conjugate solutions immediately after addition of pepsin in colloidal gold at pH=3 at two different concentrations of pepsin in solution: 10^{-7} M (curve 1) and 10^{-8} M (curve 2). b) UV-vis spectra of pepsin-Au bio-conjugate solutions after centrifugation, rinsing and re-suspension in pH = 3 buffer. Curves 1 and 2 correspond to the 10^{-7} M and 10^{-8} M pepsin-Au colloidal solutions respectively.

Figure 1A shows the UV-vis spectra of the two different concentrations of pepsin added to colloidal gold. Curve 1 corresponds to spectrum from the pepsin-colloidal gold solution with 10^{-7} M pepsin, while curve 2 is the pepsin-colloidal gold solution spectrum with 10^{-8} M pepsin. The surface plasmon resonance due to gold can be clearly seen above 500 nm (Patil et al., 1999), and the slight asymmetry in the curves (more pronounced in the case of curve 1 indicates some degree of aggregation of the gold particles. The absorbance at about 280 nm in both the cases is due to the π-π^* transitions arising from the tryptophan and tyrosine residues of the enzyme (Stoscheck, 1990). It is seen that this band is more intense in curve 1 than in curve 2 and agrees with the higher concentration of pepsin in the bioconjugate corresponding to curve 1. The bioconjugate solutions were stored for a period of 12 h at 4°C before centrifugation and resuspension. Figure 1B shows the UV-vis spectra of the two pepsin-Au solutions shown in Figure 1A after centrifugation/resuspension. While there is a small decrease in intensity of the surface plasmon resonance of colloidal gold, a large decrease in intensity of the 280 nm band can clearly be seen, indicating removal of uncoordinated pepsin from the respective solutions. It is also interesting to observe that the spectrum corresponding to the 10^{-8} M pepsin-Au bioconjugate solution is fairly sharp and does not show evidence of aggregation of the gold particles. Apparently, the process of centrifugation, washing and redispersion has removed aggregated pepsin-Au structures from the bioconjugate solution. The 10^{-7} M pepsin-Au solution indicates some degree of aggregation even in the redispersed form.

SEM and EDAX Measurements

Figure 2A shows an SEM image of the 10^{-8} M pepsin-Au bioconjugate film formed by drop-drying the bioconjugate solution on a Si-(111) substrate. The film is highly aggregated and has morphology rather similar to

that observed by Caruso et al. in multilayer films of polymer-anti-IgG composites (Caruso et al. 1998). The aggregated structure is likely to be a consequence of the solvent evaporation process used in making the films. The gold particles are too small to be resolved in the figure. The aggregation of the pepsin-Au conjugates in solution is ruled out due to the intactness of the natural conformation of the enzyme as evidenced from the FTIR, fluorescence, and catalytic activity measurements. EDAX measurements on the same film yielded a nitrogen-Au ratio of 1:40, indicating a high percentage of gold particles in the composite material. The presence of the large number of gold particles appears to stabilize the enzymes in the aggregate as will be seen subsequently; the specific activity of the enzyme in the bioconjugate material is close to that of the free enzyme in solution.

Figure 2B shows the TEM micrograph of a pepsin-Au bioconjugate film on a carbon-coated TEM grid. The image shows the extremity of one of the aggregates seen in the SEM micrograph (Figure 2A). The spherical substructures in the aggregate can clearly be resolved. In this case as well, the magnification is insufficient to see the gold particles. At higher magnification, the film was observed to melt under the electron beam, due to possible electron-induced degradation of the enzyme molecules in the film. The size of the gold particles (3.5 nm) and pepsin molecules (ca. 5 nm) are nearly the same, and it is possible that the protein molecules “condense” due to coordination with the gold particles to yield spherical structures as seen in the TEM micrograph.

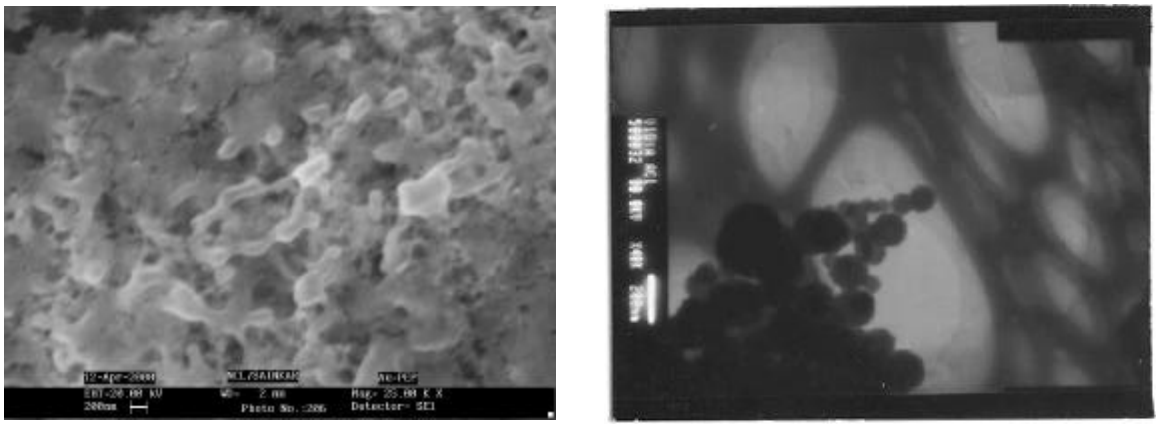

Figure 2. Scanning and transmission electron microscopic analysis of the pepsin-Au bioconjugate.

A) SEM image of a film of the pepsin-Au bio-conjugate prepared by drop drying on a Si (111) substrate.
B) TEM micrograph of a drop-dried pepsin-Au bio-conjugate film on a carbon coated copper TEM grid.

FTIR Studies

Figure 3A shows FTIR spectra recorded from a drop-dried 10^{-7} M pepsin-Au bioconjugate film on Si (111) substrates. As revealed from the figure, a broad band, centered at about 3300 cm^{-1} is due to O-H vibrations from trapped water molecules in the pepsin-Au bioconjugate film. Two small features occurring at about 2920 and 2855 cm^{-1} (feature 2) are assigned to the methylene antisymmetric and symmetric vibrations of the hydrocarbons present in the enzyme. A small broad feature at about 2520 cm^{-1} (feature 3) arises due to the free/uncoordinated -SH stretching vibrations that are present in the cysteine residues in the enzyme. The presence of this feature indicates that not all cysteine residues are bound to the gold particle surface, possibly due to uneven distribution on the enzyme surface. Figure 3B shows two prominent and sharp resonances at about 1648 and 1536 cm^{-1}, which are the amide I and II bands respectively. The amide I band (feature 1) is assigned to the stretch mode of the carbonyl group coupled to the amide linkage, whereas the amide II band arises due to the N-H stretching modes of vibration in the amide linkage. The position of these bands is close to that reported for native proteins in earlier papers (Dong et al., 1992), and indicates that the secondary structure of the enzyme is unperturbed after immobilization on the gold surface.

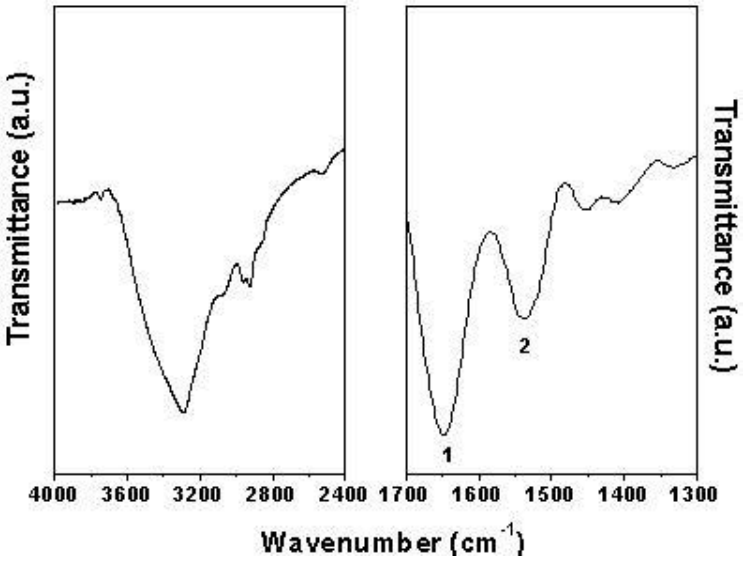

Figure 3. FTIR spectra of the pepsin-Au bioconjugate.

A) FTIR spectra recorded from a drop-dried pepsin-Au bio-conjugate film on a Si (111) substrate in the 4000 to 2400 cm^{-1} spectral region. B) FTIR spectra recorded for the same drop-dried pepsin-Au bio-conjugate film on Si (111) in the range 1700 cm^{-1} to 1300 cm^{-1}. The amide I and II bands (features 1 and 2) are indicated next to the individual resonances.

Chemical Analysis of the Bioconjugate using XPS

A drop coated 10^{-7} M pepsin-Au conjugate film on Si (111) substrate was investigated chemically using XPS. General scan spectra did not reveal the presence of any impurities in the film. The Au 4f, Si 2p (from the substrate), C 1s, N 1s, O 1s and S 2p core level spectra were recorded as mentioned in the experimental section. The signal to noise ratio of the S 2p and O 1s core levels was not good enough for carrying out an accurate chemical analysis and, therefore, will not be discussed further. The core level spectra mentioned above were decomposed into individual chemical components using a nonlinear least squares fitting procedure as shown in Figure 4. Figure 4A shows the Au 4f spectrum together with the spin-orbit components 1 and 2. The Au $4f_{7/2}$ peak occurred at a binding energy (BE) of 83.8 eV and corresponds to that of metallic Au. There was no evidence of a chemically shifted component which could arise due to co-ordination with pepsin molecules.

The C 1s spectrum could be decomposed into two chemically distinct components as shown in Figure 4B. The peak at 285 eV (curve 1) BE arises from carbons in the hydrocarbons from the various residues of the enzyme. The component at 288.6 eV BE (curve 2, Figure 4B) is assigned to electron emission from carbons in the carboxylate groups of the amino acids of the enzyme. This value agrees with reported BEs of carboxylate carbons in Langmuir-Blodgett films of fatty acids (Ganguly et al., 1993) as well as surface modified polymers (Davies et al., 1994).

The most interesting spectrum is that of the N 1s core level which could be fit to two Gaussians centered at 400.5 eV BE (curve 1) and at 403.5 eV BE (curve 2) and is shown in Figure 4C. The lower BE component is tentatively assigned to nitrogens from the un-ionized amine groups in the protein (possibly those bound to the gold surface) while the higher BE component arises due to electron emission from the amine groups in the pepsin

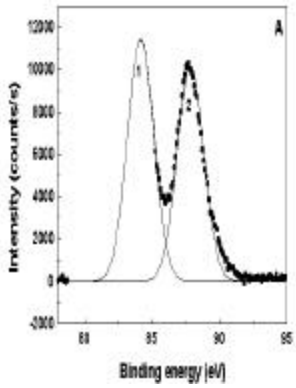

molecules. We are not aware of photoemission studies of proteins bound to colloidal gold particles and therefore, the above assignments must be viewed as tentative.

Figure 4. Chemical analysis of the pepsin-Au bioconjugates.

A) Au 4f core level spectrum recorded from a drop-dried pepsin-Au bio-conjugate film on a Si (111) substrate. The two spin-orbit components are shown in the figure. B) C 1s core level spectrum recorded from a drop-dried pepsin-Au bio-conjugate film on a Si (111) substrate. The chemically distinct components are also shown. C) N 1s core level spectrum recorded from a drop-dried pepsin-Au bio-conjugate film on a Si (111) substrate. The spectrum has been fit to two Gaussians (shown in the figure) centered at 400.5 eV and 403.5 eV respectively.

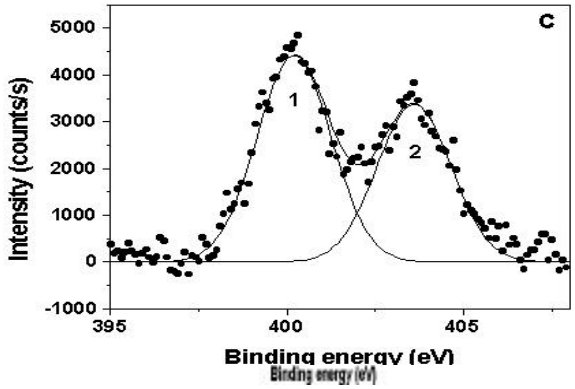

Tertiary Structure Studies

The catalytic activity of the immobilized enzyme depends on the tertiary structure of the enzyme remaining unperturbed on the surface of colloidal gold. The tertiary structure of pepsin co-ordinated to colloidal

gold particles have been monitored by excitation of the π - π^* transition in the tryptophan and tyrosine residues at 280 nm (Eftink and Ghiron, 1981). Figure 5A shows the fluorescence spectra of 5 x 10^{-9} M and 10^{-9} M pepsin solutions at pH 3 (curves 1 and 3 respectively). Curve 2 corresponds to the emission spectrum from the 10^{-8} M pepsin-Au bio-conjugate solution. The emission maxima in all the three pepsin solutions occur at about 340 nm. The nature of the curve for the pepsin-Au bio-conjugate solution is similar to that of the free enzyme in solution, which indicates that the pepsin co-ordinated to gold colloidal particles is present in its natural configuration maintaining its tertiary structure.

Fluorescence spectroscopy was also used to quantify the amount of pepsin in the bio-conjugate solution by comparing the fluorescence intensity at 340 nm with the calibration curve mentioned earlier (two spectra of which are shown in Figure 5A). The calibration curve was obtained by plotting the fluorescence intensities of different concentrations of pepsin at pH = 3 as a function of protein concentration in solution. The concentration of pepsin in the pepsin-Au bio-conjugate solution was calculated to be ca. 2 x 10^{-9} M.

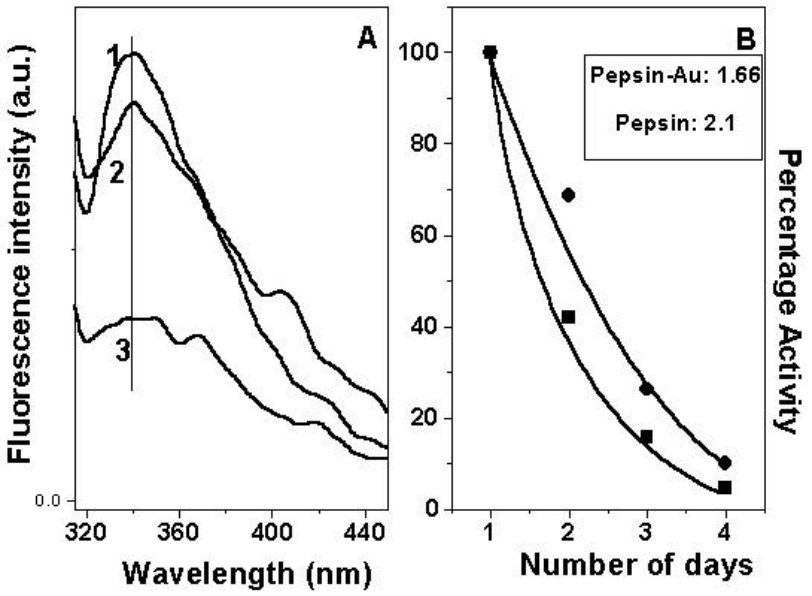

Figure 5. Structural and functional integrity analysis of pepsin-Au bioconjugate.

A) Fluorescence spectra of pepsin solution at a concentration of 5 x 10^{-9} M (curve 1), pepsin-Au bio-conjugate solution (10^{-7} M pepsin concentration in initial solution, curve 2), and pepsin solution at a concentration of 10^{-9} M (curve 3). B) Proteolytic activity measurements of a 10^{-7} M pepsin-Au bio-conjugate solution (●) and free pepsin in solution (2 x 10^{-9} M concentration, ■) as a function of number of days of storage at 4^0C. The inset indicates the specific activities of freshly prepared pepsin-Au bio-conjugates and the free enzyme solutions.

Enzymatic Activity Measurements

The most significant aspect in protein-colloid bioconjugate systems is the functional integrity of the proteins after adsorption onto the particle surface. This is of vital importance because of the ultimate application potential of the protein-coated particles in areas of medical diagnosis and drug delivery. Figure 5B shows a plot of the normalized biocatalytic activity of 10^{-7} M pepsin-Au bioconjugate solution as a function of number of days of storage of the solution at 4^0C. The error bars correspond to the standard deviation in the specific activity values measured from 6 separate pepsin-Au conjugate solutions. Each day, equal volume of the same stock solution was taken and the proteolytic activity was determined. It can be seen that there is an exponential decrease in the biocatalytic activity of the pepsin-Au solution, starting from 100% for the first day to 10 % for the 4^{th} day. The contrast with the time-dependent biocatalytic activity of free pepsin in solution (2×10^{-9} M concentration) measured in a similar manner is interesting. It is seen that the pepsin:Au solution was more stable and exhibited higher activity at each stage of measurement. Thus, the gold particles appear to stabilize the pepsin molecules to some extent in solution. The reduction in the biocatalytic activity of the enzyme with time may be primarily due to the autoproteolytic degradation of the enzyme in the solution. The numbers shown in Figure 5B are the specific activities of pepsin in the bioconjugate and as free protein in solution. It is seen that the specific activity of the enzyme in the bio-conjugate is slightly less than that of the free enzyme in solution and may be due to the partial blockage of some of the reaction sites in the protein during binding to the gold particles.

Conclusions

Pepsin-Au bioconjugates have been prepared by simple addition of pepsin to the colloidal gold solution. It is believed that thiol groups in the cysteine residues as well as amine groups in the lysine residues of the enzyme bind covalently with the gold particle surface, leading to the formation of the bioconjugate. While TEM and SEM measurements indicated aggregated structures in the drop-dried pepsin-Au bioconjugate films, estimation of the proteolytic activity of the conjugate material showed very little loss in activity due to gold particle surface binding. This clearly indicates that the enzyme secondary and tertiary structures were unperturbed on surface coordination with gold particles and was supported by FTIR and fluorescence spectroscopy studies. Comparison of the catalytic activity of the pepsin-Au conjugate material and an equivalent quantity of the free enzyme in solution as a function of time of storage indicated that the enzyme on the surface of gold is more stable than the enzyme in solution.

References

Alvarez, M. M., Khoury, J. T., Schaaf, T. G., Shafigullin, M. N., Vezmar, I., and Whetten, R. L. (1997) *J. Phys. Chem B*. **101**, 3706-3712.

Anson, M. (1938) *J. Gen. Physiol.* **22**,79-89.

Avnir, D., and Braun, S. (1996) *"Biochemical Aspects of Sol-Gel Science and Technology"* Kluwer: Hingham, MA, 1996. Bastida, A., Sabuquillo, P., Armisen, P., Fernandez-Lafuente, R., Huget, J., and Guisan, J. M. (1998) *Biotechnol. Bioeng.* **58**, 486-493.

Bosley, J. A., and Clayon, J. C. (1994) *Biotechnol. Bioeng.* **43**, 934-938.

Boussaad, A., Dziri, L., Arechabaleta, N. J., Tao, N. J., and Leblanc, R. M. (1998) *Langmuir* **14**, 6215-6219.

Burgess, J. D., Rhoten, M. C., and Hawkridge, F. M. (1998) *Langmuir* **14**, 2467-2475.

Buttry, D. A., and Ward, M.D. (1992) *Chem. Rev.* **92**, 1355-1379.

Caruso, F., and Mohwald, H. (1999) *J. Am. Chem. Soc.* **121**, 6039-6046.

Caruso, F., Furlong, D. N., Ariga, Katsuhiko, Ichinose, I., and Kunitake, T. (1998) *Langmuir* **14**, 4559-4565.

Caruso, F., Mohwald, H. (1999) *J. Am. Chem. Soc*. **121**, 6039-6046.

Caruso, F., Niikura, K., Furlong, D. N., and Okahata, Y. (1997) *Langmuir* **13**, 3427-3433.

Caruso, F., Rodda, E., Furlong, D. N., Niikura, K., and Okahata, Y. (1997) *Anal. Che*m. **69**, 2043-2049.

Chapman, D (1984) In *"Membrane structure ad function"* (Chapman, D., Eds.), Verlag chemie, Weinehim.

Chen, X., Hu, N., Zeng, Y., Rusling, J. F., and Yang, J. (1999) *Langmuir***15**, 7022-7030.

Crumbliss, A. L., Perine, S. C., Stonehuerner, J., Tubergen, K. R., Zhao, J., and O'Daly, J. P. (1992) *Biotech. Bioeng.* **40**, 483-490.

Davies, M. C., Lynn, R. A. P., Davis, S. S., Hearn, J., Watts, J. F., Vickerman, J. C., and Johnson, D. (1994) *Langmuir* **10**, 1399-1409.

deWildt, R. M. T. et al. (2000) *Nat. Biotech*. **18**, 989-994.

Dong, A., Huang, P., and Caughey, W. S. (1992) *Biochemistry* **31**,182-189.

Eftink, M. R., and Ghiron, C. A. (1981) *Anal. Biochem.* 199-227. Elgersma, A. V., Zsom, R. L. J., Norde, W., and Lyklema, J. (1990) *J. Colloid Interface Sci.* **138**,145-156.

Fang, J., and Knobler, C. M. (1996) *Langmuir* **12**, 1368-1374.

Franchina, J. G., Lackowski, W. M., Dermody, D. L., Crooks, R. M., Bergbreiter, D. E., Sirkar, K., Russell, R. J., and Pishko, M. V. (1999) *Anal. Chem.* **71**, 3133-3139.

Franchina, J. G., Lakskowski, W. M., Dermody, D. L., and Crooks, R. M. (1999) *Anal. Chem*. **71**, 3133-3139.

Ganguly, P., Pal, S., Sastry, M., and Shashikala, M. N. (1995)*Langmuir* **11**, 1078-1080.

Ganguly, P., Paranjape, D. V., Sastry, M., Chaudhary, S. K., and Patil, K. R. (1993) *Langmuir* **9**, 487-490.

Gill, I., and Ballesteros, A. (1998) *J. Am. Chem. Soc.* **120**, 8587-8598.

Gill, I., Pastor, E., and Ballesteros, A. (1999) *J. Am. Chem. Soc.* **120**, 9487-9496.

Gole, A., Dash, C., Rao, M., and Sastry, M. (2000) *Chem. Commu*n. **2000**, 297-298.

Hamachi, I., Honda, T., Noda, S., and Kunitake, T. (1991) *Chem. Lett*. 1121-1124.

Hianik, T., Snejdarkova, M., Passechnik, V I., Rehak, M., and Babincova, M. (1996) *Bioelectrochem. Bioenerg.* **41**, 221-225.

Himachi, I., Fujita, A., and Kunitake, T. (1994) *J. Am. Chem. Soc*. **116**, 8811-8812.

Himachi, I., Noda, S., and Kunitake, T. (1990) *J. Am. Chem. Soc.* **112**, 6744-6745.

Keating, C. D., Kovaleski, K. M., and Natan, M. J. (1998) *J. Phys. Chem. B*. **102**, 9404-9413.

Keating, C. D., Kovaleski, K. M., and Natan, M. J. (1998) *J. Phys. Chem. B*. **102**, 9414-9425.

Kumar, C. V. and Chaudhari, A. (2000) *J. Am. Chem. Soc.* **122**, 830-837.

Kumar, C. V., and McLendon, G. L. (1997) *Chem. Mater.* **9**, 863-870.

Lalonde, J. J., Govardhan, C., Khalaf, N., Martinez, A. G., Visuri, K., and Margolin, A. L. (1995) *J. Am. Chem. Soc.* **117**, 6845-6852.

Leff, D. V., Brandt, L., and Heath, J. R. (1996) *Langmuir* **12**, 4723-4730.

Lu, Z., Huang, Q., and Rusling, J. F. (1997) *J. Electroanal. Chem.* **423**, 59-66.

Macdonald, I. D. G., and Smith, W. E. (1996) *Langmuir* **12**, 706-713. May, S., and Ben-Shaul, A. (1999) *Biophys. J.* **76**, 751-767.

Mirkin, C. A. (2000) *Inorganic Chemistry* **39**, 2258-2272.

Mouritsen, O. G., and Bloom, M. (1984) *Biophys. J.* **46**, 141-153.

Mrksich, M., Sigal, G. B., and Whitesides, G. M. (1995) *Langmuir* **11**, 4383-4385.

Nassar, A.-E. F., Zhang, Z.; Hu, N., Rusling, J. F., and Kumosinski, T. F. (1997) *J. Phys. Chem. B* **101**, 2224-2231.

Nicolini, C., Erokhin, V., Antolini, F., Catasti, P., and Facci, P. (1993) *Biochim. Biophys. Acta* **1158**, 273-278.

Ostuni, E. et al. (2001) *Langmuir* **17**, 5605-5620.

Pal, C. Ph.D. Thesis, University of Pune, **1996**.

Patil, V., and Sastry, M. (1997) *J. Chem. Soc. Faraday Trans*. **93**, 4347-4355.

Patil, V., Malvankar, R. B., and Sastry, M. (1999) *Langmuir* **15**, 8197-8206.

Puu, G. (2001) *Anal Chem.* **73**, 72-79.

Ramsden, J. J. (1998) *Biosens. Bioelectron.* **13**, 593-598.

Rembaum, A., and Dreyer, W. J. (1980) *Science* **208**, 364-368.

Reynolds, J. A., Gallagher, J. P., and Steinhardt, J. (1970) *Biochemistry* **9**, 1232-1240.

Rui, Y., Wang, S., Low, P.S., and Thompson, D. H. (1998) *J. Am. Chem. Soc*. **120**, 11213-11215.

Rusling, J. F. (1998) *Acc. Chem. Res.* **31**, 363-369.

Salamon, Z., and Tollin, G. (1996) *Biophys. J.* **71**, 848-857.

Sasaki, Y. C., Yasuda, K., Suzuki, Y., Ishibashi, T., Satoh, I., Fujiki, Y., and Ishiwata, S. (1997) *Biophys. J.* **72**, 1842-1848. Sastry, M. (2000) *Curr. Sci.* **72**,1089-1097.

Sastry, M., Patil, V., and Sainkar, S. R. (1998) *J. Phys. Chem. B* **102**, 1404-1411.

Sauerbrey, G. (1959) *Z.Phys. (Munich)* **155**, 206-209.

Schmitt, A., Fernandez-Barbero, A., Cabrerizo-Vilchez, M., and Hidalgo-Alvarez, R. (1997) *Prog. Colloid Polym. Sci*. **104**, 144-149.

Scouten, W. H., and Konecny, P. (1992) *Anal. Biochem*. **205**, 313-316.

Shabat, D., Grynszpan, F., Saphier, S., Turniansky, A., Avnir, D., and Keinan, E. (1997) *Chem. Mater*. **9**, 2258 - 2260. Shirley, D. A. (1972) *Phys. Rev. B* **5**, 4709-4714.

Sielecki, A. R., Federov, A. A., Boodhoo, A., Andreeva, N. S., and James, M. N. (1990) *J. Mol. Biol.* **214**, 143-170. Steinhardt, J., Krijn, J., and Leidy, J. G. (1971) *Biochemistry* **10**, 4005-4011.

Stonehuerner, J. G., Zhao, J., O'Daly, J.P., Crumbliss, A. L., and Henkens, R. W. (1992) *Biosens.Bioelectron*. **7**, 421-428. Storhoff, J. J., Lazarides, A. A., Mucic, R. C., Mirkin, C. A., Letsinger, R. L., and Schatz, G. C. (2000) *J Am. Chem. Soc.* **122**, 4640-4642.

Stoscheck. C. M. (1990) *Methods Enzymol*. **182**, 50-68.

Templeton, A. C., Chen, S., Gross, S. M., and Murray, R. W. (19990 *Langmuir* **15**, 66-76.

[a]Tischer, W., and Wedekind, F., (1999)*Top. Curr. Chem.* **200**, 95-126 and references therein.

[b]Tischer, W., and Kasche, V. (1999)*Trends. Biotechnol.* **17**, 326-335.

Umana, M., and Waller, J. (1986) *Anal. Chem.* **58**, 2979-2983.

Wang, J., Frostman, L.M., and Ward, M.D. (1992) *J. Phys. Chem.* **96**, 5224-5232.

Wink, T., van Zuilen, S. J., Bult, A., and van Bennekom, W. P. (1998) *Anal. Chem.* **70**, 827-832.

Xu, H., Bjerneld, E. J., Kall, M., and Borjesson, L. (1999) *Phys. Rev. Lett.* **83**, 4357-4360.

Yang, Z., Mesiano, A. J., Venkatasubramanian, S., Gross, S. H., Harris, J. M., and Russel, A. J. (1995) *J. Am. Chem. Soc.* **117**, 4843-4850.

Zelinski, T., and Waldmann, H. (1997) *Angew. Chem. Int. Ed.* **36**, 722-724.

Zhao, J., O'Daly, J. P., Henkens, R. W., Stonehuerner, J. G., and Crumbliss, A. L. (1996) *Biosens. Bioelectron.* **11**, 493-502.

Zhu, G. et al. (2000) *Nat. Biotech*. **18**, 52-57.